Maastricht University

Orthopaedic Infections: Pre-clinical Models, Diagnostic Tools and Novel Coatings

Citation for published version (APA):

Odekerken, J. C. E. (2015). *Orthopaedic Infections: Pre-clinical Models, Diagnostic Tools and Novel Coatings*. [Doctoral Thesis, Maastricht University]. Maastricht University. https://doi.org/10.26481/dis.20150424jo

Document status and date:
Published: 01/01/2015

DOI:
10.26481/dis.20150424jo

Document Version:
Publisher's PDF, also known as Version of record

Please check the document version of this publication:

• A submitted manuscript is the version of the article upon submission and before peer-review. There can be important differences between the submitted version and the official published version of record. People interested in the research are advised to contact the author for the final version of the publication, or visit the DOI to the publisher's website.
• The final author version and the galley proof are versions of the publication after peer review.
• The final published version features the final layout of the paper including the volume, issue and page numbers.

Link to publication

General rights
Copyright and moral rights for the publications made accessible in the public portal are retained by the authors and/or other copyright owners and it is a condition of accessing publications that users recognise and abide by the legal requirements associated with these rights.

• Users may download and print one copy of any publication from the public portal for the purpose of private study or research.
• You may not further distribute the material or use it for any profit-making activity or commercial gain
• You may freely distribute the URL identifying the publication in the public portal.

If the publication is distributed under the terms of Article 25fa of the Dutch Copyright Act, indicated by the “Taverne” license above, please follow below link for the End User Agreement:

www.umlib.nl/taverne-license

Take down policy
If you believe that this document breaches copyright please contact us at:

repository@maastrichtuniversity.nl

providing details and we will investigate your claim.

Download date: 06 May. 2023

Orthopaedic Infections:

Pre-clinical Models, Diagnostic Tools and Novel Coatings

© Jim C. E. Odekerken, Klimmen, 2015

Coverdesign: Jim C. E. Odekerken & Daisy Hanssen
Production: GVO drukkers & vormgevers B.V. | Ponsen & Looijen

ISBN: 978-90-9028864-2

The printing of this thesis was financially supported by: Cam Bioceramics, Anna Fonds | NOREF, Nederlandse vereniging voor Biomaterialen en Tissue Engineering, Stichting Kliniek en Wetenschap Orthopaedie, Aelmans Adviesgroep, Buitenstate, van de Laar Financiële Dienstverlening, Ger Horsmans Timmer-montagebedrijf, Frissen Groen Techniek.

Orthopaedic Infections:
Pre-clinical Models, Diagnostic Tools and Novel Coatings

PROEFSCHRIFT

ter verkrijging van de graad van doctor
aan de Universiteit Maastricht,
op gezag van de Rector Magnificus,
Prof. dr. L.L.G. Soete,
volgens het besluit van het College van Decanen,
in het openbaar te verdedigen
op vrijdag 24 april 2015 om 12:00 uur

door

Jimmy Charles Elisabeth Odekerken
Geboren op 31 januari 1985 te Valkenburg aan de Geul

Promotor

Prof. dr. G.H.I.M Walenkamp

Copromotores

Dr. T.J.M. Welting
Dr. J.J.C. Arts

Beoordelingscommissie

Prof. dr. R.A. de Bie (Voorzitter)
Prof. dr. P.R.G. Brink
Prof. dr. P. Buma (Radboud Universiteit Nijmegen)
Prof. dr. ir. H.J. Busscher (Rijksuniversiteit Groningen)
Prof. dr. P.H.M. Savelkoul

The research presented in this thesis was conducted at the School for Public Health and Primary Care (CAPHRI), Department of Orthopaedic Surgery, of Maastricht University. CAPHRI participates in the Netherlands School of Primary Care Research (CaRe). CAPHRI was classified as "excellent" by the external evaluation committee of leading international experts that reviewed CAPHRI in December 2010.

A part of the research presented in this thesis forms part of the Project P4.01 NANTICO of the research program of the BioMedical Materials institute, co-funded by the Dutch Ministry of Economic Affairs.

"We must not forget that when radium was discovered no one knew that it would prove useful in hospitals. The work was one of pure science. And this is a proof that scientific work must not be considered from the point of view of the direct usefulness of it. It must be done for itself, for the beauty of science, and then there is always the chance that a scientific discovery may become like the radium a benefit for humanity."

Marie Curie (1867—1934), Lecture at Vassar College, New York, May 14th 1921.

Table of contents

General introduction and thesis outline

1. Orthopaedic implants and infections

In orthopaedic and trauma surgery the use of prostheses and osteosynthesis is daily practise. Currently there is a broad collection of implantable devices available for the stabilisation and fixation of bones or to maintain the movement of the body. Prostheses are available for the hip, knee, ankle, shoulder, elbow, wrist, finger and toe. Fixation devices like screws, plates and wires are mainly used in trauma surgery. Intervertebral body spacers and intramedullary nails are examples of implants for stabilisation.

Orthopaedic prostheses and fixation devices (including intramedullary nails) are mostly made of titanium, cobalt chrome or stainless steel alloys while ultra-high molecular weight polyethylene (UHMWPE) or ceramics are used for the articulating surface in order to minimize wear and friction.

The major issue with orthopaedic implants (as with many other medical implants like pacemakers, cranial defect plates, stents, dental implants) is the foreign body reaction of the host against the implant (and wear debris in case of prostheses) and the risk for bacterial infection with the accompanying biofilm formation (1-4).

In general, hip and knee and shoulder arthroplasties account for the majority of the prostheses while trauma surgery uses the majority of the fixation devices (5, 6). Currently about 0.5-1% of the total hip and 1-4% of the total knee arthroplasties eventually result in an implant infection, while the deep infection rate of osteosynthesis can range up to 30% depending the indication (5-7).

With an aging population and more patients being operated at younger age, an increase in the number of orthopaedic implants being implanted per year is to be expected (8-10). So even if the incidence of implant infections remains unchanged, the prevalence of implant infections will increase (8-10).

Prosthesis infections are mainly initiated by perioperative contamination with bacteria or via the haematogenous route during postoperative bacteraemia, resulting in prosthesis colonisation and subsequently infection (6, 11). However, an osteomyelitis can also develop due to trauma or operation without the use of an implant, the treatment regimen however remains the same (6, 12, 13).

Implant infections can be classified by onset; acute or early infection (most frequently initiated by strains of *Staphylococcus aureus* (Table 1)) if the symptoms develop in the first 3 post-operative months. Delayed infections (mainly initiated by *Staphylococcus epidermidis* strains) manifest between 3 months and 2 years after surgery while low-grade or late infections manifest after 2

years (6, 11). A less frequently used infection classification system is the classification established by the Centers of Disease Control and Prevention (CDC, USA), which is based on the condition of the tissue rather than on the time of infection onset (14). If the early infections are not treated successfully, they can result in a chronic infection which may result in loss of function of the affected joint or limb, with disability (e.g. by amputation) or in some cases even death as a consequence (15-18).

Table 1: Distribution of microorganism causing prostheses infections (6).

Microorganism	Frequency (%)
Staphylococcus aureus	33-43
Coagulase-negative *Staphylococci*	17-21
Streptococci	11-12
Gram-negative bacilli	5-14
Enterococci	3-7
Anaerobes	2-5
Polymicrobial	5-13
Unknown	5-6

The local use of antibiotic carriers in orthopaedic surgery to treat and prevent orthopaedic infections is in many clinics considered to be common practice, originating from the initial ideas of Buchholz (loading of bone cement with antibiotics, for implant fixation) and Klemm (the use of gentamicin loaded polymethyl methacrylate (PMMA) beads to treat infections locally) in the 1970's (19-23), however general consensus is lacking. Still it is a proven fact that antibiotic loaded bone cement functions as a reliable prophylactic measure for orthopaedic infections (19, 24, 25).
In general there are 2 surgical approaches for implant infection treatment, a 1-stage (1 surgical intervention; implant retraction, debridement and new prosthesis implantation) or a 2-stage revision (2 surgical interventions; implant retraction, debridement, wound closure and after a couple of weeks the implantation of a new cemented prosthesis). Both revision methods can be combined with antibiotics as a treatment/prophylaxis.

This results in mainly 4 types of actual infection treatment procedures:

- 1-stage revision; direct revision of implant with(out) conventional bone cement.
  (Clearing of infection: 58 - 59%) (26, 27)
- 1-stage revision; direct revision of implant with antibiotic loaded bone cement.
  (Clearing of infection: 82 - 86%) (26, 27)
- 2-stage revision; implant removal with debridement and eventual implant placement with (out) conventional bone cement.
  (Clearing of infection: 82 - 86%) (26, 27)
- 2-stage revision; implant removal with debridement and local antibiotics (spacers/beads) and eventual implant placement with antibiotic loaded bone cement.
  (Clearing of infection: 91 - 93%) (26, 27)

The success rates (clearing of infection) of these treatments indicate the importance of the use of local antibiotics in implant infection treatment (23, 26-28). Still the above methods mainly describe antibiotic treatment and prophylaxis in cemented prostheses, while prophylaxis and treatment with uncemented prostheses remains a challenging topic. A possible solution is the application of an antibiotic- or antiseptic-releasing coating on the implant surface. Up till now a few studies have been published, reporting on the *in vitro* (29-31) and *in vivo* (32-36) efficacy of these antibiotic- (gentamicin, vancomycin, tobramycin and rifampicin) releasing coatings, without clinical reports.
Although antibiotic treatment with surgical debridement remains the most effective treatment in the majority of the infection cases, unfortunately the number of antibiotic resistant strains as methicillin resistant *Staphylococcus aureus* (MRSA), methicillin resistant *Staphylococcus epidermidis* (MRSE) and vancomycin resistant *Staphylococcus aureus* (VRSA) is increasing and is frequently the cause for unsuccessful infection treatment (6, 13, 37). Therefore the use of an antiseptic compound instead of an antibiotic could be preferable.

2. Infection development and prevention

The tolerance of the body towards an implanted foreign material (prostheses or osteosyntheses), is expressed by the growth of host tissue around or on the surface of such a device. The principle of timely adherence of host cells or bacteria on the implant surface is known as "*the race for the surface*" (Figure 1) (3). This hypothesis postulates that when the surface of an implanted inert

biomaterial is occupied by host tissue cells (before bacterial adhesion to that same surface), the implant surface would be less susceptible for bacterial colonisation (1-4).

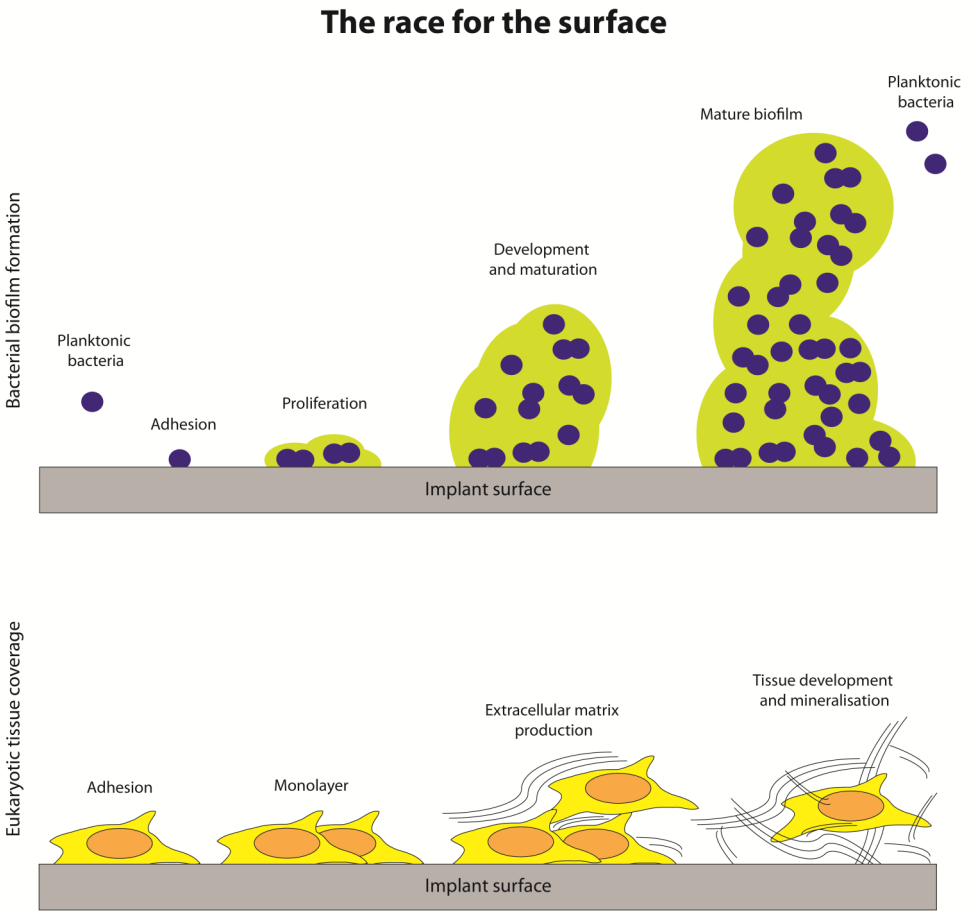

Figure 1: The general principle of "The race for the surface". **Bacteria:** Bacterial colonisation of the surface followed by encapsulation with a protecting matrix, enabling maturation towards a mature biofilm which releases bacteria (including toxins and virulence factors) from the biofilm for secondary colonisation sites. **Eukaryotic cells:** Cell adhesion on the surface followed by proliferation, differentiation with matrix-production leading to tissue development surrounding the surface.

In healthy aseptic situations, the host cells (in the case of orthopaedic implants, osteoblasts) adhere to the surface of the implant and start to proliferate and differentiate with the production

of a collagenous matrix. The calcification of this matrix (carried out by osteoblasts) will eventually result in bone apposition on the implant surface (Figure 1) (38).

However, in the case of unfortunate septic conditions, bacteria will settle on the implant surface, encapsulating themselves in a protective layer called a biofilm. In such a biofilm, bacteria are protected from the host's immune system and many antibiotics (1-4, 39). Bacteria are able to proliferate within the biofilm, colonizing the implant surface. When the biofilm becomes mature it starts to excrete toxins and other virulence factors and planktonic bacteria are being released from the biofilm to initiate new biofilm formation elsewhere in the body (Figure 1) (1, 2, 4). This indicates the importance of the prevention of biofilm formation or to disrupt the already existing biofilm on the implant surface.

The established method for infection prevention is the systemic and local use of prophylactic antibiotics to hamper bacterial growth and colonisation (6). Also disruption of the already present biofilm, by antibiotics (rifampicin), can be an effective treatment option (11, 40). Another important possible method to achieve biofilm prevention could be the modification of the implant surface to promote adherence of e.g. osteoblasts to the implant surface and subsequent bone apposition and so prevent adhesion by bacteria, and win the race for that surface.

Taken together current regimens do not offer full protection against implant infection, especially when an already infected prosthesis is being removed and should be replaced by a new prosthesis. In such cases the risk for infection remains high (12, 39). An ideal solution would be an implant coating which allows bone apposition as well as the local release of an antimicrobial compound in a high dosage to prevent bacterial colonisation at the implant location. Currently such coatings are not yet commercially available for clinical use (5).

3. Diagnostic tools

3.1 Detection of orthopaedic infections

Clinical infection diagnostics are multifactorial (Figure 2), consisting of a wide pallet of e.g. clinical, haematological, bacteriological parameters in combination with imaging modalities (11). The most general symptoms describing the general condition of the patient and the local aspect of the wound are in case of orthopaedic implant infections: redness of the peri-implant tissue, soft tissue swelling and a locally elevated tissue temperature. Haematological parameters like leucocyte

differentiation, erythrocyte sedimentation rate (ESR) and C-reactive protein (CRP) levels are systemic factors which are indicative for an infection (11).

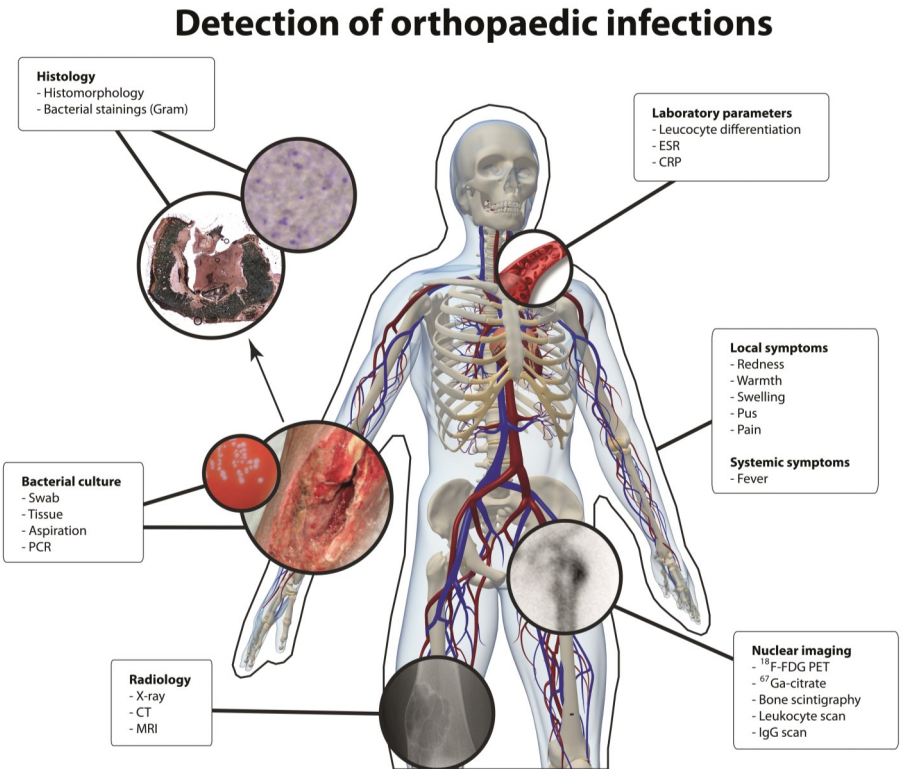

Figure 2: Clinical modalities to detect orthopaedic infections.

The leucocyte differentiation describes the percentage of lymphocytes, neutrophilic granulocytes, monocytes, basophilic granulocytes, eosinophilic granulocytes in the blood pool. In case of a bacterial infection, an increase in neutrophils (shift to the left) is typically seen. E.g. lymphocytes are more prone to react to viral infections, while neutrophilic granulocytes are more prone to react to bacterial presence and thus the percentage of neutrophillic granulocytes is expected to increase at the expense of the percentage of lymphocytes. Eosinophilic and basophilic granulocytes are mainly seen in case of allergic responses and monocytes support the neutrophilic granulocytes in a reaction against bacteria. This suggests that the differentiation of leucocytes is indicative for the diagnosis (bacterial or viral infection or allergy) (11, 41, 42).

The erythrocyte sedimentation rate is a non-specific parameter for infection, which is based on the sedimentation of erythrocytes as function of the fibrinogen content in the blood. In case of an infection the fibrinogen content in the blood increases causing agglutination of the erythrocytes which leads to an increased sedimentation rate (41, 42).

C-reactive protein is an acute phase protein which is produced in the liver as a result of the release of e.g. interleukin-6 after the infiltration of bacteria in the host-organism. CRP is also a marker for inflammation (41, 42).

Several imaging modalities can be applied to gather insight in the local morphological aspect concerning orthopaedic infection. This regards two aspects: is an infection present and where is it located. X-ray radiography and its volumetric equivalent computed tomography (CT) are frequently used in infection diagnostics and are based on absorption of radiation as a result of the density of the tissue (bone is more dense than soft tissue and is therefore capable of absorbing the radiation when passing through bone tissue). As a result X-ray and CT only describe bone morphological changes which are caused by an infection; they do not provide insight on the activity or the progression of an infection.

3.2 Nuclear imaging of infection

Nuclear imaging is being applied since the early 1970's for the detection of infections (Table 2) (43). The first (non-specific) tracer compound for this application was ^{67}Ga-citrate which binds to transferrin as an iron analogue and uses the transferrin receptors (CD71) to access the cell (43-45). ^{67}Ga also binds to lactoferrin which is highly present in infected tissue (43-45). The binding to transferrin results in a low specificity and a high background signal, furthermore ^{67}Ga emits high-energy γ-radiation and has a relatively long half-life of 3.26 days (43-45).

The labelling of diphosphonates with technetium results in a tracer which allows imaging in 3 phases: the perfusion phase (local hyper perfusion), the circulation phase (local hyperaemia) and the bone imaging phase (local bone remodelling) (43-45). Although the sensitivity is high, the specificity of the 3-phase bone scan is mainly depending on bone remodelling, not limited to osteomyelitis mediated remodelling but also bone apposition on an implant surface or physiological bone remodelling (43-45).

Another approach is the visualisation of leucocytes (directly or indirect), since they are involved in the host immune response towards an infection and are expected to be present in elevated levels

at the infection site, resulting in elevated tracer levels. In general these methods are sensitive and relatively specific. However the direct labelling of leucocytes requires isolation of the patient's leucocytes which are subsequently labelled in the laboratory and then injected back in the patient before the initial imaging can be performed, making it a laborious and expensive approach (43-45). Instead of using patient material, it is possible to label leucocyte antibodies. Unfortunately the antibodies diffuse slowly into the infected area (making it less sensitive than the directly labelled leucocytes) and there is a slow systemic clearance of the labelled antibodies (43-45).

All the above mentioned tracers are used in scintigraphy or SPECT (Single photon emission computed tomography) imaging, which is based on the detection of single emitted photons, making exact localisation of the source of emission more difficult compared to positron emission tomography (PET), which detects 2 photons emitted in opposite directions (43-45).

Table 2: Nuclear imaging approaches for infection detection (43-47).

Imaging modality	Technique	Measures	Sensitivity	Specificity
^{67}Ga-citrate	Scintigraphy/ SPECT	Blood flow Transferrin/lactoferrin	+	±
3-phase bone scan (^{99m}Tc)	Scintigraphy/ SPECT	Focal hyper perfusion Focal hyperaemia Focal bone uptake	++	-
Labelled IgG (^{99m}Tc & ^{111}In)	Scintigraphy/ SPECT	Leucocyte localisation	+	±
Labelled leucocytes (^{99m}Tc & ^{111}In)	Scintigraphy/ SPECT	Leucocyte localisation	++	±
^{68}Ga	PET	Blood flow	+	±
^{18}F-FDG	PET	Metabolic glucose uptake	++	±

PET is a nuclear imaging modality used for the detection of implant infections. PET is an upcoming imaging modality in the clinic since its initial development in the mid 1970's (48, 49). The working mechanism is based on the annihilation of a proton (originating from the tracer) with an electron (originating from the organism) resulting in the formation of 2 photons (511 keV) travelling in the

opposite direction of each other. These 2 photons are then detected in coincidence by 2 scintillation detectors which allow calculation of the origin of the annihilation (48-50). This is called a true coincidence event (Figure 3A). As in all detection methods, PET can have a considerable amount of background noise. This is caused by scatter and random coincidence events. Scatter coincidence events are events from 1 annihilation event detected by the scintillation detectors, only in this case one or both of the photons are being redirected by a high density object (e.g. a metallic implant), resulting in a miscalculation of the origin of the annihilation (Figure 3B). A random coincidence event (also called single events) is an event from 1 annihilation event detected by the scintillation detector, in this case as a result of the direction of the travelling photons only 1 photon is detected by the scintillation detector (Figure 3C) (50).

Image reconstruction can be performed in various ways, the most common are the filtered back projection and 2-dimensional ordered-subsets expectation maximisation (OSEM-2D). The filtered back projection method is based on the assumption that a locally concentrated amount of image tracer results in photon emission in all directions without preference, because they happen in a random fashion. This means that the coincidence pairs (photons) that enter the detector ring can be calculated back into the imaging field to the proposed point of origin, resulting in a calculated image of the object. Still the filtered back-projection method is negatively influenced by noise in the imaging dataset (50). The OSEM-2D algorithm is less influenced by noise since it includes anatomical data into the equation gathered by an attenuation scan. The attenuation scan gathers information on the object in the scanner gantry by the use of a point source (e.g. ^{57}Co) rotating in the gantry around the object of interest. The hereby gathered information on e.g. scattering, allows noise reduction in the initial image reconstruction, resulting in a higher imaging quality (less noise) (50).

A widely used method for the quantification of the imaging data is the calculation of the standardized uptake value (SUV), which is calculated from the formula below (50).

$$SUV = \frac{\text{Detected activity in the tissue by the PET scanner (Bq/g)}}{\text{Injected systemic activity (Bq) / Body weight (g)}}$$

The SUV provides in a quantifiable value for local PET tracer uptake in static detection conditions.

There are various tracers available for clinical applications concerning PET-imaging. One of those tracers is ^{68}Ga, of which the physiological principle is comparable to that of ^{67}Ga (47).

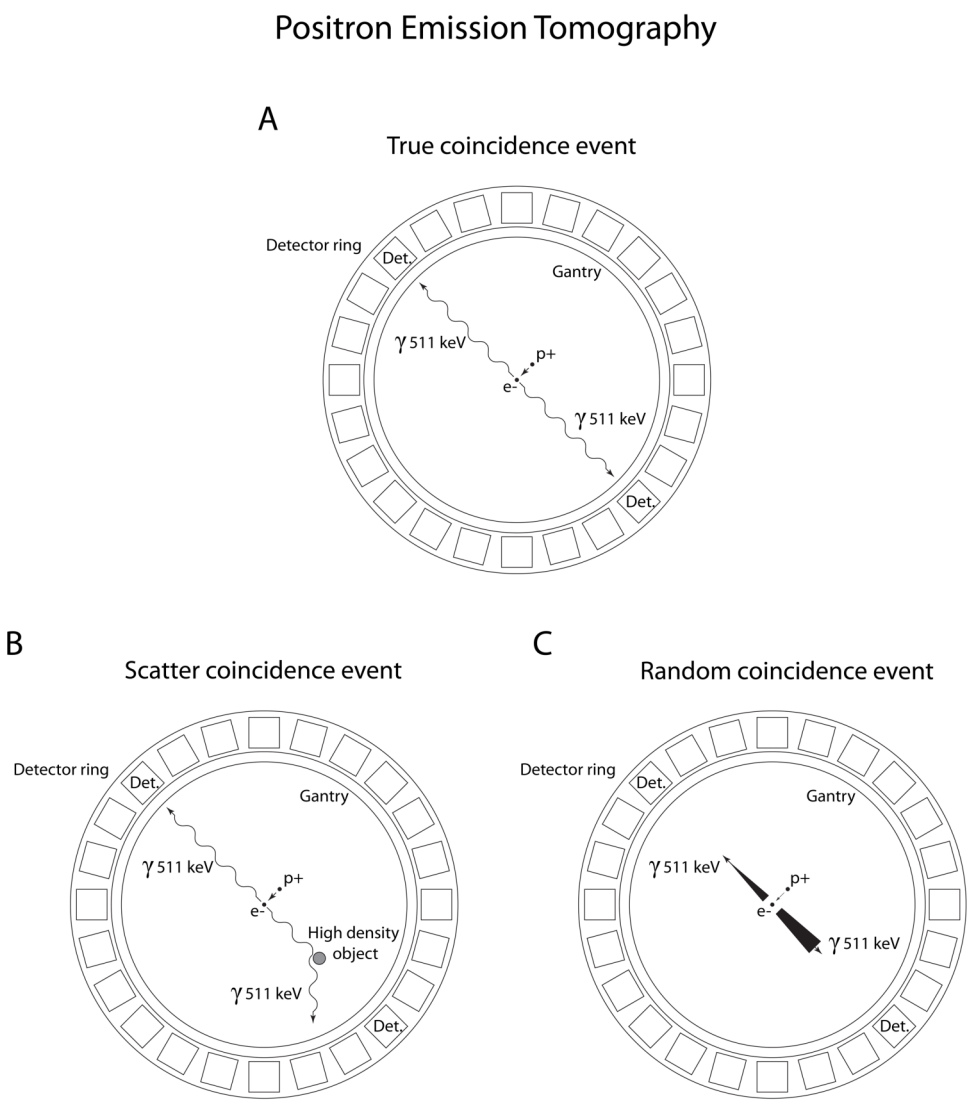

Figure 3: The principle of PET detection and the generation of noise. **A:** True coincidence is the detection of the 2 photons of a single annihilation event in coincidence on 2 opposite detectors (Det.) in the detector ring. **B:** Scatter is induced by the presence of a high density object which redirects 1 of the 2 photons from a single annihilation event, resulting in the detection of a neighbouring detector in the detector ring. In general this results in the miscalculation of the point of origin. **C:** A random coincidence event is when only 1 of the 2 photons of a single annihilation event is detected by the detector ring while the other is travelling outside of the detector ring.

The most common PET tracer however is ^{18}fluor-fluorodeoxyglucose (^{18}F-FDG), a radioactively labelled glucose-derivative (50-52). This tracer originates from the field of oncology mainly due to the high glucose uptake of tumour tissue, which allows highly specific imaging of malignant cells (50-52). Since acute implant infections are considered highly metabolically active, ^{18}F-FDG is proposed as an infection tracer. Currently clinical application of this tracer for the detection of orthopaedic implant infection is limited (11, 53).

3.3 Detection of antibiotics

In prevention and treatment of orthopaedic infections, antibiotics are used systemically or locally. Local delivery of antibiotics can be achieved by implantation of antibiotic-containing PMMA, which releases its antibiotic in a high concentration during the first days (23). To study the efficacy of local antibiotic therapy it is necessary to determine the antibiotic concentration in exudate and tissues. This often requires complex systems and protocols (like high performance liquid chromatography (HPLC)) which can be heavily influenced by protein presence in the samples (54, 55). Antibiotics being released by coatings or biomaterials have been determined in the past by the semi-quantitative evaluation of growth inhibition zones on agar plates in correspondence with known stock solutions (29, 56). The use of fluorescence- or spectrophotometric-based detection methods resulted in improved detection limits, which were further improved by the introduction of HPLC based protocols (30, 31, 55, 57-59). However both methods were highly influenced by high protein concentrations within the measured samples, which are unavoidably present in clinical samples.

Enzyme-linked immunosorbent assay (ELISA)-based methods have been established to detect gentamicin in dairy products like milk (60) or in sera (61, 62). However these methods were not directly applicable to the human situation or suitable for the assessment of releasing biomaterials or coatings, neither did they allow modification to detect other antibiotics like vancomycin.

4. Experimental models for orthopaedic infections

Osteomyelitis is one of the most severe complications in orthopaedic and trauma surgery. The disease itself is probably as old as the existence of vertebrates, since its occurrence has been demonstrated in dinosaurs and Neanderthals (63-65). Furthermore symptoms and disease

treatment have been described through ancient literature (Egyptian, Greek, Roman and Mayan) and late renaissance literature (Paracelsus, Paré and Scultetus) (64, 66, 67). One of the first reports on osteomyelitis in "modern era" literature, described it as a complication after gunshot wounds in the American civil war, describing the morphological changes of the diseased bone (68). However the bacterial cause of osteomyelitis (a micrococcus, later described as *Staphylococcus aureus*) was found in 1883 by Becker (group of Koch) (69). They were also the first to culture *S. aureus* and to use it in an experimental osteomyelitis in which they inoculated animals with bone fractures with the cultured bacterium, resulting in pus formation and animal death within 14 days (69).

The first actually published report dedicated on an experimental haematogenic osteomyelitis was conducted by Rodet, who in 1884 reported that the intravenous injection of a micrococcus (presumably *S. aureus*) in rabbits resulted in development of osteomyelitis. He described periosteal lifting, loss of cortical integrity and the presence of sequesters in the affected bone tissue (70). Dedicated models to study osteomyelitis were established in the early 1970's by Norden (71, 72), Bowers (73) and Andriole (74, 75). The model of Norden focused on the development of osteomyelitis by the intramedullary administration of *S. aureus* in rabbit tibiae and was followed-up by evaluating blood and bone cultures, the differences in erythrocyte sedimentation rate and whole white blood cell count, X-ray and histology (71, 72). The model of Bowers focused on antibiotic prophylaxis for osteomyelitis in a dog model, in this model the osteomyelitis was initiated by an intramedullary per-operative contamination with *S. aureus* of the femur and assessed by bacterial cultures of the affected tissue and blood (73). The model described by Andriole was the first to include an intramedullary nail to study implant-related infections. The main procedure was the perioperative contamination of the intramedullary cavity of the tibia of a rabbit in the presence or absence of an intramedullary nail, with or without a fracture (the implantation of a foreign object initiates the host's immune response). The infection was assessed by bacterial culture, X-rays and histology (74, 75).

To facilitate the initiation of osteomyelitic development many studies included the use of a sclerosing agent like sodium morrhuate to locally initiate vascular thrombosis (less angiogenesis), resulting in local aseptic necrosis of the bone and a decreased transport of nutrients and host immune cells, making the bone more susceptible to an infection (71, 74, 76-78). However the necessity of a sclerosing agent is debatable since many studies did not require a sclerosing agent to obtain a reproducible osteomyelitic lesion (34, 73, 79-87). Still it appears that the use of a

sclerosing agent speeds up the development of an osteomyelitic lesion by the forced absence of a local host immune response (71, 74, 76-78).

Post-mortem bacterial culture is currently the golden standard for infection diagnosis in these experimental models. Since bacterial culture allows false negative cultures, the diagnostic pallet is often supplemented with the accompanying radiological and histological findings to increase the accuracy of these models (11). Furthermore, the use of sequential time points during follow-up, instead of only endpoint measurements, could monitor disease progression during the experimental follow-up (88, 89). Besides, such a sequential follow-up would also allow detailed monitoring of infection prophylaxis and treatment efficacy (88, 89).

An overview of the different models studying osteomyelitis and its treatment modalities is presented in table 3. Overall these models describe the induction of osteomyelitis by perioperative bacterial contamination of the surgical site or by bacteraemia caused by i.v. injection. The *radius*, *ulna*, *humerus*, *tibia* and *femur* have been used in mice, rats, guinea pigs, chinchilla's, rabbits, chickens, dogs, sheep or goats.

It is to be expected that sequential and precise measurements of a broad spectrum of parameters can provide detailed information about the progression of an infection and the efficacy of its treatment, and even could deliver unexpected findings. The use of sequential measurements of such multiple parameter follow-up may reduce the amount of animals necessary to achieve statistically relevant data, since the sacrifice of animals at multiple time points is avoided. E.g. the use of several calcium binding fluorophores enables the histological detection of bone apposition on multiple time points during the experimental follow-up in each animal. This could also be achieved by the sequential use of radiological (X-ray) or nuclear imaging techniques (^{18}F-FDG microPET), were X-ray radiographs indicate bone morphological changes and ^{18}F-FDG microPET would detect metabolic activity in the implant area, monitoring disease progression during the experimental follow-up. So this approach enhances the power of the study and reduces the amount of subjects needed to achieve statistically relevant data.

Table 3: Overview of experimental osteomyelitis models and their experimental parameters

Author, year	Experimental animal	Sclerosing agent	Implant material	Antimicrobial compound	Bacterial contaminant	Inoculation route	Clinical parmeters (weight, temp.)	Haematology (ESR, CRP, leucoc.)	Radiology (X-ray (x), CT (c), MRI (m))	Nuclear imaging (Scint. (s), PET (p))	Bioluminescence	*Post-mortem* culture	Calcium binding fluorophores	Histology	Reference
Becker, 1883	rabbit	no	-	-	*S. aureus*	i.v.						x			(69, 90)
Rodet, 1884	rabbit	no	-	-	*S. aureus*	i.v.						x			(70, 91)
Lexer, 1894	rabbit, dog	no	-	-	*S. aureus* *S. pyogenes*	i.v.						x		x	(92)
Lexer, 1896	rabbit	no	-	-	*S. aureus* *S. pyogenes*	i.v.			x			x		x	(93)
Scheman, 1941	rabbit	yes	-	-	*S. aureus*	i.v. local						x		x	(94)
Norden, 1970	rabbit	yes	-	-	*S. aureus*	local	x	x	x			x			(71)
Andriole, 1973	rabbit	no	Stainless steel	-	*S. aureus*	local			x			x		x	(74)
Bowers, 1973	dog	no	-	Cephaloridine	*S. aureus*	local	x					x			(73)
Andriole, 1974	rabbit	no	Stainless steel	-	*S. aureus*	local			x			x			(75)
Elson, 1977	rat	no	PMMA	Fucidin, Gentamicin	*S. aureus* *P. aeruginosa* *P. mirabilis* *S. canis*	local						x			(95)
Norden, 1980	rabbit	yes	-	Sisomicin, Carbenicillin	*P. aeruginosa*	local	x		x			x			(77)
Blomgren, 1980	rabbit	no	PMMA	-	*S. aureus*	i.v.						x			(79)
Blomgren, 1980	rabbit	no	TKA, PMMA	-	*S. aureus*	i.v.			x			x		x	(80)
Blomgren, 1981	rabbit	no	TKA, PMMA	Gentamicin	*S. aureus*	i.v.						x			(96)
Blomgren, 1981	rabbit	no	TKA	-	*P. acnes*	i.v.			x	s		x		x	(81)
Zimmerli, 1982	guinea pig	no	PMMA, PTFE	-	*S. aureus*	local		x				x			(97)
Fitzgerald, 1983	dog	no	PMMA	Gentamicin	*S. aureus*	local			x			x		x	(98)
Norden, 1983	rabbit	yes	-	Vancomycin, Rifampin	*S. aureus*	local			x			x			(99)

Author, year	Experimental animal	Sclerosing agent	Implant material	Antimicrobial compound	Bacterial contaminant	Inoculation route	Clinical parmeters (weight, temp.)	Haematology (ESR, CRP, Leucoc.)	Radiology (X-ray (x), CT (c), MRI (m))	Nuclear imaging (Scint. (s), PET (p))	Bioluminescence	*Post-mortem* culture	Calcium binding fluorophores	Histology	Reference
Emslie, 1983	chicken	no	-	-	*S. aureus*	i.v.	x					x		x	(100)
Rodeheaver, 1983	rabbit	no	PMMA	Erythromycin, Colistin	*S. aureus, E. coli*	local			x			x		x	(101)
Norden, 1983	rabbit	yes	-	Rifampin, Sisomicin, Cephalothin, Trimethoprim	*S. aureus*	local						x			(102)
Norden, 1985	rabbit	yes	-	Ciprofloxacin	*P. aeruginosa*	local			x			x			(103)
Petty, 1985	dog	no	Stainless steel, Cobalt chrome, HD-PE, PMMA	-	*S. aureus, S. epidermidis, E. coli*	local						x		x	(84)
Southwood, 1985	rabbit	no	pHA (fem. comp.), PMMA	-	*S. aureus*	i.v.	x					x			(86)
Petty, 1988	dog	no	PMMA	Gentamicin	*S. aureus, S. epidermidis, E. coli*	local						x			(104)
Worlock, 1988	rabbit	no	Stainless steel	-	*S. aureus*	local			x			x		x	(105)
Nelson, 1990	rat	no	Bone wax	-	*S. aureus*	local						x		x	(106)
Power, 1990	rat	yes	-	-	*S. aureus*	local						x		x	(78)
Jacob, 1991	rabbit	yes	PL:PG	Ampicillin	*S. aureus*	local			x			x			(107)
Gerhart, 1993	rat	no	TCP, PMMA	-	*S. aureus*	local			x			x			(108)
Laurencin, 1993	rat		PolyA, PMMA	Gentamicin	*S. aureus*	local						x		x	(109)
Melcher,1994	rabbit & chinchilla	no	Stainless steel	-	*S. aureus*	local			x			x			(110)
Garvin, 1994	dog	no	PMMA, PL:PG	Gentamicin	*S. aureus*	local						x		x	(111)
Sanzén, 1995	rabbit	no	Titanium, PMMA	-	*S. aureus, S. epidermidis*	local	x		x			x		x	(112)

Author, year	Experimental animal	Sclerosing agent	Implant material	Antimicrobial compound	Bacterial contaminant	Inoculation route	Clinical parmeters (weight, temp.)	Haematology (ESR, CRP, Leucoc.)	Radiology (X-ray (x), CT (c), MRI (m))	Nuclear imaging (Scint. (s), PET (p))	Bioluminescence	*Post-mortem* culture	Calcium binding fluorophores	Histology	Reference
Fialkov, 1996	rabbit	no	Bone graft	-	*S. aureus*	local						x	x	x	(113)
Nelson, 1997	rabbit	no	PolyA	Gentamicin	*S. aureus*	local			x			x		x	(114)
An, 1997	rabbit	no	Titanium-BSA	-	*S. epidermidis*	local			x			x		x	(115)
Calhoun, 1997	rabbit	no	PLA-PL:CG	Vancomycin	*S. aureus*	local			x			x			(82)
Smeltzer, 1997	rabbit	no	Bone graft	-	*S. aureus*	local			x			x		x	(85)
Kaarsemakers, 1997	sheep	yes	Gelatin sponge	-	*S. aureus*	local	x	x	x			x		x	(76)
Awasthi, 1998	rabbit	yes	-	-	*S. aureus*	local			x	s		x		x	(116)
Nie, 1998	rabbit	no	PL:PG	Ofloxacin	*P. aeruginosa*	local			x			x		x	(117)
Vogely, 2000	rabbit	no	Titanium-HA	-	*S. aureus*	local			x			x		x	(87)
Nijhof, 2000	rabbit	no	PMMA	Tobramycin, Cefazolin	*S. aureus*	local	x	x	x			x		x	(83)
Gürsel, 2001	rabbit	no	PHA	Sulbactam, Cefoperazone, Ampicillin	*S. aureus*	local			x			x			(118)
Lucke, 2002	rat	no	Stainless steel	-	*S. aureus*	local	x	x	x			x		x	(119)
Mader, 2002	rabbit	no	PMMA, Fibrin	Tobramycin	*S. aureus*	local	x		x			x		x	(120)
Shirtliff, 2002	rabbit	yes	PMMA, HA	Vancomycin	MRSA	local			x			x			(121)
Rutledge, 2003	rabbit	yes	PCL	Tobramycin	S. aureus	local						x		x	(122)
Huneault, 2004	dog	no	CLHAS	Ciprofloxacin	*S. aureus*	local			x			x		x	(123)
Ambrose, 2004	rabbit	no	PLGA, PMMA	Tobramycin, Cefazolin	*S. aureus*	local			x			x		x	(124)
Koort, 2004	rabbit	no	PMMA	-	*S. aureus*	local			x, c	p		x		x	(125)
Koort, 2005	rabbit	no	PLA	Ciprofloxacin	*S. aureus*	local			c	p		x		x	(126)
Craig, 2005	rabbit	no	Stainless steel, PMMA, UHMWPE	-	MRSA	local						x			(127)
Mendel, 2005	rat	yes	Collagen sponge, PMMA	Cefazolin, Gentamicin	*S. aureus*	local			x			x		x	(128)

Author, year	Experimental animal	Sclerosing agent	Implant material	Antimicrobial compound	Bacterial contaminant	Inoculation route	Clinical parmeters (weight, temp.)	Haematology (ESR, CRP, Leucoc.)	Radiology (X-ray (x), CT (c), MRI (m))	Nuclear imaging (Scint. (s), PET (p))	Bioluminescence	*Post-mortem* culture	Calcium binding fluorophores	Histology	Reference
Fukushima, 2005	rat	no	-	-	*S. aureus*	local	x		x			x		x	(129)
Jones-Jackson, 2005	rabbit	no	-	-	*S. aureus*	local			x	p		x		x	(130)
Mäkinen, 2005	rat	yes	-	-	*S. aureus*	local			x, c	p		x		x	(47)
Mäkinen, 2005	rabbit	no	PLGA,	Ciprofloxacin	*S. aureus*	local			x	p		x		x	(131)
Beardmore, 2005	goat	no	PMMA, Calcium sulphate, Demineral. bone	Tobramycin	*S. aureus*	local						x			(132)
Joosten, 2005	rabbit	yes	HAC,	Vancomycin	*S. aureus, MRSA*	local	x	x				x		x	(133)
Salgado, 2005	goat	yes	-	-	*S. aureus*	local	x		x			x		x	(134)
Alt, 2006	rabbit	no	Stainless steel	-	*S. aureus*	local						x		x	(33)
Kälicke, 2006	rabbit	no	Titanium-PLLA	Rifampin, Fusidic acid, Octenidin, Irgasan	*S. aureus*	local						x		x	(36)
Darouiche, 2007	rabbit	no	Titanium-Ab	Minocycline, Rifampin	*S. aureus*	local						x			(135)
Poultsides, 2008	rabbit	no	Tantalum	-	MRSA	i.v.	x	x	x			x		x	(136)
Williams, 2008	rabbit	no	Titanium, Tantalum	-	*S. aureus*	local						x			(137)
Laure, 2008	sheep	no	Stainless steel-HA, Stainless steel, PMMA	-	*S. epidermidis*	local			x			x		x	(138)
Kanellakopoulou, 2008	rabbit	no	PLA,	Ciprofloxacin	*P. aeruginosa*	local						x		x	(139)
Hamel, 2008	rabbit	no	Stainless steel	-	MRSA	local			x			x			(140)
Moojen, 2009	rabbit	no	Titanium-PA,	Tobramycin	*S. aureus*	local	x	x				x		x	(34)
Moojen, 2009	rabbit	no	PMMA, Silver	-	*S. aureus*	local	x	x				x		x	(141)
Bernthal, 2010	mouse	no	Stainless steel	-	*S. aureus*	local					x	x		x	(142)

Author, year	Experimental animal	Sclerosing agent	Implant material	Antimicrobial compound	Bacterial contaminant	Inoculation route	Clinical parmeters (weight, temp.)	Haematology (ESR, CRP, Leucoc.)	Radiology (X-ray (x), CT (c), MRI (m))	Nuclear imaging (Scint. (s), PET (p))	Bioluminescence	*Post-mortem* culture	Calcium binding fluorophores	Histology	Reference
Moskowitz, 2010	rabbit	no	PMMA, Titanium-Ab	Gentamicin	*S. aureus*	local						x			(35)
Jacqueline, 2010	rabbit	no	-	Ceftaroline	MRSA	local						x		x	(143)
Stewart, 2010	rat	no	Stainless steel, PPF	-	*S. aureus* *E. coli*	local			x			x		x	(144)
Robinson, 2011	rat	no	Stainless steel	-	*S. aureus*	local			x			x		x	(145)
Vergidis, 2011	rat	no	Titanium	Linezolid, Vancomycin, Rifampin	MRSA	local						x			(146)
Gaudin, 2011	rabbit	no	-	-	MRSA	local						x		x	(147)
Alt, 2011	rat	no	Stainless steel	-	S. aureus	local			x, c			x		x	(148)
Poeppl, 2011	rat	no	-	Fosfomycin	MRSA	local			x			x		x	(149)
Lankinen, 2012	rabbit	Yes	PMMA	-	*S. aureus*, *S. epidermidis*	local			x, c	p		x		x	(89)
Pribaz, 2012	mouse	no	Stainless steel	-	*S. aureus*	local					x	x			(150)
Niska, 2012	mouse	no	Stainless steel, Titanium	Daptomycin, Tigecycline, Vancomycin	*S. aureus*, MRSA	local					x	x			(151)
Horst, 2012	mouse	no	-		*S. aureus*	i.v.	x	x	x, m			x		x	(152)
Li, 2012	rabbit	yes	-	L-PRP	MRSA	local			c			x		x	(153)
Johansen, 2013	pig	no	-	-	*S. aureus*	i.v.			x			x			(154)
Yin, 2013	rabbit	yes	-	-	MRSA, *K. pneumoniae*, *P. aeruginosa*, *A. baumannii*	local			x			x			(155)
Xing, 2013	rabbit	no	Alginate beads	Vancomycin	*S. aureus*	local			x, c			x		x	(156)
Xie, 2013	rabbit	yes	Bioactive glass	Gentamicin	*E. coli*	local			x			x		x	(157)
Søe, 2013	rat	no	Stainless steel, HD-PE	-	*S. aureus*	local	x	x	x			x		x	(158)
Tran, 2013	goat	no	Stainless steel	Silver	*S. aureus*	local		x	x, c			x		x	(159)
Odekerken, 2013-2014	rabbit	no	Titanium	-	*S. aureus*	local	x	x	x, c	p		x	x	x	(160, 161)

Author, year	Experimental animal	Sclerosing agent	Implant material	Antimicrobial compound	Bacterial contaminant	Inoculation route	Clinical parmeters (weight, temp.)	Haematology (ESR, CRP, Leucoc.)	Radiology (X-ray (x), CT (c), MRI (m))	Nuclear imaging (Scint. (s), PET (p))	Bioluminescence	*Post-mortem* culture	Calcium binding fluorophores	Histology	Reference
Helbig, 2014	rabbit	no	Titanium	Vancomycin	MRSA	local	x	x				x		x	(162)
Crémieux, 2014	rabbit	yes	-	-	MRSA	local		x				x		x	(163)
Varrone, 2014	mouse	no	Stainless steel	Gmd-1C11	MRSA	local			c		x	x		x	(164)
McLaren, 2014	sheep	no	PLGA-PEG	Gentamicin, Clindamycin	*S. aureus*	local			c			x		x	(165)
Inanmaz, 2014	rat	no	Stainless steel	Teicoplanin	*S. aureus*	local			x			x			(166)
Gahukamble, 2014	rabbit	no	Stainless steel	-	*P. acnes* *S. lugdunensis*	local		x	x			x		x	(167)
Zhu, 2014	mouse	no	-	Anisomycin	MRSA	local	x	x				x		x	(168)
Freiberg, 2014	rabbit	yes	Dextran		*S. pyogenes*	local						x		x	(169)
Chen, 2014	dog	no	Gelatin, Titanium	Cefazolin, Gentamicin	*S. aureus*	local			m			x			(170)
Ding, 2014	rabbit	yes	Bioactive glass, Calcium sulphate	Vancomycin	MRSA	local			x			x		x	(171)
Cui, 2014	rabbit	yes	Bioactive glass, Calcium sulphate	Vancomycin	MRSA	local			x			x		x	(172)
Odekerken, 2014	rabbit	no	-	-	*S. aureus*	local	x	x	x, c	p		x	x	x	(173)
Shishatskaya, 2014	chinchilla, rabbit	no	P3HB, P3HB/HA, Xenograft	-	*S. aureus*	local			x			x		x	(174)
Poeppl, 2014	rat	no	Titanium	Fosfomycin, Vancomycin	MRSA	local						x		x	(175)
Gatin, 2014	rabbit	no	Silicon	Ceftaroline-Fosamil, Vancomycin, Rifampin	MRSA	local						x			(176)
Odekerken	rabbit	no	Titanium	Chlorhexidine	*S. aureus*	local	x	x	x, c	p		x	x	x	Prep

Table 3 legend

Abbreviations "Implant material" and "Antimicrobial compound":

-Ab: coated with antibiotic, **-BSA:** coated with bovine serum albumin, **-HA:** coated with hydroxyapatite, **-PA:** coated with peri-apatite, **-PLLA:** coated with poly-L-lactide, **CLHAS:** cross-linked high amylose starch, **Gmd-1C11:** anti-glucosamidase monoclonal antibody, **HA(C):** hydroxyapatite (cement), **HD-PE:** high density polyethylene, **L-PRP:** leucocyte- and platelet-rich plasma, **P3HB:** poly-3-hydroxybutyrate, **P3HB/HA:** poly-3-hydroxybutyrate/hydroxyapatite, **PCL:** polycarprolactone, **pHA:** partial hip arthroplasty, **PHA:** polyhydroxyalkanoate, **PLA:** polylactic acid, **PLA-PL:CG:** polylactic acid-polylactide/polyglycolide, **PL:PG:** polylactide/polyglycolide, **PLGA:** polylactic-co-glycolic acid, **PLGA-PEG:** polylactic-co-glycolic acid – polyethylene glycol, **PMMA:** polymethyl methacrylate, **PolyA:** polyanhydride, **PPF:** polypropylene fumarate, **PTFE:** polytetrafluoroethylene, **TCP:** tricalcium phosphate, **TKA:** Total knee arthroplasty, **UHMWPE:** ultra-high molecular weight polyethylene.

Abbreviations "Bacterial contaminant":

E. coli: *Escherichia coli,* ***MRSA:*** Methicillin resistant *Staphylococcus aureus,* ***P. acnes:*** *Propionibacterium acnes,* ***P. aeruginosa:*** *Pseudomonas aeruginosa,* ***P. mirabilis:*** *Proteus mirabilis,* ***S. aureus:*** *Staphylococcus aureus,* ***S. canis:*** *Streptococcus canis,* ***S. epidermidis:*** *Staphylococcus epidermidis.*

General abbreviations:

CRP: C-reactive protein, **CT:** computed tomography, **ESR:** erythrocyte sedimentation rate, **i.v.:** intravenous, **leucoc.:** leucocyte count/differentiation, **PET:** positron emission tomography, **scint.:** scintigraphy, **temp.:** temperature.

5. Aims and outline of this thesis

Due to the current incidence of implant infections and the increasing number of orthopaedic and trauma implants being placed, there is a need for a prophylactic coating for metal-based implants within the field of orthopaedic and trauma surgery. Although such coatings will be specifically designed for orthopaedic and trauma (prostheses and osteosynthesis), they could also contribute as a prophylactic measure for other implants like pacemakers, skull defect plates, stents and dental implants.

In prostheses such a prophylactic coating must allow bone apposition on the coating surface to promote subsequent firm fixation to bone.

When established, a novel prophylactic coating requires thorough evaluation requiring determination of the prophylactic efficacy *in vitro* and *in vivo*.

A prophylactic coating requires a tool which allows the determination of the concentration of the released antibiotic compound to assess if clinically effective dosages can be achieved. Immunological detection of antibiotics by ELISA may provide a solution to this problem since this method allows highly specific detection of antibiotics by specific antibodies (Chapter 3). An animal infection model has to be available which allows the establishment of an implant infection and the sequential monitoring of relevant infection parameters during the experimental follow-up to assess infection progression and to correlate disease parameters with clinical outcome to allow differentiation in future coating efficacy (Chapter 4). Furthermore the potential of imaging modalities, like ^{18}F-FDG PET, should be explored to monitor infection progression since imaging tools are frequently used in (pre-)clinical diagnostics were they allow specific imaging of the affected tissues (Chapter 5 and 6). Combined, the above approaches will be able to assess the *in vivo* efficacy of a novel implant coating for infection prophylaxis (Chapter 7).

Four main research goals were formulated:

1 Establish an ELISA-based assay to determine gentamicin and vancomycin concentrations in protein rich samples to allow future evaluation of novel antibiotic release systems *in vitro* and *in vivo*.

2 Establish a reproducible orthopaedic infection model in rabbits for the evaluation of novel antimicrobial orthopaedic implant coatings and bone replacement materials.

3 Assess the potential of ^{18}F-FDG PET as an infection specific imaging tool for the detection of orthopaedic infections and investigate if ^{18}F-FDG PET allows assessment of disease progression and treatment efficacy.

4 Evaluate a novel drug-releasing implant coating on its antimicrobial efficacy and assess bone remodelling in the area surrounding the coated implant.

References

1. Arciola CR, Campoccia D, Speziale P, Montanaro L, Costerton JW. Biofilm formation in staphylococcus implant infections. A review of molecular mechanisms and implications for biofilm-resistant materials. Biomaterials. 2012 Sep;33(26):5967-82.
2. Busscher HJ, van der Mei HC, Subbiahdoss G, Jutte PC, van den Dungen JJ, Zaat SA, Schultz MJ, Grainger DW. Biomaterial-associated infection: Locating the finish line in the race for the surface. Science Translational Medicine. 2012 Sep 26;4(153):153rv10.
3. Gristina AG. Biomaterial-centered infection: Microbial adhesion versus tissue integration. Science. 1987 Sep 25;237(4822):1588-95.
4. Hoiby N, Ciofu O, Johansen HK, Song ZJ, Moser C, Jensen PO, Molin S, Givskov M, Tolker-Nielsen T, Bjarnsholt T. The clinical impact of bacterial biofilms. Int J Oral Sci. 2011 Apr;3(2):55-65.
5. Montanaro L, Speziale P, Campoccia D, Ravaioli S, Cangini I, Pietrocola G, Giannini S, Arciola CR. Scenery of staphylococcus implant infections in orthopedics. Future Microbiology. 2011 Nov;6 (11):1329-49.
6. Trampuz A, Zimmerli W. Antimicrobial agents in orthopaedic surgery: Prophylaxis and treatment. Drugs. 2006;66(8):1089-105.
7. Adeli B, Parvizi J. Strategies for the prevention of periprosthetic joint infection. Journal of Bone and Joint Surgery (British Volume). 2012 Nov;94(11 Suppl A):42-6.
8. Acklin YP, Widmer AF, Renner RM, Frei R, Gross T. Unexpectedly increased rate of surgical site infections following implant surgery for hip fractures: Problem solution with the bundle approach. Injury. 2011 Feb;42(2):209-16.
9. Dale H, Hallan G, Espehaug B, Havelin LI, Engesaeter LB. Increasing risk of revision due to deep infection after hip arthroplasty. Acta Orthopaedica. 2009 Dec;80(6):639-45.
10. Kurtz SM, Lau E, Ong KL, Carreon L, Watson H, Albert T, Glassman S. Infection risk for primary and revision instrumented lumbar spine fusion in the medicare population. Journal of Neurosurgery: Spine. 2012 Oct;17(4):342-7.
11. Zimmerli W. Infection and musculoskeletal conditions: Prosthetic-joint-associated infections. Best Practice & Research: Clinical Rheumatology. 2006 Dec;20(6):1045-63.
12. Geurts J, Chris Arts JJ, Walenkamp GH. Bone graft substitutes in active or suspected infection. Contra-indicated or not? Injury. 2011 Sep;42 Suppl 2:S82-6.
13. Trampuz A, Zimmerli W. Diagnosis and treatment of infections associated with fracture-fixation devices. Injury. 2006 May;37 Suppl 2:S59-66.
14. Horan TC, Andrus M, Dudeck MA. Cdc/nhsn surveillance definition of health care-associated infection and criteria for specific types of infections in the acute care setting. American Journal of Infection Control. 2008 Jun;36(5):309-32.
15. Sanders J, Mauffrey C. Long bone osteomyelitis in adults: Fundamental concepts and current techniques. Orthopedics. 2013 May;36(5):368-75.
16. Darouiche RO. Treatment of infections associated with surgical implants. New England Journal of Medicine. 2004 Apr 1;350(14):1422-9.
17. Waldvogel FA, Medoff G, Swartz MN. Osteomyelitis: A review of clinical features, therapeutic considerations and unusual aspects. New England Journal of Medicine. 1970 Jan 22;282(4):198-206.
18. Noskin GA, Rubin RJ, Schentag JJ, Kluytmans J, Hedblom EC, Jacobson C, Smulders M, Gemmen E, Bharmal M. National trends in staphylococcus aureus infection rates: Impact on economic burden and mortality over a 6-year period (1998-2003). Clinical Infectious Diseases. 2007 Nov 1;45(9):1132-40.
19. Buchholz HW, Engelbrecht H. (depot effects of various antibiotics mixed with palacos resins). Chirurg. 1970 Nov;41(11):511-5.
20. Klemm K. (gentamicin-pmma-beads in treating bone and soft tissue infections (author's transl)). Zentralblatt für Chirurgie. 1979;104(14):934-42.
21. Walenkamp GH, van Rens TJ. (chains of gentamicin-pmma beads: A new method for the local treatment of osteomyelitis). Nederlands Tijdschrift voor Geneeskunde. 1982 Nov 20;126(47):2136-42.
22. Walenkamp GH, Vree TB, van Rens TJ. Gentamicin-pmma beads. Pharmacokinetic and nephrotoxicological study. Clinical Orthopaedics and Related Research. 1986 Apr(205):171-83.

23. Walenkamp GH, Kleijn LL, de Leeuw M. Osteomyelitis treated with gentamicin-pmma beads: 100 patients followed for 1-12 years. Acta Orthopaedica Scandinavica. 1998 Oct;69(5):518-22.
24. Parvizi J, Saleh KJ, Ragland PS, Pour AE, Mont MA. Efficacy of antibiotic-impregnated cement in total hip replacement. Acta Orthopaedica. 2008 Jun;79(3):335-41.
25. Engesaeter LB, Lie SA, Espehaug B, Furnes O, Vollset SE, Havelin LI. Antibiotic prophylaxis in total hip arthroplasty: Effects of antibiotic prophylaxis systemically and in bone cement on the revision rate of 22,170 primary hip replacements followed 0-14 years in the norwegian arthroplasty register. Acta Orthopaedica Scandinavica. 2003 Dec;74(6):644-51.
26. Garvin KL, Evans BG, Salvati EA, Brause BD. Palacos gentamicin for the treatment of deep periprosthetic hip infections. Clinical Orthopaedics and Related Research. 1994 Jan(298):97-105.
27. Langlais F. Can we improve the results of revision arthroplasty for infected total hip replacement? Journal of Bone and Joint Surgery (British Volume). 2003 Jul;85(5):637-40.
28. Walenkamp GH. Gentamicin pmma beads and other local antibiotic carriers in two-stage revision of total knee infection: A review. Journal of Chemotherapy. 2001 Nov;13 Spec No 1(1):66-72.
29. Castelli C, Marone P, Monzillo V, Segú K. Antistaphylococcal activity of antibiotic impregnated bone cement. The Knee. 1995;2(2):219-22.
30. Lewis G, Janna S. The in vitro elution of gentamicin sulfate from a commercially available gentamicin-loaded acrylic bone cement, versabond ab. J Biomed Mater Res B Appl Biomater. 2004 Oct 15;71(1):77-83.
31. Neut D, Kluin OS, Crielaard BJ, van der Mei HC, Busscher HJ, Grijpma DW. A biodegradable antibiotic delivery system based on poly-(trimethylene carbonate) for the treatment of osteomyelitis. Acta Orthopaedica. 2009 Oct;80(5):514-9.
32. Alt V, Bitschnau A, Bohner F, Heerich KE, Magesin E, Sewing A, Pavlidis T, Szalay G, Heiss C, Thormann U, Hartmann S, Pabst W, Wenisch S, Schnettler R. Effects of gentamicin and gentamicin-rgd coatings on bone ingrowth and biocompatibility of cementless joint prostheses: An experimental study in rabbits. Acta Biomater. 2011 Mar;7(3):1274-80.
33. Alt V, Bitschnau A, Osterling J, Sewing A, Meyer C, Kraus R, Meissner SA, Wenisch S, Domann E, Schnettler R. The effects of combined gentamicin-hydroxyapatite coating for cementless joint prostheses on the reduction of infection rates in a rabbit infection prophylaxis model. Biomaterials. 2006 Sep;27(26):4627-34.
34. Moojen DJ, Vogely HC, Fleer A, Nikkels PG, Higham PA, Verbout AJ, Castelein RM, Dhert WJ. Prophylaxis of infection and effects on osseointegration using a tobramycin-periapatite coating on titanium implants--an experimental study in the rabbit. Journal of Orthopaedic Research. 2009 Jun;27(6):710-6.
35. Moskowitz JS, Blaisse MR, Samuel RE, Hsu HP, Harris MB, Martin SD, Lee JC, Spector M, Hammond PT. The effectiveness of the controlled release of gentamicin from polyelectrolyte multilayers in the treatment of staphylococcus aureus infection in a rabbit bone model. Biomaterials. 2010 Aug;31(23):6019-30.
36. Kalicke T, Schierholz J, Schlegel U, Frangen TM, Koller M, Printzen G, Seybold D, Klockner S, Muhr G, Arens S. Effect on infection resistance of a local antiseptic and antibiotic coating on osteosynthesis implants: An in vitro and in vivo study. Journal of Orthopaedic Research. 2006 Aug;24(8):1622-40.
37. Patel A, Calfee RP, Plante M, Fischer SA, Arcand N, Born C. Methicillin-resistant staphylococcus aureus in orthopaedic surgery. Journal of Bone and Joint Surgery (British Volume). 2008 Nov;90(11):1401-6.
38. Albrektsson T, Johansson C. Osteoinduction, osteoconduction and osseointegration. European Spine Journal. 2001 Oct;10 Suppl 2:S96-101.
39. Brady RA, Leid JG, Calhoun JH, Costerton JW, Shirtliff ME. Osteomyelitis and the role of biofilms in chronic infection. FEMS Immunology and Medical Microbiology. 2008 Jan;52(1):13-22.
40. Zimmerli W, Moser C. Pathogenesis and treatment concepts of orthopaedic biofilm infections. FEMS Immunology and Medical Microbiology. 2012 Jul;65(2):158-68.
41. Paakkonen M, Kallio MJ, Kallio PE, Peltola H. C-reactive protein versus erythrocyte sedimentation rate, white blood cell count and alkaline phosphatase in diagnosing bacteraemia in bone and joint infections. Journal of Paediatrics and Child Health. 2013 Mar;49(3):E189-92.
42. Shih LY, Wu JJ, Yang DJ. Erythrocyte sedimentation rate and c-reactive protein values in patients with total hip arthroplasty. Clinical Orthopaedics and Related Research. 1987 Dec(225):238-46.

43. Glaudemans AW, Galli F, Pacilio M, Signore A. Leukocyte and bacteria imaging in prosthetic joint infection. Eur Cell Mater. 2013;25:61-77.
44. Palestro CJ, Love C, Bhargava KK. Labelled leukocyte imaging: Current status and future directions. Quarterly Journal of Nuclear Medicine and Molecular Imaging. 2009 Feb;53(1):105-23.
45. Palestro CJ, Love C, Miller TT. Infection and musculoskeletal conditions: Imaging of musculoskeletal infections. Best Practice & Research: Clinical Rheumatology. 2006 Dec;20(6):1197-218.
46. Al-Zahrani A, El-Saban K, Al-Sakhri H. Diagnosis of bone infection by complementary role of technetium -99m mdp and technetium-99m hexamethylpropylene-amineoxime-leukocytes. Indian Journal of Nuclear Medicine. 2012 Jul;27(3):164-71.
47. Makinen TJ, Lankinen P, Poyhonen T, Jalava J, Aro HT, Roivainen A. Comparison of 18f-fdg and 68ga pet imaging in the assessment of experimental osteomyelitis due to staphylococcus aureus. European Journal of Nuclear Medicine and Molecular Imaging. 2005 Nov;32(11):1259-68.
48. Hoffmann EJ, Phelps ME, Mullani NA, Higgins CS, Ter-Pogossian MM. Design and performance characteristics of a whole-body positron transaxial tomograph. Journal of Nuclear Medicine. 1976 Jun;17(6):493-502.
49. Phelps ME, Hoffman EJ, Mullani NA, Ter-Pogossian MM. Application of annihilation coincidence detection to transaxial reconstruction tomography. Journal of Nuclear Medicine. 1975 Mar;16(3):210-24.
50. Kim EE. Clinical pet : Principles and applications. New York: Springer; 2004. xviii, 394 p. p.
51. Schlyer DJ. Pet tracers and radiochemistry. Annals of the Academy of Medicine, Singapore. 2004 Mar;33(2):146-54.
52. Bleeker-Rovers CP, Vos FJ, Corstens FH, Oyen WJ. Imaging of infectious diseases using (18f) fluorodeoxyglucose pet. Quarterly Journal of Nuclear Medicine and Molecular Imaging. 2008 Mar;52 (1):17-29.
53. Schmitz A, Risse HJ, Kalicke T, Grunwald F, Schmitt O. (fdg-pet for diagnosis and follow-up of inflammatory processes: Initial results from the orthopedic viewpoint). Zeitschrift für Orthopädie und Ihre Grenzgebiete. 2000 Sep-Oct;138(5):407-12.
54. Baietto L, D'Avolio A, De Rosa FG, Garazzino S, Michelazzo M, Ventimiglia G, Siccardi M, Simiele M, Sciandra M, Di Perri G. Development and validation of a simultaneous extraction procedure for hplc-ms quantification of daptomycin, amikacin, gentamicin, and rifampicin in human plasma. Anal Bioanal Chem. 2010 Jan;396(2):791-8.
55. Manyanga V, Kreft K, Divjak B, Hoogmartens J, Adams E. Improved liquid chromatographic method with pulsed electrochemical detection for the analysis of gentamicin. Journal of Chromatography A. 2008 May 2;1189(1-2):347-54.
56. Rauschmann MA, Wichelhaus TA, Stirnal V, Dingeldein E, Zichner L, Schnettler R, Alt V. Nanocrystalline hydroxyapatite and calcium sulphate as biodegradable composite carrier material for local delivery of antibiotics in bone infections. Biomaterials. 2005 May;26(15):2677-84.
57. Stypulkowska K, Blazewicz A, Fijalek Z, Sarna K. Determination of gentamicin sulphate composition and related substances in pharmaceutical preparations by lc with charged aerosol detection. Chromatographia. 2010 Dec;72(11-12):1225-9.
58. Stallmann HP, Faber C, Bronckers AL, Nieuw Amerongen AV, Wuisman PI. In vitro gentamicin release from commercially available calcium-phosphate bone substitutes influence of carrier type on duration of the release profile. BMC Musculoskeletal Disorders. 2006;7:18.
59. Wilson JF, Davis AC, Tobin CM. Evaluation of commercial assays for vancomycin and aminoglycosides in serum: A comparison of accuracy and precision based on external quality assessment. Journal of Antimicrobial Chemotherapy. 2003 Jul;52(1):78-82.
60. Haasnoot W, Stouten P, Cazemier G, Lommen A, Nouws JF, Keukens HJ. Immunochemical detection of aminoglycosides in milk and kidney. Analyst. 1999 Mar;124(3):301-5.
61. Jin Y, Jang JW, Han CH, Lee MH. Development of elisa and immunochromatographic assay for the detection of gentamicin. Journal of Agricultural and Food Chemistry. 2005 Oct 5;53(20):7639-43.
62. Jin Y, Jang JW, Lee MH, Han CH. Development of competitive direct enzyme-linked immunosorbent assay for the detection of gentamicin residues in the plasma of live animals. Asian-Australasian Journal of Animal Sciences. 2005 Oct;18(10):1498-504.

63. Rega E, Holmes RB, Tirabaso A. Habitual locomotor behaviour inferred from manual pathology in two late cretaceous chasmosaurine ceratopsid dinosaurs, chamsosaurus irvinensis (cmn41357) and chasmosaurus belli (rom 843). In: Ryan MJ, editor. New perspectives on horned dinosaurs: The royal tyrrell museum ceratopsian symposium. Life of the past: Indiana University Press; 2010.
64. Burri C. Posttraumatische osteitis. Bern: Hans Huber; 1979.
65. Schulp AS, Walenkamp GHIM, Hofman PAM, Stuip Y, Rothschild BM. Chronic bone infection in the jaw of mosasaurus hoffmanni (squamata). Oryctos. 2006;6:41-52.
66. Breasted JH. The edwin smith surgical papyrus: Published in fascimile and hieroglyphic transliteration with translation and commentary in 2 volumes: University of Chicago; 1930.
67. Scultetus J. Armamentarium chirurgicum. Ulmae suevorum imp: B. Kühnemann; 1655.
68. Longmore T. Remarks upon osteo-myelitis consequent on gunshot wounds of the upper and lower extremities, and especially upon the treatment of stumps affected with osteomyelitis after amputation necessitated by such injuries. Medico-Chirurgical Transactions. 1865;48:43-64 1.
69. Vanarsdale WW. Ii. On the present state of knowledge in bacterial science in its surgical relations (continued): Osteomyelitis. Annals of Surgery. 1886 Mar;3(3):221-6.
70. Rodet A. The classic. An experimental study on infectious osteomyelitis. Clinical Orthopaedics and Related Research. 1973 Oct;99(96):3-4.
71. Norden CW. Experimental osteomyelitis. I. A description of the model. Journal of Infectious Diseases. 1970 Nov;122(5):410-8.
72. Norden CW. Experimental osteomyelitis. Ii. Therapeutic trials and measurement of antibiotic levels in bone. Journal of Infectious Diseases. 1971 Dec;124(6):565-71.
73. Bowers WH, Wilson FC, Greene WB. Antibiotic prophylaxis in experimental bone infections. Journal of Bone and Joint Surgery (American Volume). 1973 Jun;55(4):795-807.
74. Andriole VT, Nagel DA, Southwick WO. A paradigm for human chronic osteomyelitis. Journal of Bone and Joint Surgery (American Volume). 1973 Oct;55(7):1511-5.
75. Andriole VT, Nagel DA, Southwick WO. Chronic staphylococcal osteomyelitis: An experimental model. Yale Journal of Biology and Medicine. 1974 Mar;47(1):33-9.
76. Kaarsemaker S, Walenkamp GH, vd Bogaard AE. New model for chronic osteomyelitis with staphylococcus aureus in sheep. Clinical Orthopaedics and Related Research. 1997 Jun(339):246-52.
77. Norden CW, Keleti E. Experimental osteomyelitis caused by pseudomonas aeruginosa. Journal of Infectious Diseases. 1980 Jan;141(1):71-5.
78. Power ME, Olson ME, Domingue PA, Costerton JW. A rat model of staphylococcus aureus chronic osteomyelitis that provides a suitable system for studying the human infection. Journal of Medical Microbiology. 1990 Nov;33(3):189-98.
79. Blomgren G, Lindgren U. Postoperative infections resulting from bacteremia. An experimental study in rabbits. Acta Orthopaedica Scandinavica. 1980 Oct;51(5):761-5.
80. Blomgren G, Lindgren U. The susceptibility of total joint replacement to hematogenous infection in the early postoperative period: An experimental study in the rabbit. Clinical Orthopaedics and Related Research. 1980 Sep(151):308-12.
81. Blomgren G, Lundquist H, Nord CE, Lindgren U. Late anaerobic haematogenous infection of experimental total joint replacement. A study in the rabbit using propionibacterium acnes. Journal of Bone and Joint Surgery (British Volume). 1981;63B(4):614-8.
82. Calhoun JH, Mader JT. Treatment of osteomyelitis with a biodegradable antibiotic implant. Clinical Orthopaedics and Related Research. 1997 Aug(341):206-14.
83. Nijhof MW, Stallmann HP, Vogely HC, Fleer A, Schouls LM, Dhert WJ, Verbout AJ. Prevention of infection with tobramycin-containing bone cement or systemic cefazolin in an animal model. Journal of Biomedical Materials Research. 2000 Dec 15;52(4):709-15.
84. Petty W, Spanier S, Shuster JJ, Silverthorne C. The influence of skeletal implants on incidence of infection. Experiments in a canine model. Journal of Bone and Joint Surgery (American Volume). 1985 Oct;67(8):1236-44.
85. Smeltzer MS, Thomas JR, Hickmon SG, Skinner RA, Nelson CL, Griffith D, Parr TR, Jr., Evans RP. Characterisation of a rabbit model of staphylococcal osteomyelitis. Journal of Orthopaedic Research. 1997 May;15(3):414-21.

86. Southwood RT, Rice JL, McDonald PJ, Hakendorf PH, Rozenbilds MA. Infection in experimental hip arthroplasties. Journal of Bone and Joint Surgery (British Volume). 1985 Mar;67(2):229-31.
87. Vogely HC, Oosterbos CJ, Puts EW, Nijhof MW, Nikkels PG, Fleer A, Tonino AJ, Dhert WJ, Verbout AJ. Effects of hydrosyapatite coating on ti-6a1-4v implant-site infection in a rabbit tibial model. Journal of Orthopaedic Research. 2000 May;18(3):485-93.
88. Patel M, Rojavin Y, Jamali AA, Wasielewski SJ, Salgado CJ. Animal models for the study of osteomyelitis. Seminars in Plastic Surgery. 2009 May;23(2):148-54.
89. Lankinen P, Lehtimaki K, Hakanen AJ, Roivainen A, Aro HT. A comparative 18f-fdg pet/ct imaging of experimental staphylococcus aureus osteomyelitis and staphylococcus epidermidis foreign-body-associated infection in the rabbit tibia. EJNMMI Res. 2012 Jul 23;2(1):41.
90. Becker. Deutsche Medizinische Wochenschrift. 1883;9(46).
91. Rodet A. Etude expérimentale sur l'osteomyelite infectieuse. Comptes rendus hebdomadaires des Séances de l'Académie des Sciences. 1884;99:569-71.
92. Lexer E. Zur experimentellen erzeugung osteomyelitischer herde. Archiv für Klinische Chirurgie. 1894;48:181-200.
93. Lexer E. Experimente uber osteomyelitis. Archiv für Klinische Chirurgie. 1896;53:266-77.
94. Scheman L, Janota M, Lewin P. The production of experimental osteomyelitis: Preliminary report. JAMA. 1941;117(18):1525-9.
95. Elson RA, Jephcott AE, McGechie DB, Verettas D. Bacterial infection and acrylic cement in the rat. Journal of Bone and Joint Surgery (British Volume). 1977 Nov;59-B(4):452-7.
96. Blomgren G, Lindgren U. Late hematogenous infection in total joint replacement: Studies of gentamicin and bone cement in the rabbit. Clinical Orthopaedics and Related Research. 1981 Mar-Apr(155):244-8.
97. Zimmerli W, Lew PD, Waldvogel FA. Pathogenesis of foreign body infection. Evidence for a local granulocyte defect. Journal of Clinical Investigation. 1984 Apr;73(4):1191-200.
98. Fitzgerald RH, Jr. Experimental osteomyelitis: Description of a canine model and the role of depot administration of antibiotics in the prevention and treatment of sepsis. Journal of Bone and Joint Surgery (American Volume). 1983 Mar;65(3):371-80.
99. Norden CW, Shaffer M. Treatment of experimental chronic osteomyelitis due to staphylococcus aureus with vancomycin and rifampicin. Journal of Infectious Diseases. 1983 Feb;147(2):352-7.
100. Emslie KR, Nade S. Acute hematogenous staphylococcal osteomyelitis. A description of the natural history in an avian model. American Journal of Pathology. 1983 Mar;110(3):333-45.
101. Rodeheaver GT, Rukstalis D, Bono M, Bellamy W. A new model of bone infection used to evaluate the efficacy of antibiotic-impregnated polymethylmethacrylate cement. Clinical Orthopaedics and Related Research. 1983 Sep(178):303-11.
102. Norden CW. Experimental chronic staphylococcal osteomyelitis in rabbits: Treatment with rifampicin alone and in combination with other antimicrobial agents. Reviews of Infectious Diseases. 1983 Jul-Aug;5 Suppl 3:S491-4.
103. Norden CW, Shinners E. Ciprofloxacin as therapy for experimental osteomyelitis caused by pseudomonas aeruginosa. Journal of Infectious Diseases. 1985 Feb;151(2):291-4.
104. Petty W, Spanier S, Shuster JJ. Prevention of infection after total joint replacement. Experiments with a canine model. Journal of Bone and Joint Surgery (American Volume). 1988 Apr;70(4):536-9.
105. Worlock P, Slack R, Harvey L, Mawhinney R. An experimental model of post-traumatic osteomyelitis in rabbits. British Journal of Experimental Pathology. 1988 Apr;69(2):235-44.
106. Nelson DR, Buxton TB, Luu QN, Rissing JP. The promotional effect of bone wax on experimental staphylococcus aureus osteomyelitis. Journal of Thoracic and Cardiovascular Surgery. 1990 Jun;99 (6):977-80.
107. Jacob E, Setterstrom JA, Bach DE, Heath JR, 3rd, McNiesh LM, Cierny G, 3rd. Evaluation of biodegradable ampicillin anhydrate microcapsules for local treatment of experimental staphylococcal osteomyelitis. Clinical Orthopaedics and Related Research. 1991 Jun(267):237-44.
108. Gerhart TN, Roux RD, Hanff PA, Horowitz GL, Renshaw AA, Hayes WC. Antibiotic-loaded biodegradable bone cement for prophylaxis and treatment of experimental osteomyelitis in rats. Journal of Orthopaedic Research. 1993 Mar;11(2):250-5.

109. Laurencin CT, Gerhart T, Witschger P, Satcher R, Domb A, Rosenberg AE, Hanff P, Edsberg L, Hayes W, Langer R. Bioerodible polyanhydrides for antibiotic drug delivery: In vivo osteomyelitis treatment in a rat model system. Journal of Orthopaedic Research. 1993 Mar;11(2):256-62.
110. Melcher GA, Claudi B, Schlegel U, Perren SM, Printzen G, Munzinger J. Influence of type of medullary nail on the development of local infection. An experimental study of solid and slotted nails in rabbits. Journal of Bone and Joint Surgery (British Volume). 1994 Nov;76(6):955-9.
111. Garvin KL, Miyano JA, Robinson D, Giger D, Novak J, Radio S. Polylactide/polyglycolide antibiotic implants in the treatment of osteomyelitis. A canine model. Journal of Bone and Joint Surgery (American Volume). 1994 Oct;76(10):1500-6.
112. Sanzen L, Linder L. Infection adjacent to titanium and bone cement implants: An experimental study in rabbits. Biomaterials. 1995 Nov;16(16):1273-7.
113. Fialkov JA, Phillips JH, Walmsley SL, Morava-Protzner I. The effect of infection and lag screw fixation on revascularisation and new bone deposition in membranous bone grafts in a rabbit model. Plastic and Reconstructive Surgery. 1996 Aug;98(2):338-45.
114. Nelson CL, Hickmon SG, Skinner RA. Treatment of experimental osteomyelitis by surgical debridement and the implantation of bioerodable, polyanhydride-gentamicin beads. Journal of Orthopaedic Research. 1997 Mar;15(2):249-55.
115. An YH, Bradley J, Powers DL, Friedman RJ. The prevention of prosthetic infection using a cross-linked albumin coating in a rabbit model. Journal of Bone and Joint Surgery (British Volume). 1997 Sep;79 (5):816-9.
116. Awasthi V, Goins B, Klipper R, Loredo R, Korvick D, Phillips WT. Imaging experimental osteomyelitis using radiolabelled liposomes. Journal of Nuclear Medicine. 1998 Jun;39(6):1089-94.
117. Nie L, Nicolau DP, Tessier PR, Kourea HP, Browner BD, Nightingale CH. Use of a bioabsorbable polymer for the delivery of ofloxacin during experimental osteomyelitis treatment. Journal of Orthopaedic Research. 1998 Jan;16(1):76-9.
118. Gursel I, Korkusuz F, Turesin F, Alaeddinoglu NG, Hasirci V. In vivo application of biodegradable controlled antibiotic release systems for the treatment of implant-related osteomyelitis. Biomaterials. 2001 Jan;22(1):73-80.
119. Lucke M, Schmidmaier G, Sadoni S, Wildemann B, Schiller R, Stemberger A, Haas NP, Raschke M. A new model of implant-related osteomyelitis in rats. J Biomed Mater Res B Appl Biomater. 2003 Oct 15;67 (1):593-602.
120. Mader JT, Stevens CM, Stevens JH, Ruble R, Lathrop JT, Calhoun JH. Treatment of experimental osteomyelitis with a fibrin sealant antibiotic implant. Clinical Orthopaedics and Related Research. 2002 Oct(403):58-72.
121. Shirtliff ME, Calhoun JH, Mader JT. Experimental osteomyelitis treatment with antibiotic-impregnated hydroxyapatite. Clinical Orthopaedics and Related Research. 2002 Aug(401):239-47.
122. Rutledge B, Huyette D, Day D, Anglen J. Treatment of osteomyelitis with local antibiotics delivered via bioabsorbable polymer. Clinical Orthopaedics and Related Research. 2003 Jun(411):280-7.
123. Huneault LM, Lussier B, Dubreuil P, Chouinard L, Desevaux C. Prevention and treatment of experimental osteomyelitis in dogs with ciprofloxacin-loaded crosslinked high amylose starch implants. Journal of Orthopaedic Research. 2004 Nov;22(6):1351-7.
124. Ambrose CG, Clyburn TA, Louden K, Joseph J, Wright J, Gulati P, Gogola GR, Mikos AG. Effective treatment of osteomyelitis with biodegradable microspheres in a rabbit model. Clinical Orthopaedics and Related Research. 2004 Apr(421):293-9.
125. Koort JK, Makinen TJ, Knuuti J, Jalava J, Aro HT. Comparative 18f-fdg pet of experimental staphylococcus aureus osteomyelitis and normal bone healing. Journal of Nuclear Medicine. 2004 Aug;45(8):1406-11.
126. Koort JK, Makinen TJ, Suokas E, Veiranto M, Jalava J, Knuuti J, Tormala P, Aro HT. Efficacy of ciprofloxacin-releasing bioabsorbable osteoconductive bone defect filler for treatment of experimental osteomyelitis due to staphylococcus aureus. Antimicrobial Agents and Chemotherapy. 2005 Apr;49 (4):1502-8.
127. Craig MR, Poelstra KA, Sherrell JC, Kwon MS, Belzile EL, Brown TE. A novel total knee arthroplasty infection model in rabbits. Journal of Orthopaedic Research. 2005 Sep;23(5):1100-4.

128. Mendel V, Simanowski HJ, Scholz HC, Heymann H. Therapy with gentamicin-pmma beads, gentamicin-collagen sponge, and cefazolin for experimental osteomyelitis due to staphylococcus aureus in rats. Archives of Orthopaedic and Trauma Surgery. 2005 Jul;125(6):363-8.
129. Fukushima N, Yokoyama K, Sasahara T, Dobashi Y, Itoman M. Establishment of rat model of acute staphylococcal osteomyelitis: Relationship between inoculation dose and development of osteomyelitis. Archives of Orthopaedic and Trauma Surgery. 2005 Apr;125(3):169-76.
130. Jones-Jackson L, Walker R, Purnell G, McLaren SG, Skinner RA, Thomas JR, Suva LJ, Anaissie E, Miceli M, Nelson CL, Ferris EJ, Smeltzer MS. Early detection of bone infection and differentiation from post-surgical inflammation using 2-deoxy-2-(18f)-fluoro-d-glucose positron emission tomography (fdg-pet) in an animal model. Journal of Orthopaedic Research. 2005 Nov;23(6):1484-9.
131. Makinen TJ, Veiranto M, Knuuti J, Jalava J, Tormala P, Aro HT. Efficacy of bioabsorbable antibiotic containing bone screw in the prevention of biomaterial-related infection due to staphylococcus aureus. Bone. 2005 Feb;36(2):292-9.
132. Beardmore AA, Brooks DE, Wenke JC, Thomas DB. Effectiveness of local antibiotic delivery with an osteoinductive and osteoconductive bone-graft substitute. Journal of Bone and Joint Surgery (American Volume). 2005 Jan;87(1):107-12.
133. Joosten U, Joist A, Gosheger G, Liljenqvist U, Brandt B, von Eiff C. Effectiveness of hydroxyapatite-vancomycin bone cement in the treatment of staphylococcus aureus induced chronic osteomyelitis. Biomaterials. 2005 Sep;26(25):5251-8.
134. Salgado CJ, Jamali AA, Mardini S, Buchanan K, Veit B. A model for chronic osteomyelitis using staphylococcus aureus in goats. Clinical Orthopaedics and Related Research. 2005 Jul(436):246-50.
135. Darouiche RO, Mansouri MD, Zakarevicz D, Alsharif A, Landon GC. In vivo efficacy of antimicrobial-coated devices. Journal of Bone and Joint Surgery (American Volume). 2007 Apr;89(4):792-7.
136. Poultsides LA, Papatheodorou LK, Karachalios TS, Khaldi L, Maniatis A, Petinaki E, Malizos KN. Novel model for studying hematogenous infection in an experimental setting of implant-related infection by a community-acquired methicillin-resistant s. Aureus strain. Journal of Orthopaedic Research. 2008 Oct;26(10):1355-62.
137. Williams D, Bloebaum R, Petti CA. Characterisation of staphylococcus aureus strains in a rabbit model of osseointegrated pin infections. J Biomed Mater Res A. 2008 May;85(2):366-70.
138. Laure B, Besnier JM, Bergemer-Fouquet AM, Marquet-Van Der Mee N, Damie F, Quentin R, Favard L, Rosset P. Effect of hydroxyapatite coating and polymethylmethacrylate on stainless steel implant-site infection with staphylococcus epidermidis in a sheep model. J Biomed Mater Res A. 2008 Jan;84(1):92-8.
139. Kanellakopoulou K, Thivaios GC, Kolia M, Dontas I, Nakopoulou L, Dounis E, Giamarellos-Bourboulis EJ, Andreopoulos A, Karagiannakos P, Giamarellou H. Local treatment of experimental pseudomonas aeruginosa osteomyelitis with a biodegradable dilactide polymer releasing ciprofloxacin. Antimicrobial Agents and Chemotherapy. 2008 Jul;52(7):2335-9.
140. Hamel A, Caillon J, Jacqueline C, Rogez JM, Potel G. Internal device decreases antibiotic's efficacy on experimental osteomyelitis. Journal of Children's Orthopaedics. 2008 Jun;2(3):239-43.
141. Moojen DJ, Vogely HC, Fleer A, Verbout AJ, Castelein RM, Dhert WJ. No efficacy of silver bone cement in the prevention of methicillin-sensitive staphylococcal infections in a rabbit contaminated implant bed model. Journal of Orthopaedic Research. 2009 Aug;27(8):1002-7.
142. Bernthal NM, Stavrakis AI, Billi F, Cho JS, Kremen TJ, Simon SI, Cheung AL, Finerman GA, Lieberman JR, Adams JS, Miller LS. A mouse model of post-arthroplasty staphylococcus aureus joint infection to evaluate in vivo the efficacy of antimicrobial implant coatings. PloS One. 2010;5(9):e12580.
143. Jacqueline C, Amador G, Caillon J, Le Mabecque V, Batard E, Miegeville AF, Biek D, Ge Y, Potel G, Hamel A. Efficacy of the new cephalosporin ceftaroline in the treatment of experimental methicillin-resistant staphylococcus aureus acute osteomyelitis. Journal of Antimicrobial Chemotherapy. 2010 Aug;65(8):1749-52.
144. Stewart RL, Cox JT, Volgas D, Stannard J, Duffy L, Waites KB, Chu TM. The use of a biodegradable, load-bearing scaffold as a carrier for antibiotics in an infected open fracture model. Journal of Orthopaedic Trauma. 2010 Sep;24(9):587-91.
145. Robinson DA, Bechtold JE, Carlson CS, Evans RB, Conzemius MG. Development of a fracture osteomyelitis model in the rat femur. Journal of Orthopaedic Research. 2011 Jan;29(1):131-7.

146. Vergidis P, Rouse MS, Euba G, Karau MJ, Schmidt SM, Mandrekar JN, Steckelberg JM, Patel R. Treatment with linezolid or vancomycin in combination with rifampicin is effective in an animal model of methicillin-resistant staphylococcus aureus foreign body osteomyelitis. Antimicrobial Agents and Chemotherapy. 2011 Mar;55(3):1182-6.
147. Gaudin A, Amador Del Valle G, Hamel A, Le Mabecque V, Miegeville AF, Potel G, Caillon J, Jacqueline C. A new experimental model of acute osteomyelitis due to methicillin-resistant staphylococcus aureus in rabbit. Letters in Applied Microbiology. 2011 Mar;52(3):253-7.
148. Alt V, Lips KS, Henkenbehrens C, Muhrer D, Oliveira Cavalcanti MC, Sommer U, Thormann U, Szalay G, Heiss C, Pavlidis T, Domann E, Schnettler R. A new animal model for implant-related infected non-unions after intramedullary fixation of the tibia in rats with fluorescent in situ hybridisation of bacteria in bone infection. Bone. 2011 May 1;48(5):1146-53.
149. Poeppl W, Tobudic S, Lingscheid T, Plasenzotti R, Kozakowski N, Georgopoulos A, Burgmann H. Efficacy of fosfomycin in experimental osteomyelitis due to methicillin-resistant staphylococcus aureus. Antimicrobial Agents and Chemotherapy. 2011 Feb;55(2):931-3.
150. Pribaz JR, Bernthal NM, Billi F, Cho JS, Ramos RI, Guo Y, Cheung AL, Francis KP, Miller LS. Mouse model of chronic post-arthroplasty infection: Noninvasive in vivo bioluminescence imaging to monitor bacterial burden for long-term study. Journal of Orthopaedic Research. 2012 Mar;30(3):335-40.
151. Niska JA, Shahbazian JH, Ramos RI, Pribaz JR, Billi F, Francis KP, Miller LS. Daptomycin and tigecycline have broader effective dose ranges than vancomycin as prophylaxis against a staphylococcus aureus surgical implant infection in mice. Antimicrobial Agents and Chemotherapy. 2012 May;56(5):2590-7.
152. Horst SA, Hoerr V, Beineke A, Kreis C, Tuchscherr L, Kalinka J, Lehne S, Schleicher I, Kohler G, Fuchs T, Raschke MJ, Rohde M, Peters G, Faber C, Loffler B, Medina E. A novel mouse model of staphylococcus aureus chronic osteomyelitis that closely mimics the human infection: An integrated view of disease pathogenesis. American Journal of Pathology. 2012 Oct;181(4):1206-14.
153. Li GY, Yin JM, Ding H, Jia WT, Zhang CQ. Efficacy of leukocyte- and platelet-rich plasma gel (l-prp gel) in treating osteomyelitis in a rabbit model. Journal of Orthopaedic Research. 2013 Jun;31(6):949-56.
154. Johansen LK, Svalastoga EL, Frees D, Aalbaek B, Koch J, Iburg TM, Nielsen OL, Leifsson PS, Jensen HE. A new technique for modeling of hematogenous osteomyelitis in pigs: Inoculation into femoral artery. Journal of Investigative Surgery. 2013 Jun;26(3):149-53.
155. Yin LY, Manring MM, Calhoun JH. A rabbit osteomyelitis model to simulate multibacterial war wound infections. Military Medicine. 2013 Jun;178(6):696-700.
156. Xing J, Hou T, Luobu B, Luo F, Chen Q, Li Z, Jin H, Xu J. Anti-infection tissue engineering construct treating osteomyelitis in rabbit tibia. Tissue engineering Part A. 2013 Jan;19(1-2):255-63.
157. Xie Z, Cui X, Zhao C, Huang W, Wang J, Zhang C. Gentamicin-loaded borate bioactive glass eradicates osteomyelitis due to escherichia coli in a rabbit model. Antimicrobial Agents and Chemotherapy. 2013 Jul;57(7):3293-8.
158. Soe NH, Jensen NV, Nurnberg BM, Jensen AL, Koch J, Poulsen SS, Pier G, Johansen HK. A novel knee prosthesis model of implant-related osteomyelitis in rats. Acta Orthopaedica. 2013 Feb;84(1):92-7.
159. Tran N, Tran PA, Jarrell JD, Engiles JB, Thomas NP, Young MD, Hayda RA, Born CT. In vivo caprine model for osteomyelitis and evaluation of biofilm-resistant intramedullary nails. Biomed Research International. 2013;2013:674378.
160. Odekerken JC, Arts JJ, Surtel DA, Walenkamp GH, Welting TJ. A rabbit osteomyelitis model for the longitudinal assessment of early post-operative implant infections. Journal of Orthopaedic Surgery and Research. 2013;8(1):38.
161. Odekerken JC, Brans BT, Welting TJ, Walenkamp GH. 18f-fdg micropet imaging differentiates between septic and aseptic wound healing after orthopedic implant placement a longitudinal study of an implant osteomyelitis in the rabbit tibia. Acta Orthopaedica. 2014;85(3):9.
162. Helbig L, Simank HG, Lorenz H, Putz C, Wolfl C, Suda AJ, Moghaddam A, Schmidmaier G, Guehring T. Establishment of a new methicillin resistant staphylococcus aureus animal model of osteomyelitis. International Orthopaedics. 2014 Apr;38(4):891-7.
163. Cremieux AC, Saleh-Mghir A, Danel C, Couzon F, Dumitrescu O, Lilin T, Perronne C, Etienne J, Lina G, Vandenesch F. Alpha-hemolysin, not panton-valentine leukocidin, impacts rabbit mortality from severe sepsis with methicillin-resistant staphylococcus aureus osteomyelitis. Journal of Infectious Diseases. 2014 Jun 1;209(11):1773-80.

164. Varrone JJ, de Mesy Bentley KL, Bello-Irizarry SN, Nishitani K, Mack S, Hunter JG, Kates SL, Daiss JL, Schwarz EM. Passive immunisation with anti-glucosaminidase monoclonal antibodies protects mice from implant-associated osteomyelitis by mediating opsonophagocytosis of staphylococcus aureus megaclusters. Journal of Orthopaedic Research. 2014 Oct;32(10):1389-96.
165. McLaren JS, White LJ, Cox HC, Ashraf W, Rahman CV, Blunn GW, Goodship AE, Quirk RA, Shakesheff KM, Bayston R, Scammell BE. A biodegradable antibiotic-impregnated scaffold to prevent osteomyelitis in a contaminated in vivo bone defect model. Eur Cell Mater. 2014;27:332-49.
166. Inanmaz ME, Uslu M, Isik C, Kaya E, Tas T, Bayram R. Extracorporeal shockwave increases the effectiveness of systemic antibiotic treatment in implant-related chronic osteomyelitis: Experimental study in a rat model. Journal of Orthopaedic Research. 2014 Jun;32(6):752-6.
167. Gahukamble AD, McDowell A, Post V, Salavarrieta Varela J, Rochford ET, Richards RG, Patrick S, Moriarty TF. Propionibacterium acnes and staphylococcus lugdunensis cause pyogenic osteomyelitis in an intramedullary nail model in rabbits. Journal of Clinical Microbiology. 2014 May;52(5):1595-606.
168. Zhu C, Wang J, Cheng T, Li Q, Shen H, Qin H, Cheng M, Zhang X. The potential role of increasing the release of mouse beta- defensin-14 in the treatment of osteomyelitis in mice: A primary study. PloS One. 2014;9(1):e86874.
169. Freiberg JA, McIver KS, Shirtliff ME. In vivo expression of streptococcus pyogenes immunogenic proteins during tibial foreign body infection. Infection and Immunity. 2014 Sep;82(9):3891-9.
170. Chen WH, Kang YJ, Dai LY, Wang B, Lu C, Li J, Lu GH. Bacteria detected after instrumentation surgery for pyogenic vertebral osteomyelitis in a canine model. European Spine Journal. 2014 Apr;23(4):838-45.
171. Ding H, Zhao CJ, Cui X, Gu YF, Jia WT, Rahaman MN, Wang Y, Huang WH, Zhang CQ. A novel injectable borate bioactive glass cement as an antibiotic delivery vehicle for treating osteomyelitis. PloS One. 2014;9(1):e85472.
172. Cui X, Zhao C, Gu Y, Li L, Wang H, Huang W, Zhou N, Wang D, Zhu Y, Xu J, Luo S, Zhang C, Rahaman MN. A novel injectable borate bioactive glass cement for local delivery of vancomycin to cure osteomyelitis and regenerate bone. Journal of Materials Science: Materials in Medicine. 2014 Mar;25(3):733-45.
173. Odekerken JCE, Walenkamp GHIM, Brans BT, Welting TJM, Arts JJC. The longitudinal assessment of osteomyelitis development by molecular imaging in a rabbit model. Biomed Research International. 2014;424652.
174. Shishatskaya EI, Kamendov IV, Starosvetsky SI, Vinnik YS, Markelova NN, Shageev AA, Khorzhevsky VA, Peryanova OV, Shumilova AA. An in vivo study of osteoplastic properties of resorbable poly-3-hydroxybutyrate in models of segmental osteotomy and chronic osteomyelitis. Artif Cells Nanomed Biotechnol. 2014 Oct;42(5):344-55.
175. Poeppl W, Lingscheid T, Bernitzky D, Schwarze UY, Donath O, Perkmann T, Kozakowski N, Plasenzotti R, Reznicek G, Burgmann H. Efficacy of fosfomycin compared to vancomycin in treatment of implant-associated chronic methicillin-resistant staphylococcus aureus osteomyelitis in rats. Antimicrobial Agents and Chemotherapy. 2014 Sep;58(9):5111-6.
176. Gatin L, Saleh-Mghir A, Tasse J, Ghout I, Laurent F, Cremieux AC. Ceftaroline-fosamil efficacy against methicillin-resistant staphylococcus aureus rabbit prosthetic joint infection. Antimicrobial Agents and Chemotherapy. 2014 Aug 18.

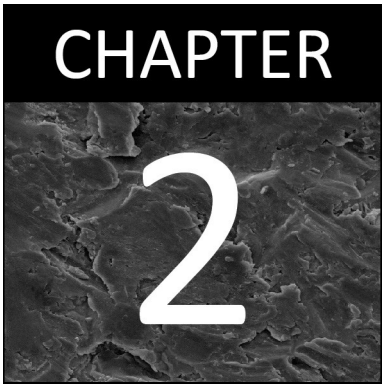

Modern orthopaedic implant coatings: their pro's, con's and evaluation methods

J.C.E. Odekerken

T.J.M. Welting

J.J.C. Arts

G.H.I.M. Walenkamp

P.J. Emans

Modern Surface Engineering Treatments, InTech. ISBN: 978-953-51-1149-8.

1. Introduction

Metal implants in the field of orthopaedic and trauma surgery have been used for a long time to restore joint function, reduce pain or stabilize fractures (1-3). Both prevention of infection as well as integration of the implant with the host-tissue (mostly bone) are factors of concern. The most frequently used implants for these purposes are made of metallic alloys (plates and nails for fracture repair and for total joint arthroplasties) and polyethylene (PE) (used in the articulating parts of a prosthesis).

Infection of orthopaedic implants and prostheses is a medical issue that has intrigued people since their very first use over two-and-a-half millennia ago. Since that early beginning, lack of fixation and infection has been the major problem with such medical devices. In many cases, it may result in serious discomfort, limb amputation, illness and in many cases it may have even resulted in death of the patient. Even after 2500 years of medical progression we are still not able to fully conquer these major health risks. Since they are not isolated to the field of orthopaedics and trauma, their multi-factorial character indicates the complexity of the problems concerning healthcare-associated infections (HAI) (4, 5).

The purpose of this chapter is to give an insight in the quest to decrease the percentage of infections and increase the amount of osteointegration by coatings on metallic alloys in the field of orthopaedic and trauma surgery. Finally an overview will be provided of the available methods to examine and evaluate the properties of coatings *in vitro* and *in vivo*.

1.1 Healthcare-associated infections and orthopaedics

Healthcare-associated infections, also called nosocomial infections, are considered to be the biggest healthcare related complication worldwide. HAI annually affects hundreds of millions of patients worldwide with approximately 4.1 million patients in Europe and about 1.7 million patients in the United States (6, 7). These infections can be related to the cause of death of a considerable number of patients annually. Together with the tremendous economic burden of HAI, HAI is a major point of interest in medical research.

With urinary tract infections as the most frequent implant related HAI in developed countries, orthopaedic implant infections is another major sub-populations within the multifactorial group of HAI (together with infections related to cardiovascular, neurological and gastrointestinal

interventions). Infections due to implantation of total hip and total knee prostheses account for about 2% of the HAI, without taking trauma implants into account (7). Trauma implants or implants for fracture fixation and stabilisation, like plates, screws and stabilizing frames, have been described to have an even higher risk for infection, mainly due to the fact that they are used to repair complex injuries and open fractures. Infection together with the eventual loosening of an orthopaedic implant explains the limited lifespan of an orthopaedic device (generally up to 15 years for an artificial joint (5, 8, 9)).

Since the discovery of antibiotics, (implant) infections have been reduced and implant infections have become less lethal and can even be cured. Still, the extensive use of antibiotics has resulted in an increasing amount of resistant bacterial strains, which makes infections caused by those pathogens challenging. Medical device implantation remains troublesome also in the case of orthopaedic implants.

Table 1: Epidemiological data on HAI (6, 7).

Area	# Patients (million/yr)	Prevalence (%)	Death (%)	Costs (billion)	Neonatal death rate (caused by HAI)
Europe	4.1	7.1	3.7%	(€) 7	< 5%
USA	1.7	4.5	5.8%	($) 6.5	< 5%
Worldwide	> 100	8.5 - 15.5			Up to 75% in South-East Asia and Africa

1.2 The race for the surface

After implantation of an orthopaedic device, a competition between bacterial colonisation versus tissue integration takes place to conquer the surface of the implant. This phenomenon is often described as "the race for the surface" (Figure 1) (10, 11). The first stage of bacterial biofilm formation is the settling of a planktonic bacterium on the surface of the implant. After adhering to the surface, the bacterium starts to divide and encapsulate itself for protection against the host organism's immune response. This layer of protective matrix, mostly consisting out of polysaccharides, also shields the bacteria from effective antibiotic treatment. The first stage of the biofilm formation is complete and subsequently the present bacteria start to form colonies increasing the internal pressure in the biofilm, which starts to expand. At a certain point the

bacterial load within the mature biofilm becomes so high that planktonic bacteria are released from the biofilm. These bacteria can then result in the infection of the surrounding tissue or in the expansion of the biofilm on a different location (Figure 1) (10-12). Eukaryotic cell adhesion (e.g. adhesion of osteoblasts) on the other hand, can result in implant ingrowth by settling of the osteoblast on the implant surface, followed by cell division and collagen matrix production. Eventual calcification of the collagen matrix allows bone apposition on the implant surface (Figure 1) (10, 12). In general the inability of the body and its immune system to cope with infected implants is one of the biggest issues when implants are used for medical treatment. Due to infection, local bone resorption takes place, leading to bone loss and implant loosening. As such it is essential to treat the infection, avoiding the risk of tremendous damage to the bone and the bony peri-implant tissue. After removal of an infected implant, the accompanying bone fractures, soft tissue infection, and inflammation result in fixation issues and an increased infection risk during revision surgery (13).

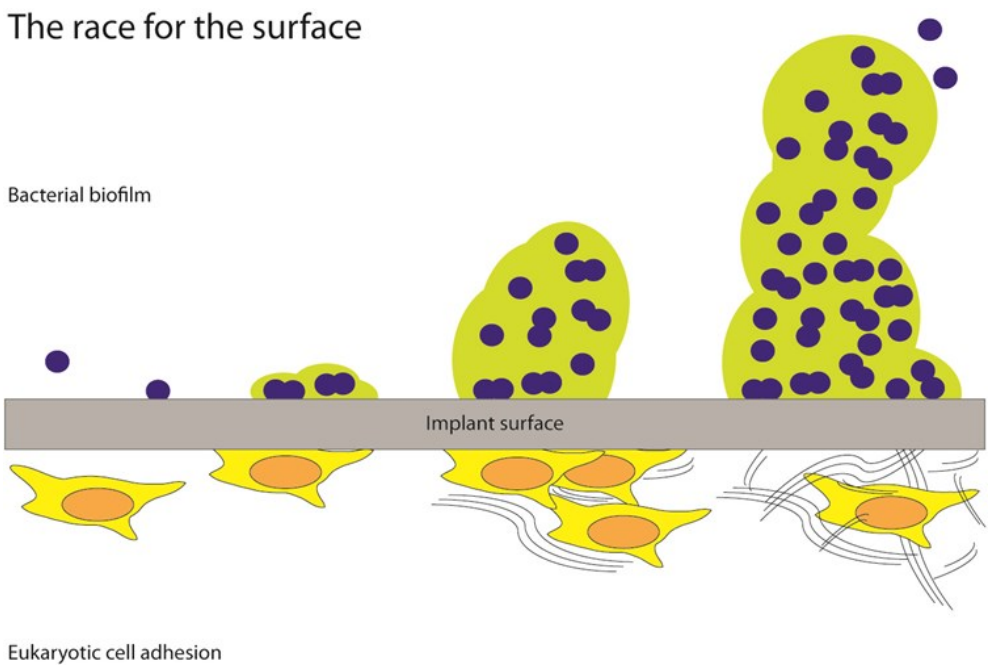

Figure 1: A schematic representation of "the race for the surface", between the bacterial biofilm colonisation and eukaryotic cell adhesion with subsequent bone apposition on the implant surface.

1.3 Implant coatings

In order to decrease the amount of implant infections and prevent the implants from loosening, coatings can be applied to the surface of the implant. These coatings may vary from (antibiotic) releasing to non-releasing coatings. In general non-releasing coatings (like hydroxyapatite (HA)) are applied by thermal-processes, while releasing coatings (like RGD or antibiotic-containing coatings) are mostly applied to the surface by dip or spray coating, due to their limited thermal stability.
Since the principle of "the race for the surface" dictates that early tissue integration may also reduce the infection risk, a coating promoting tissue integration may also be regarded as a passive method to reduce the amount of infections. In order to promote this tissue integration, one of the biggest leaps forward in the improvement of implant fixation and "the race for the surface" in favour of eukaryotic cells might be the use of hydroxyapatite coatings on the surface of a metallic implant (12, 14-16). Although in the beginning it was believed that uncemented prostheses, including the HA-coated implants, would have a higher infection percentage compared to implants fixated with an antibiotic-releasing bone-cement, long-term studies showed a comparable infection percentage and a longer survival in favour of the uncemented prosthesis (5, 17). These HA-based coatings (and their derivatives) are still one of the most frequently used implant coatings in the field of orthopaedic surgery and trauma, resulting in improved implant ingrowth and a longer lifespan of the prosthesis (8). A combined situation of a coating with both antimicrobial and osteoconductive properties, is yet to be found.

2. Active and passive implant coatings

2.1 Osteoconductive coatings

The definition of osteoconduction means that a material or coating "guides" the bone healing or formation. In case of coatings this means that the bone formation is "guided" to grow or attach to the coating surface (a passive coating) (18). An orthopaedic implant with such a surface treatment or coating provides an ideal substrate for bone apposition which results in improved implant fixation and a possible prolonged lifespan, with a decreased risk of implant loosening and possibly infection (10, 12).

2.1.1 Apatite coatings

The initial idea of hydroxyapatite coatings originated from the use of calcium phosphates as a material to stimulate osteogenesis, like tricalcium phosphate (TCP). During the last decades, studies have shown that HA and TCP are suitable for the production of ceramic scaffolds to serve as a bone substitute. Studies on the stability of sintered TCP ($Ca_3(PO_4)_2$) and HA ($Ca_{10}(PO_4)_6(OH)_2$) have shown that TCP ceramics dissolve over 10 times faster in acidic and alkaline environments compared to HA (19). Explaining the rationale behind the current use of TCP for resorbable bone scaffolds and the use of HA for implant coatings.

Since the proposed use of HA as a coating, in the late 1980's by Geesink *et al.* (14-16), several implant designs have been used in the clinic, e.g. partially coated or fully coated hip implants. Fully coated implants achieved complete bone remodelling around the implant, with very good fixation properties. The major disadvantage of these fully coated implants was that in case of revision surgery (either for implant infection or component failure) removal of the implant resulted in massive bone trauma due to the fixation of the implant to the bone. By redefining the coating location to the taper only, a good fixation could be achieved with limited problems at the time of a revision surgery (15). However this design allowed the formation of stress shielding due to the pressure of the stem against the cortical wall. Due to this strain an implant can get loose, resulting in bone loss or a cortical wall fracture. Still HA coatings sintered to an implant surface have proven to be the most successful implant coating made, with 20 years of clinical experience (8, 20).

2.1.2 Hydroxyapatite application methods for metallic surfaces

There are several ways to coat a metallic alloy, like titanium or stainless steel, with HA. The techniques to coat such a metallic implant include; dip coating (21), sputter coating (22), pulsed laser deposition (23), hot pressing and hot isostatic pressing (24), electrophoretic deposition(25), electrostatic spraying (26, 27), thermal spraying (28), and sol–gel (29). Some of these techniques are still experimental, thermal spraying, in particular. Plasma spraying is the most accepted method for the production of HA coatings (30). Plasma spraying requires high temperatures which may damage the HA crystallinity and create unwanted or amorphous phases, with HA ablation from the coated surface as a possible result (28).

Table 2: Different coating techniques for hydroxyapatite (HA) application.

Technique	Advantage	Disadvantage	Thickness	Ref
Sol-Gel	• Coats 3D complex porous substrates • Low processing temperatures • Relatively cheap • Very thin coatings	• Processing in controlled atmosphere	< 1 µm	(29)
Sputter coating	• Uniform coating thickness on flat substrates	• Only coats visible area • Expensive and time consuming • Unable to coat complex 3D porous substrates • Risk for amorphous coating	0.02 - 2 µm	(22)
Pulsed Laser Deposition	• See sputter coating	• See sputter coating	1 - 10 µm	(23, 25)
Electrostatic Spray Deposition	• Uniform coating thickness on flat substrates • Relatively cheap	• Only coats visible area • Fragility	1 - 10 µm	(26, 27, 31)
Electrophoretic Deposition	• Uniform coating thickness • High deposition rates • Coats complex 3D porous substrates	• Cracks in coating • High sintering temperature	0.1 - 200 µm	(25)
Thermal spraying, Plasma spraying	• High deposition rates	• Only coats visible area • Coating decomposition due to high temperature • Rapid cooling may result in amorphous coating	30 – 200 µm	(25, 28)
Dip Coating	• Inexpensive • Coatings applied quickly • Coats complex 3D porous substrates	• High sintering temperature • Thermal expansion results in amorphous coating • Fragile due to thickness	0.05 - 2 mm	(21, 25)
Hot Pressing, Hot Isostatic Pressing and Sintering	• Dense coatings	• Unable to coat complex 3D porous substrates • Differences in coating elasticity • Expensive • Interaction with or changes due to the encapsulation material	0.1 – 10 mm	(24, 25, 32)

Every technique has its advantages and disadvantages. For example, the thickness, the bonding strength and the properties of the HA-composition may be influenced by the application technique. Techniques such as thermal spraying and sputter coating are used for surfaces or substrates (e.g. porous titanium implants) which are difficult to coat. Techniques such as electrophoretic deposition and sol-gel may coat more complex substrates such as porous alloys, still the production of crack free coatings remains challenging (Table 2).

2.2 Osteoinductive coatings

Although biomimetic HA coatings improve the osteoconductivity of metal implants, they do not influence the osteoinductivity. In general osteoinductive coatings are described as coatings which induce bone formation of undifferentiated cells in the surrounding tissue to ultimately promote osteointegration of bone to the coating (active coatings). In order to promote the differentiation of immature progenitor cells to an osteoblastic lineage, attempts to integrate functional biological agents such as growth factors into biomimetic coatings have been realized (33, 34). Several of these coatings have been studied extensively, the most important coatings are described below.

2.2.1 RGD coatings

Extracellular matrix proteins contain a short functional domain of three amino acids, arginine (R), glycine (G) and asparagine (D), the so-called RGD-domain. This domain plays an important role in cell adhesion, cell proliferation and differentiation. RGD peptides coated to a surface can initiate these processes in their direct vicinity. The major advantage of using peptide coatings instead of protein coatings is that peptides are smaller and more stable compared to proteins. This allows more peptides to be coated to a surface, which results in a more dense coating. Studies have shown that the flanking amino acids in a RGD containing peptide are of great importance for their efficiency. *In vitro* studies show promising results, where RGD enhances (human) cell adhesion, proliferation and differentiation in the osteogenic lineage (35). An *in vivo* study of an HA/HA-RGD coating with antibiotic release showed that the HA-RGD coating performed at least equally well as the HA-only coating (33). Still these coatings remain experimental by application.

2.2.2 BMP coatings

Bone morphogenetic proteins (BMP's), which belong to the transforming growth factor-β (TGF-β) superfamily, are generally accepted osteoinductive additives for per-operative use to enhance bone remodelling. Due to the lack of a local delivery system, capable of a sustained release, relatively high dosages of BMP's (e.g. BMP-2) are being used in the clinic. The use of BMP's has a locally higher incidence of tumourigenesis as a major disadvantage. Other osteogenic BMP's, such as BMP-4 (36, 37) and BMP-7 (38), are also potent inducers of bone regeneration. Knippenberg et al showed that BMP-7, in contrast to BMP-2 may be a more chondrogenic growth factor in contrast to BMP-2 which was described as a more osteogenic growthfactor (39). BMP-2 works in 2 concentration dependent directions, at low dosages it promotes bone remodelling, while at high dosage it promotes bone resorption. Therefore a low-dose releasing BMP-2 coated implant may be the most optimal (40). While many techniques to incorporate BMP's result in a burst release, they can also be incorporated into the crystal latticework of coatings to establish a gradual release system (34, 40). As such the incorporated proteins can be released gradually and steadily at a low pharmacological level; not rapidly as in a single high-dose burst (41). In conclusion, incorporation of osteoinductive coatings may seem attractive but, release rate, potential carcinogenesis, inactivation of the compound (e.g. due to changes in temperature, pH), and bonding to the implant remain of concern.

3. Antimicrobial coatings

Since vascularisation of infected tissue is often compromised and a bacterial biofilm is formed, which results in poor penetration of antibiotics, systemic antibiotics are not sufficient to treat a bone infection properly (10-12). To achieve a local dose high enough to treat the infection, this would involve a systemic overdose of the antibiotic (possibly resulting in kidney and liver failure and damage to the function of the inner ear). The best solution to this problem is to have a local delivery system, this suggests an approach for the treatment of orthopaedic infections. Still in many cases the prosthesis can be rescued by infection treatment *in situ*, without a surgical procedure (13, 42, 43). The use of local antibiotics by antibiotic-loaded bone cement, either as beads or spacers often placed after implant removal in the remaining infected cavity. The general treatment procedure requires at least two surgical procedures, one to remove the infected

implant and the surrounding affected tissue, combined with the placement of a spacer or antibiotic-loaded beads to fill up to void (44-46). The second operation is required to remove the spacer or beads after a couple of weeks or months. Once the infection is regarded as treated sufficiently, a new implant or prosthesis is implanted. If the treatment was not successful, new beads can be placed, which will require a third operation for the removal of the beads (44-46). Due to the high costs and the tremendous burden for the patient a one-step procedure would be preferable. An antimicrobial coating directly on the surface of the newly placed implant, in case of revision surgery after infection, could prevent the infection form re-occurring, besides such coatings may also work as a prophylactic in the case of the placement of a primary hip.

3.1 Antibiotic releasing coatings

Already in clinical use in other medical specialties (e.g. in sutures and central venous and urinary tract catheters), antibiotic releasing coatings remain mainly experimental in the field of orthopaedic and trauma surgery. For orthopaedic applications gentamicin, vancomycin, rifampicin, and tobramycin are the most frequently used local antibiotics in case of an implant infection. There are several published *in vitro* and *in vivo* studies based on the use of these antibiotic drugs for an orthopaedic implant coating. Poly-L-lactide (PLLA) coatings with rifampicin on a fracture fixation plate, placed on the tibia of rabbits, showed good results on both antimicrobial properties and acceptance of the host-tissue within 28 days after surgery (47). Also the direct application of minocycline and rifampicin on titanium, placed in the distal femur of a rabbit, lead to good results on prevention of device colonisation and infection prevention within a week after surgery (48). A combined osteoconductive/antimicrobial coating (HA/tobramycin) on titanium, evaluated in the proximal tibia of a rabbit indicated the potential of a combined coating for infection prevention as well as implant incorporation (49). A recent study on a combined osteoconductive/osteoinductive/ antimicrobial coating (HA/RGD/gentamicin) on stainless steel showed promising results on bone integration and antibiotic release characteristics (33). Furthermore antibiotic releasing coatings on biodegradable substances could replace antibiotic containing polymethyl methacrylate (PMMA)-beads, in this case no implant coating would be necessary. A study on gentamicin coated poly(trimethylene carbonate) (PMTC), a biodegradable polymer, showed good results on antibiotic release, biofilm inhibition and biodegradability, suggesting to be a good substitute for PMMA-beads (50). A recent report on a prospective study of the first antibiotic releasing tibial nail

has shown promising clinical results with no deep surgical wound infections within the first six months after implantation (51). The major disadvantage for these coatings which they will face in the near future is the increasing number of antibiotic-resistant bacterial strains. This is the main reason why antimicrobial coatings, based on disinfectants or non-traditional antibiotics, are of great interest in research and development of such coatings.

3.2 Silver-based coatings

Silver is (amongst copper, lead and mercury) a potent antimicrobial heavy metal which has been related to medicine for many centuries. Instead of its metallic state, only the ionic state of silver is considered to be antimicrobial and its mode of function is multifactorial. Ionic silver not only reacts easily with amines and microbial DNA to prevent bacterial replication, but also with sulfhydryl groups of metabolic enzymes of the bacterial electron transport chain, resulting in their inactivation (52, 53). This also forms its treat to large scale clinical applications, since it can also inhibit eukaryotic metabolic function in a patient. Therefore a local release of silver ions is preferable. In contrast to lead and mercury silver does not appear to have cumulative toxic effects in the body, suggesting its potential as a coating component. The use of silver in releasing coatings currently spans from central venous catheters to urinary tract catheters and coated orthopaedic implants, with limited *in vivo* antimicrobial effectiveness as a main problem. While some studies show that silver coated surfaces can minimize the infection risk by lowering the bacterial load (54-57), to date, pre-clinical studies and randomized controlled trials of silver coated catheters, implants and external fixation pins were not able to prove its antimicrobial efficacy (52, 58-61).

4. Coating evaluation

Newly developed coatings need evaluation before implementation in the clinic to prevent possible adverse reactions to the coating. This evaluation includes mechanical testing and cytotoxicity and biocompatibility tests. In general these tests can be subdivided in three categories: *in vitro*, *in vivo* and *ex vivo* testing.

4.1 *In vitro* evaluation

This is defined as all testing modalities performed in controlled laboratory conditions, so outside of a living organism or its natural setting (Table 3).

4.1.1 Cytotoxicity tests

Cytotoxicity tests can be subdivided in cell viability, cell adhesion and cell spreading assays and are usually performed with fibroblastic cell lines (e.g. A529 (62), MC3T3-E1 (62-65), L929 (66), MG-63 (67, 68)). Cell viability assays evaluate the toxicity of a compound present in the vicinity of the cells either in solution or in a solid state. During these tests the material to be tested is incubated in cell culture medium. The resulting pre-conditioned culture medium is then used for cell-culture to evaluate the viability of the cells after exposure to the extracted medium from the material to be tested. Depending on the material, also direct cell culture on the material surface can be performed. The viability of the cells can e.g. be assessed by performing an MTT-assay.

- The MTT-assay is based on the reduction of 3-(4,5-dimethylthiazol-2-yl)-2,5-diphenyltetrazolium bromide (MTT, or another tetrazolium salt) to formazan by the enzyme succinate dehydrogenase in the mitochondria of living cells. The formed purple product can be measured spectrophotometrically and provides a direct measurement of the cell viability based on mitochondrial activity, hence energy metabolism (55, 64-70).
- Cell adhesion assays evaluate the potential of an implant surface to allow cell adhesion by culturing cells directly on the surface of the material to be tested. After allowing the cells to adhere to the surface, non-adhering cells are washed of the implant surface after which the adhering cells are double-stained with fluorescein diacetate (FDA) and ethidium bromide. In this live/death staining, FDA will stain the cytoplasm of intact cells green, while ethidium bromide will stain the DNA of dead cells red. The cell adhesion can be assessed by fluorescence microscopy. The ratio between the FDA-positive and ethidium bromide-positive cells provides insight into the live-dead percentage and thus biocompatibility of the culture surface. If the cells are only incubated with FDA, cell lysis allows quantification by fluorescence spectrophotometry. The level of fluorescent signal is an indication of cell adhesion on the material surface (64, 70, 71).

Table 3: *In vitro* analytical methods – part 1

Analytical method	Detection method	Detects	Ref.
Eukaryotic cultures			
Tetrazolium based assay • MTT • XTT • MTS	Spectrophotometric	Cell viability by metabolic activity • Reduction of a tetrazolium salt (yellow) to formazan (purple) by metabolically active cells	(55, 64-70)
FDA based assay • Fluorescein diacetate • DAPI	Fluorescence	Cell adhesion • Fluorescein diacetate→ cytoplasm of healthy cells (green) • DAPI → nuclei of every cell (blue)	(64, 70, 71)
Crystal violet	Spectrophotometric	Cell viability by DNA content • DNA staining, released dye indicates level of cell viability compared to control situation	(62)
SRB • Sulforhodamine B	Spectrophotometric	Cell density based on protein content • protein staining, released dye indicates amount of cells present compared to control situation	(72)
Phalloidinbased assay • Rhodamine • DAPI	Fluorescence	Actin staining • Rhodamine→ actin cytoskeleton (red) • DAPI → nuclei (blue)	(64, 68, 69, 73)
Alizarin Red S	Fluorescence	Osteogenic cells→ staining of calcium deposition (red)	(62)
ALP • Alkaline phosphatase	Spectrophotometric • Enzymatic assay	ALP activity is a marker for osteogenic potential of a cell • Enzymatic turnover of p-nitrophenyl phosphate to p-nitrophenol	(62, 63, 69, 74)
Live/dead staining • Fluorescein diacetate • Ethidium bromide	Fluorescence	Cell viability • Fluorescein diacetate→ cytoplasm of healthy cells (green) • Ethidium bromide → nuclei of death cells (red)	(65, 70)

Table 3: *In vitro* analytical methods – part 2

Analytical method	Detection method	Detects	Ref.
Prokaryotic cultures			
JIS Z 2801	Bacterial growth	Bacterial growth inhibition	(70, 73)
ASTM E-2810	Bacterial growth	Bacterial growth inhibition	(70)
Agar diffusion	Bacterial growth • Colony formation	Zone of inhibition, antibiotic potential of test compound • Distance antibiotic containing object to colony defines potency of antibiotic compound and its release system	(65)
MIC-MBC-assay	Bacterial growth • OD 600 measurements (MIC) • Quantitative bacterial culture (MBC)	Bacterial growth inhibition • Elevation in OD 600 indicates bacterial growth • Colony formation	(54, 55, 65, 69)
Other			
Immunocytochemistry	Light microscopy	Tissue specific staining	(62, 75)
Optical imaging	Fluorescence or bioluminescence • Fluorescence → emission after excitation • Bioluminescence → auto-emission	Presence of light emitting cells (e.g. cell growth or biofilm) • Fluorescence → GFP • Bioluminescence → luciferase	(76)
PCR	Fluorescence • SYBR-green related dyes	DNA/RNA expression	(62, 63)
Western blot	Chemiluminescence	Protein expression	(63)
SEM/TEM • Scanning electron microscopy • Transmission electron microscopy	Electron microscopy • Sputtering with gold or carbon for visualization	Evaluation of bacterial biofilm or extracellular matrix formation • SEM → Cell to surface interactions • TEM → Cell to cell interactions	(62-64, 66, 67, 73, 74)

- Cell spreading assays evaluate the potential of a surface to allow cell adhesion and proliferation including matrix formation in the case of e.g. osteocytes. There are multiple ways to assess this surface property. One of the methods described is the use of cell staining directly on the surface after cell culture on the material surface by e.g. crystal violet staining or by an actin staining based on phalloidin. The crystal violet staining is a DNA staining in which cells are fixed on the cultured surface, then incubated with crystal violet to stain the cellular DNA. After washing the stained cells the dye is released by the incubation in a weak acid. The released dye can be measured on a spectrophotometer and providing a quantitative measure for the amount of cells present on the surface. A phalloidin-based staining allows staining of the actin cytoskeleton and cellular organisation on the surface of a material. This is a direct cell staining which is visualized by fluorescence microscopy. In most cases the phalloidin based stainings are counterstained with DAPI (4',6-diamidino-2-phenylindole) to stain the cells nuclei, which allows visualisation of the individual cells and their cytoskeleton (62, 64, 68, 69, 73).
- Assays to assess the osteogenic potential, quantify the osteogenic potential of a coating. This can be determined by using cultured cells on the coating surface for an alkaline phosphatase assay (ALP). The ALP assay determines the ALP activity within the tissue, which is related to osteogenesis and bone deposition on the coating surface. Another method to assess the osteogenic potential of a coated surface is an alizarin red s staining, which stains calcified tissue (62, 63, 69, 74).

4.1.2 Antimicrobial coating tests

In the case of antimicrobial coatings the effect of the coating on bacteria can be assessed with a wide variety of assays, with the most well-known being the agar diffusion test where the release of an antimicrobial compound into the agar leads to an inhibition zone around the releasing material.

- Bacterial viability can be assessed by a minimal inhibitory concentration (MIC)/ minimal bactericidal concentration (MBC) assay. In this assay the releasing material is allowed to release its effective compound into a buffer or culture medium over a certain time span. The acquired pre-conditioned buffer/medium is then used in a bacterial culture setting in which a standardized amount of bacteria is exposed to the preconditioned buffer/medium. After 24 hours of incubation the optical density can be measured at 600 nm, the lowest concentration

which shows no increased optical density compared to the uncultured control condition defines the MIC, while the lowest concentration which shows no bacterial growth after incubation of the MIC-cultures on agar plates for another 24 hours defines the MBC (55).

- *In vitro* biofilm formation on a surface can be confirmed by incubating the surface in a bacterial suspension, rinsing the surface with an isotonic buffer (phosphate buffered saline, PBS) and use sonication to release the bacteria from the surface for quantitative culture.Or fix the bacteria on the surface with 2.5% glutaraldehyde/PBS for evaluation with SEM. This method can easily be transferred to the *in vivo* situation.
- International standards provide guidelines of how to assess coating stability and function, e.g. ISO 10993-5 provides guidelines for *in vitro* medical device evaluation. The Japanese Industrial Standard Z 2801 (JIS) describes a test for contact killing by the incubation of bacteria on a potential antimicrobial surface. Culturing of this surface provides insight on the antimicrobial properties of the evaluated coating (70, 73). The American Standard E-2810 (American Society for Testing and Materials, ASTM)) describes a test for contact killing by the application of a bacteria loaded agar onto the coated surface, after incubation the number of viable bacteria is determined (70).

4.2 *In vivo* evaluation

This is defined as all testing modalities performed in a controlled group of living organisms, often including clinically relevant parameters and a broad range of imaging techniques (Table 4).

The first models concerning orthopaedic conditions date back to the late 19th century, primarily focusing on osteomyelitis (77). Rodet described 2 basic methods to establish an osteomyelitis in a rabbit, the first one by inflicting a fracture and subsequent intravenous injection of the bacterium, resulting in an osteomyelitic lesion in the area of the fracture. The second method was performed by merely injecting bacteria intravenously, which resulted in a systemic infection with periosteal lesions leading to local osteomyelitis (77).

The most well-known model for osteomyelitis is the model by Norden *et al.*; this model describes the direct percutaneous injection, directly into the tibial intramedullary cavity of a rabbit, of both a sclerosing agent (sodium morrhuate, bile salts from codfish) and *S. aureus* (78). Andriole *et al.* however, established one of the first osteomyelitis models with a foreign object. Their model was based on a tibial fracture and subsequent tibial stabilisation by a stainless steel pin, contaminated

with *S. aureus* (79). Together with the model by Norden, the model of Andriole mainly forms the basis for current animal models used for the evaluation of implant coatings. In general, rabbits are still the most frequently used animal species for these experimental studies, but there have also been successful models in mice, rats, dogs and sheep. During the years, models increased in complexity and included multifactorial parameters.

The bone bonding properties of apatite-coated implants were first evaluated in dogs by Geesink *et al*. (16). After the development of these apatite-coated implants, Vogely *et al.* described a rabbit proximal tibial model for the evaluation of hydroxyapatite coated titanium implants in an implant site infection (80). Darouiche was one of the first to described a rabbit lateral femoral condyle model for the evaluation of antimicrobial coatings on titanium (48). Poultsides *et al*. described a haematogeneous implant contamination model by MRSA (81). Moojen evaluated a combined coating with both osteoconductive (peri-apatite) and antimicrobial (tobramycin) properties in a proximal tibial implant infection model in rabbits (49). Also, Moskowitz *et al*. developed antibiotic multilayer implant coatings with an antibiotic release of over 4 weeks in a 2 stage rabbit distal femoral condyle infection model. The first surgical stage contained the initial infection with the insertion of a pre-colonized peg, the second surgical stage was the removal of the peg and implantation of the antibiotic coated implant (65). Alt *et al*. was one of the first to describe a coating which combined osteoconductive (hydroxyapatite), osteoinductive (RGD) and antibiotic (gentamicin) properties in an experimental rabbit implant infection model (33).

4.2.1 Clinical parameters

Body weight and temperature provide general information about the animal's physical condition, with weight loss and fever in case of an infection. Leucocyte differentiation provides a detailed overview of the percentages of lymphocytes, neutrophillic granulocytes, monocytes, basophilic granulocytes and eosinophilic granulocytes in the total leucocyte population. An elevated number of leucocytes or a shift in differentiation indicates a bacterial infection. The ESR is based on the fibrinogen balance in the blood. In case of an inflammation or infection the fibrinogen levels increase, resulting in agglutination of erythrocytes with sedimentation as a result. CRP is an acute phase protein whose levels rapidly increase in case of inflammation or infection. ESR and CRP both only indicate the presence of inflammation or infection, never the cause or the location (82).

4.2.2 Imaging modalities

- Optical imaging (based on fluorescence and bioluminescence) is based on the detection of light emitted from the body. The use of fluorescently labelled antibodies results in a very specific signal, although resulting in a very local detection, it also requires a large amount of antibodies when used in humans. This renders large scale use in humans not yet profitable (76). Also bioluminescence can be used to visualize infection. The main disadvantage of bioluminescence is the requirement of the luciferase gene in the cell to be detected, meaning the use of genetically modified organisms in case of detection by either autologous cells or bacteria. E.g. a bacterium expressing luciferase can be used to monitor an implant infection initiated with that bacterium (76). Both methods are currently available in laboratory animal setting.
- X-ray radiographs are by far the oldest imaging technique and the most frequently used imaging technique to assess fractures, implant fixation, location and loosening but also for the differential diagnosis of bone diseases like osteomyelitis. The use of X-rays is cost effective, they are easy to obtain and have a relatively low burden for the patient. An X-ray only provides detailed information about the mineralized tissue (or the lack thereof) and the disease related bone morphological changes accompanied with it (15, 83, 84).
- CT (computed tomography) is a 3D-imaging technique which uses X-rays to construct a 3D image of the mineralized tissue in a patient. It generally provides more in-depth data about the density of the mineralized tissue and bone remodelling compared to X-rays, however imaging of metallic implants can result in scattering of the X-rays resulting in a blur around the implant, rendering data-analysis difficult (76, 85, 86).
- DEXA (dual energy X-ray absorptiometry) is often incorrectly stated as a bone scan. The use of 2 different energy levels of the X-ray beam allows accurate determination of the bone mineral density. DEXA is the most common imaging technique to diagnose osteoporosis and is seldomly used in *in vivo* coating assessment studies (86).
- MRI (magnetic resonance imaging) does, in contrast to other imaging techniques, not rely on ionizing radiation but on the magnetic spin of protons. Due to the high water content (and thus protons) of soft tissue, MRI is one of the main imaging techniques to assess the musculoskeletal tissues, like cartilage and tendons. MRI only allows indirect imaging of bony structures due to the limited water content of the bone. The main drawbacks for MRI are the

duration of the imaging acquisition and the inability for it to be used in combination with metallic implants (76, 84).

- PET (positron emission tomography) is based on the detection of the annihilation event of a positron with an electron (beta-decay). Every annihilation-event results in 2 gamma-photons in an opposite direction from the point of decay. The detections of the photons on the detectorring of the scanner results in a 3D image (97). ^{18}F is one of the most frequently used isotopes (connected to a carrier molecule) to serve as a PET-tracer in orthopaedic research. ^{18}F-fluorodeoxyglucose (FDG) is used for the detection of infection and inflammation (figure 2) and ^{18}F-sodium fluoride as a tracer for bone remodelling (85, 94, 98). With signal specificity as its advantage, PET does not provide anatomical information, merely the location of the tracer uptake. This is the main reason why PET and CT are often combined in the clinic.
- Bone scan (bone scintigraphy) is based on the direct detection of gamma radiation originating from the injected tracer molecule (often ^{99m}Tc, ^{67}Ga or ^{111}In) connected to a specific ligand which allows tissue specific binding and thus imaging. A bone scan provides two-dimensional images of the patient, which are sufficient in the clinic for the diagnosis (84).
- SPECT (single photon emission computed tomography) on the other hand allows acquisition of three-dimensional images, providing more insight in size and localisation of certain pathology. In general, bone scan/SPECT-tracers have a longer half-life than PET tracers making them more cost-effective to produce. Just like PET, SPECT provides limited anatomical information and is therefore often combined with CT in the clinic (76).

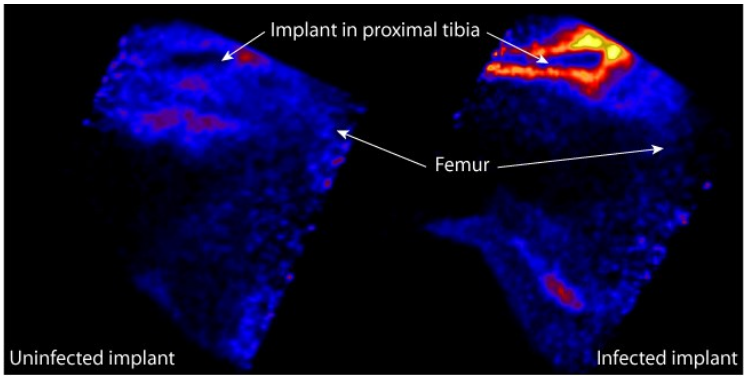

Figure 2: ^{18}F-FDG PET of an uninfected implant versus an infected implant in the proximal part of a rabbit tibia, six weeks after surgery. The increased tracer uptake around the infected implant (black area) depicts the local osteomyelitic lesion.

Table 4: *In vivo* analytical methods – part 1

Analytical method	Detection method	Detects	Ref.
Clinical parameters			
Body weight	Weighing scale	General physical condition • Weight loss after surgical intervention, returns to pre-operative values within first weeks after intervention. • Persistent weight loss indicates animal discomfort, infection or another systemic event related to device or intervention.	(49, 78, 79, 81, 87)
Temperature	Thermal probe	General physical condition • Post-operative thermal elevation, returns to normal within days after surgery. • Persistent elevation indicates infection or another systemic event related to device or intervention.	(49, 81)
ESR • Erythrocyte sedimentation rate	Anticoagulated blood • Capillary tube	Infection by increase of erythrocyte sedimentation • Elevation in first post-operative week due to surgical intervention. • Remains elevated in case of infection.	(49, 78, 80, 81, 88)
CRP • C-reactive protein	Serum/plasma • ELISA	Infection by increase of CRP levels • Elevation in first post-operative week due to surgical intervention. • Remains elevated in case of infection.	(84)
Leucocyte count and Leucocyte differentiation	Anticoagulated blood • Cell count	Infection by shift in leucocyte distribution • ↑ Neutrophils and monocytes → bacterial infection • ↑ Lymphocytes → viral infection or tumor • ↑ Basophils and eosinophils→ inflammatory processes and/or allergic reactions	(49, 65, 78, 80, 81, 84, 88)

Table 4: *In vivo* analytical methods – part 2

Analytical method	Detection method	Detects	Ref.
Imaging modalities			
Optical imaging	Fluorescence or bioluminescence • Fluorescence → emission after excitation • Bioluminescence → auto-emission	Presence of light emitting cells • Fluorescence → GFP • Bioluminescence → luciferase	(76)
X-ray	Electromagnetic radiation	Bone, bone pathology and metal objects	(33, 49, 76, 78-81, 84, 87-94)
CT • Computed tomography	Electromagnetic radiation • X-ray (3D)	Bone, bone pathology and metal objects	(76, 84, 86, 88, 91, 94)
DEXA • Dual energy X-ray absorptiometry	Electromagnetic radiation • Dual energy X-ray of same object	Bone density • Difference between X-rays allows calculation of bone density	(86)
MRI • Magnetic resonance imaging	Nuclear magnetic resonance • Proton magnetic spin resonance (3D)	Soft tissue • Detection of tissues with a high water content	(76, 84, 88)
Bone scintigraphy	γ-radiation • Single photon emission (2D)	Active bone remodeling • ^{99m}Tc –MDP → increased osteogenesis • ^{67}Ga-citrate → leucocyte activation (e.g. infection)	(84, 88, 95)
SPECT • Single photon emission computed tomography	γ-radiation • Single photon emission (3D)	Active bone remodeling • ^{99m}Tc –MDP → increased osteogenesis • ^{67}Ga-citrate → leucocyte activation (e.g. infection)	(76, 88)
PET • Positron emission tomography	γ-radiation • Positron mediated dual photon emission (3D)	Active bone remodeling and infection • ^{18}F-Fluorodeoxyglucose → inflammation and infection • ^{18}F-Sodium fluoride→ active bone remodeling	(76, 84, 88, 91-94)

Table 4: *In vivo* analytical methods – part 3

Analytical method	Detection method	Detects	Ref.
Other – *Ex vivo*			
Calcium binding fluorophores • Calcein blue • Calcein green • Tetracycline • Xylenol orange • Alizarin red S	Fluorescence (excitation/emission) • Calcein blue (370 / 435 nm) • Calcein green (470 / 530 nm) • Tetracycline (390 / 570 nm) • Xylenol orange (470 / 610 nm) • Alizarin red S (550 / 620 nm)	Calcium deposition during bone remodeling (color) • Calcein blue →blue • Calcein green →green • Tetracycline → yellow • Xylenol orange→ orange/red • Alizarin red S → red	(96)
Histology • Paraffin • PMMA	Light microscopy	Tissue specific staining (including bacteria) • Haematoxylin/eosin staining (general) • Masson Goldnertrichrome staining (general) • Gram staining (bacteria) • Wear particles (e.g. polyethylene by polarized light) • Immunostaining (antibody specific)	(33, 49, 75, 79-81, 84, 87, 90-94)
SEM • Scanning electron microscopy	Electron microscopy	Surface treatment, bacterial biofilm, wear particles • Surface assessment of non-metallic substrates by gold or carbon sputtering • Metallic substrates can be assessed directly	(65, 80)
Bacterial/bone culture • Tissue swaps • Bone homogenates	(Selective) culture media • Tryptic soy agar/broth • Tellurite glycine agar (selective for coagulase negative Staphylococci)	Bacterial growth under specific circumstances • Quantification by colony count or OD 600 measurements	(48, 49, 65, 78-81, 84, 87, 89-94)

4.3 *Ex vivo* analysis

- Calcium binding fluorophores (like calcein green, blue and xylenol orange) are being used for the *in vivo* labeling of the calcium deposition at the time of injection. The use of different fluorophores, emitting at different wavelengths, allow post-mortem visualisation of the calcium deposition during the experimental follow-up (96). This provides the opportunity to determine implant ingrowth and bone remodelling in a normal healthy situation and periosteal elevation and calcification during the progression of an osteomyelitis (Figure 3).

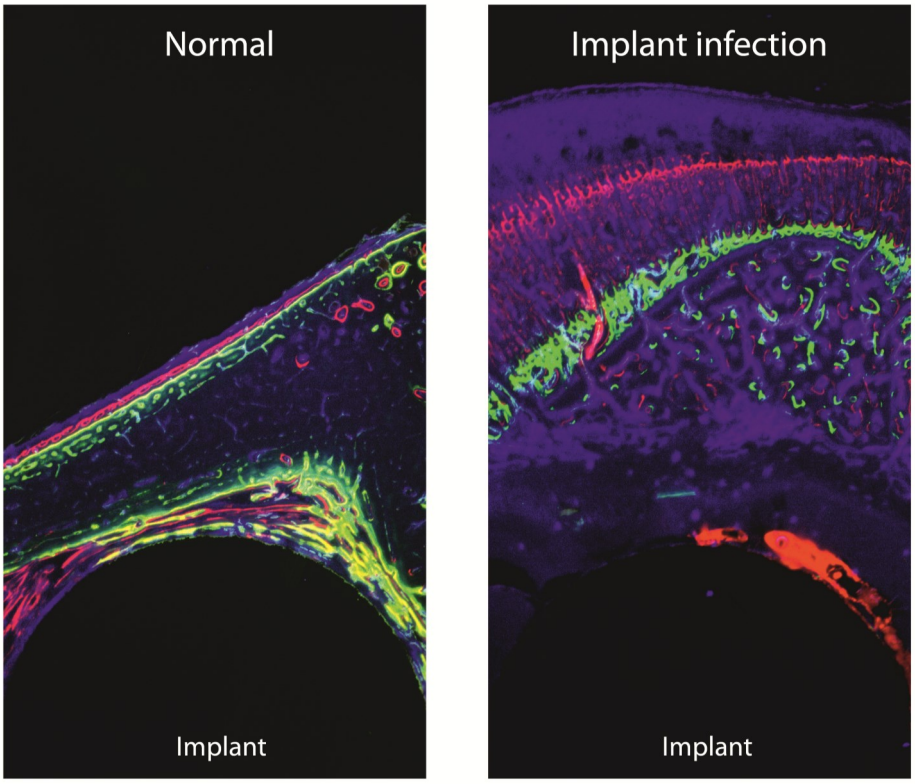

Figure 3: The use of calcium binding fluorophores, depicted in 50 micron PMMA sections, of a rabbit tibial intramedullary nail model, to address normal bone remodelling and bone remodelling in case of an implant infection. Calcein green was injected at 2 weeks, xylenol orange at 4 weeks and calcein blue at 6 weeks. In the case of normal bone remodelling, calcium deposition is detected around the implant, combined with bone remodelling of the cortical wall. In case of an implant infection the most calcium deposition is located in the outer cortical wall depicting the periosteal elevation and calcification during the 6 week follow-up.

- Histology is a commonly used method to assess the tissue in the implant area on e.g. tissue morphology or bacterial presence. Tissue sections with metallic implants generally require embedding in methyl methacrylate, instead of paraffin, with the inability to allow immunostainings as a major drawback. Still it provides the unique opportunity to assess the tissue-implant interface (33, 49, 57, 80).
- Electronmicroscopy allows analysis of the implant surface (with or without coating) after distraction from the surrounding tissue. This can include analysis of the bone matrix-implant interface but also analysis of a formed biofilm (31).

5. Conclusion

Both osteointegration and infections are of concern in implants and prosthesis used in the field of orthopaedic and trauma surgery. Metallic alloys used for plating and nailing of fractures and joint replacements are the largest group of these implants. Hydroxyapatite coatings have proven to be successful to promote osseous integration of uncemented total hip prosthesis. During the last years the focus on coating development has shifted from osteoconductive coatings (like hydroxyapatite) towards osteoinductive coatings to support bone remodelling (like RGD and BMP coatings) and antimicrobial coatings for implant infection treatment and prophylaxis (like silver or antibiotic releasing coatings).

Plasma spraying is the most used and accepted method for hydroxyapatite coatings. Other coating techniques which do not require high temperatures are necessary for the application of bioactive coatings that promote osteogenesis and/or prevent infections.

With the current palette of *in vitro* (e.g. MTT, ALP and SEM), *in vivo* (e.g. ESR, CT and PET) and *ex vivo* techniques (e.g. bacterial culture, calcium binding fluorophores and histology), we can thoroughly evaluate novel implant coatings in a qualitative and quantitative fashion. The strength of such an evaluation will always lie in the combination of the individual methods, leading to a complete, broad-spectrum analysis on coating toxicity and efficacy.

References

1. Adams JE. A simple method of mechanical fixation for fracture of long bones. British Medical Journal. 1918 Jan 5;1(2975):12-3.
2. Devas MB. Arthroplasty of the hip: A review of 110 cup and replacement arthroplasties. Journal of Bone and Joint Surgery (British Volume). 1954 Nov;36-B(4):561-6.
3. Judet J, Judet R. The use of an artificial femoral head for arthroplasty of the hip joint. Journal of Bone and Joint Surgery (British Volume). 1950 May;32-B(2):166-73.
4. Surveillance report: Annual epidemiological report, reporting on 2009 surveillance data and 2010 epidemic intelligence data. http://ecdc.europa.eu/en/publications/publications/0910_sur_annual_epidemiological_report_on_communicable_diseases_in_europe.pdf (Accessed December 2012): European Centre for Disease prevention and Control; 2011.
5. Dale H, Hallan G, Espehaug B, Havelin LI, Engesaeter LB. Increasing risk of revision due to deep infection after hip arthroplasty. Acta Orthopaedica. 2009 Dec;80(6):639-45.
6. Healthcare-associated infections - fact sheet. http://www.who.int/gpsc/country_work/gpsc_ccisc_fact_sheet_en.pdf (Accessed December 2012): World Health organisation; 2012.
7. Surveillance of healthcare-associated infections in europe. http://www.ecdc.europa.eu/en/publications/Publications/120215_SUR_HAI_2007.pdf (Accessed December 2012): European Centre of Disease prevention and Control; 2007.
8. Capello WN, D'Antonio JA, Jaffe WL, Geesink RG, Manley MT, Feinberg JR. Hydroxyapatite-coated femoral components: 15-year minimum followup. Clinical Orthopaedics and Related Research. 2006 Dec;453:75-80.
9. Tannast M, Najibi S, Matta JM. Two to twenty-year survivorship of the hip in 810 patients with operatively treated acetabular fractures. Journal of Bone and Joint Surgery (American Volume). 2012 Sep 5;94(17):1559-67.
10. Gristina AG. Biomaterial-centered infection: Microbial adhesion versus tissue integration. Science. 1987 Sep 25;237(4822):1588-95.
11. Busscher HJ, van der Mei HC, Subbiahdoss G, Jutte PC, van den Dungen JJ, Zaat SA, Schultz MJ, Grainger DW. Biomaterial-associated infection: Locating the finish line in the race for the surface. Science Translational Medicine. 2012 Sep 26;4(153):153rv10.
12. Arciola CR, Campoccia D, Speziale P, Montanaro L, Costerton JW. Biofilm formation in staphylococcus implant infections. A review of molecular mechanisms and implications for biofilm-resistant materials. Biomaterials. 2012 Sep;33(26):5967-82.
13. Geurts J, Chris Arts JJ, Walenkamp GH. Bone graft substitutes in active or suspected infection. Contra-indicated or not? Injury. 2011 Sep;42 Suppl 2:S82-6.
14. Geesink RG. Osteoconductive coatings for total joint arthroplasty. Clinical Orthopaedics and Related Research. 2002 Feb(395):53-65.
15. Geesink RG, de Groot K, Klein CP. Chemical implant fixation using hydroxyl-apatite coatings. The development of a human total hip prosthesis for chemical fixation to bone using hydroxyl-apatite coatings on titanium substrates. Clinical Orthopaedics and Related Research. 1987 Dec(225):147-70.
16. Geesink RG, de Groot K, Klein CP. Bonding of bone to apatite-coated implants. Journal of Bone and Joint Surgery (British Volume). 1988 Jan;70(1):17-22.
17. Smabrekke A, Espehaug B, Havelin LI, Furnes O. Operating time and survival of primary total hip replacements: An analysis of 31,745 primary cemented and uncemented total hip replacements from local hospitals reported to the norwegian arthroplasty register 1987-2001. Acta Orthopaedica Scandinavica. 2004 Oct;75(5):524-32.
18. LeGeros RZ. Properties of osteoconductive biomaterials: Calcium phosphates. Clinical Orthopaedics and Related Research. 2002 Feb(395):81-98.
19. Jarcho M. Calcium phosphate ceramics as hard tissue prosthetics. Clinical Orthopaedics and Related Research. 1981 Jun(157):259-78.
20. Geesink RG. Hydroxyapatite-coated total hip prostheses. Two-year clinical and roentgenographic results of 100 cases. Clinical Orthopaedics and Related Research. 1990 Dec(261):39-58.

21. Charles LF, Shaw MT, Olson JR, Wei M. Fabrication and mechanical properties of plla/pcl/ha composites via a biomimetic, dip coating, and hot compression procedure. Journal of Materials Science: Materials in Medicine. 2010 Jun;21(6):1845-54.
22. Ding SJ. Properties and immersion behavior of magnetron-sputtered multi-layered hydroxyapatite/ titanium composite coatings. Biomaterials. 2003 Oct;24(23):4233-8.
23. Saju KK, Reshmi R, Jayadas NH, James J, Jayaraj MK. Polycrystalline coating of hydroxyapatite on tial6v4 implant material grown at lower substrate temperatures by hydrothermal annealing after pulsed laser deposition. Proceedings of the Institution of Mechanical Engineers Part H: Journal of Engineering in Medicine. 2009 Nov;223(8):1049-57.
24. Zhao J, Xiao S, Lu X, Wang J, Weng J. A study on improving mechanical properties of porous ha tissue engineering scaffolds by hot isostatic pressing. Biomed Mater. 2006 Dec;1(4):188-92.
25. Boccaccini AR, Keim S, Ma R, Li Y, Zhitomirsky I. Electrophoretic deposition of biomaterials. J R Soc Interface. 2010 Oct 6;7 Suppl 5:S581-613.
26. Leeuwenburgh S, Wolke J, Schoonman J, Jansen J. Electrostatic spray deposition (esd) of calcium phosphate coatings. J Biomed Mater Res A. 2003 Aug 1;66(2):330-4.
27. Leeuwenburgh SC, Wolke JG, Siebers MC, Schoonman J, Jansen JA. In vitro and in vivo reactivity of porous, electrosprayed calcium phosphate coatings. Biomaterials. 2006 Jun;27(18):3368-78.
28. Heimann RB. Thermal spraying of biomaterials. Surf Coat Technol. 2006 Oct 25;201(5):2012-9.
29. Kim HW, Knowles JC, Salih V, Kim HE. Hydroxyapatite and fluor-hydroxyapatite layered film on titanium processed by a sol-gel route for hard-tissue implants. J Biomed Mater Res B Appl Biomater. 2004 Oct 15;71(1):66-76.
30. Vidigal GM, Jr., Groisman M, de Sena LA, Soares Gde A. Surface characterisation of dental implants coated with hydroxyapatite by plasma spray and biomimetic process. Implant Dentistry. 2009 Aug;18 (4):353-61.
31. Leeuwenburgh SC, Wolke JG, Lommen L, Pooters T, Schoonman J, Jansen JA. Mechanical properties of porous, electrosprayed calcium phosphate coatings. J Biomed Mater Res A. 2006 Sep 1;78(3):558-69.
32. O'Flynn KP, Stanton KT. Optimisation of the enamelling of an apatite-mullite glass-ceramic coating on ti6al4v. Journal of Materials Science: Materials in Medicine. 2011 Sep;22(9):2035-44.
33. Alt V, Bitschnau A, Bohner F, Heerich KE, Magesin E, Sewing A, Pavlidis T, Szalay G, Heiss C, Thormann U, Hartmann S, Pabst W, Wenisch S, Schnettler R. Effects of gentamicin and gentamicin-rgd coatings on bone ingrowth and biocompatibility of cementless joint prostheses: An experimental study in rabbits. Acta Biomater. 2011 Mar;7(3):1274-80.
34. Liu Y, Hunziker EB, Layrolle P, De Bruijn JD, De Groot K. Bone morphogenetic protein 2 incorporated into biomimetic coatings retains its biological activity. Tissue Engineering. 2004 Jan-Feb;10(1-2):101-8.
35. Ardjomandi N, Klein C, Kohler K, Maurer A, Kalbacher H, Niederlander J, Reinert S, Alexander D. Indirect coating of rgd peptides using a poly-l-lysine spacer enhances jaw periosteal cell adhesion, proliferation, and differentiation into osteogenic tissue. J Biomed Mater Res A. 2012 Aug;100(8):2034-44.
36. Wang YJ, Lin FH, Sun JS, Huang YC, Chueh SC, Hsu FY. Collagen-hydroxyapatite microspheres as carriers for bone morphogenic protein-4. Artificial Organs. 2003 Feb;27(2):162-8.
37. Sun JS, Lin FH, Wang YJ, Huang YC, Chueh SC, Hsu FY. Collagen-hydroxyapatite/tricalcium phosphate microspheres as a delivery system for recombinant human transforming growth factor-beta 1. Artificial Organs. 2003 Jul;27(7):605-12.
38. Haidar ZS, Tabrizian M, Hamdy RC. A hybrid rhop-1 delivery system enhances new bone regeneration and consolidation in a rabbit model of distraction osteogenesis. Growth Factors. 2010 Feb;28(1):44-55.
39. Knippenberg M, Helder MN, Zandieh Doulabi B, Wuisman PI, Klein-Nulend J. Osteogenesis versus chondrogenesis by bmp-2 and bmp-7 in adipose stem cells. Biochemical and Biophysical Research Communications. 2006 Apr 14;342(3):902-8.
40. Liu Y, Wu G, de Groot K. Biomimetic coatings for bone tissue engineering of critical-sized defects. J R Soc Interface. 2010 Oct 6;7 Suppl 5:S631-47.
41. Liu Y, de Groot K, Hunziker EB. Bmp-2 liberated from biomimetic implant coatings induces and sustains direct ossification in an ectopic rat model. Bone. 2005 May;36(5):745-57.
42. Crockarell JR, Hanssen AD, Osmon DR, Morrey BF. Treatment of infection with debridement and retention of the components following hip arthroplasty. Journal of Bone and Joint Surgery (American Volume). 1998 Sep;80(9):1306-13.

43. Kim YH, Kim JS, Park JW, Joo JH. Cementless revision for infected total hip replacements. Journal of Bone and Joint Surgery (British Volume). 2011 Jan;93(1):19-26.
44. Walenkamp GH. Gentamicin pmma beads and other local antibiotic carriers in two-stage revision of total knee infection: A review. Journal of Chemotherapy. 2001 Nov;13 Spec No 1(1):66-72.
45. Walenkamp GH, Kleijn LL, de Leeuw M. Osteomyelitis treated with gentamicin-pmma beads: 100 patients followed for 1-12 years. Acta Orthopaedica Scandinavica. 1998 Oct;69(5):518-22.
46. Rasyid HN, van der Mei HC, Frijlink HW, Soegijoko S, van Horn JR, Busscher HJ, Neut D. Concepts for increasing gentamicin release from handmade bone cement beads. Acta Orthopaedica. 2009 Oct;80 (5):508-13.
47. Kalicke T, Schierholz J, Schlegel U, Frangen TM, Koller M, Printzen G, Seybold D, Klockner S, Muhr G, Arens S. Effect on infection resistance of a local antiseptic and antibiotic coating on osteosynthesis implants: An in vitro and in vivo study. Journal of Orthopaedic Research. 2006 Aug;24(8):1622-40.
48. Darouiche RO, Mansouri MD, Zakarevicz D, Alsharif A, Landon GC. In vivo efficacy of antimicrobial-coated devices. Journal of Bone and Joint Surgery (American Volume). 2007 Apr;89(4):792-7.
49. Moojen DJ, Vogely HC, Fleer A, Nikkels PG, Higham PA, Verbout AJ, Castelein RM, Dhert WJ. Prophylaxis of infection and effects on osseointegration using a tobramycin-periapatite coating on titanium implants--an experimental study in the rabbit. Journal of Orthopaedic Research. 2009 Jun;27(6):710-6.
50. Neut D, Kluin OS, Crielaard BJ, van der Mei HC, Busscher HJ, Grijpma DW. A biodegradable antibiotic delivery system based on poly-(trimethylene carbonate) for the treatment of osteomyelitis. Acta Orthopaedica. 2009 Oct;80(5):514-9.
51. Fuchs T, Stange R, Schmidmaier G, Raschke MJ. The use of gentamicin-coated nails in the tibia: Preliminary results of a prospective study. Archives of Orthopaedic and Trauma Surgery. 2011 Oct;131 (10):1419-25.
52. Darouiche RO. Anti-infective efficacy of silver-coated medical prostheses. Clinical Infectious Diseases. 1999 Dec;29(6):1371-7; quiz 8.
53. Petering HG. Pharmacology and toxicology of heavy metals: Silver. Pharmacology & Therapeutics Part A: Chemotherapy, Toxicology and Metabolic Inhibitors. 1976;1(2):4.
54. Shimazaki T, Miyamoto H, Ando Y, Noda I, Yonekura Y, Kawano S, Miyazaki M, Mawatari M, Hotokebuchi T. In vivo antibacterial and silver-releasing properties of novel thermal sprayed silver-containing hydroxyapatite coating. J Biomed Mater Res B Appl Biomater. 2010 Feb;92(2):386-9.
55. Chen W, Liu Y, Courtney HS, Bettenga M, Agrawal CM, Bumgardner JD, Ong JL. In vitro anti-bacterial and biological properties of magnetron co-sputtered silver-containing hydroxyapatite coating. Biomaterials. 2006 Nov;27(32):5512-7.
56. Moseke C, Gbureck U, Elter P, Drechsler P, Zoll A, Thull R, Ewald A. Hard implant coatings with antimicrobial properties. Journal of Materials Science: Materials in Medicine. 2011 Dec;22(12):2711-20.
57. Badiou W, Lavigne JP, Bousquet PJ, O'Callaghan D, Mares P, de Tayrac R. In vitro and in vivo assessment of silver-coated polypropylene mesh to prevent infection in a rat model. Int Urogynecol J. 2011 Mar;22 (3):265-72.
58. Moojen DJ, Vogely HC, Fleer A, Verbout AJ, Castelein RM, Dhert WJ. No efficacy of silver bone cement in the prevention of methicillin-sensitive staphylococcal infections in a rabbit contaminated implant bed model. Journal of Orthopaedic Research. 2009 Aug;27(8):1002-7.
59. Coester LM, Nepola JV, Allen J, Marsh JL. The effects of silver coated external fixation pins. Iowa Orthopaedic Journal. 2006;26:48-53.
60. Masse A, Bruno A, Bosetti M, Biasibetti A, Cannas M, Gallinaro P. Prevention of pin track infection in external fixation with silver coated pins: Clinical and microbiological results. Journal of Biomedical Materials Research. 2000 Sep;53(5):600-4.
61. Pickard R, Lam T, MacLennan G, Starr K, Kilonzo M, McPherson G, Gillies K, McDonald A, Walton K, Buckley B, Glazener C, Boachie C, Burr J, Norrie J, Vale L, Grant A, N'Dow J. Antimicrobial catheters for reduction of symptomatic urinary tract infection in adults requiring short-term catheterisation in hospital: A multicentre randomised controlled trial. Lancet. 2012 Dec 1;380(9857):1927-35.
62. Evans ND, Gentleman E, Chen X, Roberts CJ, Polak JM, Stevens MM. Extracellular matrix-mediated osteogenic differentiation of murine embryonic stem cells. Biomaterials. 2010 Apr;31(12):3244-52.
63. Jung GY, Park YJ, Han JS. Effects of ha released calcium ion on osteoblast differentiation. Journal of Materials Science: Materials in Medicine. 2010 May;21(5):1649-54.

64. Kapoor R, Sistla PG, Kumar JM, Raj TA, Srinivas G, Chakraborty J, Sinha MK, Basu D, Pande G. Comparative assessment of structural and biological properties of biomimetically coated hydroxyapatite on alumina (alpha-al2o3) and titanium (ti-6al-4v) alloy substrates. J Biomed Mater Res A. 2010 Sep 1;94(3):913-26.
65. Moskowitz JS, Blaisse MR, Samuel RE, Hsu HP, Harris MB, Martin SD, Lee JC, Spector M, Hammond PT. The effectiveness of the controlled release of gentamicin from polyelectrolyte multilayers in the treatment of staphylococcus aureus infection in a rabbit bone model. Biomaterials. 2010 Aug;31 (23):6019-30.
66. Qiang F, Rahaman MN, Nai Z, Wenhai H, Deping W, Liying Z, Haifeng L. In vitro study on different cell response to spherical hydroxyapatite nanoparticles. Journal of Biomaterials Applications. 2008 Jul;23 (1):37-50.
67. De Carlos A, Lusquinos F, Pou J, Leon B, Perez-Amor M, Driessens FC, Hing K, Best S, Bonfield W. In vitro testing of nd:Yag laser processed calcium phosphate coatings. Journal of Materials Science: Materials in Medicine. 2006 Nov;17(11):1153-60.
68. Kazemzadeh-Narbat M, Noordin S, Masri BA, Garbuz DS, Duncan CP, Hancock RE, Wang R. Drug release and bone growth studies of antimicrobial peptide-loaded calcium phosphate coating on titanium. J Biomed Mater Res B Appl Biomater. 2012 Jul;100(5):1344-52.
69. Hu H, Zhang W, Qiao Y, Jiang X, Liu X, Ding C. Antibacterial activity and increased bone marrow stem cell functions of zn-incorporated tio2 coatings on titanium. Acta Biomater. 2012 Feb;8(2):904-15.
70. Khalilpour P, Lampe K, Wagener M, Stigler B, Heiss C, Ullrich MS, Domann E, Schnettler R, Alt V. Ag/sio (x)c(y) plasma polymer coating for antimicrobial protection of fracture fixation devices. J Biomed Mater Res B Appl Biomater. 2010 Jul;94(1):196-202.
71. Lanfer B, Seib FP, Freudenberg U, Stamov D, Bley T, Bornhauser M, Werner C. The growth and differentiation of mesenchymal stem and progenitor cells cultured on aligned collagen matrices. Biomaterials. 2009 Oct;30(30):5950-8.
72. Vichai V, Kirtikara K. Sulforhodamine b colorimetric assay for cytotoxicity screening. Nature Protocols. 2006;1(3):1112-6.
73. Necula BS, van Leeuwen JP, Fratila-Apachitei LE, Zaat SA, Apachitei I, Duszczyk J. In vitro cytotoxicity evaluation of porous tio(2)-ag antibacterial coatings for human fetal osteoblasts. Acta Biomater. 2012 Nov;8(11):4191-7.
74. Goransson A, Arvidsson A, Currie F, Franke-Stenport V, Kjellin P, Mustafa K, Sul YT, Wennerberg A. An in vitro comparison of possibly bioactive titanium implant surfaces. J Biomed Mater Res A. 2009 Mar 15;88(4):1037-47.
75. Woods GL, Walker DH. Detection of infection or infectious agents by use of cytologic and histologic stains. Clinical Microbiology Reviews. 1996 Jul;9(3):382-404.
76. Tremoleda JL, Khalil M, Gompels LL, Wylezinska-Arridge M, Vincent T, Gsell W. Imaging technologies for preclinical models of bone and joint disorders. EJNMMI Res. 2011;1(1):11.
77. Rodet A. The classic. An experimental study on infectious osteomyelitis. Clinical Orthopaedics and Related Research. 1973 Oct;99(96):3-4.
78. Norden CW. Experimental osteomyelitis. I. A description of the model. Journal of Infectious Diseases. 1970 Nov;122(5):410-8.
79. Andriole VT, Nagel DA, Southwick WO. A paradigm for human chronic osteomyelitis. Journal of Bone and Joint Surgery (American Volume). 1973 Oct;55(7):1511-5.
80. Vogely HC, Oosterbos CJ, Puts EW, Nijhof MW, Nikkels PG, Fleer A, Tonino AJ, Dhert WJ, Verbout AJ. Effects of hydrosyapatite coating on ti-6a1-4v implant-site infection in a rabbit tibial model. Journal of Orthopaedic Research. 2000 May;18(3):485-93.
81. Poultsides LA, Papatheodorou LK, Karachalios TS, Khaldi L, Maniatis A, Petinaki E, Malizos KN. Novel model for studying hematogenous infection in an experimental setting of implant-related infection by a community-acquired methicillin-resistant s. Aureus strain. Journal of Orthopaedic Research. 2008 Oct;26(10):1355-62.
82. Shih LY, Wu JJ, Yang DJ. Erythrocyte sedimentation rate and c-reactive protein values in patients with total hip arthroplasty. Clinical Orthopaedics and Related Research. 1987 Dec(225):238-46.
83. Calhoun JH, Manring MM, Shirtliff M. Osteomyelitis of the long bones. Seminars in Plastic Surgery. 2009 May;23(2):59-72.

84. Zimmerli W. Infection and musculoskeletal conditions: Prosthetic-joint-associated infections. Best Practice & Research: Clinical Rheumatology. 2006 Dec;20(6):1045-63.
85. Monjo M, Lamolle SF, Lyngstadaas SP, Ronold HJ, Ellingsen JE. In vivo expression of osteogenic markers and bone mineral density at the surface of fluoride-modified titanium implants. Biomaterials. 2008 Oct;29(28):3771-80.
86. MacNeil JA, Boyd SK. Accuracy of high-resolution peripheral quantitative computed tomography for measurement of bone quality. Medical Engineering and Physics. 2007 Dec;29(10):1096-105.
87. Sanzen L, Linder L. Infection adjacent to titanium and bone cement implants: An experimental study in rabbits. Biomaterials. 1995 Nov;16(16):1273-7.
88. El-Maghraby TA, Moustafa HM, Pauwels EK. Nuclear medicine methods for evaluation of skeletal infection among other diagnostic modalities. Quarterly Journal of Nuclear Medicine and Molecular Imaging. 2006 Sep;50(3):167-92.
89. Melcher GA, Claudi B, Schlegel U, Perren SM, Printzen G, Munzinger J. Influence of type of medullary nail on the development of local infection. An experimental study of solid and slotted nails in rabbits. Journal of Bone and Joint Surgery (British Volume). 1994 Nov;76(6):955-9.
90. An YH, Bradley J, Powers DL, Friedman RJ. The prevention of prosthetic infection using a cross-linked albumin coating in a rabbit model. Journal of Bone and Joint Surgery (British Volume). 1997 Sep;79 (5):816-9.
91. Koort JK, Makinen TJ, Knuuti J, Jalava J, Aro HT. Comparative 18f-fdg pet of experimental staphylococcus aureus osteomyelitis and normal bone healing. Journal of Nuclear Medicine. 2004 Aug;45(8):1406-11.
92. Jones-Jackson L, Walker R, Purnell G, McLaren SG, Skinner RA, Thomas JR, Suva LJ, Anaissie E, Miceli M, Nelson CL, Ferris EJ, Smeltzer MS. Early detection of bone infection and differentiation from post-surgical inflammation using 2-deoxy-2-[18f]-fluoro-d-glucose positron emission tomography (fdg-pet) in an animal model. Journal of Orthopaedic Research. 2005 Nov;23(6):1484-9.
93. Makinen TJ, Veiranto M, Knuuti J, Jalava J, Tormala P, Aro HT. Efficacy of bioabsorbable antibiotic containing bone screw in the prevention of biomaterial-related infection due to staphylococcus aureus. Bone. 2005 Feb;36(2):292-9.
94. Lankinen P, Lehtimaki K, Hakanen AJ, Roivainen A, Aro HT. A comparative 18f-fdg pet/ct imaging of experimental staphylococcus aureus osteomyelitis and staphylococcus epidermidis foreign-body-associated infection in the rabbit tibia. EJNMMI Res. 2012 Jul 23;2(1):41.
95. Guhlmann A, Brecht-Krauss D, Suger G, Glatting G, Kotzerke J, Kinzl L, Reske SN. Fluorine-18-fdg pet and technetium-99m antigranulocyte antibody scintigraphy in chronic osteomyelitis. Journal of Nuclear Medicine. 1998 Dec;39(12):2145-52.
96. van Gaalen SM, Kruyt MC, Geuze RE, de Bruijn JD, Alblas J, Dhert WJ. Use of fluorochrome labels in in vivo bone tissue engineering research. Tissue engineering Part B, Reviews. 2010 Apr;16(2):209-17.
97. Schlyer DJ. Pet tracers and radiochemistry. Annals of the Academy of Medicine, Singapore. 2004 Mar;33 (2):146-54.
98. Segall G, Delbeke D, Stabin MG, Even-Sapir E, Fair J, Sajdak R, Smith GT, Snm. Snm practice guideline for sodium 18f-fluoride pet/ct bone scans 1.0. Journal of Nuclear Medicine. 2010 Nov;51(11):1813-20.

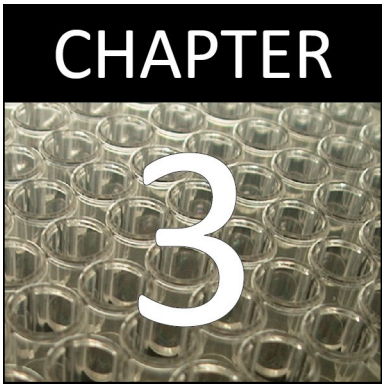

ELISA-based detection of gentamicin and vancomycin in protein-containing samples

J.C.E. Odekerken

D.M.W. Logister

L. Assabre

J.J.C. Arts

G.H.I.M. Walenkamp

T.J.M. Welting

Submitted, 2015

Abstract

Background: Orthopaedic implant infections are treated by rigorous surgical debridement, systematic antibiotic treatment and eventually supported by local antibiotic treatment with antibiotic-loaded PMMA beads. Currently antibiotic concentrations in wound exudate, serum, urine or tissue samples are investigated by HPLC or by a fluorescent spectrometric assay. Both methods are heavily influenced by the presence of proteins in the samples.

Purpose: Evaluate the potential of an antibiotic-specific ELISA to detect antibiotic concentrations in protein rich samples.

Methods: Two specific competitive ELISA-assays were set-up to detect either gentamicin or vancomycin in a protein-rich environment. An antibiotic-BSA hapten was generated for use as a coatable antigen and commercially available antibodies were applied for downstream immunodetection.

Results: The developed ELISAs perform at a detection range of 2 - 500 ng/ml gentamycin and 20 - 5000 ng/ml vancomycin. Both ELISAs were also capable of detecting these antibiotics in human serum and wound exudate without being compromised by the presence of proteins. We did not detect cross-reactivity for gentamicin in the vancomycin ELISA or *vice versa*.

Conclusions: Our results indicate that the antibiotic ELISAs are able to detect gentamicin and vancomycin readily at low concentrations in protein-rich samples and that they can be used as a high throughput and cost-effective alternative for chromatographic or fluorescent methods .

Clinical Relevance: These ELISAs can be used to determine gentamicin or vancomycin concentrations in clinical samples, assess novel orthopaedic antibiotic release systems as well as allowing quantitative detection of antibiotics released from biomaterials in *in vitro* and *in vivo* studies at very low concentrations in protein-rich samples.

Keywords: ELISA, gentamicin, vancomycin, drug release, drug delivery

1. Introduction

Orthopaedic infections are complex disorders, making prevention essential and treatment a challenging task (1-3). Often the only possible treatment regimen to successfully treat a patient for orthopaedic infections is aggressive surgical debridement with intensive systemic antibiotic treatment, often supported by local antibiotic delivery (1, 4, 5). Gentamicin and vancomycin are two important antibiotics with a broad spectrum towards micro-organisms in severe orthopaedic infections (3, 6, 7). Gentamicin is an aminoglycoside-antibiotic and is mostly used to treat gram-negative species and *Staphylococci*, while vancomycin is a glycopeptide-antibiotic and is used against specific antibiotic-resistant strains of *Staphylococci (3, 4, 6, 7)*. These antibiotics are the most frequently used antibiotics admixed in polymethyl methacrylate (PMMA) bone cements for prosthesis fixation or as beads, both to serve as a local antibiotic delivery system in the prevention or treatment of orthopaedic infections (7-9). Local antibiotic treatment is not only effective, but also avoids the toxicity of these antibiotics during systemic treatment such as ototoxicity and nephrotoxicity. (10-14).

To follow the release of antibiotics from e.g. beads or spacers or determine systemic antibiotic concentrations in patient material (e.g. serum, urine, wound exudate and tissue samples), the quantification of the release of these antibiotics is essential (8). Initially these quantifications have been performed by fluorescent detection methods (Roche Diagnostics, approximate detection range 1-10 µg/ml) or chromatographic methods (e.g. high performance liquid chromatography (HPLC) with a minimal detection limit of 50 ng/ml) (15-17). In food and dairy applications gentamicin levels have been determined with enzyme-linked immunosorbent assays (ELISA) with more sensitive detection limits (as low as 1 ng/ml) (18-20) and only recently an ELISA-based method to measure vancomycin was published, (21, 22). However, the use of such ELISA-based methods in human material has been minimally reported, possibly due to antibody restrictions and clinical diagnostic product regulations.

The goal of this study was to develop an indirect competitive ELISA-based detection method for gentamicin and vancomycin . In this setup a coated steady state antibiotic-hapten competes with the antibiotic in the sample for anti-antibiotic antibody binding. Due to this competition only antibodies bound to the steady state antibiotic-hapten will be detected by the conjugated secondary antibody, resulting in an horseradish peroxidase (HRP) conjugate-dependent colorimetric signal which is inversely correlated to the antibiotic concentration in the sample.

Therefore a low concentration of antibiotic in the sample will result in a high colorimetric absorbance value in the assay and *vice versa*. See the figure 1 for a schematic representation of the ELISA setup. To meet future requirements for (pre-) clinical use, our ELISA-based approach should be able to detect gentamicin and vancomycin in samples with a clinically relevant protein concentration and preferably in human serum and wound exudate as well.

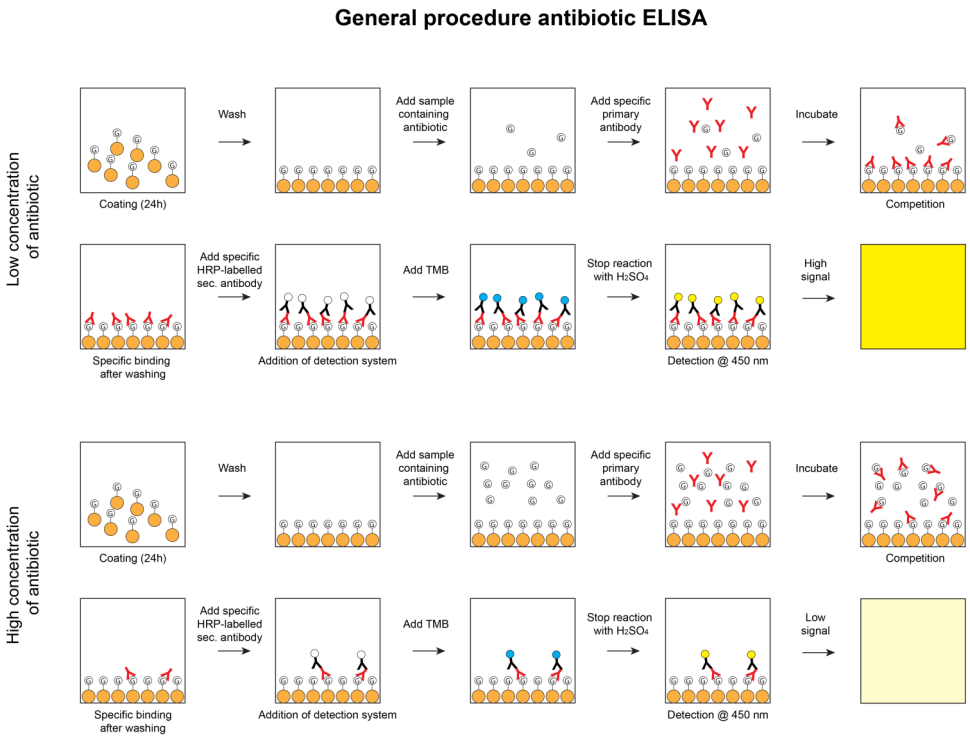

Figure 1: Schematic representation of the antibiotic ELISA procedure and detection. The antibiotic-BSA hapten is coated to a microtiter plate. An antibody directed against the antibiotic compound can interact with either the antibiotic in the sample or the antibiotic-hapten coated to the microtiter plate. After washing only the microtiter plate-bound antibodies remain present and can be detected by HRP-conjugated secondary antibodies in combination with TMB (colorimetric detection at 450 nm). A high concentration of antibiotics in a sample will lead to more interaction with an antibiotic-specific antibody in solution and thus result in less bound antibodies to the microtiter plate leading to a low signal when detected at 450 nm. This indicates that the measured signal is inversely correlated with the concentration of antibiotic in the measured sample. Samples with a known concentration of antibiotics can be used for a calibration curve; regression from this curve will allow calculation of the antibiotic concentration in unknown samples.

2. Materials and methods

2.1 Material collection, ethics and protein content

The used human serum originated from a single healthy volunteer. The collection of patient material (wound exudate) was approved by the Medical Ethics Committee of the Maastricht University Medical Centre (MEC approval number AZM/UM 11-4-023) and originated from a single patient.

Total protein concentration in human serum, human wound exudate (from hip revision surgery) and foetal calf serum (FCS, PAA Laboratories, Germany) was determined using the BCA method (Sigma-Aldrich, USA).

2.2 Hapten preparation

Gentamicin sulphate (Sigma-Aldrich, USA) and vancomycin hydrochloride (Sigma–Aldrich, USA) were individually coupled to bovine serum albumin (BSA, PAA Laboratories, Germany) using N-(3-Dimethylaminopropyl)-N'-ethylcarbodiimide hydrochloride (EDC, Sigma-Aldrich, USA). The gentamicin-BSA hapten was prepared as follows: 50 mg BSA was dissolved in 1.5 ml phosphate buffered saline (PBS, pH 7.4) which was subsequently added drop-wise to 24.5 mg gentamicin sulphate. Three hundred milligram EDC was dissolved in 1 ml demineralized water and added drop -wise to the gentamicin-BSA mixture under continuous agitation. After 1 hour incubation at room temperature the mixture was stored over night at 4 ^{o}C. The procedure for the vancomycin-BSA hapten preparation was comparable with the gentamicin-BSA hapten, only with 70 mg BSA in 18 ml PBS added to 77.8 mg vancomycin hydrochloride. The same amount of EDC was used only in 12 ml demineralized water. After 1 hour incubation at room temperature the mixture was stored over night at 4 ^{o}C.

The combination hapten of both gentamicin and vancomycin with BSA was prepared using 33 mg BSA in 24 ml PBS added to 12 mg gentamicin sulphate and 36.7 mg vancomycin hydrochloride. Also 300 mg of EDC in 12 ml demineralized water was subsequently added drop-wise to the gentamicin-vancomycin-BSA mixture. After 1 hour incubation at room temperature the mixture was stored over night at 4 ^{o}C.

After the 4 °C incubation step, uncoupled gentamicin and vancomycin as well as left-over EDC was removed from the preparation by dialysis (membrane cut-off value 12-14 kDa, Sigma-Aldrich, USA) at 4 °C over a period of 3 days with daily refreshment of the dialysis solution (phosphate buffered saline (PBS), pH 7.4). After dialysis the haptens were stored in aliquots at -80 °C.

2.3 Assessment of cross-linking of antibiotic compounds to BSA in hapten preparations

Polypeptides in hapten preparations were separated by sodium dodecyl sulphate polyacrylamide gel electrophoresis (SDS-PAGE) and transferred to polyvinylidene fluoride (PVDF, GE Healthcare Life Sciences, USA) membranes (for gentamicin-BSA, G-BSA) and nitrocellulose membranes (Protran BA 83, GE Healthcare Life Sciences, USA) (for vancomycin-BSA, V-BSA) by electroblotting. Immuno-blotting was performed with the same antibodies that are also used in the ELISA assay: mouse anti-gentamicin monoclonal antibody (clone 26.16, Abcam, USA) and rabbit anti-vancomycin polyclonal antibody (AbD Serotec, UK). Secondary antibodies conjugated with HRP (Dako, Denmark) were used to assess the bound primary antibody fraction to the antibiotic-BSA haptens on the membranes which is subsequently visualized by enhanced chemiluminescence (ECL).

2.4 Indirect competitive ELISA for gentamicin or vancomycin

The generated haptens were individually coated overnight at 4 °C to the surface of a 96-wells ELISA plate (10 ng coupled G-BSA, 1 µg V-BSA or 1.34 µg coupled G/V-BSA per well) in a 50 mM carbonate/bicarbonate buffer (pH 9.6). After incubation the plate was washed 3 times with wash-buffer (PBS/Tween-20 (0.05% v/v)). Subsequently wells were blocked (1 hour incubation with wash -buffer/BSA (5% wt./v)) Calibration curve samples were prepared in PBS/BSA (5% wt./v) (range gentamicin: 0 - 1000 ng/ml and vancomycin: 0 - 5000 ng/ml) also the test samples (clinical isolates or serum spiked with a known concentration of antibiotics) were diluted 1000x in PBS/BSA before the initial measurement. Fifty microliter of the calibration curve sample or diluted test sample was pipetted in each well of the ELISA plate. Fifty microliter of diluted primary antibody (mouse anti-gentamicin monoclonal antibody (Abcam, USA), 7000x diluted in PBS/BSA; rabbit anti-vancomycin polyclonal antibody (Abd Serotec, UK), 5000x diluted in PBS/BSA) was added to the samples and incubated for 1 hour at room temperature (conditions and antibody dilutions were based on

experimental optimisation, data not shown). After incubation, the ELISA plate was washed 4 times with wash-buffer followed by an additional blocking step with wash-buffer/BSA (5% wt./v) for 1 hour. One-hundred microliter diluted secondary antibody (for gentamicin: rabbit anti-mouse peroxidase (RAMPO, Dako, Denmark), 5000x diluted in PBS/BSA; for vancomycin: swine anti-rabbit peroxidase (SWARPO, Dako, Denmark), 2000x diluted in PBS/BSA) was added to the wells and incubated for 1 hour at room temperature after which the plate is washed 4 times with wash-buffer. After washing, 100 µl 3,3',5,5'-tetramethylbenzidine (TMB, Sigma-Aldrich, USA) was added to each well to allow chromogenic detection of bound secondary antibodies. The reaction was stopped with 3M sulphuric acid at the moment the absorbance of the negative control sample (0 ng/ml antibiotic) reached 0.5 at 650 nm. After stopping the reaction, the absorbance at 450 nm was measured using an ELISA reader (MultiSkan FC, Thermo Scientific). Due to the setup of the ELISA, the measured absorbance is inversely correlated with the antibiotic concentration present in the sample (for a detailed representation of the experimental procedure see supplementary figure). The antibiotic concentration present in the sample can be calculated based on the used calibration standards in a log-log scale.

2.5 Regression analysis

Calibration curve fitment was calculated in Microsoft Excel 2010 by the use of the Visual Basic for Applications (VBA) Analysis ToolPak (Microsoft, USA). Graphical representation of the data was performed in GraphPad Prism 5 (GraphPad, USA).

3. Results

3.1 Protein concentration

Total protein concentration measurements of human serum, wound exudate or FCS showed that these contained 56, 46 and 37 mg total protein/ml, respectively. Based on these findings we decided to develop the ELISA assays in the presence of 50 mg/ml BSA to represent the protein concentration that generally occurs in the samples that we aim to measure.

3.2 Hapten evaluation

The development of these ELISAs required the coating of gentamicin or vancomycin to standard polystyrene ELISA wells. As the antibiotics themselves cannot be coated directly to well plates, we generated BSA haptens of each individual antibiotic by EDC-mediated coupling between a BSA carrier and the antibiotic. To acquire evidence of successful hapten generation we separated freshly prepared BSA-gentamicin and BSA-vancomycin haptens by SDS-PAGE, transferred the separated proteins to nitrocellulose membranes and performed anti-gentamicin or anti-vancomycin immunoblotting. To first visualize the total amount of SDS-PAGE-loaded hapten/ protein, membranes were stained with Ponceau S after electro-blotting of SDS-PAGE gels. BSA runs at 66 kDa in SDS-PAGE and besides a major 66 kDa band, we were able to confirm the presence of ~140 kDa (BSA dimer) and ~210 kDa (BSA trimer) main bands, as well as a smear of higher molecular weight BSA species which were generated as a result of the EDC cross-linking (Figure 2A). A band running at the size for BSA was found in the BSA-vancomycin hapten preparation, but no other higher molecular weight BSA species were detected by Ponceau S staining (Figure 2A).

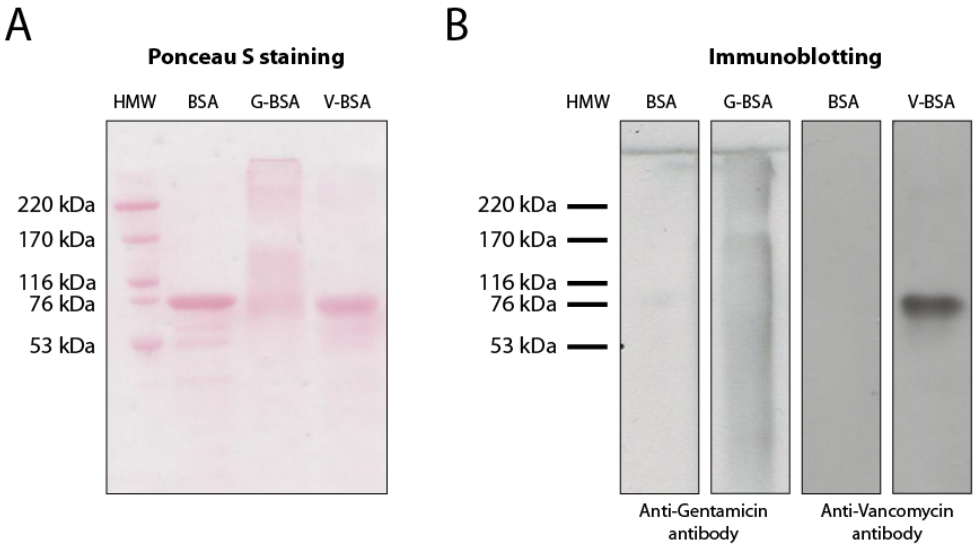

Figure 2: Hapten evaluation. **A:** Ponceau S staining indicates protein presence in the coupled haptens. **B:** Immunoblotting indicates corresponding antibiotic presence in both coupled haptens specifically.

To confirm the coupling of each individual antibiotic to BSA, antibiotic-specific immunodetection was performed. As presented in Figure 2B, immuno-blotting against gentamicin specifically generated a signal in the lane loaded with the BSA-gentamicin hapten and not in the BSA-only lane. Similarly, a specific signal was detected in the BSA-vancomycin lane as compared to the BSA-only lane after anti-vancomycin immuno-blotting. These data show that we were successful in covalently coupling gentamicin or vancomycin to BSA for use as a hapten in the ELISA.

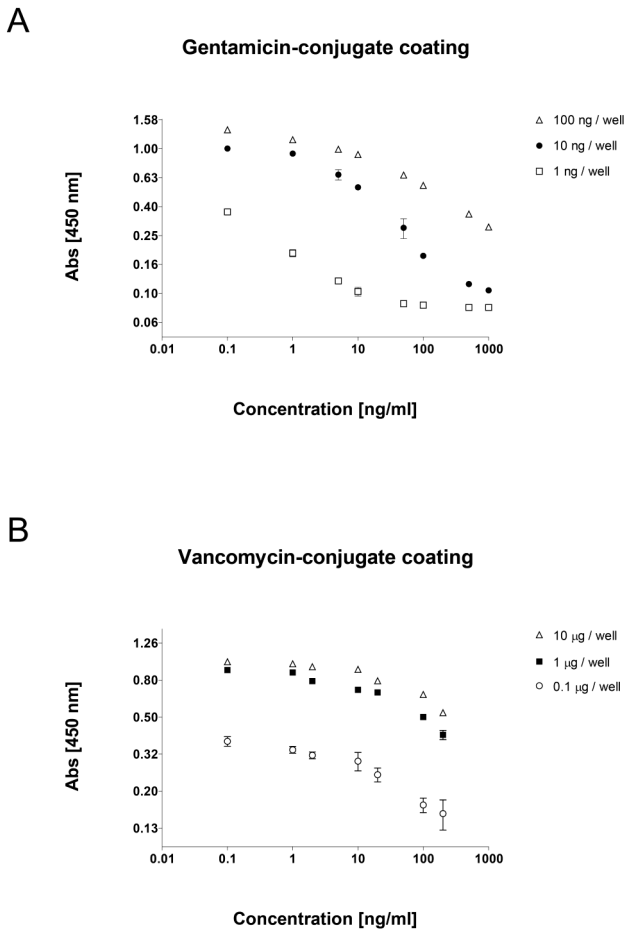

Figure 3: Coating optimisation **A:** The optimal concentration of the gentamicin-BSA hapten was based on the pattern of the calibration curve, which indicated a concentration dependant absorbance. **B:** The optimal concentration of the vancomycin-BSA hapten was determined on the relation between coating concentration and absorbance level.

3.3 Optimal hapten amount for coating of the microtiter plate

To determine the optimal coating amount for the hapten, three different hapten concentrations were coated on a microtiter plate. The gentamicin-BSA (G-BSA) hapten was coated at 1 ng, 10 ng or 100 ng per well, while the vancomycin-BSA (V-BSA) hapten was coated at an amount of 0.1 µg, 1 µg or 10 µg per well. Subsequently gentamicin or vancomycin detection properties of these amounts were evaluated. Performing the ELISA with a gentamicin concentration series indicated an inversely correlated gentamicin concentration-dependant signal in all G-BSA hapten coated wells. The 10 ng/well G-BSA hapten coating showed the broadest interpretable relation between gentamicin concentration and the A450 signal (Figure 3A).
Performing the ELISA on the different hapten coating amounts with a vancomycin concentration series also indicated an inversely correlated vancomycin concentration-dependent signal in all V-BSA coated wells. Here, the 1 µg/well V-BSA hapten coating provided an optimal relation between the vancomycin concentration and the A450 signal. The 10 µg/well V-BSA hapten coating performed equally well and thus the 1 µg/well V-BSA became our condition of choice (Figure 3B). From here on forward 10 ng/well G-BSA or 1 µg/well V-BSA were used to coat wells for any further experiments.

3.4 Specificity and sensitivity of the gentamicin and vancomycin ELISAs

The specificity of the gentamicin ELISA was assessed by performing the gentamicin ELISA using a concentration series of either gentamicin or vancomycin. If the gentamicin ELISA would be aspecific for distinguishing gentamicin from vancomycin, it is expected that with increasing vancomycin concentrations a vancomycin-induced A450 shift would take place. The same principle was used for the *vice versa* situation where we determined the specificity of the vancomycin ELISA with a concentration series of gentamicin. The presence of vancomycin in the gentamicin ELISA did not result in a change of A450 absorbance in any of the tested concentrations, indicating that this ELISA setup is highly specific for gentamicin (Figure 4A). These data also show that with this high specificity, the gentamicin ELISA is very sensitive and allows reliable detection of gentamicin in a range between 2 and 500 ng/ml. Gentamicin did not influence the vancomycin ELISA at any of the concentrations that were tested, indicating that also the vancomycin ELISA setup is very specific for vancomycin (Figure 4B). The detection range of the vancomycin ELISA was determined to be

reliable between 20 and 5000 ng/ml vancomycin. To determine how the sensitivity of the ELISAs might depend on the antibiotic concentration in the sample, we used two separately prepared antibiotic concentration series. One series was used to generate a calibration curve and the other concentration series ("validation series" in the Figure) was subsequently measured and calculated for the antibiotic concentration in the series by using the calibration curve. This was done for both ELISAs separately. As shown in Figure 4C/D we found that for both ELISAs the samples in the validation series generated absorbances that were within the 10% deviation range of the measured absorbance of the calibration curve (often used in commercial kits, to compensate for potential pipetting errors, differences between wells and the standard deviation of the measurements) (Figure 4C/D).

3.5 Antibiotic concentration in high-protein samples

In an orthopaedic context, the gentamicin and vancomycin ELISAs are expected to be used, amongst others, for determining antibiotic concentrations in clinical samples such as wound exudate from post-surgical drainage. To determine the performance of our ELISAs in this context, human wound exudate (total protein concentration was 56.8 mg/ml) was spiked with vancomycin to a final concentration of 50 µg/ml, to simulate a sample acquired from a patient undergoing antibiotic treatment. Before performing the ELISA, the sample was pre-diluted (1000x) in PBS/BSA. The vancomycin ELISA showed that the sample contained 53.5 µg/ml vancomycin, indicating a calculated recovery of 107%. The wound exudate was not spiked with gentamicin since the patient from whom the exudate was acquired was under gentamicin treatment. However this offered us the opportunity to determine whether we could detect the presence of gentamicin in the patient's wound exudate. Using our gentamicin ELISA we found that the wound exudate contained 5.0 µg gentamicin/ml. In addition we spiked human serum with gentamicin to a final concentration of 5 µg/ml to simulate a sample acquired from a patient undergoing antibiotic treatment. After initial sample dilution (1000x) the gentamicin ELISA determined that the serum sample contained 4.5 µg gentamicin/ml, indicating a calculated recovery of 90%. Also, concentration series of gentamicin (Table 1) and vancomycin (Table 2) in PBS/BSA indicated calculated recovery ranges between 91.6% and 108.8%.

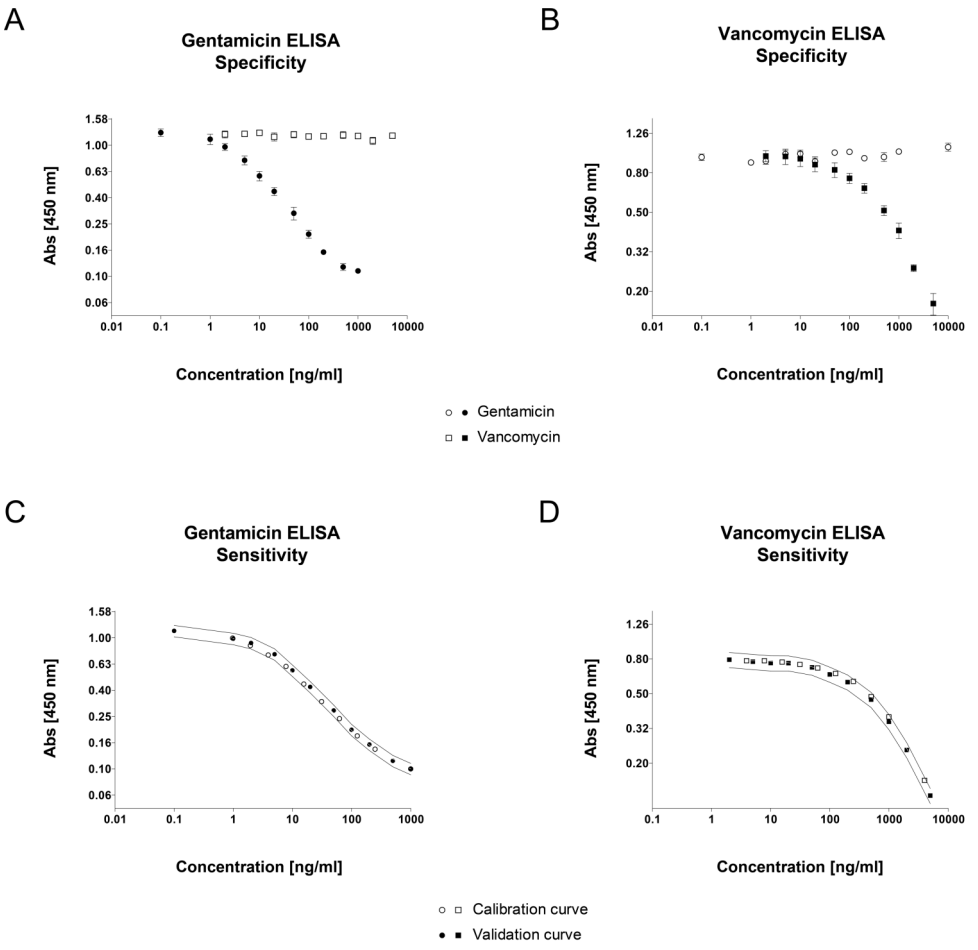

Figure 4: Specificity and sensitivity of the antibiotic ELISAs. **A:** The influence of vancomycin on the gentamicin ELISA. **B:** The influence of gentamicin on the vancomycin ELISA. **C:** The validation of the calibration curve of the gentamicin ELISA. Lines indicate upper and lower 10% range of the calibration curve. **D:** The validation of the calibration curve of the vancomycin ELISA. Lines indicate upper and lower 10% range of the calibration curve. Error bars indicate standard deviation.

Table 1: Accuracy gentamicin ELISA

Gentamicin concentration in validation series (ng/ml)	Concentration determined by linear regression from calibration series (ng/ml)	Recovery (%)
7.8	8.3	105.8
15.6	16.8	107.5
31.3	33.9	108.4
62.5	67.3	107.7
125.0	134.9	107.9
250.0	230.2	92.1
Human serum (5 ng/ml)	4.5	90.0

Table 2: Accuracy vancomycin ELISA

Vancomycin concentration in validation series (ng/ml)	Concentration determined by polynomial regression from calibration series (ng/ml)	Recovery (%)
31.3	33.0	105.6
62.5	68.0	108.8
125.0	114.5	91.6
250.0	258.6	103.4
750.0	766.3	102.2
4000.0	4282.1	107.1
Hum. wound exudate (50 ng/ml)	53.5	107.0

3.6 Multiple conjugates in one hapten

By using BSA as a coatable protein for generating the gentamicin and vancomycin haptens, we explored the possibility of combining different antibiotics in one hapten coupling reaction. This potentially offers the opportunity to generate a combined assay for the detection of both antibiotics by using the same hapten in separate dedicated ELISAs. A combined hapten of both

gentamicin and vancomycin cross-linked to BSA indeed allowed the detection of either gentamicin or vancomycin by their respective antibodies, in a comparable range as the individual ELISA protocols (Figure 5). Furthermore, when this hapten was used for the ELISA detection of gentamicin, it was not influenced by vancomycin presence in the sample and *vice versa*.

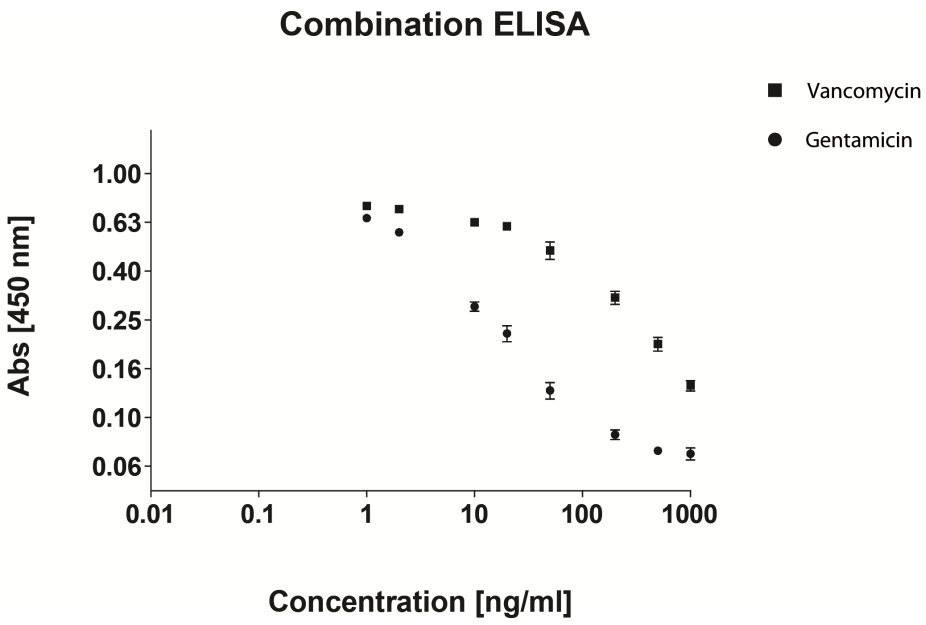

Figure 5: ELISA for gentamicin and vancomycin. A combined hapten of both gentamicin and vancomycin was used to coat wells for the detection of either gentamicin (black circles) or vancomycin (black squares) in a calibrations series of the respective antibiotics. Error bars indicate standard deviation.

4. Discussion

Orthopaedic infections are complex disorders which often require surgical treatment and implantation of a local antibiotic delivery system. The use of antibiotic containing PMMA bone cement, beads or spacers is considered effective to prevent and treat such infections in combination with systemic antibiotics (7, 8, 23-25). Gentamicin beads and spacers generally

remain implanted in the patient for a couple of weeks, before being surgically removed and substituted by a prosthesis or osteosynthesis materials (7, 23).

Currently HPLC and fluorescence-based methods are used to detect antibiotics in patient material (15-17). These methods often require sample pre-treatments, are expensive, often insensitive or prone to be influenced by the high protein content in (patient) sample material (15-17). Currently, these methods are the method of choice to assess novel antibiotic release systems and coatings for clinical use. ELISA-based methods have been sparsely used for this purpose, possibly due to the lack of ready-to-use protocols for ELISA-based antibiotic detection methods. ELISA-based methods are generally cheaper per sample, and better suited for high-throughput applications, compared to HPLC.

Based on protocols derived from dairy and food-industry applications we established ELISA-based assays to determine the concentration of gentamicin and vancomycin in patient material (serum and wound exudate). The gentamicin ELISA has a reliable detection range of 2-500 ng/ml with no detectable cross-reactivity with vancomycin. The vancomycin ELISA is reliable between 20-5000 ng/ml without cross-reactivity with gentamicin. Due to the graph characteristics of the concentration-dependent calibration curve of gentamicin a linear regression can be used to calculate the concentration in unknown samples. For vancomycin a linear regression is not preferable due to the bending of the curve. Therefor a polynomial regression was used to calculate the vancomycin concentrations of unknown samples. The sensitivity and accuracy of both ELISA's is high, especially when compared to the detection limits of the frequently used fluorescence-based detection systems and when compared to HPLC, where high-protein content is a notoriously hampering factor (17-20).

Recently novel experimental approaches to detect gentamicin and vancomycin have been reported in literature (21, 22). The group of Chianella recently described the use of a specific synthetic coatable molecularly imprinted polymer nanoparticle (nanoMIP) for the detection of vancomycin in an ELISA-like way, instead of a conventional antibiotic-protein hapten (21). Very low concentration ranges (pM) are achieved by using the high-tech nanoMIP method. However, depending on the relevant concentrations to be measured, our low-tech ELISA setup provides an easy accessible and low-cost method for an in-house generated ELISA assay in the nM range. The group of Fujiwara described the use of a hapten consisting of an antibiotic cross-linked to a protein like BSA. Only they choose a different cross-linking agent resulting in an antibiotic-cross-linker-BSA hapten (22). In our approach we use a zero-length cross-linker (EDC) which results in an antibiotic-

BSA hapten without the cross-linker in the hapten. A possible interaction of a cross-linker in the assay is thereby avoided.

Our data shows that the gentamicin ELISA requires a lower amount of hapten to be coated to the surface of the microtiter plate well as compared to the vancomycin ELISA. This difference might be related to the size of the individual antibiotic compounds. Gentamicin is a relatively small molecule in comparison to vancomycin (about 1/3 in molecular weight). To achieve the coating of an equimolar amount of vancomycin as compared to gentamicin, it is imperative that more V-BSA hapten is coated to the well. However this does not fully explain the 100-fold larger coating dose required for the vancomycin ELISA. In addition this could also be attributed by a difference in cross-linking efficiency during hapten formation, as seen in the immunoblotting results where the cross-linking of gentamicin resulted in BSA di-mers and tri-mers. Furthermore, the applied individual antibodies for the detection of gentamicin and vancomycin are different and will differ in their antibody-antigen binding affinity. This difference in antibodies might thus influence the detection ranges in the assays and provide an explanation why we need to coat more V-BSA hapten to the well than G-BSA hapten. Although the gentamicin antibody does not detectably interact with vancomycin and the vancomycin antibody does not interact with gentamicin, we cannot exclude that other antibiotics might cause aspecific interactions with the herein described antibodies, potentially resulting in incorrect calculations of the antibiotic concentration in the measured sample. Future application-specific evaluation of this potential bias should be performed, depending on the antibiotic.

Due to the nature of our ELISA setup, the protocol can be easily converted to establish ELISA tests for other antibiotics, provided the availability of antibodies and that such antibiotics possess carboxyl-groups or primary amines (like tobramycin, kanamycin, sisomicin and cefuroxime). This is due to the use of EDC as a cross-linking agent to establish the antibiotic-BSA hapten. The versatility of this ELISA setup also allowed the detection of both vancomycin and gentamicin by one hapten source, in which the two different antibiotics were combined. From an efficiency point-of-view this is particularly interesting, since only one hapten has to be produced to allow detection of a variable set of antibiotics.

5. Conclusion

We here describe an easy-to-use protocol for the detection of gentamicin and vancomycin by ELISA. The protocol can be adapted relatively easy to other antibiotics, enabling the detection of antibiotics from experimental and clinical antibiotic release studies in several types of liquids, including high-protein samples.

References

1. Calhoun JH, Manring MM, Shirtliff M. Osteomyelitis of the long bones. Seminars in Plastic Surgery. 2009 May;23(2):59-72.
2. Miclau T, Schmidt AH, Wenke JC, Webb LX, Harro JM, Prabhakara R, Shirtliff ME. Infection. Journal of Orthopaedic Trauma. 2010 Sep;24(9):583-6.
3. Trampuz A, Zimmerli W. Antimicrobial agents in orthopaedic surgery: Prophylaxis and treatment. Drugs. 2006;66(8):1089-105.
4. Zimmerli W. Infection and musculoskeletal conditions: Prosthetic-joint-associated infections. Best Practice & Research: Clinical Rheumatology. 2006 Dec;20(6):1045-63.
5. Zimmerli W, Ochsner PE. Management of infection associated with prosthetic joints. Infection. 2003 Mar;31(2):99-108.
6. Fraimow HS. Systemic antimicrobial therapy in osteomyelitis. Seminars in Plastic Surgery. 2009 May;23 (2):90-9.
7. Walenkamp GH, Kleijn LL, de Leeuw M. Osteomyelitis treated with gentamicin-pmma beads: 100 patients followed for 1-12 years. Acta Orthopaedica Scandinavica. 1998 Oct;69(5):518-22.
8. Wahlig H, Dingeldein E, Bergmann R, Reuss K. The release of gentamicin from polymethylmethacrylate beads. An experimental and pharmacokinetic study. Journal of Bone and Joint Surgery (British Volume). 1978 May;60-B(2):270-5.
9. Walenkamp GH. Gentamicin pmma beads and other local antibiotic carriers in two-stage revision of total knee infection: A review. Journal of Chemotherapy. 2001 Nov;13 Spec No 1(1):66-72.
10. Contreiras C, Legal M, Lau TT, Thalakada R, Shalansky S, Ensom MH. Identification of risk factors for nephrotoxicity in patients receiving extended-duration, high-trough vancomycin therapy. Canadian Journal of Hospital Pharmacy. 2014 Mar;67(2):126-32.
11. Han H, An H, Shin KH, Shin D, Lee S, Kim JH, Cho SH, Kang HR, Jang IJ, Yu KS, Lim KS. Trough concentration over 12.1 mg/l is a major risk factor of vancomycin-related nephrotoxicity in patients with therapeutic drug monitoring. Therapeutic Drug Monitoring. 2014 Feb 26.
12. Nagai J, Takano M. Entry of aminoglycosides into renal tubular epithelial cells via endocytosis-dependent and -independent pathways. Biochemical Pharmacology. 2014 May 29.
13. Ojano-Dirain CP, Antonelli PJ, Le Prell CG. Mitochondria-targeted antioxidant mitoq reduces gentamicin-induced ototoxicity. Otology & Neurotology. 2014 Mar;35(3):533-9.
14. Walenkamp GH, Vree TB, van Rens TJ. Gentamicin-pmma beads. Pharmacokinetic and nephrotoxicological study. Clinical Orthopaedics and Related Research. 1986 Apr(205):171-83.
15. Baietto L, D'Avolio A, De Rosa FG, Garazzino S, Michelazzo M, Ventimiglia G, Siccardi M, Simiele M, Sciandra M, Di Perri G. Development and validation of a simultaneous extraction procedure for hplc-ms quantification of daptomycin, amikacin, gentamicin, and rifampicin in human plasma. Anal Bioanal Chem. 2010 Jan;396(2):791-8.
16. Manyanga V, Kreft K, Divjak B, Hoogmartens J, Adams E. Improved liquid chromatographic method with pulsed electrochemical detection for the analysis of gentamicin. Journal of Chromatography A. 2008 May 2;1189(1-2):347-54.
17. Wilson JF, Davis AC, Tobin CM. Evaluation of commercial assays for vancomycin and aminoglycosides in serum: A comparison of accuracy and precision based on external quality assessment. Journal of Antimicrobial Chemotherapy. 2003 Jul;52(1):78-82.
18. Jin Y, Jang JW, Han CH, Lee MH. Development of elisa and immunochromatographic assay for the detection of gentamicin. Journal of Agricultural and Food Chemistry. 2005 Oct 5;53(20):7639-43.
19. Jin Y, Jang JW, Lee MH, Han CH. Development of competitive direct enzyme-linked immunosorbent assay for the detection of gentamicin residues in the plasma of live animals. Asian-Australasian Journal of Animal Sciences. 2005 Oct;18(10):1498-504.
20. Haasnoot W, Stouten P, Cazemier G, Lommen A, Nouws JF, Keukens HJ. Immunochemical detection of aminoglycosides in milk and kidney. Analyst. 1999 Mar;124(3):301-5.
21. Chianella I, Guerreiro A, Moczko E, Caygill JS, Piletska EV, De Vargas Sansalvador IM, Whitcombe MJ, Piletsky SA. Direct replacement of antibodies with molecularly imprinted polymer nanoparticles in elisa --development of a novel assay for vancomycin. Analytical Chemistry. 2013 Sep 3;85(17):8462-8.

22. Fujiwara K, Yoshizaki Y, Shin M, Miyazaki T, Saita T, Nagata S. Immunocytochemistry for vancomycin using a monoclonal antibody that reveals accumulation of the drug in rat kidney and liver. Antimicrobial Agents and Chemotherapy. 2012 Nov;56(11):5883-91.
23. Geurts J, Chris Arts JJ, Walenkamp GH. Bone graft substitutes in active or suspected infection. Contra-indicated or not? Injury. 2011 Sep;42 Suppl 2:S82-6.
24. Klemm K. [gentamicin-pmma-beads in treating bone and soft tissue infections (author's transl)]. Zentralblatt für Chirurgie. 1979;104(14):934-42.
25. Wahlig H, Buchholz HW. [experimental and clinical studies on the release of gentamicin from bone cement]. Chirurg. 1972 Oct;43(10):441-5.

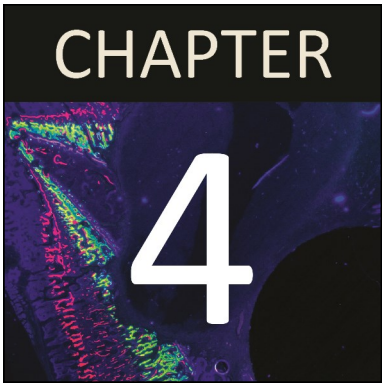

A rabbit osteomyelitis model for the longitudinal assessment of early post-operative implant infections

J.C.E. Odekerken

J.J.C. Arts

D.A.M. Surtel

G.H.I.M. Walenkamp

T.J.M. Welting

Journal of Orthopaedic Surgery and Research. 2013;8:38

Abstract

Background: Implant infection is one of the most severe complications within the field of orthopaedic surgery, associated with an enormous burden for the healthcare system. During the last decades attempts have been made to lower the incidence of implant-related infections. In the case of cemented prostheses the use of antibiotic-containing bone cement can be effective. However in the case of non-cemented prostheses, osteosynthesis and spinal surgery, local antibacterial prophylaxis is not a standard procedure. For the development of implant coatings with antibacterial properties, there is need for a reliable animal model to evaluate the preventive capacity of such coatings during a specific period of time. Existing animal models generally present a limited follow-up, with a limited number of outcome parameters and relatively large animal numbers in multiple groups.

Methods: To represent an early post-operative implant infection, we established an acute tibial intramedullary nail infection model in rabbits by contamination of the tibial nail with $3.8x10^5$ colony forming units of *Staphylococcus aureus.* Clinical, haematological and radiological parameters for infection were weekly assessed during a 6 week follow-up with *post-mortem* bacteriological and histological analyses.

Results: *Staphylococcus aureus,* implant infection was confirmed by the above parameters. A saline control group did not develop osteomyelitis. By combining the clinical, haematological, radiological, bacteriological and histological data collected during the experimental follow-up, we were able to differentiate between the control and infected condition and assess the severity of the infection at sequential timepoints in a parameter-dependent fashion.

Conclusion: We here present an acute early post-operative rabbit implant infection model which, in contrast to previously published models, combines improved in-time insight into the development of an implant osteomyelitis with a relatively low amount of animals.

Keywords: Implant infection; osteomyelitis; animal model; rabbit; *Staphylococcus aureus*

1. Background

The implantation of orthopaedic prostheses/trauma implants is an invasive surgical procedure with an increased risk for post-operative infections compared to non-implant related orthopaedic interventions. Since the lifespan and quality of orthopaedic implants is gradually improving and more biomaterials are implanted every year, the prevalence of post-operative infections is expected to increase (1-3).

Most orthopaedic implant infections and osteomyelitises are of Staphylococcal origin (3-5). The most frequent direct post-operative (acute) deep implant infections are the result of trauma, while infection after a total joint replacement is less frequent (6, 7). Antibiotic treatment of these infections often fails due to biofilm formation by the infecting pathogen on the implant surface (6, 7).

Most orthopaedic implants are based on titanium or cobalt-chrome alloys and their overall biocompatibility is good, however these materials do not possess antimicrobial properties. Applying antimicrobial functionality to an implant, by e.g. coatings to prevent biofilm formation, could provide an effective way to minimize the risk for bacterial colonisation. For evaluating the efficacy of novel antimicrobial implant coatings, *in vivo* testing is essential to establish a reliable coating, suitable for orthopaedic implants.

One of the most well-known *in vivo* models is the model by Norden (8), in which rabbits receive an intramedullary contamination of *Staphylococcus aureus* after the administration of a sclerosing agent (sodium morrhuate). To mimic the presence of an orthopaedic implant, the rabbit model by Andriole (9, 10) introduced an intramedullary pin in a contaminated tibial intramedullary cavity. Over the years these models have been modified for the clinical evaluation of implant materials and coatings (11-16) or for the evaluation of antibiotic treatment efficacy, like antibiotic-containing bone cements (14, 17-19). Despite the many published rabbit infection models, these studies seldom report on time course measurements of infection parameters in the same animal in follow-up studies. Determining infection parameters in individual animals overtime is expected to provide important information about the development of the osteomyelitis and the in-time bone integrity surrounding the implant, as well as bone apposition dynamics on the implant. Furthermore such an experimental setup would also require less animals without making any concessions on the experimental significance (according to the 3R guidelines proposed by Russell and Burch (20).

To address the current lack of a model providing data on above parameters in individual animals during the course of osteomyelitic development, we aimed to establish an improved rabbit implant infection model, based on several previously published models resembling clinical orthopaedic implant infections (8-10, 12, 15). By combining haematological parameters (leucocyte differentiation, erythrocyte sedimentation rate (ESR) and C-reactive protein (CRP)) with clinical parameters (body weight and -temperature) and bone integrity parameters (determined by X-ray, microCT and histology) during a 6-week follow-up in rabbit osteomyelitic development, a broad spectrum insight on the development of the infection status in individual subjects was acquired, using a minimal number of animals.

2. Methods

2.1 Inoculum preparation

Staphylococcus aureus strain, UAMS-1, (a clinical methicillin sensitive isolate, obtained from the American Type Culture Collection (ATCC 49230, ATCC, USA)) (5, 21) was used in these experiments. Bacteria were cultured in tryptic soy broth (Bacto, Beckton Dickinson, France). Bacterial inoculum was created from a fresh overnight culture which was subsequently diluted with sterile saline to a concentration within the range of $1x10^6$ – $1x10^7$ CFU/ml, based on OD600 (Amersham Biosciences, GE Healthcare, USA) measurements. The range of the inoculum was based on our previous *in vivo* dose finding experiments in New Zealand White rabbits (data not shown). A contamination with 100 µl of this inoculum generally led to distinctive clinical and bone morphological changes related to osteomyelitis, with limited cases of spontaneous remission. The bacterial count of every inoculum was verified by quantitative culture on tellurite glycine agar (Difco, Becton Dickinson, France) before and after surgery. The inoculum size used in this study was $3.8x10^5$ CFU per contamination.

2.2 Surgery, animal welfare and health

Twenty-two Specified Pathogen Free (SPF) female New Zealand White (NZW) rabbits (Charles River, France), with a weight of 3.5 - 4 kg (approximately 6 months of age) were used in this study. After arrival the animals were allowed to acclimatize for 2 weeks before surgery was performed.

Anaesthesia was initiated by ketamine (35 mg/kg i.m.) (Nimatek, Eurovet Animal Health, the Netherlands) and xylazine (5 mg/kg i.m.) (Xylalin, Ceva Santé Animale, France), while maintained by fentanyl (2 µg/kg/h i.v.) (Fentanyl, Hameln Pharmaceuticals, Germany), midazolam (1 mg/kg/h i.v.) (Midazolam, Actavis, Switzerland) and if necessary supported by isoflurane (1%) (Isoflo, Abbott Laboratories, USA). The right hind leg of the animal was clipped (not shaved) and disinfected with 2% iodine solution (Eurovet Animal Health, the Netherlands).

The animals were randomly assigned to two separate surgical groups (based on a power calculation according to Sachs (22)), a contamination group (n=11) and a sterile saline control group (n=11). By sequential reaming, a 4 mm wide defect was drilled by hand into the tibial plateau to open the tibial intramedullary canal. After reaming, the tibial intramedullary cavity was flushed with sterile saline to remove bone fragments and haematoma. Each animal received a 20 mm long, 4 mm wide grit-blasted titanium nail (TiAl6V4) (DePuy, USA) in the proximal part of the tibia by transpatellar incision (Figure 1A).

Immediately before insertion of the implant the contamination group received an intramedullary contamination of $3.8x10^5$ CFU *S. aureus* in 100 µl saline. In the control group 100 µl saline was administered. The implant was press-fit into the tibial defect (Figure 1B), and positioned just below the tibial articulating cartilage surface (Figure 1C). After insertion the defect was sealed with bone wax (Syneture, Covidien, USA) and the surrounding tissue was flushed with sterile saline as an extra prophylaxis for soft tissue infection. The wound was closed in layers with resorbable sutures (Syneture, Covidien, USA) and furthermore Aluminium-spray (Eurovet Animal Health, the Netherlands) was applied to protect the wound.

For the first 2 days after surgery animals were treated with subcutaneous injection of buprenorphine (twice a day 0.05 mg/kg bodyweight, Temgesic, Reckitt Benckiser, UK). Pain-treatment, with buprenorphine, was continued if pain persisted after these 2 days.

Animals were housed in groups to promote movement of the operated leg. Housing groups were based on the random assignment of the animals to a specific operating day, resulting in mixed housing groups containing both infected and uninfected animals. The animals were monitored during the 6 week follow-up for using their hind legs, the appearance of the wound and on general signs of infection (redness, swelling and fever). Food and water was available *ad libitum*. The daily diet was supplemented with Critical Care (Oxbow Animal Health, USA).

Body weight and temperature were measured pre-operative at the day of surgery and every week thereafter until the end of the experiment. Blood was collected by venipuncture from the jugular

vein of the rabbit from which approximately 2 ml blood was drawn to determine the leucocyte differentiation (Euregio Laboratory, the Netherlands), ESR (Kabe Labortechnik, Germany) and CRP (E-15CRP, Immunology Consulants Laboratory, USA)

Tibial fracture, soft tissue infection with a large abscess or fistula and sepsis were defined as humane endpoints which would directly lead to termination of the animal. In case of 20% weight loss, a veterinarian was consulted and the animal treated accordingly (either euthanisation or additional individual feeding with Critical Care). According to the experimental procedure, all remaining animals were sacrificed six weeks after surgery by a pentobarbital (Euthanimal, Alfasan Diergeneesmiddelen, the Netherlands) overdose.

This study was approved by the Maastricht University Animal Ethics Committee (DEC-UM, Protocol 2010-089, Maastricht, the Netherlands). Dutch law guidelines for animal experiments were strictly followed while designing and conducting this study.

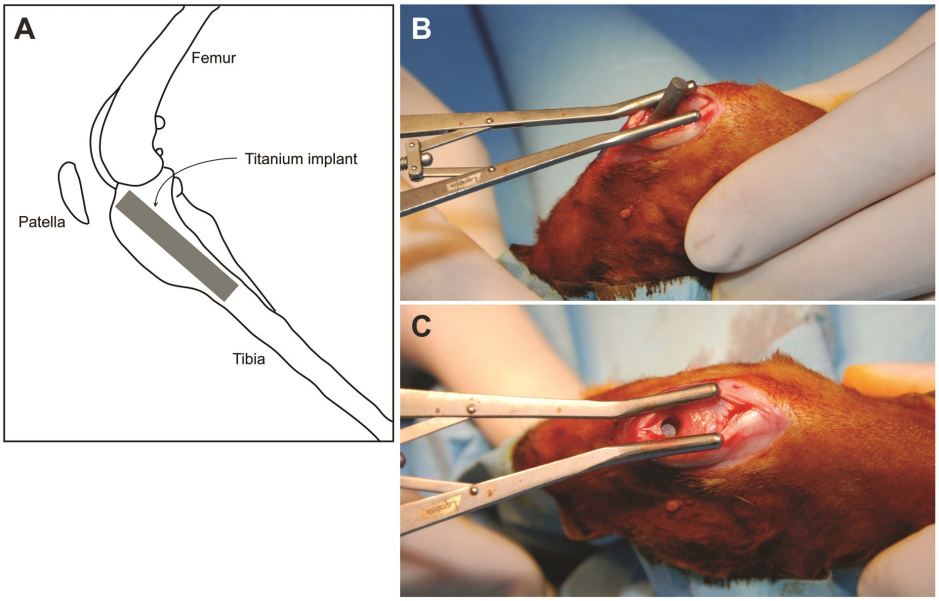

Figure 1: Implant localisation and implantation. **A:** Localisation of the titanium implant in the proximal tibia. **B:** transpatellar insertion of the implant. **C:** Implant positioning after implantation, before sealing with bone wax.

2.3 Imaging

Antero-posterior and medio-lateral X-rays of the tibia were made under tiletamine-zolazepam sedation (15 mg/kg i.m., Zoletil 100, Virbac Laboratories, France) at 85kV, 20mAs (Polymobil, Siemens, Germany) on Kodak PQ-phosphor screens (Carestream Healthcare, USA) with a phosphor screen to source distance of approximately 70 cm. Data were digitized by a CR-975 plate reader (Carestream Healthcare, USA). Images were assessed with the Philips iSite (version 3.5) software package (Royal Philips Electronics, the Netherlands). A modified X-ray scoring system (based on the classification by Calhoun and Mader (17)) were used for describing the specific changes around the infected intramedullary implant in a rabbit (Table 1 and 2). All individual X-ray radiographs were scored (according to Table 1) by 3 independent, blinded observers. *Ex vivo* microCT imaging of the implant and the surrounding area was performed on the excised tibiae after 6 weeks follow-up. The microCT-images were acquired on an X-rad 225 (Precision X-ray, USA), with a field of view of 10 cm in diameter, a source-to-axis distance of 30 cm and a source-to-detector distance of 62 cm. Images were made at 80kVp, with an isotropic spacing of 102 µm and 2.14 mm Al added filtration. Data were assessed with the GE MicroView software package (version 2.1.2, GE Healthcare, USA). Individual microCT images were scored by 3 independent, blinded observers (according to table 2).

2.4 Calcium binding fluorophores

Three different calcium binding fluorophores were administered, by subcutaneous injection, to follow bone apposition and mineralisation over time. At week 2 in follow-up, 25 mg/kg Calcein Green (Fluka, Sigma Aldrich, Germany) was injected, 30 mg/kg Xylenol Orange (Fluka, Sigma Aldrich, Germany) was injected at week 4 and 25 mg/kg Calcein Blue (Fluka, Sigma Aldrich, Germany) was injected on day 41 (the day before sacrifice), resulting in a green, orange and blue zone, indicating active bone formation at that particular timepoint.

2.5 *Post-mortem* bacterial culture

After sacrifice the tibiae were dissected aseptically. Swabs were taken from the knee joint cavity and tibial plateau. To assess soft tissue infection, swabs were evaluated for the presence of *S. aureus* on tellurite glycine agar plates. A 5 mm piece of the distal part of the *tuberositas tibiae* was

excised from the tibia with a surgical drill (SM 12, Nouvag, Switzerland). After weight measurement it was homogenized (Ultra-Turrax T25, Ika, Germany) and cultured on tellurite glycine agar plates. After 24 hours, culture dishes were quantified for specific bacterial growth.

Table 1: Osteomyelitis scoring system – X-ray (also see page 227)

Osteomyelitis grade	Morphological changes
0	No radiologic abnormalities
1	Mild periosteal reaction Mild osteolysis directly around the implant
2	Periosteal reaction Evident osteolysis around the implant
3	Periosteal reaction with subperiostal calcification More extensive metaphyseal osteolysis
4	Cortical thickening Osteolysis extending into diaphysis

Table 2: Osteomyelitis scoring system - MicroCT (also see page 229)

Osteomyelitis grade	Morphological changes
0	No radiologic abnormalities
1	Mild periosteal reaction Mild cortical thickening
2	Evident periosteal reaction Evident cortical thickening Mild osteolysis
3	Extensive cortical thickening Focal loss of cortical wall Evident osteolysis
4	Extensive cortical thickening Loss of cortical morphology Loss of spongeous morphology Extensive osteolysis

2.6 Histology

After sampling for bone culture, tibiae were fixated in 4% formaldehyde/PBS and subsequently embedded in polymethyl methacrylate (PMMA) (Technovit 9100, Hereaus-Kulzer, Germany). Fifty micrometer thick sections were prepared using a saw microtome (Leica SP1600, Germany) and each section was stained according to Masson-Goldner (Carl Roth, Germany) or Gram (without safranin-O counterstain). Sections were analysed and digitized by light microscopy (Axioscope A1, Axiovision LE release 4.8.2, Carl Zeiss, Germany). The localisation of calcium binding fluorophores in the bony tissue was visualized by fluorescence microscopy (Leica DMRB, Leica IM50 version 1.2 release 19, Leica, Germany) on unstained PMMA sections. Acquired images were merged using Photoshop CS3 (Adobe Systems, USA) to generate overview images. Histological sections were scored by 3 blinded, independent observers (according to Table 3).

Table 3: Osteomyelitis scoring system - Histology (also see page 230)

Morphological abnormality	Histological staining	Score (per abnormality)
Cortical thickening	Masson-Goldner	0: Absent 1: Mild to moderate 2: Moderate to severe
Presence of microabcesses		
Enlarged Haversian canals		
Periosteal elevation	Calcium binding fluorophores	
Gram stain	Modified Gram stain	0: Negative 2: Positive

Total histological score	Osteomyelitis grade
0 – 3	Not infected
>3 – 5	Mild
>5 – 7	Moderate
>7 – 10	Severe

2.7 Statistical analysis

SPSS 19 (IBM, USA) was used for the statistical analyses. Data were checked for normality using the Shapiro-Wilk test. Differences between groups were determined by a Mann-Whitney U test for non-parametric one-tailed significance. The significance level was determined at $p<0.05$. Graphical representation of the data was performed in GraphPad Prism 5 (GraphPad, USA).

3. Results

3.1 Surgery and follow-up

In total 22 rabbits received an implant by a transpatellar incision, of which 11 received an intramedullary inoculation with $3.8x10^5$ CFU *S. aureus*. The inoculum size was checked before and after surgery to ensure a constant intra operative bacterial load (Figure 2). Due to respiratory depression, 3 rabbits did not recuperate from anaesthesia during the follow-up (2 animals from the control group and 1 from the contaminated implant group). Another 3 animals (all from the contaminated implant group) had to be sacrificed during follow-up due to humane endpoint complications. Blood cultures were taken after sacrifice to exclude sepsis. All blood cultures were negative for *S. aureus* and *S. epidermidis*. In total, these 6 animals, including the corresponding data, were considered as loss to follow-up, resulting in a control group of 9 animals and a contaminated implant group of 7 animals.

3.2 Physical examination and haematological analysis

After recuperation, the control group returned to full weight bearing of the operated leg in the first week after surgery, while most animals in the contaminated implant group did not recover to full weight bearing within the six-week follow-up period. Weight loss was noted in the first weeks after surgery in both groups. The contaminated implant group had significantly more weight loss compared to the uncontaminated control implant group at the third, fifth and sixth post-operative week ($p=0.071$, 0.176, 0.028, 0.071, 0.006 and 0.006, respectively) (Figure 3A).
There was no incidence of fever in both groups. Temperature range of the control group was 37.7 – 39.9 °C, while the range in the contaminated implant group was 37.9 – 39.8 °C. The body

temperature in the contaminated implant group was significantly higher compared to the uncontaminated implant group at the fourth post-operative week only (p=0.046) (Figure 3B).

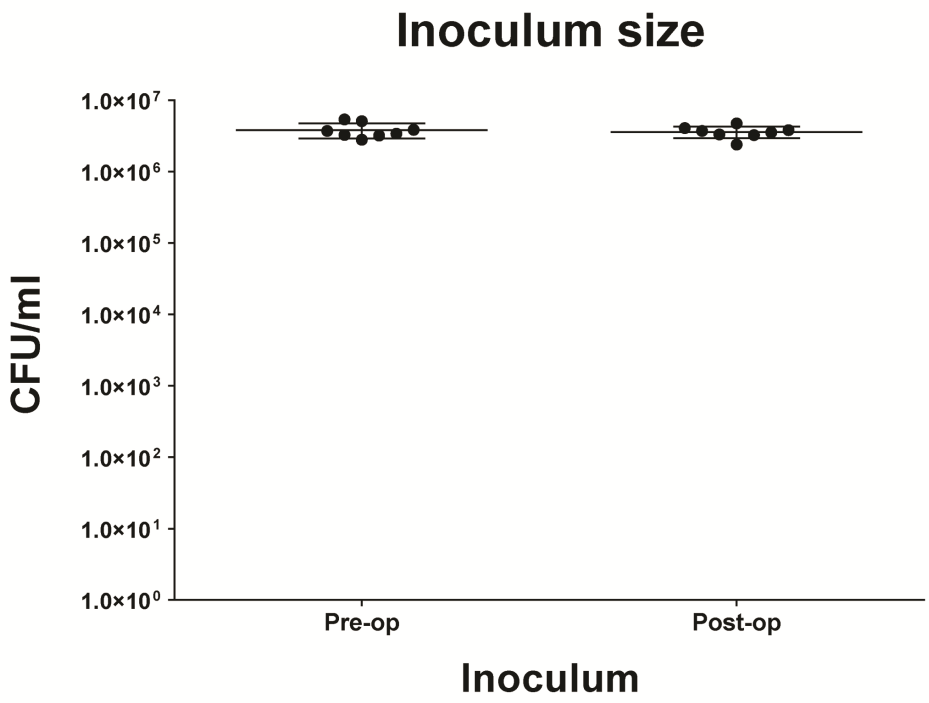

Figure 2: Inoculum size verification before and after surgery.

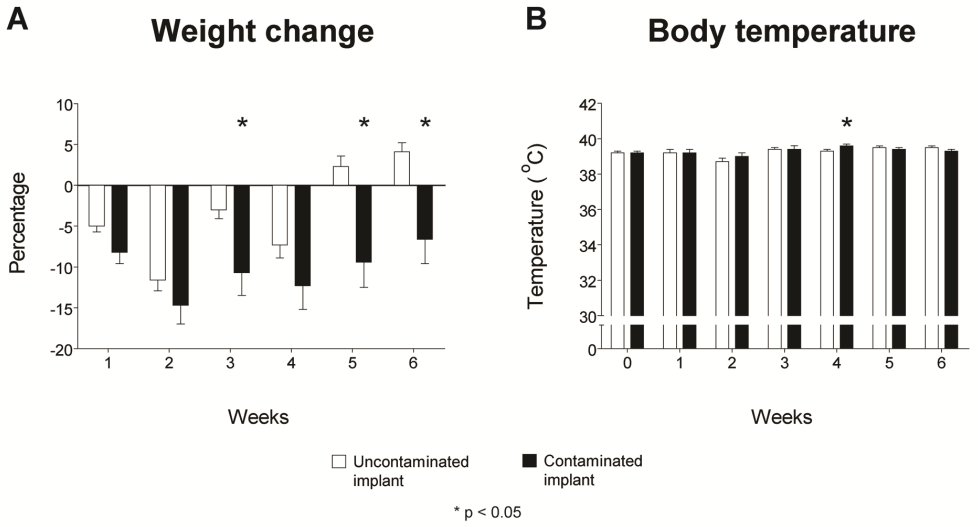

Figure 3 (above): Physiological parameters. **A:** Weight change during follow-up. **B:** Body temperature during the follow-up. White bars represent the control population while the black bars represent the contaminated implant group. Error bars represent standard error of mean. Asterisk indicates $p<0.05$.

Figure 4 (right page): Haematological parameters. **A:** Summary of the leucocyte differentiation. **B:** Percentage of Lymphocytes. **C:** Percentage of neutrophils. **D:** Percentage of monocytes. **E:** Erythrocyte sedimentation rate. **F:** The C-reactive protein levels. White bars represent the control population while the black bars represent the contaminated implant group. Error bars represent standard error of mean. Asterisk indicates $p<0.05$.

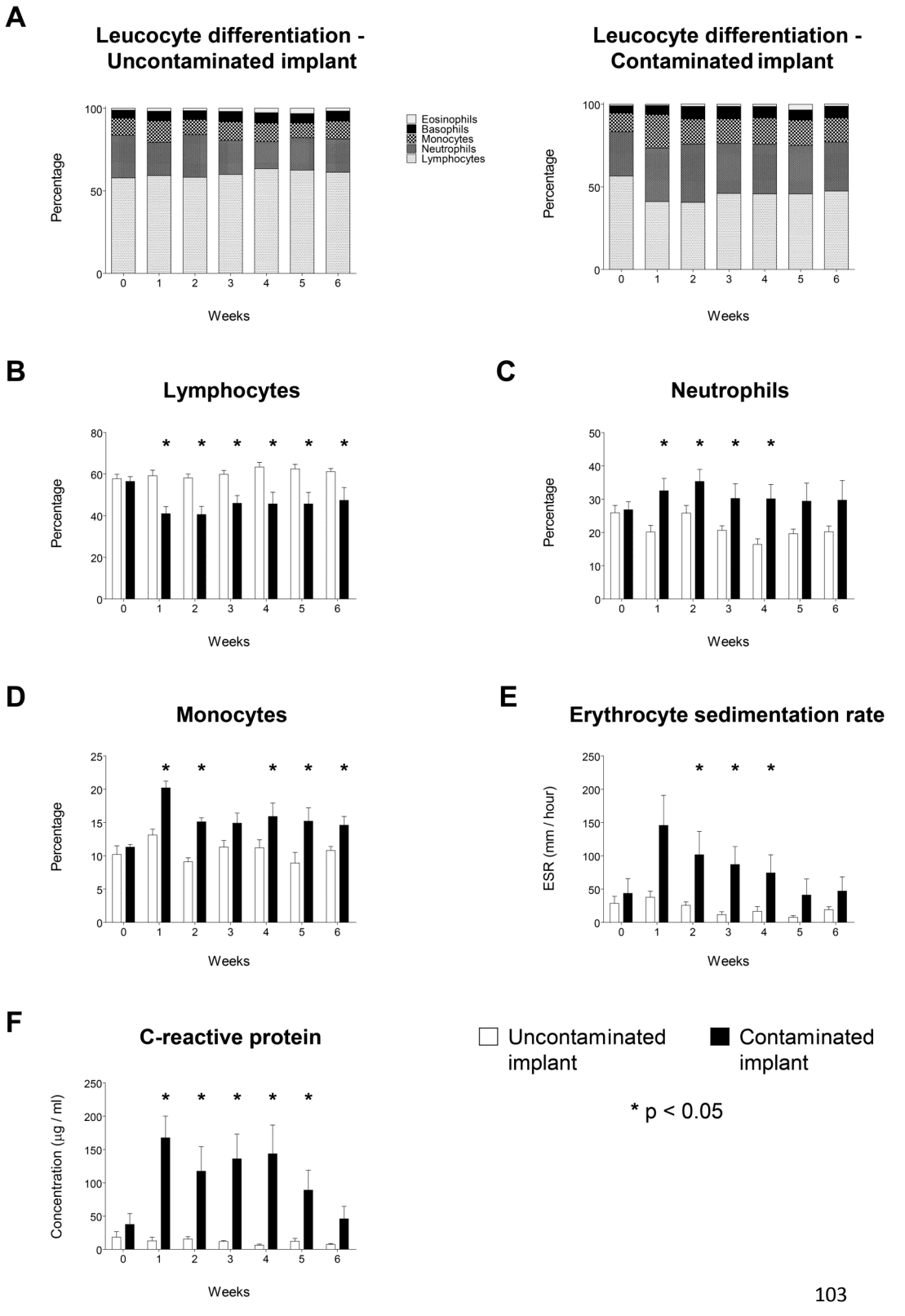
A
Leucocyte differentiation - Uncontaminated implant
Leucocyte differentiation - Contaminated implant
Eosinophils
Basophils
Monocytes
Neutrophils
Lymphocytes
Percentage
Weeks
B
Lymphocytes
C
Neutrophils
D
Monocytes
E
Erythrocyte sedimentation rate
ESR (mm / hour)
F
C-reactive protein
Concentration (µg / ml)
Uncontaminated implant
Contaminated implant
* p < 0.05

The leucocyte differentiation in the control group remained unchanged throughout follow-up, while the contaminated implant group presented with a clear shift in differentiation after surgery, compared to the pre-operative and control group levels. During follow-up, the contaminated implant group showed a relative decrease of the percentage of lymphocytes in favour of the neutrophil- and monocyte-fraction (Figure 4A), resulting in a significantly lower lymphocyte percentage in the contaminated implant group compared to the controls in the entire follow-up (p=0.001, 0.001, 0.001, 0.001, 0.003, 0.021, respectively) (Figure 4B). Neutrophilic granulocyte fractions were significantly higher in the first 4 post-operative weeks only (p=0.010, 0.047, 0.016, 0.001, 0.055 and 0.105, respectively) (Figure 4C). The percentage of monocytes in the contaminated implant group was significantly higher at nearly all postoperative weeks except for the third post-operative week (p=0.001, 0.0001, 0.055, 0.028, 0.016 and 0.006, respectively) (Figure 4D).

The ESR, was significantly higher in the contaminated implant group at the second, third and fourth week (p=0.076, 0.012, 0.006, 0.036, 0.051 and 0.126, respectively) as compared to the uncontaminated control group (Figure 4E). Plasma CRP levels were specifically elevated in the contaminated implant group, for up to 5 weeks after surgery (p=0.0001, 0.021, 0.0001, 0.001, 0.012 and 0.057, respectively) (Figure 4F).

3.3 Radiology

Several clinical radiological parameters for infection, like bone morphological changes, periosteal elevation and thickening together with meta- and diaphyseal osteolysis were observed on X-ray radiographs, enabling the use of our modified scoring system for osteomyelitis (Table 1). After 6 weeks of follow-up the control group showed no signs of osteomyelitis or abnormal morphology of the bone tissue with correct implant placement. Still radiologically visible artefacts from the surgical procedure may suggest the presence of osteolysis around the implant in the direct post-operative images (Figure 5A, small arrowhead).

The contaminated implant group however showed the first signs of osteomyelitis with periosteal reactivity at 2 weeks after surgery (Figure 5A, solid arrowhead). Osteolysis, starting at the metaphyseal level and calcification of the initial periosteal reaction, was observed around the 4th week (Figure 5A, asterisk and double arrowhead, respectively). Diaphyseal osteolysis, with resorption of the cortex and involucrum formation, was generally observed at the 6th week (Figure

5A, hash-sign). Scoring of the individual timed radiographs, using the modified osteomyelitis scoring system (Table 1), resulted in a significantly higher score for animals with a contaminated implant from the second post-operative week onwards (p=0.204, 0.046, 0.036, 0.003, 0.0001 and 0.001, respectively) (Figure 5B). This indicates that infected and uninfected implants can be distinguished in this model from 2 weeks after surgery.

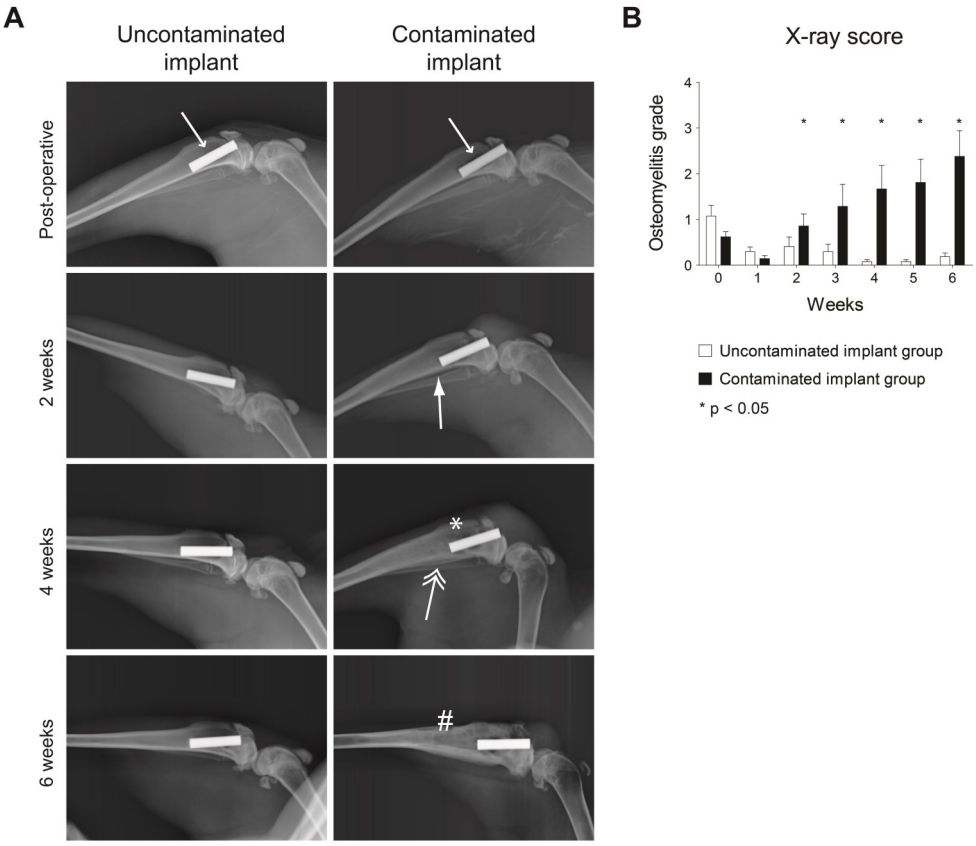

Figure 5: Quantitative radiological *in vivo* imaging. **A:** X-ray images taken during follow-up. The small arrowhead at the post-operative images indicates the possible inter-operative damage to the peri-implant tissue. The solid arrow at 2 weeks indicates the presence of a periosteal reaction. The asterisk at 4 weeks indicates metaphyseal osteolysis, while the double arrowhead points at calcification of the periosteal reaction noted at 2 weeks. The hash-sign at 6 weeks indicates diaphyseal osteolysis. **B:** Quantification of the X-ray images. White bars represent the control population while the black bars represent the contaminated implant group. Error bars represent standard error of mean. Asterisk indicates p<0.05.

Post-mortem microCT imaging at 6 weeks was carried out to acquire in depth overview of the implant/infection area in an axial direction, focussing on bone remodelling around the implant. The control group showed clearly mineralized cortices with sharp boundaries, correct implant positioning and bone apposition on the implant surfaces. No signs of osteolysis were observed. (Figure 6A, far left panels). All contaminated implants on the other hand showed distinctive infection characteristics visible on microCT (Figure 6A, right panels). Remodelling of the tibial cortex, metaphyseal and diaphyseal osteolysis, resorption of the tibial cortex, deformity of the tibial plateau and limited to no bone apposition on the implant were observed. Furthermore, while the sagittal planes allowed comparison with the X-ray radiographs (Figure 5), the transversal planes allowed comparison between the histological sections and provided more information in the axial direction with regard to histomorphological changes in the peri-implant tissue (Figure 8). Blinded scoring of the microCT images (Table 2) allowed quantification of the osteomyelitic status of the rabbit tibia after the 6-week follow-up period. This resulted in a significant differentiation between the control group and the infected implant group ($p=0.0001$) (Figure 6B).

3.4 Bacterial culture

Post-mortem tissue swabs and bone homogenates were selectively cultured on tellurite glycine agar to determine the presence of *S. aureus* and other bacterial species. All swabs and bone homogenates taken from control group animals were negative for bacterial growth, while samples from 6 out of 7 animals of the contaminated implant group were positive for *S. aureus* growth (Figure 7). No growth of *S. epidermidis* was detected in these samples.

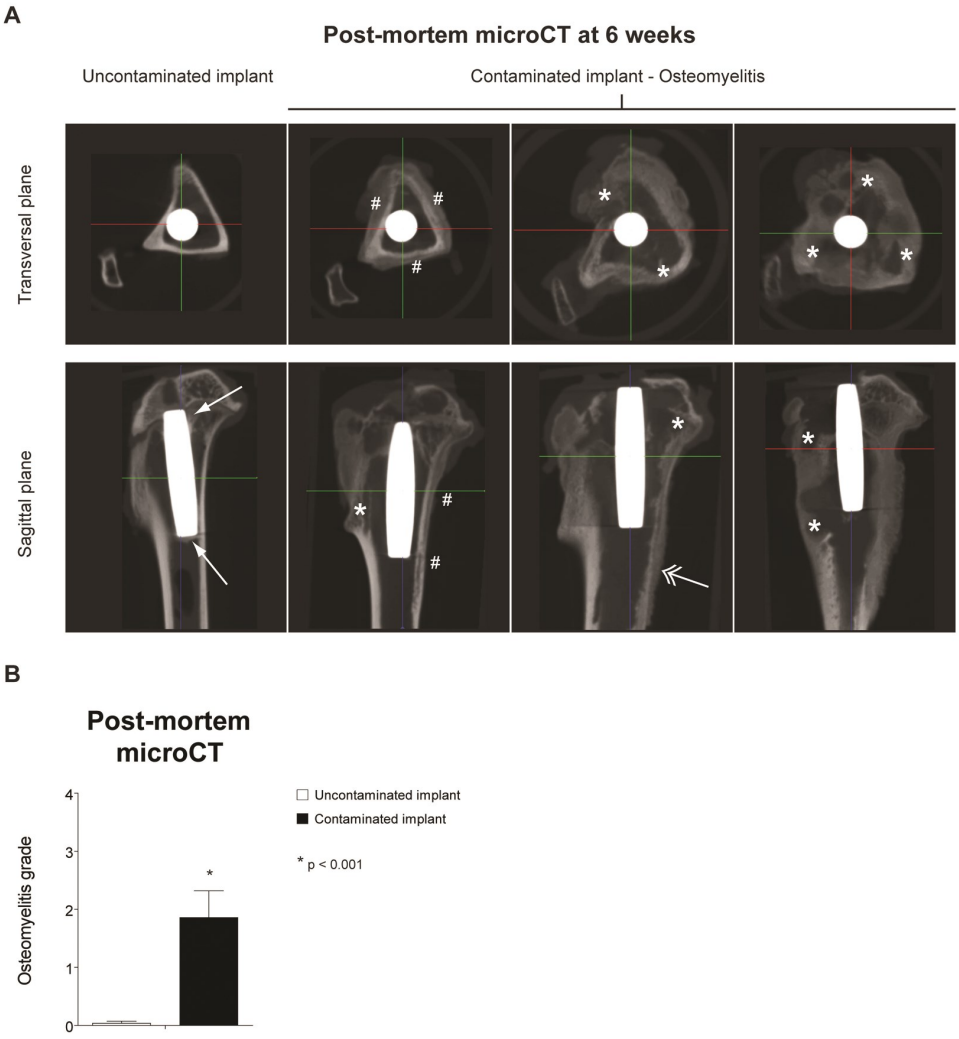

Figure 6: Quantitative radiological *ex vivo* imaging. **A**: Representative *post-mortem* microCT images taken after 6 weeks follow-up. The hash sign indicates calcification of the periosteal reaction, the asterisk indicates osteolysis the solid arrow points at bone apposition at the implant surface and the double headed arrow indicates the presence of an involucrum. **B**: Quantification of the microCT images allows differentiation between the control group (white bar) and the implant infection group (black bar). Error bars represent standard error of mean. Asterisk indicates p<0.001

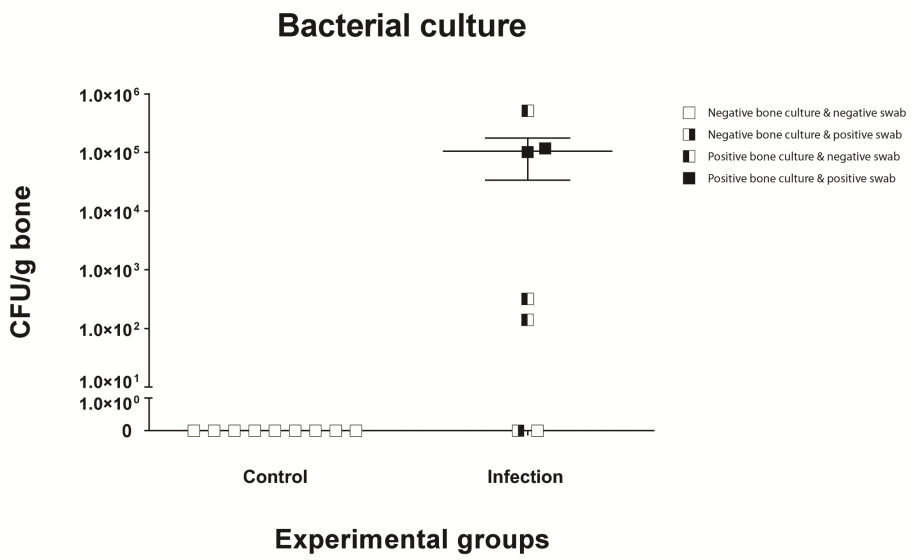

Figure 7: *Post-mortem* bacterial culture. Swabs and bone samples were obtained from each animal and cultured on tellurite glycine agar. Graph indicates culture negativity in all control group samples, while 6 out of 7 animals of the contaminated implant group cultured positive for *S. aureus* infection.

3.5 Histology

Masson-Goldner stained sections revealed normal tibial cortex morphology, bone apposition around the titanium implant and no indication of bacterial presence in PMMA sections of all control tibiae (Figure 8A, left panel). This was in sharp contrast to every contaminated tibia, where Masson-Goldner stained sections show the destructive effect of the infection by cortical thickening, absence of implant ingrowth, abscesses in the bone marrow cavity and enlarged Haversian canals (Figure 8A, right panel). A modified Gram staining was performed to address the presence of bacterial cells (live or dead). Confirming an infected state of the tibiae, Gram positive cocci were found in all contaminated tibiae, whereas these were not microscopically detectable in control tibiae (Figure 8A, inserts). Three different calcium binding fluorophores (Figure 8B, upper panels) allowed tracking of active bone apposition and remodelling on specified timepoints during the follow-up period. Fluorescent signals from the three different fluorophores were detected in sections of control tibiae, where the cortex showed sharp fluorescent linings with overlapping regions, as well as clear signals around the implant surface (Figure 8B, lower left panels). This

indicates local bone apposition and remodelling in an organized and confined manner. In the contaminated tibiae all fluorescent signals were also found, however showing highly disorganized patterning, representing mineralizing periosteal elevation and local remodelling due to osteolytic processes (Figure 8B, lower right panels). The modified scoring system (Table 3), allowed quantitative discrimination of the osteomyelitic status, between uncontaminated and contaminated tibiae. Scoring the histological sections according to this system resulted in two distinct groups that were significantly different (p=0.001) and fully consistent with the contaminated and uncontaminated group.

4. Discussion

Several animal models exist which generally focus on a select number of parameters for monitoring the activity of an osteomyelitis. These models mainly focus on haematological parameters for comparing contaminated and control groups, others on radiological parameters in combination with histology (11, 17, 23) or bacterial culture (16, 18, 24-27). The use of multiple experimental animal groups, sacrificed at pre-defined time points is a frequently used method to specifically gain insight in infection development (28, 29). Yet, this approach requires a large number of animals. Our approach is partially based on previously published models (10, 12, 15), but we combined many of the most relevant infection parameters in one model and measured most of these parameters repeatedly throughout the 6 week follow-up in every animal. Besides lowering the number of required animals, this contributes to the dynamic analysis of the development of an implant infection in individual subjects over time. This broad collection of infection-related outcome parameters allows a selection to be made to establish tailored models in the future to evaluate novel antimicrobial coatings, to study implant fixation and bone apposition on the implant surface or to study the development of osteomyelitis or an implant infection. Still some parameters were not included in our model, like the use of bioluminescent bacteria to induce the implant infection or the assessment of biofilm formation on the implant surface. These remain an option for dedicated models. Also the use of an antibiotic resistant strain, like MRSA, could further broaden the applicability of this acute model. However, as antibiotic sensitive strains are most commonly found to cause orthopaedic implant infections in the clinic (3, 30, 31), at this stage we deliberately chose to establish this model with an antibiotic sensitive strain. Debridement is a commonly used approach in the clinic to treat existing osteomyelitises.

When this model will be used for the evaluation of novel therapeutic antimicrobial approaches like bioactive glass, antibiotic containing bone fillers and cements or resorbable microparticles (32, 33), debridement should be included in this infection model as well. The herein described repeated use of anaesthetics in our model (7 episodes in total, for each rabbit) is not yet optimal, since there is a risk of having an animal not recuperating from the anaesthesia. This was also recognized by Lankinen and colleagues (34). Although kept to a minimum, this severe side effect could not be totally prevented in our present study. We lost 3 animals due to handling issues and respiratory depression related to the anaesthesia. These issues were considered as learning curve-related problems and might be prevented by the use of another combination of anaesthetics. A combination of ketamine-medetomidine-isoflurane should be considered for future experiments as a possible alternative with possibly a lower incidence of respiratory depression. Also the loss of follow-up due to reaching humane endpoints (in our experiments this only occurred in 3 animals of the contaminated implant group), are inevitable (12, 25). Still, daily check-up during follow-up and general supplementation of the daily diet with "Critical Care" (extra fibres and vitamins) positively contributed to the overall animal health throughout the study. Furthermore, many studies based their experiments on individually caged animals (11-13, 15, 19). We chose to house the animals in mixed groups. We regard this as an important aspect of this model, because mixed group housing of the experimental groups stimulates the physical activity of the animals within a housing group and therefore encourages the use of the operated leg, thereby optimally maintaining the function of the operated limb.

The uncontaminated and contaminated groups could be distinguished relatively early by several systemic haematological parameters like ESR, CRP and leucocyte differentiation. As all haematological data consistently separated both groups early in the infection process, measuring a selected parameter may be sufficient for future animal studies in rabbits. For this purpose we suggest to use an ELISA-based measurement of plasma CRP levels as the most sensitive and optimal parameter to determine the presence of a developing implant infection. ESR and leucocyte differentiation can also be used in specific cases but may be more prone to experimental misinterpretation due to the used capillary approach or is relatively expensive, respectively.

In the development of our model some limitations were encountered in the imaging of each animal over time. As an *in vivo* microCT was not at our disposal we were not able to visualize bone development in all three dimensions over time *in vivo*. Instead we applied weekly medio-lateral X-ray radiographs to visualize the tibiae in the sagittal plane over time and added *post-mortem*

microCT to analyse the tibiae in three dimensions at the 6-week timepoint only. By combining the overtime X-ray imaging with the single timepoint microCT as well as histology and fluorescent imaging of the calcium binding fluorophores, the overall bone development during follow-up could be visualized in great detail. Although true three-dimensional information on bone development over-time is lacking, the herein described approach provides adequate information on bone activity for future interpretation of the efficacy of antimicrobial implant coatings.

Due to the complexity of the model the need of clearly defined scoring systems for radiology and histology to allow proper discrimination of the infection status of an implant is evident. Several scoring systems have been described in the past, like the well known X-ray scoring system of Calhoun and Mader (17) or the histological scoring system used by Petty and colleagues (35), modified by Vogely (15). Due to the high number of parameters in our study, these scoring systems could not be implemented in our model without necessary modifications. This resulted in three independent modified scoring systems for the assessment of X-ray radiographs, microCT and histology (Table 1). When developing these scoring systems we used the original scoring systems (17, 35), but incorporated additional results from X-ray radiographs, microCT and histology in our modified scoring systems. The X-ray radiographs and microCT score is based on infection-induced morphological changes of the tibia and the histological scoring system is a cumulative score based on the presence of multiple histomorphological infection parameters. Using the scoring systems on the herein described experimental groups, we were able to faithfully discriminate infected from uninfected tibiae. As detailed parameters were included in the scoring systems we expect that these will be able to also detect more subtle changes due to e.g. persisting low-grade infections.

Bacterial culturing of homogenized bone fragments and swabs showed specific growth of *Staphylococcus aureus* in 6 out of the 7 contaminated implants. The remaining implant was inconclusive for bacterial growth. This could either be the result of clearing of the infection by the host-immune system, or by stress acting on the bacterial cells during homogenisation. This animal however also showed less severe radiological and histological symptoms of infection, while the damage to the peri-implant tissue and the haematological data in this contaminated animal indisputably pointed to an infection. As it seems that even within the same species identically administered bacterial contaminations do not develop equal infections (8, 15, 24), it stresses the use of multiple independent infection parameters to analyse the development of an osteomyelitic infection, to avoid large experimental groups and false negative scores based solely on negative bacterial cultures.

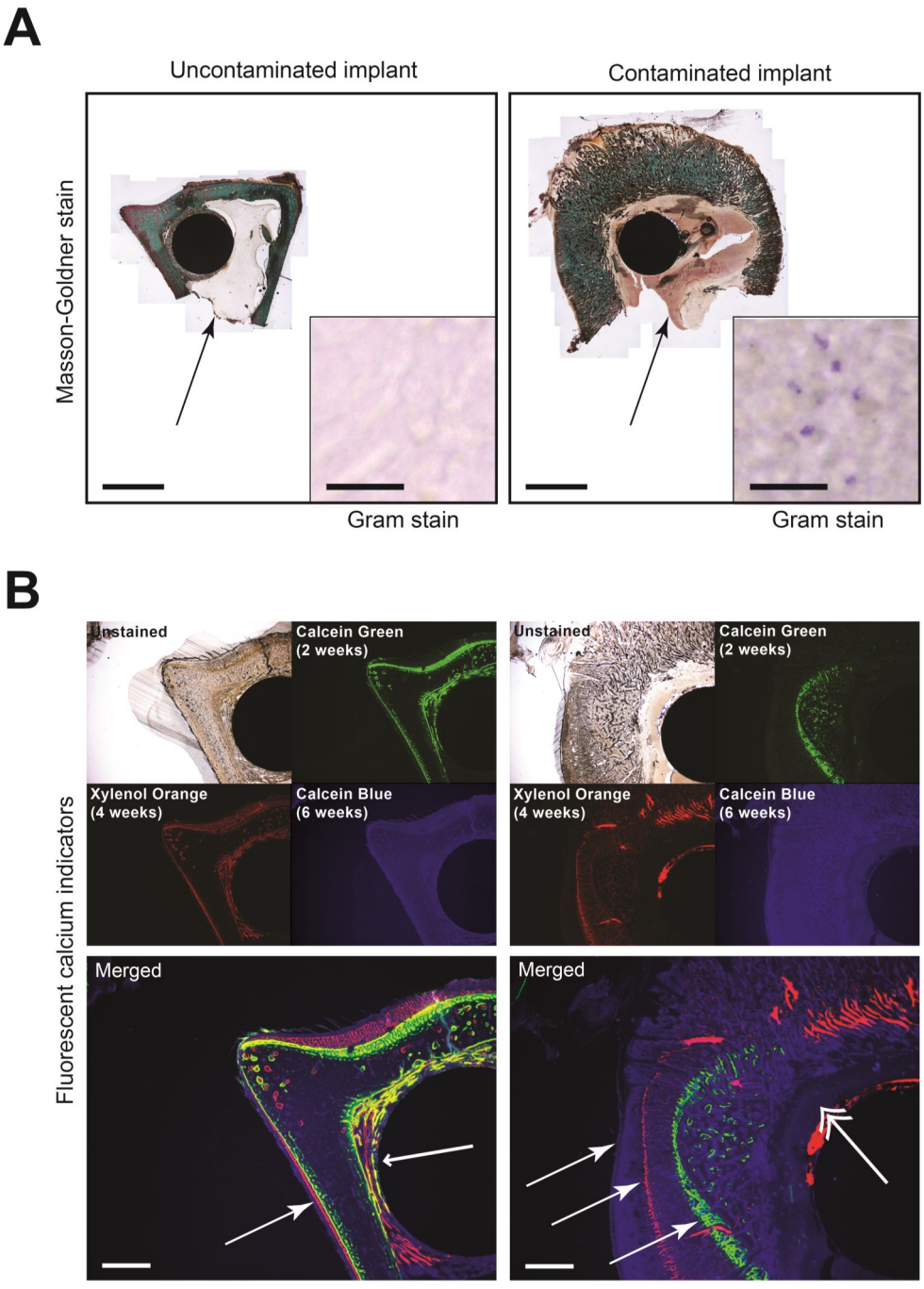
A
Uncontaminated implant
Contaminated implant
Masson-Goldner stain
Gram stain
Gram stain
B
Fluorescent calcium indicators
Unstained
Calcein Green
(2 weeks)
Xylenol Orange
(4 weeks)
Calcein Blue
(6 weeks)
Merged
Unstained
Calcein Green
(2 weeks)
Xylenol Orange
(4 weeks)
Calcein Blue
(6 weeks)
Merged

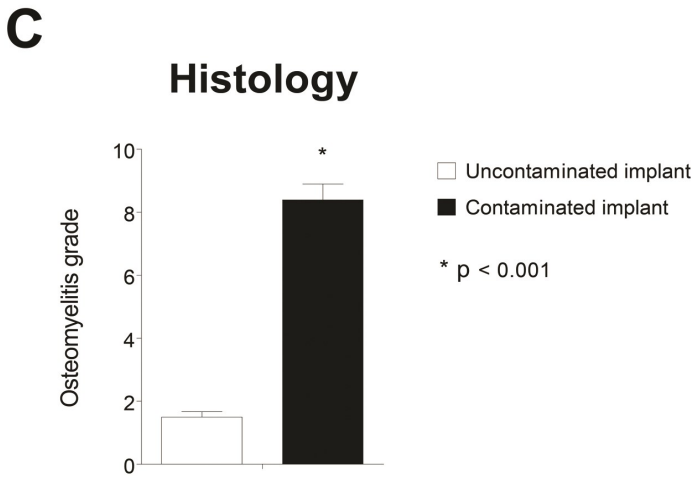

Figure 8: Quantitative histology. **A**: Histological sections of the distal part of the implant region. Sections show distinctive morphological changes in the contaminated implant group, with bone apposition on the implant surface in the uncontaminated implant group and cortical thickening in the contaminated implant group. Black arrow indicates an intramedullary abscess in the contaminated implant group only (bars represent 4 mm). Gram staining (insert) shows gram positive cells in the contaminated implant group while the uncontaminated group remains negative (bars represent 20 µm). **B**: Calcium binding fluorophores represent calcium deposition at the time of injection, indicating bone development (large arrowhead) and implant ingrowth (small arrowhead) in the uncontaminated implant group. In the contaminated implant group these indicators point at calcification of the periosteum due the periosteal elevation (3 identical white arrows) caused by the presence of bacteria. The double arrowhead indicates osteolysis in the peri-implant tissue (bars represent 1 mm). **C**: Quantification of the histological symptoms of implant infection shows a distinct, significant difference between the control group (white bar) and the infected implant group (black bar). Error bars represent standard error of mean. Asterisk indicates $p<0.001$.

Although histological staining of PMMA-sections clearly showed whether or not an infection was present in the tested tibiae ((12, 15) and this study), analysis of this *post-mortem* material does not provide insight into infection related bone remodelling over-time. To overcome this hurdle we additionally incorporated three different commonly used calcium binding fluorophores in this animal model (36). This allows assessment of bone remodelling/calcification caused by the initial

infection and detection of subtle local changes that might be missed by other techniques. In our study both calcein green and xylenol orange were injected at earlier timepoints, whereas calcein blue was injected only 24 hours before sacrifice. The short time frame before sacrifice could explain why the fluorescent signal for calcein blue was more diffuse as for the other two fluorophores (due to slow systemic clearance). This suggests that a calcium binding fluorophore should be injected several days before sacrifice to obtain sharp fluorescent signals.

5. Conclusion

The present study has shown that we established a per-operative orthopaedic implant contamination model resulting in early post-operative infection in rabbits with a comprehensive multi-analytical six-week follow-up. The modified scoring systems of several imaging techniques and histology allow a clear classification of the infection grade of the peri-implant tissue. The longitudinal assessment of the animals' infection status reduces the required number of test animals, without making concessions on the outcome data and statistics. In addition to the gained information on the longitudinal development of an acute implant infection, the above-mentioned suggestions (anaesthesia and nutritional supplementation) can improve future experimental survival. Our experimental and analytical setup may be used for the thorough longitudinal assessment of novel prophylactic antimicrobial coatings and antimicrobial treatments in a relatively small population of individual animals. Furthermore our study suggests that a combination of weekly weight measurements, CRP, and X-rays combined with bi-weekly injections of calcium binding fluorophores and *post-mortem* bacterial bone culture provide the most optimal insight on infection development and status.

Acknowledgements

This research forms part of the Project P4.01 NANTICO of the research program of the BioMedical Materials institute, co-funded by the Dutch Ministry of Economic Affairs.

The authors would like to thank the employees of the animal facility of the Maastricht University Medical Centre for their assistance during this study. We would also like to thank J. Geurts for scoring the X-ray radiographs and microCT images and A. Cremers and D. Logister for scoring the histological sections (Department of Orthopaedic Surgery, Maastricht University Medical Centre, the Netherlands), Dr. D. Moojen and Dr. H. Vogely for their valuable input during the preparations of this study (Department of Orthopaedic Surgery, University Medical Centre Utrecht, the Netherlands) and S. Bout and P. Dijkstra (Maastricht University Medical Centre) for their overall assistance during this study.

References

1. Zimmerli W, Lew PD, Waldvogel FA. Pathogenesis of foreign body infection. Evidence for a local granulocyte defect. Journal of Clinical Investigation. 1984 Apr;73(4):1191-200.
2. Zimmerli W, Waldvogel FA, Vaudaux P, Nydegger UE. Pathogenesis of foreign body infection: Description and characteristics of an animal model. Journal of Infectious Diseases. 1982 Oct;146 (4):487-97.
3. Montanaro L, Speziale P, Campoccia D, Ravaioli S, Cangini I, Pietrocola G, Giannini S, Arciola CR. Scenery of staphylococcus implant infections in orthopedics. Future Microbiology. 2011 Nov;6 (11):1329-49.
4. Montanaro L, Testoni F, Poggi A, Visai L, Speziale P, Arciola CR. Emerging pathogenetic mechanisms of the implant-related osteomyelitis by staphylococcus aureus. International Journal of Artificial Organs. 2011 Sep;34(9):781-8.
5. Smeltzer MS, Thomas JR, Hickmon SG, Skinner RA, Nelson CL, Griffith D, Parr TR, Jr., Evans RP. Characterisation of a rabbit model of staphylococcal osteomyelitis. Journal of Orthopaedic Research. 1997 May;15(3):414-21.
6. Miclau T, Schmidt AH, Wenke JC, Webb LX, Harro JM, Prabhakara R, Shirtliff ME. Infection. Journal of Orthopaedic Trauma. 2010 Sep;24(9):583-6.
7. Trampuz A, Zimmerli W. Diagnosis and treatment of infections associated with fracture-fixation devices. Injury. 2006 May;37 Suppl 2:S59-66.
8. Norden CW. Experimental osteomyelitis. I. A description of the model. Journal of Infectious Diseases. 1970 Nov;122(5):410-8.
9. Andriole VT, Nagel DA, Southwick WO. A paradigm for human chronic osteomyelitis. Journal of Bone and Joint Surgery (American Volume). 1973 Oct;55(7):1511-5.
10. Andriole VT, Nagel DA, Southwick WO. Chronic staphylococcal osteomyelitis: An experimental model. Yale Journal of Biology and Medicine. 1974 Mar;47(1):33-9.
11. An YH, Bradley J, Powers DL, Friedman RJ. The prevention of prosthetic infection using a cross-linked albumin coating in a rabbit model. Journal of Bone and Joint Surgery (British Volume). 1997 Sep;79 (5):816-9.
12. Moojen DJ, Vogely HC, Fleer A, Nikkels PG, Higham PA, Verbout AJ, Castelein RM, Dhert WJ. Prophylaxis of infection and effects on osseointegration using a tobramycin-periapatite coating on titanium implants--an experimental study in the rabbit. Journal of Orthopaedic Research. 2009 Jun;27(6):710-6.
13. Poultsides LA, Papatheodorou LK, Karachalios TS, Khaldi L, Maniatis A, Petinaki E, Malizos KN. Novel model for studying hematogenous infection in an experimental setting of implant-related infection by a community-acquired methicillin-resistant s. Aureus strain. Journal of Orthopaedic Research. 2008 Oct;26(10):1355-62.
14. Sanzen L, Linder L. Infection adjacent to titanium and bone cement implants: An experimental study in rabbits. Biomaterials. 1995 Nov;16(16):1273-7.
15. Vogely HC, Oosterbos CJ, Puts EW, Nijhof MW, Nikkels PG, Fleer A, Tonino AJ, Dhert WJ, Verbout AJ. Effects of hydrosyapatite coating on ti-6a1-4v implant-site infection in a rabbit tibial model. Journal of Orthopaedic Research. 2000 May;18(3):485-93.
16. Darouiche RO, Mansouri MD, Zakarevicz D, Alsharif A, Landon GC. In vivo efficacy of antimicrobial-coated devices. Journal of Bone and Joint Surgery (American Volume). 2007 Apr;89(4):792-7.
17. Calhoun JH, Mader JT. Treatment of osteomyelitis with a biodegradable antibiotic implant. Clinical Orthopaedics and Related Research. 1997 Aug(341):206-14.
18. Darouiche RO, Mansouri MD, Schneidkraut MJ. Comparative efficacies of telavancin and vancomycin in preventing device-associated colonisation and infection by staphylococcus aureus in rabbits. Antimicrobial Agents and Chemotherapy. 2009 Jun;53(6):2626-8.
19. Moojen DJ, Vogely HC, Fleer A, Verbout AJ, Castelein RM, Dhert WJ. No efficacy of silver bone cement in the prevention of methicillin-sensitive staphylococcal infections in a rabbit contaminated implant bed model. Journal of Orthopaedic Research. 2009 Aug;27(8):1002-7.
20. Russell W, Burch R. The principles of humane experimental technique. United States of America: Johns Hopkins University; 1959.

21. Jones RC, Deck J, Edmondson RD, Hart ME. Relative quantitative comparisons of the extracellular protein profiles of staphylococcus aureus uams-1 and its sara, agr, and sara agr regulatory mutants using one-dimensional polyacrylamide gel electrophoresis and nanocapillary liquid chromatography coupled with tandem mass spectrometry. Journal of Bacteriology. 2008 Aug;190(15):5265-78.
22. Sachs L. Applied statistics: A handbook of techniques. New York, Heidelberg, Berlin: Springer-Verlag; 1982. 706 p.
23. Alt V, Bitschnau A, Bohner F, Heerich KE, Magesin E, Sewing A, Pavlidis T, Szalay G, Heiss C, Thormann U, Hartmann S, Pabst W, Wenisch S, Schnettler R. Effects of gentamicin and gentamicin-rgd coatings on bone ingrowth and biocompatibility of cementless joint prostheses: An experimental study in rabbits. Acta Biomater. 2011 Mar;7(3):1274-80.
24. Melcher GA, Claudi B, Schlegel U, Perren SM, Printzen G, Munzinger J. Influence of type of medullary nail on the development of local infection. An experimental study of solid and slotted nails in rabbits. Journal of Bone and Joint Surgery (British Volume). 1994 Nov;76(6):955-9.
25. Williams D, Bloebaum R, Petti CA. Characterisation of staphylococcus aureus strains in a rabbit model of osseointegrated pin infections. J Biomed Mater Res A. 2008 May;85(2):366-70.
26. Gaudin A, Amador Del Valle G, Hamel A, Le Mabecque V, Miegeville AF, Potel G, Caillon J, Jacqueline C. A new experimental model of acute osteomyelitis due to methicillin-resistant staphylococcus aureus in rabbit. Letters in Applied Microbiology. 2011 Mar;52(3):253-7.
27. Jacqueline C, Amador G, Caillon J, Le Mabecque V, Batard E, Miegeville AF, Biek D, Ge Y, Potel G, Hamel A. Efficacy of the new cephalosporin ceftaroline in the treatment of experimental methicillin-resistant staphylococcus aureus acute osteomyelitis. Journal of Antimicrobial Chemotherapy. 2010 Aug;65(8):1749-52.
28. He F, Yang G, Wang X, Zhao S. Bone responses to rough titanium implants coated with biomimetic ca -p in rabbit tibia. J Biomed Mater Res B Appl Biomater. 2009 Aug;90(2):857-63.
29. Lankinen P, Makinen TJ, Poyhonen TA, Virsu P, Salomaki S, Hakanen AJ, Jalkanen S, Aro HT, Roivainen A. (68)ga-dotavap-p1 pet imaging capable of demonstrating the phase of inflammation in healing bones and the progress of infection in osteomyelitic bones. European Journal of Nuclear Medicine and Molecular Imaging. 2008 Feb;35(2):352-64.
30. Moran E, Masters S, Berendt AR, McLardy-Smith P, Byren I, Atkins BL. Guiding empirical antibiotic therapy in orthopaedics: The microbiology of prosthetic joint infection managed by debridement, irrigation and prosthesis retention. Journal of Infection. 2007 Jul;55(1):1-7.
31. Trampuz A, Zimmerli W. Antimicrobial agents in orthopaedic surgery: Prophylaxis and treatment. Drugs. 2006;66(8):1089-105.
32. Le Ray AM, Gautier H, Laty MK, Daculsi G, Merle C, Jacqueline C, Hamel A, Caillon J. In vitro and in vivo bactericidal activities of vancomycin dispersed in porous biodegradable poly(epsilon-caprolactone) microparticles. Antimicrobial Agents and Chemotherapy. 2005 Jul;49(7):3025-7.
33. Hamel A, Caillon J, Jacqueline C, Rogez JM, Potel G. Internal device decreases antibiotic's efficacy on experimental osteomyelitis. Journal of Children's Orthopaedics. 2008 Jun;2(3):239-43.
34. Lankinen P, Lehtimaki K, Hakanen AJ, Roivainen A, Aro HT. A comparative 18f-fdg pet/ct imaging of experimental staphylococcus aureus osteomyelitis and staphylococcus epidermidis foreign-body-associated infection in the rabbit tibia. EJNMMI Res. 2012 Jul 23;2(1):41.
35. Petty W, Spanier S, Shuster JJ, Silverthorne C. The influence of skeletal implants on incidence of infection. Experiments in a canine model. Journal of Bone and Joint Surgery (American Volume). 1985 Oct;67(8):1236-44.
36. van Gaalen SM, Kruyt MC, Geuze RE, de Bruijn JD, Alblas J, Dhert WJ. Use of fluorochrome labels in in vivo bone tissue engineering research. Tissue engineering Part B, Reviews. 2010 Apr;16(2):209-17.

CHAPTER

5

^{18}F-FDG microPET imaging differentiates between septic and aseptic wound healing after orthopaedic implant placement

J.C.E. Odekerken

B.T. Brans

T.J.M. Welting

G.H.I.M. Walenkamp

Acta Orthopaedica. 2014;85:3

Abstract

Background and purpose: ^{18}F-FDG PET is a widely used tool for molecular imaging of oncological, cardiovascular and neurological disorders. We evaluated ^{18}F-FDG microPET as an implant osteomyelitis imaging tool using a *Staphylococcus aureus*-induced per-operative implant infection in rabbits.

Methods: Intramedullary titanium nails were implanted in contaminated and uncontaminated (control) proximal right tibiae of rabbits. Tibiae were quantitatively assessed with microPET for ^{18}F-FDG uptake before and sequentially at 1, 3 and 6 weeks after surgery. Tracer uptake was assessed in soft tissue and bone in both treatment groups with an additional comparison between the operated and non-operated limb. MicroPET analysis was combined with radiological assessment and complementary histology of the tibiae.

Results: At the first post-operative week the ^{18}F-FDG uptake in the contaminated implant group was significantly higher compared to the pre-operative measurement, without a significant difference between the contaminated and uncontaminated tibiae. From the third post-operative week onward, ^{18}F-FDG uptake allowed discrimination between osteomyelitis and post-operative aseptic bone healing, as well as quantification of the infection at distinct locations around the implant.

Interpretation: ^{18}F-FDG-based microPET imaging allows differentiation between deep infection and undisturbed wound healing after implantation of a titanium intramedullary nail in this rabbit model. Furthermore, our results indicate that ^{18}F-FDG PET may provide a tool in human clinical diagnostics and for the evaluation of antimicrobial strategies in animal models for orthopaedic implant infection.

Key words

^{18}F-FDG; microPET; implant; osteomyelitis; animal

1. Introduction

With more prostheses and osteosyntheses being implanted every year and a suggested increase in infection rate, the absolute number of implant infections will increase (1-3). Deep orthopaedic implant infections are difficult to diagnose in the early post-operative weeks, while infection diagnosis in this period is important for adequate patient treatment and implant survival. A specific diagnostic tool to monitor implant infections is therefore imperative.

Current diagnostics to detect orthopaedic implant infections are based on clinical symptoms, haematological parameters, radiology and nuclear scintigraphy. However, in the early post-operative phase as in low-grade infections, changes like periosteal reactions and cortical thickening (4-6) or osteolysis and calcifications (4-7) are not specific enough to differentiate between implant/ soft tissue infection, and aseptic wound problems. More discriminative power is needed to distinguish aseptic wound healing from bacterial infection and to follow implant infection quantitatively over time. ^{18}F-fluorodeoxyglucose (^{18}F-FDG) is widely used as a positron emission tomography (PET) tracer to diagnose and monitor several pathological conditions in the clinic (8-13). The use of ^{18}F-FDG as a tracer is based on a locally increased metabolic turnover of glucose. Since the presence of bacteria and increased leukocyte infiltration in an infected area generates such a locally increased glucose turnover and thus increased ^{18}F-FDG uptake (8, 14, 15), it allows for local detection of bacterial infections.

We hypothesized that ^{18}F-FDG PET scanning is able to provide the discriminative power needed to distinguish aseptic wound healing from orthopaedic implant infection. To address this hypothesis we longitudinally determined the development of implant osteomyelitis by ^{18}F-FDG microPET scanning of contaminated and uncontaminated rabbit tibiae and explored its potential use in implant infection diagnostics.

2. Materials and methods

2.1 Experimental group

Twenty-two specified pathogen free (SPF), female New Zealand White (NZW) rabbits (Charles River, France), within a weight range of 3.5 – 4 kg were used in this study. Animals were allowed to acclimatize for 2 weeks, before the initial start of the experiments. Thirteen animals, randomly

chosen from the population, were scanned 2 weeks before surgery with ^{18}F-FDG microPET to define the background tracer uptake level in a healthy animal without surgical intervention. At the day of surgery, the population was subdivided into 2 equally sized, randomly assigned research groups, an uncontaminated implant group (sterile saline control) and a contaminated implant group.

Anaesthesia was initiated by ketamine (35 mg/kg i.m.) (Nimatek, Eurovet Animal Health, the Netherlands) and xylazine (5 mg/kg i.m.) (Xylalin, Ceva Santé Animale, France), while maintained by fentanyl (2 µg/kg/h i.v.) (Fentanyl, Hameln Pharmaceuticals, Germany), midazolam (1 mg/kg/h i.v.) (Midazolam, Actavis, Switzerland) and if necessary supported by isoflurane (1%) (Isoflo, Abbott Laboratories, USA). A 2% iodine solution in ethanol (Aesculaap, the Netherlands) was used for the disinfection of the shaved right hind leg of the animal.

A transpatellar incision was made to acquire access to the tibial plateau. A 4 mm wide opening was drilled, by sequential reaming, with a hand drill into the tibial plateau to gain access to the intramedullary cavity. Residual bone fragments and haematoma were removed by irrigation. Each animal received a 4 mm wide, 20 mm long, grit blasted titanium-alloy (TiAl6V4) implant (DePuy, Johnson & Johnson, UK) into the tibial intramedullary cavity.

The uncontaminated implant group received a 100 µl sterile saline injection into the intramedullary cavity, before implantation of the titanium implant. The implant infection group received a single dose of on average $3.8x10^5$ colony forming units (CFU) *S. aureus* (UAMS-1, ATCC 49230, ATCC, USA) in 100 µl saline, into the intramedullary cavity before implantation. The implant was positioned distal to the tibial articulating surface. The bone defect was sealed with bonewax (Syneture, Covidien, USA) and the surrounding soft tissues were flushed with sterile saline. The wound was closed in layers with single resorbable sutures and protected by the application of "Aluminium spray" (Eurovet Animal Health, the Netherlands).

Animals were housed in groups to stimulate physical activity of the animal and thus movement of the operated leg. Animals were randomly assigned to a housing group based on the day of surgery, resulting in mixed housing of animals with contaminated and uncontaminated implants. Animals received food and water *ad libitum,* daily diet was supplemented with 20 g "Critical Care" (Oxbow Animal Health, USA) to support animal physical condition. The animals were checked daily for general health and experiment-related discomfort during a period of 6 weeks. Pain treatment by injection of buprenorphine (0.05 mg/kg bodyweight, Temgesic, Reckitt Benckiser, UK) was applied twice a day, for the first 2 days after surgery and continued if pain persisted.

Tibial fracture, sepsis, and extensive formation of soft tissue abscesses and fistula were defined in accordance with the institutional animal ethics committee as humane endpoints. In case of 20% weight loss, a veterinarian was consulted and the animal was treated accordingly by either additional individual feeding with "Critical Care" or euthanisation of the animal. All remaining animals were sacrificed 6 weeks after surgery by a pentobarbital (Euthanimal, Alfasan Diergeneesmiddelen, the Netherlands) overdose.
This study was approved in September 2010 by the Maastricht University Animal Ethics Committee (DEC-UM, Protocol 2010-089, Maastricht, the Netherlands).

2.2 Radiological imaging

Radiographs were acquired under tiletamine-zolazepam anaesthesia (15 mg/kg body weight, Zoletil 100, Virbac Laboratories, France), to assess bone quality and implant positioning applied weekly, starting directly post-operative. Antero-posterior and lateral images were acquired at 85 kV and 20 mAs (Polymobil, Siemens, Germany) on Kodak PQ-phosphor screens (Carestream Healthcare, USA). Acquired data were digitized by a CR-975 phosphor screen reader (Carestream Healthcare, USA). Digitized images were visualized with the Philips iSite (version 3.5) software package (Royal Philips Electronics, the Netherlands). Radiographs were assessed for signs for osteomyelitis (periosteal elevation, cortical thickening and osteolysis) (4, 6).
After 6 weeks follow-up the animals were sacrificed and the hindleg excised in a sterile fashion. *Ex vivo* microCT imaging of these excised hindlegs was performed directly *post-mortem*. Images were acquired on an X-rad 225 (Precision X-ray, USA), with a field of view of 10 cm in diameter, a source-to-axis distance of 30 cm and a source-to-detector distance of 62 cm. Images were acquired at 80 kVp, with an isotropic spacing of 102 µm and 2.14 mm Al added filtration. The GE MicroView (version 2.1.2) software package (GE Healthcare, USA) was used for the image evaluation.

2.3 ^{18}F-FDG microPET imaging

The entire microPET procedure of approximately 2 hours was performed under tilatamine-zolazepam sedation, initiated by a 15 mg/kg intramuscular dose and 3 additional intramuscular injections of 7.5 mg/kg. The time between the first and the subsequent second dose was 20 minutes, al injections following thereafter were given with 45 minute intervals. A pre-operative

scan and 3 post-operative scans (respectively at 1, 3 and 6 weeks after surgery) were made to assess the progress of implant infection in each animal. The rabbits were fixed in a custom made PVC restrainer (Figure 1), which allowed the rabbit to breath freely without allowing movements of the hind legs. Fifty MBq ^{18}F-FDG (GE Healthcare Medical Diagnostics, Eindhoven, the Netherlands) was diluted with sterile saline to a volume of 1 ml and was subsequently injected in the ear vein of the rabbit. Residual activity in the syringe was measured on a CRC-25R dose calibrator (Capintec, USA) to calculate the initially injected ^{18}F-FDG dose. A 1 hour incubation period was taken into account to allow uptake of the ^{18}F-FDG in the area of interest.

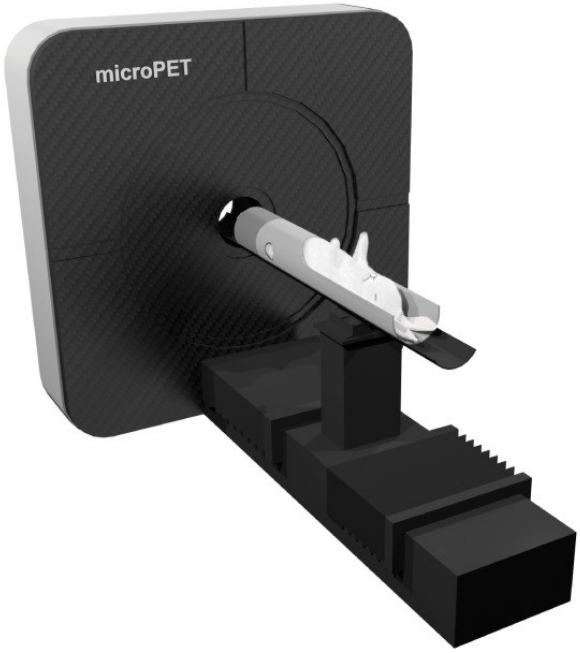

Figure 1: Representation of the experimental setup. Animal positioning in the custom made restrainer on the Siemens Focus 120 microPET scanner.

The microPET scans of the rabbit hind legs were performed on a Focus 120 microPET scanner (Siemens, Germany) (Figure 1) with an axial field of view of 7.6 cm consisting of 95 slices of 0.796 mm thick. The spatial resolution was 1.4 mm at the centre of the field of view. A 773 second static transmission scan, using a ^{57}CO rod source for attenuation correction, was obtained before the

initial 900 second static emission scan. Transmission scan data were acquired using an energy window of 120-125 keV and the emission data were acquired using an energy window of 350-650 keV, both had a coincidence timing window of 6 ns. Acquired data were reconstructed iteratively in a 128x128x95 matrix using attenuation-weighed 2-dimensional ordered-subsets expectation maximisation (OSEM2D).

Data were analysed with the ASIPRO VM software package (version 6.7.1.2, Concorde Microsystems, Siemens, Germany). The imaging data were reconstructed by the OSEM2D protocol with an isotropic voxel size of 0.87 mm to align the implant with the coronal, sagittal and transversal planes to keep the regions and volumes of interest (ROI and VOI) of all scans equal. A cylindrical VOI of 10.4 mm in diameter and 25.1 mm long (12 voxels in diameter and 29 voxels long) was used as a contour around the implant (of 4x20 mm) and the surrounding bony tissue. An equally sized VOI was placed in the contralateral leg on the equivalent location where an implant was placed in the other leg. Each leg also contained an equally sized VOI in the *vastus lateralis* to serve as a measurement for the soft tissue ^{18}F-FDG-uptake. Additionally 3 circular ROI (10.4 mm in diameter (respectively 12 voxels), and 0.87 mm in thickness (respectively 1 voxel)) were constructed at the proximal, central and distal part of each implant. The standardized uptake value (SUV) was calculated from the total activity in the selected ROI and VOI, corrected for the weight of the animal and the activity of ^{18}F-FDG in the animal at the time of emission scanning. Activity at the time of the scan was corrected for the injected activity and the calibration factor of the microPET and dose calibrator.

2.4 Quantification of infection

Weekly assessment of clinical, haematological and radiological infection parameters, combined with *post-mortem* microCT was performed to confirm the absence or presence of an infection in the uncontaminated and contaminated implants. Furthermore *post-mortem* bone tissue culture was performed to verify the presence of bacteria. Bacterial growth was assessed on tellurite glycine agar after 24 hours of culture. After sampling for bacterial culture, the remaining part of the tibiae, which included the implant, was fixated in a 4% formaldehyde/PBS solution for 4 weeks, followed by alcohol dehydration and embedding in polymethyl methacrylate (PMMA) (Technovit 9100, Hereaus-Kulzer, Germany). Once polymerized, 50 µm sections were acquired on a saw microtome (SP 1600, Leica, Germany), stained according to Masson-Goldner (Carl Roth, Germany)

or Gram and glued on a microscope slide with UV-polymerizing glue (Permacol, the Netherlands). The sections were digitized by light microscopy (Axioscope A1, Axiovison LE release 4.8.2, Carl Zeiss, Germany). Acquired images were fused with Photoshop CS3 (Adobe Systems, USA) to generate overview images.

2.5 Statistical analysis

Significant differences between the contaminated and uncontaminated implant group were determined by Student's T-test for independent-samples. The significant differences between the operated and non-operated contralateral legs were determined by a paired-samples T-test. Statistical significance was set at a p-value below 0.05. Experimental drop-out resulted in an experimental population of 15 animals with a complete post-operative follow-up: 8 animals with an uncontaminated implant and 7 animals with a contaminated implant.
Statistical analysis was performed with SPSS 21 (IBM, USA). Graphical representation of the statistical data was performed in GraphPad Prism 5 (GraphPad, USA).

3. Results

3.1 Surgery and follow-up

The animals with an uncontaminated implant recovered to full weight bearing within the first 2 weeks after surgery, while in the contaminated implant group the animals only showed partial weight bearing of the operated leg throughout the experiment. From the initial 22 animals, 3 animals did not recover from anaesthesia, 3 other animals (all in the contaminated implant group) had to be sacrificed before the end of the study because of humane endpoints, related to the bacterial infection. Furthermore, the use of tiletamine-zolazepam for anaesthesia caused muscle contractions in 1 animal which therefore could not be scanned on the microPET on all time points. Complete datasets were acquired from 8 animals with an uncontaminated implant and 7 animals with a contaminated implant. Acquired datasets of animals that did not complete the experimental follow-up were excluded from data analysis.

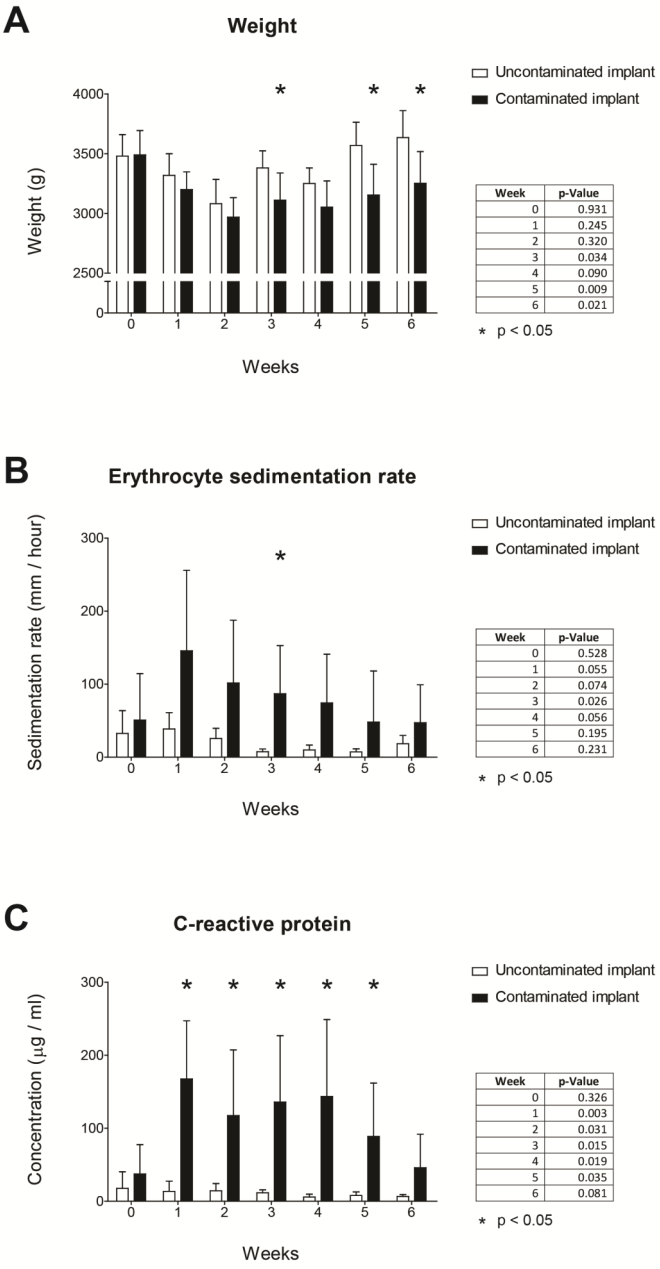

Figure 2: A: Animal weight. **B:** erythrocyte sedimentation rate. **C:** C-reactive protein levels. Asterisk indicates $p < 0.05$, tables beside the graphs describe the corresponding p-values. Error bars represent 95% confidence intervals.

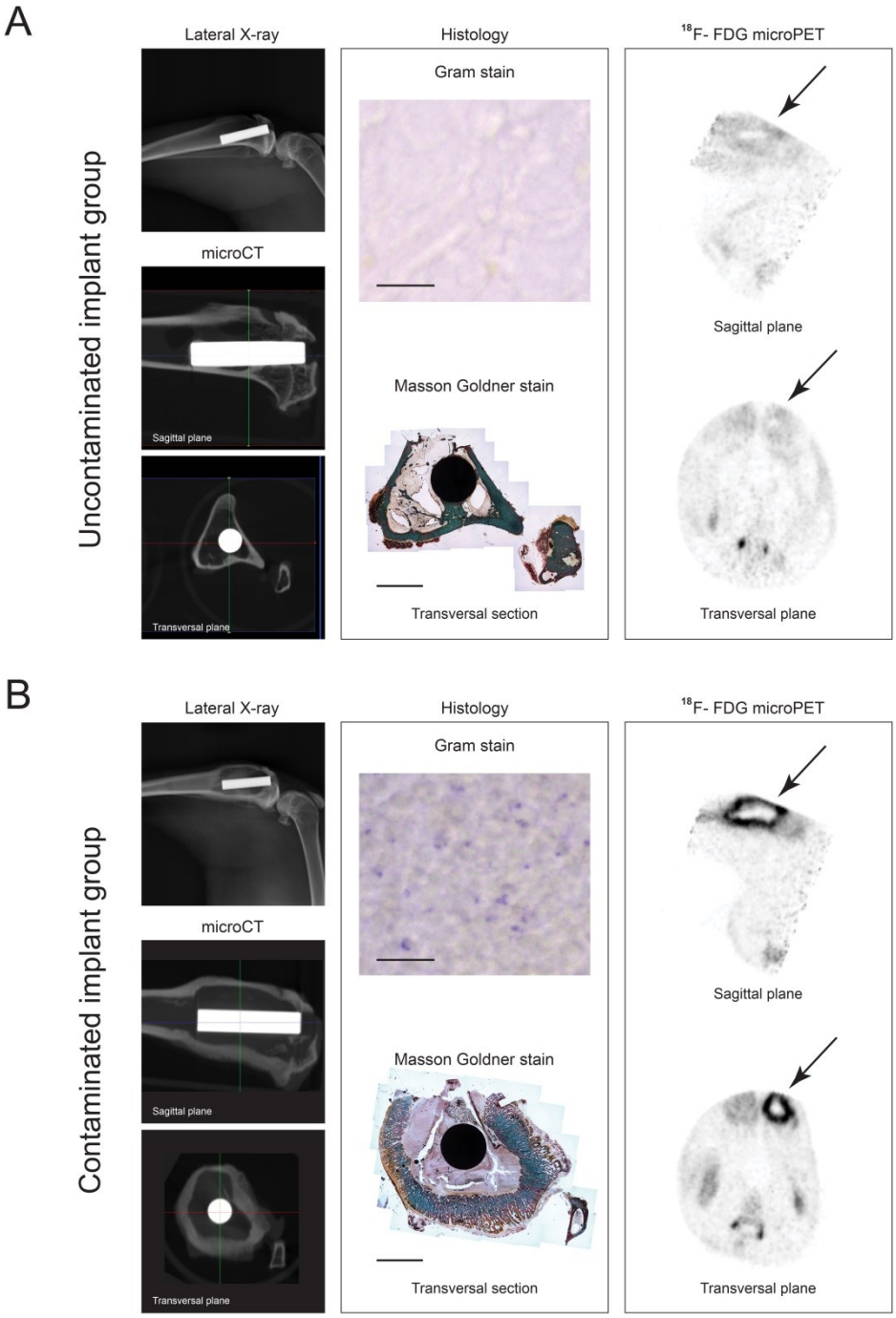
A
Uncontaminated implant group
Lateral X-ray
microCT
Sagittal plane
Transversal plane
Histology
Gram stain
Masson Goldner stain
Transversal section
18F- FDG microPET
Sagittal plane
Transversal plane
B
Contaminated implant group
Lateral X-ray
microCT
Sagittal plane
Transversal plane
Histology
Gram stain
Masson Goldner stain
Transversal section
18F- FDG microPET
Sagittal plane
Transversal plane

Figure 3 (left page): Radiology, histology and microPET, 6 weeks after surgery. **A:** Uncontaminated implant group. Lateral X-ray (upper left panel) shows normal bone morphology. MicroCT (lower left panels) indicates a healthy cortex with bone apposition on the implant surface. Transversal microCT corresponds to the transversal histological section (lower middle panel, bar represents 4 mm), which indicates bone apposition on the implant besides a normal bone morphology. Absence of Gram positive bacteria confirms absence of infection (upper middle panel, bar represents 20 µm). Reconstructed ^{18}F-FDG microPET planes (right panel) indicate tracer uptake and implant location (arrows). **B:** Contaminated implant group. Lateral X-ray (upper left panel) indicates cortical thickening and osteolysis. MicroCT (lower left panels) supports the X-ray images with cortical thickening and extensive osteolysis. Transversal microCT plane corresponds to the transversal histology section (lower middle panel, bar represents 4 mm) additionally indicating the presence of an intramedullary abscess. Presence of Gram positive bacteria confirms the presence of a bacterial infection (upper middle panel, bar represents 20 µm). Reconstructed ^{18}F-FDG microPET planes (right panel) indicate implant location combined with increased tracer uptake (arrows).

3.2 Infection status

To confirm that the bacterial contamination led to an implant infection, infection development was first determined. The experimental procedure resulted in initial weight loss during the first post-operative weeks in all animals. Only the uncontaminated control group recovered to their pre-operative weight within 4 weeks, while animals in the contaminated implant group remained below their pre-operative weight (Figure 2 A). Erythrocyte sedimentation rate (ESR) and C-reactive protein (CRP) were increased in the contaminated implant group (Figure 2 B and C). During the 6 weeks follow-up the severity of the radiological signs of osteomyelitis (periosteal elevation, cortical thickening and osteolysis) increased in the contaminated implant group (Figure 3B). In the uncontaminated control group radiological signs of osteomyelitis were absent (Figure 3A). *Post-mortem* microCT imaging of the operated tibiae confirmed the X-ray findings by the presence of osteolysis, cortical thickening and implant loosening, specifically in the contaminated implant group (Figure 3B). Bone apposition on the implant surface was detected in the uncontaminated implant group (Figure 3A), but not in the contaminated implant group (Figure 3B).

Bacterial culture of the peri-implant tissue on tellurite glycine agar showed *S. aureus* culture positivity in 6 out of 7 contaminated implants, while none of the uncontaminated implants were culture positive for *S. aureus*. Finally, to acquire histological confirmation of infection, PMMA histological sections were prepared. Microscopic analysis of the histological sections clearly

differentiated between the uncontaminated implant group and the contaminated implant group. Undisturbed cortex integrity was observed in the uncontaminated implant group, with bone apposition on the implant surface (Figure 3A). In sharp contrast the contaminated implant group showed cortical thickening, abscess formation and osteolysis around the implant (Figure 3B). Gram staining of similar sections showed the presence of Gram-positive cocci specifically in the contaminated implant group (Figure 3B).

Overall, these data confirm that the uncontaminated group did not develop an osteomyelitis, whereas the contaminated group showed all signs of an implant infection leading to osteomyelitis.

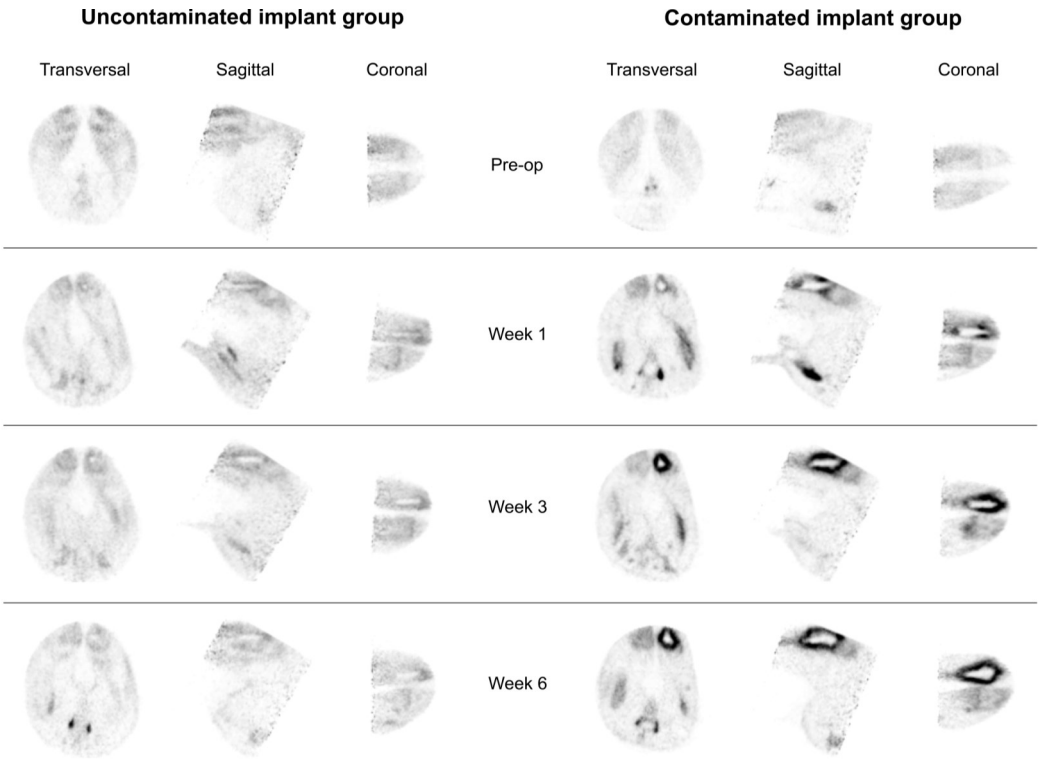

Figure 4: Representative images of the ^{18}F-FDG uptake in the uncontaminated implant group (left) and the contaminated implant group (right) during the 6 week follow-up.

3.3 ^{18}F-FDG uptake in bone and soft tissue around the implant

OSEM2D reconstructed microPET images of the contaminated implant group indicated that the ^{18}F-FDG uptake was localized in the morphologically affected bone tissue (according to radiographs, microCT and histology) (Figure 3B). Furthermore the reconstructed images of the implant infection group showed an increased ^{18}F-FDG uptake around the implants compared to the uncontaminated implant group throughout the experimental follow-up (Figure 4).

To quantify the ^{18}F-FDG uptake in both groups and investigate whether ^{18}F-FDG micro-PET enables differentiation between control and infected implants, the ^{18}F-FDG uptake by the soft tissues as well as the uptake by the bone tissue around the implants was separately determined and compared. In the uncontaminated control group quantification of ^{18}F-FDG uptake in the soft tissues (*vastus lateralis*) of the uncontaminated control group showed no difference between the uptake in the soft tissue of the tibia containing an implant compared to the non-operated contra-lateral tibia of the same animal throughout the entire follow-up (Figure 5A, left panel). The ^{18}F-FDG uptake by the bone tissue surrounding the uncontaminated implant was compared to the uptake of the same region in the contralateral non-operated tibia. An almost significant difference between SUV's from both regions was found at the first post-operative week only (Figure 5A, right panel; $p_{week\,0}$ = 0.987, $p_{week\,1}$ = 0.054, $p_{week\,3}$ = 0.496 and $p_{week\,6}$ = 0.397). The soft tissues in the contaminated implant group showed no difference in ^{18}F-FDG uptake between the operated and non-operated tibia at all time points (Figure 5B, left panel). In contrast, the bone tissue surrounding the contaminated implant showed a significantly higher uptake of ^{18}F-FDG as compared to the same region in the non-operated contra-lateral tibia at all three post-operative time points (Figure 5B, right panel; $p_{week\,0}$ = 0.561, $p_{week\,1}$ = 0.002, $p_{week\,3}$ = 0.011 and $p_{week\,6}$ = 0.005). The soft tissue uptake in the uncontaminated group showed a minimal, but significantly higher uptake than the soft tissue of contaminated implant group (p = 0.049) at 3 weeks only (Figure 5C, left panel). The ^{18}F-FDG uptake in the bone surrounding the implant showed a significantly higher uptake in the contaminated implant group compared to the uncontaminated implant group on the 3rd and 6th post-operative week (Figure 5C, right panel; $p_{week\,3}$ = 0.026 and $p_{week\,6}$ = 0.004, respectively), but not in the first post-operative week ($p_{week\,1}$ = 0.308).

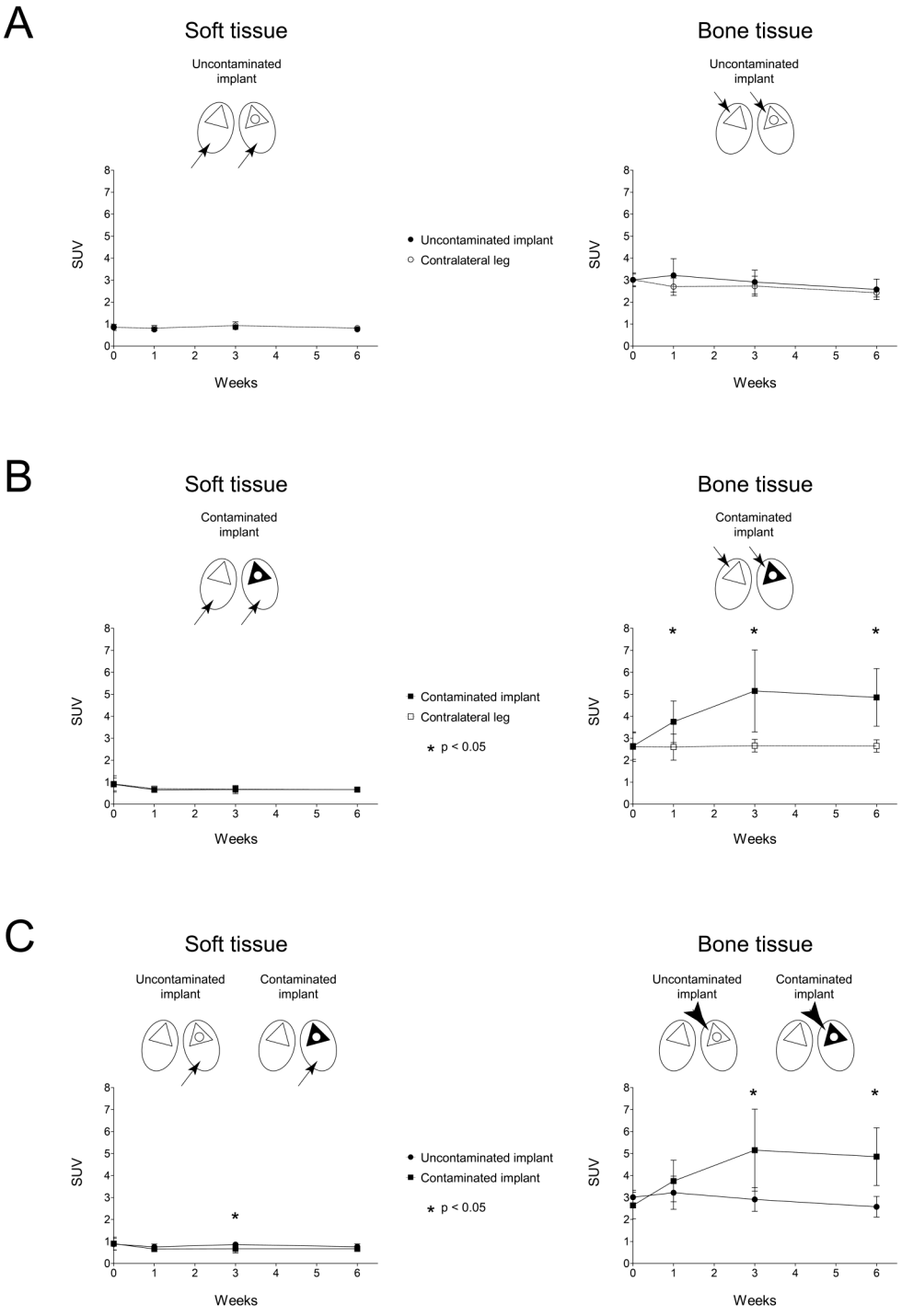
A
Soft tissue
Uncontaminated implant
SUV
Weeks
Uncontaminated implant
Contralateral leg
Bone tissue
Uncontaminated implant
SUV
Weeks
B
Soft tissue
Contaminated implant
SUV
Weeks
Contaminated implant
Contralateral leg
* p < 0.05
Bone tissue
Contaminated implant
SUV
Weeks
C
Soft tissue
Uncontaminated implant
Contaminated implant
SUV
Weeks
Uncontaminated implant
Contaminated implant
* p < 0.05
Bone tissue
Uncontaminated implant
Contaminated implant
SUV
Weeks

Figure 5 (left page): Quantification of the ^{18}F-FDG tracer uptake. Illustrations above the graph are a schematic representation of a transverse section of the rabbits hind legs, with the implant containing tibia on the right (ellipsoids depict the soft tissues, triangles depict the tibiae (black triangles depict the contaminated tibiae) and circles depict the implants). Black arrows indicate the compared tissues in the corresponding graph. **A:** Uncontaminated implant group. Quantification of the soft tissue uptake (left graph) and the tracer uptake in both tibia (right graph) of the uncontaminated implant group. **B:** Contaminated implant group. Quantification of the soft tissue uptake (left graph) and the tracer uptake in both tibia (right graph) of the contaminated implant group. **C:** Comparison of the uptake in the operated leg of the uncontaminated with the contaminated implant group. Asterisk indicates $p < 0.05$. Error bars represent 95% confidence intervals.

To determine whether the magnitude of the infection-associated ^{18}F-FDG signal from the bone surrounding the implants was related to a specific region around the implant, circular regions of interest were placed in the OSEM2D reconstructed microPET images from both groups at positions corresponding with the proximal, centre or distal part of the implant (Figure 6A). The uptake in bone surrounding the proximal part of the implants was significantly higher in the contaminated implant group compared with the uncontaminated implant group at the 3rd and 6th post-operative week (Figure 6B; $p_{week\,3}$ = 0.006 and $p_{week\,6}$ = 0.004, respectively). Similarly, around the central part of the contaminated implant the uptake was significantly higher compared to the uncontaminated implant at the 3rd and 6th post-operative week (Figure 6C; $p_{week\,3}$ = 0.012 and $p_{week\,6}$ = 0.006). At the distal part of the contaminated implant the uptake was significantly higher at the 6th postoperative week only (Figure 6D; $p = 0.047$).

4. Discussion

In this study we aimed to evaluate the use of ^{18}F-FDG microPET as a quantitative diagnostic approach for monitoring an implant infection, in the early post-operative weeks, using a *Staphylococcus aureus*-based orthopaedic implant infection model (6). We determined if ^{18}F-FDG microPET scanning is able to differentiate between septic and aseptic conditions in orthopaedic implant ingrowth, and if the development of an implant infection can be quantitatively followed over time.

^{18}F-FDG is suggested as an infection specific tracer in the field of orthopaedics (14, 16-20). However, most of these studies specifically focus on osteomyelitis without implants (14, 15, 21).

Few other studies focus on osteomyelitis in combination with the introduction of an antibiotic-containing bioresorbable screw or bone cement (22-24). However, metal-based implants are the most commonly used orthopaedic implants for fracture fixation (nails, screws and plates) and joint replacement and suffer from bacterial infection risk. Surprisingly, experimental osteomyelitis studies focussing on metal-based implants using microPET to quantify the osteomyelitis have not been reported. Since the early detection of implant infection is difficult in current clinical diagnostics, the use of ^{18}F-FDG PET could potentially contribute to early infection diagnosis (19, 25, 26). Especially, since implant infection treatment in an early stage is positively correlated with treatment success and implant survival, this may potentially reduce healthcare costs and hospital stay for the patient (27, 28).

Experimental implant infection models generally focus on clinical rather than imaging endpoints, due to the potential risk of losing animals as a result of repeated periods of general anaesthesia needed to obtain imaging data (24). Rats are not heavily influenced by the repeated use of anaesthesia and are more resilient to heavy antibiotic treatment (29, 30), this species may be preferable for such studies (31). On the other hand rats need a far higher bacterial dose to achieve a persistent implant infection and bones of rats are rather small for the study of larger orthopaedic implants (15). Therefore the rabbit has been the preferred species for experimental osteomyelitis studies since the late 19th century (32).

In contrast to other authors we have used a microPET scanner, suitable for small animals, instead of a normal PET scanner for patients (14, 15, 21, 24). The main reason, for not using microPET in rabbit studies was the limited size of the gantry of a microPET scanner. Since these microPET scanners are mainly meant for experiments using mice and rats, they do not allow positioning of a rabbit without a special fixation device. Our fixation device allowed proper fixation of the rabbit during the whole period of the ^{18}F-FDG incubation after injection and during the microPET scan with the rabbit under anaesthesia. This way we were able to scan at a higher resolution as compared with the resolution of a conventional clinical PET scanner, so providing a more detailed insight in the localisation of the ^{18}F-FDG uptake.

Work by Jones-Jackson and colleagues (21) showed that in a within-subject longitudinal follow-up in an osteomyelitis model in the forelimb of a rabbit without implant, increased FDG uptake could be detected at the first post-operative week. A subsequent drop in uptake in the uncontaminated control group was found in the following weeks, while the uptake of the infected group continued to increase up to the third post-operative week (21). Our results are in agreement with this study

and show that also in the presence of an orthopaedic titanium implant, the development of an osteomyelitis shows a comparable ^{18}F-FDG uptake pattern by the infected bone tissue. In clinical practice the differentiation between the post-operative inflammation and infection-related inflammation is a well-known problem, troubling early infection intervention (33, 34). Our microPET data suggests the presence (with a trend towards significance) of a post-operative aseptic wound healing response at the first post-operative week in the uncontaminated implant group. The earliest differentiation between ^{18}F-FDG uptake by aseptic wound healing versus septic wound healing, in our experimental setting, was possible from the 3rd post-operative week onwards.

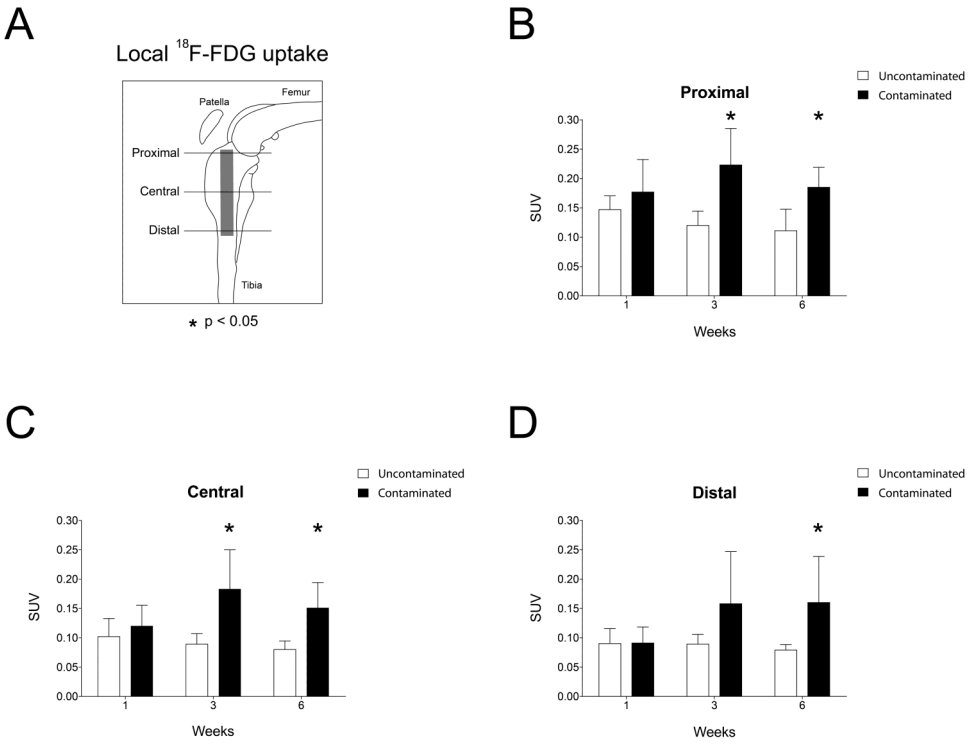

Figure 6: Quantification of localized tracer uptake. **A:** Graphical representation of the implant positioning and the location of the placed ROI. **B-D:** Comparison between the tracer uptake of the uncontaminated implant group and the contaminated implant group based on ROI location. Asterisk indicates $p < 0.05$. Error bars represent 95% confidence intervals.

^{18}F-FDG is rather a specific tracer for increased metabolic glucose turnover than an infection specific tracer. However, infection or post-operative tissue healing is related to a locally increased metabolic turnover of glucose. In the case of an infection this is mainly caused by leucocytes, neutrophilic granulocytes and macrophages, but also by bacteria present in the infected tissue (8, 14, 15, 35). Our findings for the first time show that microPET is able to differentiate aseptic from septic wound healing in an orthopaedic implant animal model using ^{18}F-FDG. As a statistically not significant post-operative peak in ^{18}F-FDG uptake was found at the first post-operative week in the uncontaminated implant group, while the uptake in the contaminated implant group reached its peak at the third post-operative week, this suggests that the most optimal time point to perform the initial imaging in this particular implant model may be at the third post-operative week.
Most of the FDG uptake was located at the proximal part of the contaminated implant. This may reflect a locally more intense infection. However, as there are differences in bone thickness between the proximal and distal tibiae, this may also indicate that the thickness of the affected epiphyseal and metaphyseal bone tissue in that area contributes to the observed increased local FDG uptake. Based on clinical experience in chronic implant infections, the intramedullary abscess is expected to spread under influence of gravity to the more distal tibia. We found that the uptake at the distal part of the contaminated implant became significantly higher (compared to the uncontaminated control group) at the 6th post-operative week, supporting this clinical observation. Therefore scanning at later time points in follow-up is expected to provide more insight in the spread of the infection.

5. Conclusion

In summary we found that ^{18}F-FDG can be used as a sensitive post-operative infection tracer in an *S. aureus*-induced implant infection in the tibia of a rabbit. From the third post-operative week onward, microPET scanning can differentiate implant infection from aseptic wound healing and bone remodelling. This highlights its potential value in human clinical diagnostics to detect early post-operative orthopaedic infections. Furthermore, our data support the use of ^{18}F-FDG microPET for future antimicrobial implant coating assessment.

Acknowledgements

This research forms part of the Project P4.01 NANTICO of the research program of the BioMedical Materials institute, co-funded by the Dutch Ministry of Economic Affairs.
The authors would like to thank the employees of the animal facility of the Maastricht University Medical Centre for their assistance during this study. We would also like to thank I. Pooters, M. Visser and C. Urbach from the Nuclear Medicine department of the Maastricht University Medical Centre for their support during this study and R. Odekerken for his assistance with the design of the experimental setup. And we would like to thank S. Bout and P. Dijkstra for their overall support during this study.

References

1. Dale H, Hallan G, Espehaug B, Havelin LI, Engesaeter LB. Increasing risk of revision due to deep infection after hip arthroplasty. Acta Orthopaedica. 2009 Dec;80(6):639-45.
2. Acklin YP, Widmer AF, Renner RM, Frei R, Gross T. Unexpectedly increased rate of surgical site infections following implant surgery for hip fractures: Problem solution with the bundle approach. Injury. 2011 Feb;42(2):209-16.
3. Kurtz SM, Lau E, Ong KL, Carreon L, Watson H, Albert T, Glassman S. Infection risk for primary and revision instrumented lumbar spine fusion in the medicare population. Journal of Neurosurgery: Spine. 2012 Oct;17(4):342-7.
4. Calhoun JH, Mader JT. Treatment of osteomyelitis with a biodegradable antibiotic implant. Clinical Orthopaedics and Related Research. 1997 Aug(341):206-14.
5. Smeltzer MS, Thomas JR, Hickmon SG, Skinner RA, Nelson CL, Griffith D, Parr TR, Jr., Evans RP. Characterisation of a rabbit model of staphylococcal osteomyelitis. Journal of Orthopaedic Research. 1997 May;15(3):414-21.
6. Odekerken JC, Arts JJ, Surtel DA, Walenkamp GH, Welting TJ. A rabbit osteomyelitis model for the longitudinal assessment of early post-operative implant infections. Journal of Orthopaedic Surgery and Research. 2013;8(1):38.
7. Vogely HC, Oosterbos CJ, Puts EW, Nijhof MW, Nikkels PG, Fleer A, Tonino AJ, Dhert WJ, Verbout AJ. Effects of hydrosyapatite coating on ti-6a1-4v implant-site infection in a rabbit tibial model. Journal of Orthopaedic Research. 2000 May;18(3):485-93.
8. Stumpe KD, Dazzi H, Schaffner A, von Schulthess GK. Infection imaging using whole-body fdg-pet. European Journal of Nuclear Medicine. 2000 Jul;27(7):822-32.
9. Huang T, Civelek AC, Li J, Jiang H, Ng CK, Postel GC, Shen B, Li XF. Tumor microenvironment-dependent 18f-fdg, 18f-fluorothymidine, and 18f-misonidazole uptake: A pilot study in mouse models of human non-small cell lung cancer. Journal of Nuclear Medicine. 2012 Aug;53(8):1262-8.
10. Marsboom G, Wietholt C, Haney CR, Toth PT, Ryan JJ, Morrow E, Thenappan T, Bache-Wiig P, Piao L, Paul J, Chen CT, Archer SL. Lung (1)(8)f-fluorodeoxyglucose positron emission tomography for diagnosis and monitoring of pulmonary arterial hypertension. American Journal of Respiratory and Critical Care Medicine. 2012 Mar 15;185(6):670-9.
11. Toyama H, Ichise M, Liow JS, Modell KJ, Vines DC, Esaki T, Cook M, Seidel J, Sokoloff L, Green MV, Innis RB. Absolute quantification of regional cerebral glucose utilisation in mice by 18f-fdg small animal pet scanning and 2-14c-dg autoradiography. Journal of Nuclear Medicine. 2004 Aug;45(8):1398-405.
12. Toyama H, Ichise M, Liow JS, Vines DC, Seneca NM, Modell KJ, Seidel J, Green MV, Innis RB. Evaluation of anesthesia effects on (18f)fdg uptake in mouse brain and heart using small animal pet. Nuclear Medicine and Biology. 2004 Feb;31(2):251-6.
13. van der Bruggen W, Bleeker-Rovers CP, Boerman OC, Gotthardt M, Oyen WJ. Pet and spect in osteomyelitis and prosthetic bone and joint infections: A systematic review. Seminars in Nuclear Medicine. 2010 Jan;40(1):3-15.
14. Koort JK, Makinen TJ, Knuuti J, Jalava J, Aro HT. Comparative 18f-fdg pet of experimental staphylococcus aureus osteomyelitis and normal bone healing. Journal of Nuclear Medicine. 2004 Aug;45(8):1406-11.
15. Makinen TJ, Lankinen P, Poyhonen T, Jalava J, Aro HT, Roivainen A. Comparison of 18f-fdg and 68ga pet imaging in the assessment of experimental osteomyelitis due to staphylococcus aureus. European Journal of Nuclear Medicine and Molecular Imaging. 2005 Nov;32(11):1259-68.
16. Guhlmann A, Brecht-Krauss D, Suger G, Glatting G, Kotzerke J, Kinzl L, Reske SN. Fluorine-18-fdg pet and technetium-99m antigranulocyte antibody scintigraphy in chronic osteomyelitis. Journal of Nuclear Medicine. 1998 Dec;39(12):2145-52.
17. Nanni C, Marangoni A, Quarta C, Di Pierro D, Rizzello A, Trespidi S, D'Ambrosio D, Ambrosini V, Donati M, Aldini R, Zanotti-Fregonara P, Grassetto G, Rubello D, Fanti S, Cevenini R. Small animal pet for the evaluation of an animal model of genital infection. Clinical Physiology and Functional Imaging. 2009 May;29(3):187-92.

18. Schmitz A, Risse HJ, Kalicke T, Grunwald F, Schmitt O. (fdg-pet for diagnosis and follow-up of inflammatory processes: Initial results from the orthopedic viewpoint). Zeitschrift für Orthopädie und Ihre Grenzgebiete. 2000 Sep-Oct;138(5):407-12.
19. Temmerman OP, Heyligers IC, Hoekstra OS, Comans EF, Roos JC. Detection of osteomyelitis using fdg and positron emission tomography. Journal of Arthroplasty. 2001 Feb;16(2):243-6.
20. Tremoleda JL, Khalil M, Gompels LL, Wylezinska-Arridge M, Vincent T, Gsell W. Imaging technologies for preclinical models of bone and joint disorders. EJNMMI Res. 2011;1(1):11.
21. Jones-Jackson L, Walker R, Purnell G, McLaren SG, Skinner RA, Thomas JR, Suva LJ, Anaissie E, Miceli M, Nelson CL, Ferris EJ, Smeltzer MS. Early detection of bone infection and differentiation from post-surgical inflammation using 2-deoxy-2-(18f)-fluoro-d-glucose positron emission tomography (fdg-pet) in an animal model. Journal of Orthopaedic Research. 2005 Nov;23(6):1484-9.
22. Koort JK, Makinen TJ, Suokas E, Veiranto M, Jalava J, Knuuti J, Tormala P, Aro HT. Efficacy of ciprofloxacin-releasing bioabsorbable osteoconductive bone defect filler for treatment of experimental osteomyelitis due to staphylococcus aureus. Antimicrobial Agents and Chemotherapy. 2005 Apr;49 (4):1502-8.
23. Makinen TJ, Veiranto M, Knuuti J, Jalava J, Tormala P, Aro HT. Efficacy of bioabsorbable antibiotic containing bone screw in the prevention of biomaterial-related infection due to staphylococcus aureus. Bone. 2005 Feb;36(2):292-9.
24. Lankinen P, Lehtimaki K, Hakanen AJ, Roivainen A, Aro HT. A comparative 18f-fdg pet/ct imaging of experimental staphylococcus aureus osteomyelitis and staphylococcus epidermidis foreign-body-associated infection in the rabbit tibia. EJNMMI Res. 2012 Jul 23;2(1):41.
25. Zhuang H, Alavi A. 18-fluorodeoxyglucose positron emission tomographic imaging in the detection and monitoring of infection and inflammation. Seminars in Nuclear Medicine. 2002 Jan;32(1):47-59.
26. De Winter F, Vogelaers D, Gemmel F, Dierckx RA. Promising role of 18-f-fluoro-d-deoxyglucose positron emission tomography in clinical infectious diseases. European Journal of Clinical Microbiology and Infectious Diseases. 2002 Apr;21(4):247-57.
27. Geurts J, Chris Arts JJ, Walenkamp GH. Bone graft substitutes in active or suspected infection. Contra-indicated or not? Injury. 2011 Sep;42 Suppl 2:S82-6.
28. Geurts JA, Janssen DM, Kessels AG, Walenkamp GH. Good results in postoperative and hematogenous deep infections of 89 stable total hip and knee replacements with retention of prosthesis and local antibiotics. Acta Orthopaedica. 2013 Dec;84(6):509-16.
29. Cremieux AC, Carbon C. Experimental models of bone and prosthetic joint infections. Clinical Infectious Diseases. 1997 Dec;25(6):1295-302.
30. Mader JT. Animal models of osteomyelitis. American Journal of Medicine. 1985 Jun 28;78(6B):213-7.
31. Alt V, Lips KS, Henkenbehrens C, Muhrer D, Oliveira Cavalcanti MC, Sommer U, Thormann U, Szalay G, Heiss C, Pavlidis T, Domann E, Schnettler R. A new animal model for implant-related infected non-unions after intramedullary fixation of the tibia in rats with fluorescent in situ hybridisation of bacteria in bone infection. Bone. 2011 May 1;48(5):1146-53.
32. Rodet A. The classic. An experimental study on infectious osteomyelitis. Clinical Orthopaedics and Related Research. 1973 Oct;99(96):3-4.
33. Trampuz A, Zimmerli W. Diagnosis and treatment of infections associated with fracture-fixation devices. Injury. 2006 May;37 Suppl 2:S59-66.
34. Zimmerli W, Ochsner PE. Management of infection associated with prosthetic joints. Infection. 2003 Mar;31(2):99-108.
35. Stumpe KD, Strobel K. 18f fdg-pet imaging in musculoskeletal infection. Quarterly Journal of Nuclear Medicine and Molecular Imaging. 2006 Jun;50(2):131-42.

The longitudinal assessment of osteomyelitis development by molecular imaging in a rabbit model

J.C.E. Odekerken

G.H.I.M. Walenkamp

B.T. Brans

T.J.M. Welting

J.J.C Arts

BioMed Research International. 2014, Article ID 424652

Abstract

Introduction: Osteomyelitis is a severe orthopaedic complication which is difficult to diagnose and treat. Previous experimental studies mainly focussed on evaluating osteomyelitis in the presence of an implant or used a sclerosing agent to promote infection onset. In contrast we focussed on the longitudinal assessment of a non-implant related osteomyelitis.

Methods: An intramedullary tibial infection with *S. aureus* was established in NZW rabbits. Clinical and haematological infection status was evaluated weekly, combined with X-ray radiographs, bi-weekly injections of calcium binding fluorophores and *post-mortem* microCT. The development of the infection was assessed by microPET at consecutive time points using ^{18}F-FDG as an infection tracer.

Results: The intramedullary contamination of the rabbit tibia resulted in an osteomyelitis. Haematological parameters confirmed infection in mainly the first post-operative weeks (CRP at the first 5 post-operative weeks, leucocyte differentiation on the second and sixth post-operative week and ESR on the second post-operative week only), while microPET was able to detect the infection from the first post-operative week onward until the end of the study.

Conclusions: This study shows that osteomyelitis in the rabbit can be induced without use of an implant or sclerosing agent. The sequential follow-up indicates that the diagnostic value of each infection parameter is time point dependant. Furthermore, from all parameters used, the diagnostic value of ^{18}F-FDG microPET is the most versatile to assess the presence of an orthopaedic infection in this model.

Key words: Infection; osteomyelitis; rabbit; imaging; microPET; *Staphylococcus aureus*

1. Introduction

Currently, posttraumatic and postoperative osteomyelitis remains to be one of the most severe complications after bone trauma or surgery. During the last decades much research has been conducted into prevention, diagnostics and treatment modalities for orthopaedic infections. Most research studies focus on treatment or prevention and not on the diagnosis of bone infection. However, novel imaging modalities are made available in the clinical evaluation of osteomyelitic lesions, i.e. combined ^{18}F-FDG PET and MRI (1).

The pre-clinical evaluation of any diagnostic tool requires a stable and consistent experimental pre-clinical model with a broad collection of relevant read-out parameters to yield reliable data with a precise follow-up. In this way pre-clinical osteomyelitis models can be highly informative on the development of the disease and the accompanying diagnosis by novel tools like ^{18}F-FDG PET (2, 3).

To investigate the development of a non-implant related osteomyelitis over time and to define a stable pre-clinical model, we aimed to establish an osteomyelitic lesion in the tibiae of rabbits, without the use of a sclerosing agent, since this destructs the local vascularisation of the bone, and reduces the local immune capacity (4, 5).

To investigate the potential of novel diagnostic approaches we evaluated the sequential use of ^{18}F-FDG as an infection specific microPET tracer on multiple time points during follow-up.

By combining the results of this study with our previously reported studies (6, 7), we also aimed to identify the most relevant parameters to diagnose naïve osteomyelitis by experimental conditions and describe how these infection parameters may differ in case of the presence or absence of an orthopaedic implant.

2. Materials and Methods

2.1 Animal choice, welfare and ethics

Eleven specified pathogen free (SPF) female New Zealand White (NZW) rabbits (Charles River, France), with a weight of 3.5 - 4 kg (approximately 6 months of age) were used in this study. Animals were allowed to acclimatize for 2 weeks before surgery was performed.

During the study each animal served as its own control since pre-operative measurements had been performed, these functioned as a baseline measurement. The non-operated contralateral leg

was also used as a control for the uncontaminated condition (radiology, microPET and histology). Furthermore, pre-operative microPET scans were supplemented with a historic control group (7) to reduce the exposure of the animals to ionising radiation in accordance with the ALARA-guideline (8). Animal housing, feeding, pain treatment, humane endpoints and sacrifice were performed according to our previously described study (6, 7).

The experimental follow-up scheme is displayed in Table 1.

This study was approved by the Maastricht University Animal Ethics Committee (DEC-UM, protocol 2010-089, Maastricht, the Netherlands).

Table 1: Experimental parameters and follow-up

	Quantification inoculum	Weight	Temperature	ESR	CRP	Leucocyte differentiation	X-ray	MicroCT	^{18}F-FDG microPET	Calcium binding fluorphores	Bone tissue culture	Histology
Pre-op		X	X						X			
Day of surgery	X	X	X	X	X	X	X					
Week 1		X	X	X	X	X	X		X			
Week 2		X	X	X	X	X	X			X		
Week 3		X	X	X	X	X	X		X			
Week 4		X	X	X	X	X	X			X		
Week 5		X	X	X	X	X	X					
Week 6		X	X	X	X	X	X		X	X		
Post-mortem								X			X	X

2.2 Animal surgery and follow-up

Animals were anaesthetized according to our previously published study (6). Subsequently a hand reamed 4 mm wide defect was drilled into the tibial plateau to open the tibial medullary canal, remaining extra articular. After reaming, the tibial medullary cavity was flushed with sterile saline to remove bone fragments and haematoma. All animals received an intramedullary contamination of $3.8x10^5$ CFU *S. aureus* (UAMS-1, ATCC 49230) in 100 µl saline.

The inoculation dose was freshly prepared before surgery from an overnight culture and diluted with sterile saline to an average concentration of $3.8x10^5$ CFU per contamination, based on OD600 measurements (Amersham Biosciences, GE Healthcare, USA). The inoculation dose and preparation was based on previous studies (6, 7). To confirm the inoculum size, the bacterial count of every inoculum was verified by quantitative culture on tellurite glycine agar (Difco, Becton Dickinson, France) before and after surgery.

After contamination the defect was sealed with bone wax (Syneture, Covidien, USA) and the surrounding tissue was flushed with sterile saline. The patella tendon was apprimated with 4 resorbable sutures and the skin by 6 single intracutaneous inverted sutures (Syneture, Covidien, USA), Aluminium-spray (Eurovet Animal Health, the Netherlands) was applied to protect the wound.

The animals were monitored during the 6 week follow-up for the use of their hind legs, the appearance of the wound and on general signs of infection (redness, swelling and fever). Body weight and temperature were measured and blood was collected by venipuncture from the jugular vein at the day of surgery and every week thereafter until the end of the experiment. Blood samples were collected weekly and analysed for changes in erythrocyte sedimentation rate (ESR) (Kabe Labortechnik, Germany), leucocyte differentiation (Euregio Laboratory, the Netherlands) and C-reactive protein levels (CRP) (E-15CRP, Immunology Consultants Laboratory, USA).

2.3 Radiographic imaging

Standard X-ray radiographs were collected according to our previously described study (6). All radiographs were independently scored, by 3 blinded observers, for osteomyelitis mediated bone morphological changes according to our modified scoring system (6, also see page 226).

Ex vivo microCT imaging of the affected tibiae was performed after 6 weeks follow-up, directly after sacrifice. The microCT-images were acquired on an X-rad 225 (Precision X-ray, USA) as described previously (6, 7, also see page 228).

2.4 ^{18}F-FDG microPET

^{18}F-FDG microPET was conducted to assess the local metabolic glucose uptake in the contaminated tissue, since infection is associated with an increased metabolic glucose turnover. Imaging data

was collected by a pre-operative scan and three post-operative scans (respectively at one, three and six weeks after surgery) of each animal.

The entire microPET procedure of approximately 2 hours was performed under tilatamine-zolazepam sedation, initiated by a 15 mg/kg intramuscular dose and 3 additional intramuscular injections of 7.5 mg/kg. The time between the first and the subsequent second dose was 20 minutes, al injections following thereafter were given with 45 minute intervals.

The rabbits were fixed in a custom made PVC restrainer, which allowed the rabbit to breath freely without allowing movements of the hind legs (7). Fifty MBq ^{18}F-FDG (GE Healthcare Medical Diagnostics, Eindhoven, the Netherlands) was diluted with sterile saline to a volume of 1 ml and was subsequently injected in the ear vein of the rabbit. Residual activity in the syringe was measured on a CRC-25R dose calibrator (Capintec, USA) to calculate the initially injected ^{18}F-FDG dose. A 1 hour incubation period was taken into account to allow uptake of the ^{18}F-FDG in the area of interest.

Data were analysed with the ASIPRO VM software package (version 6.7.1.2, Concorde Microsystems, Siemens, Germany). The imaging data were reconstructed by the OSEM2D protocol with an isotropic voxel size of 0.87 mm to align the tibial intramedullary cavity with the coronal, sagittal and transversal planes to keep the volumes of interest (VOI) of all scans equal. A cylindrical VOI of 10.4 mm in diameter and 25.1 mm long (12 voxels in diameter and 29 voxels long) was used as a contour around the affected bony tissue. An equally sized VOI was placed in the contralateral leg on the equivalent location, to serve as an internal control. Each leg also contained an equally sized VOI in the *vastus lateralis* to serve as a measurement for the soft tissue ^{18}F-FDG-uptake. The standardized uptake value (SUV) was calculated from the total activity in the selected VOI, corrected for the weight of the animal and the activity of ^{18}F-FDG in the animal at the time of emission scanning. Activity at the time of the scan was corrected for the injected activity and the calibration factor of the microPET and dose calibrator.

2.5 Bacteriology

After sacrifice the tibiae were dissected aseptically. Swabs were taken from the knee joint cavity. To assess soft tissue infection, these swabs were evaluated for the presence of *S. aureus* on tellurite glycine agar plates. *S. aureus* growth was identified by the presence of black colonies, due to the coagulase positive character of the species. Other, coagulase negative bacterial species (e.g.

S. epidermidis) would appear as white colonies. A 5 mm piece of the distal part of the *tuberositas tibiae* was excised from the tibia with a surgical drill (SM 12, Nouvag, Switzerland). After weight measurement it was homogenized in 10 ml sterile saline (Ultra-Turrax T25, Ika, Germany) at 6000 rpm. The homogenates were cultured on tellurite glycine agar plates. After 24 hours, culture dishes were quantified for the specific bacterial growth.

2.6 Histology

During the experimental follow-up, three different calcium binding fluorophores were administered, by subcutaneous injection, to follow bone apposition and mineralisation over time, which are to be detected in histological sections. Injection of Calcein Green (25 mg/kg, Fluka, Sigma Aldrich, Germany) was performed at 2 weeks, Xylenol Orange (30 mg/kg, Fluka, Sigma Aldrich, Germany) at 4 weeks and Calcein Blue (25 mg/kg, Fluka, Sigma Aldrich, Germany) was injected on the day before sacrifice.

After sacrifice and sampling for bone culture, tibiae were fixated in 4% formaldehyde/PBS for 4 weeks and embedded in polymethyl methacrylate (PMMA) (Technovit 9100, Hereaus-Kulzer, Germany). After polymerisation sections were stained according to Masson-Goldner (Carl Roth, Germany) and Gram (without a safranin counterstain) and subsequently 50 µm sections were obtained using a saw microtome (SP 1600, Leica, Germany). Sections were analysed and digitized by light microscopy (Axioscope A1, Axiovision LE release 4.8.2, Carl Zeiss, Germany). The localisation of calcium binding fluorophores in the bony tissue was visualized by fluorescence microscopy (Leica DMRB, Leica IM50 version 1.2 release 19, Leica, Germany) on unstained PMMA sections. Acquired images were merged using Photoshop CS3 (Adobe Systems, USA) to generate overview images.

2.7 Statistical analysis

SPSS 21 (IBM, USA) was used for the statistical analyses. Each animal served as its own pre-operative healthy control. Data were checked for normality using the Shapiro-Wilk test. Differences between time points were determined by a Wilcoxon Signed Ranks Test for non-parametric significance. In case of the microPET imaging we randomly selected 3 animals to serve as a healthy pre-operative control. The data of these 3 animals were supplemented by a historic

control group of 10 animals (7), to reduce overall reduction of animal inconvenience (one, two-hour episode of anaesthesia in combination with the injection of a 50 MBq ^{18}F-FDG). Therefore the statistical analysis of the microPET-data was performed with a combination of the Wilcoxon Signed Ranks Test and the Mann-Whitney U Test. The significance level was determined at $p \leq 0.05$. Graphical representation of the data was performed in GraphPad Prism 5 (GraphPad, USA), error bars represent standard error of mean.

3. Results

3.1 Animal surgery and follow-up

Eleven rabbits were intramedullary (right proximal tibia) contaminated with 3.8×10^5 CFU *S. aureus* via a transpatellar tibial plateau administration route. Nine animals completed the 6 week follow-up, which all developed an osteomyelitis in the right proximal tibia after per-operative contamination. One animal did not recuperate from the surgical procedure and another animal was sacrificed 3 weeks after surgery due to complications (humane endpoints were defined as extensive weight loss of >20% and severe soft tissue infection).

3.2 *In vivo* and *ex vivo* data analysis

After surgery the animals were monitored daily for physical activity. After recovery from the surgical procedure all animals showed limited function of the operated leg with partial weight bearing. Body temperature and weight (clinical indicators for infection) were monitored on a weekly basis. In comparison to the pre-operative measurements, a significant increase in body temperature was noted in all but the second post-operative week (Figure 1A; $p \leq 0.049$). All animals reduced weight significantly compared to pre-operative values and did not regain their pre-operative bodyweight values during follow-up (Figure 1B; $p \leq 0.011$).

During the six week follow-up period the ESR increased during the first weeks after surgery compared to the pre-operative rate, with a significant increase only at two weeks after surgery (Figure 1C; $p = 0.042$).

CRP levels however showed a significant increase in the first 5 weeks after surgery (Figure 1D; $p \leq 0.038$).

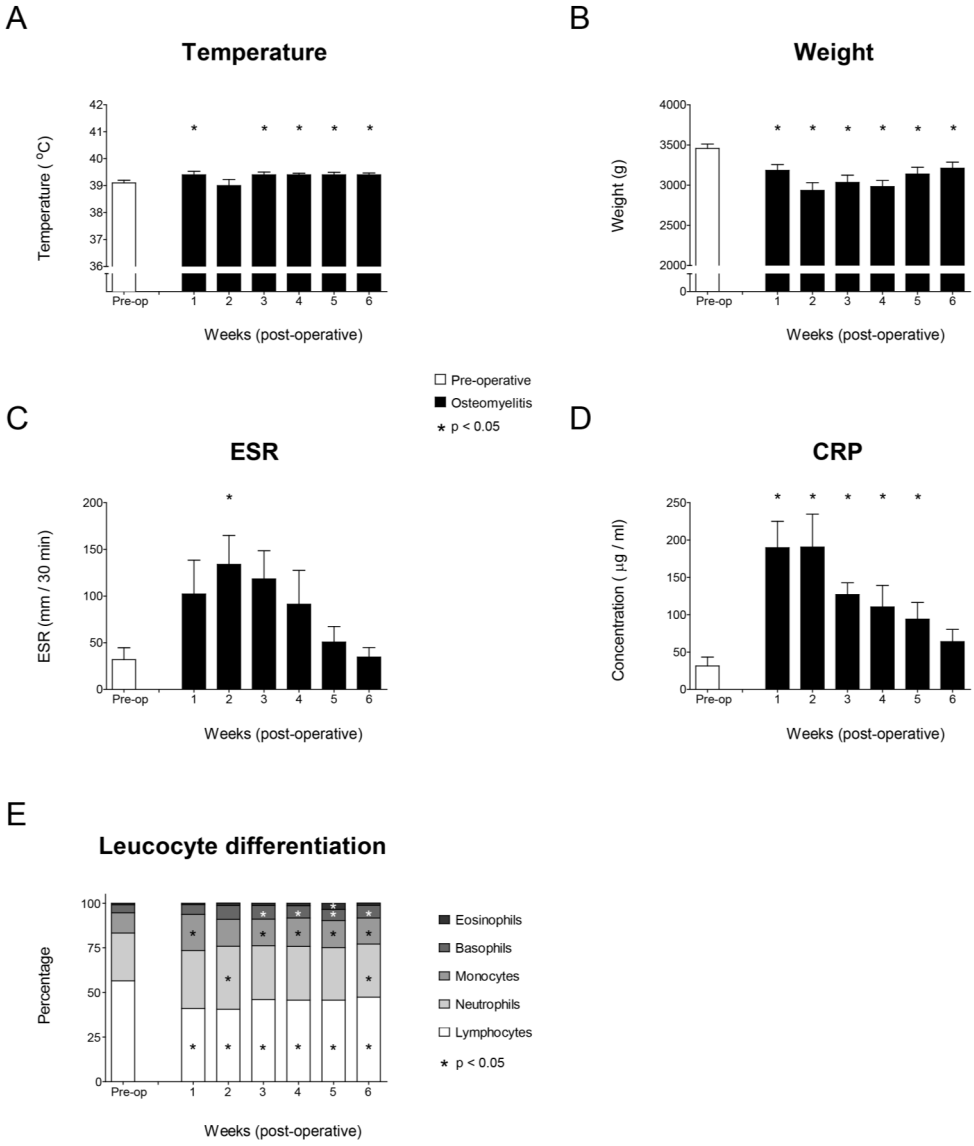

Figure 1: Physiological and haematological parameters. **A:** Body temperature during follow-up. **B:** Body weight during follow-up. **C:** Erythrocyte sedimentation rate. **D:** C-reactive protein levels. **E:** Leucocyte differentiation. All post-operative values are compared with the pre-operative values, in case on significant differences, asterisk indicates p≤0.05 and the error bars represent standard error of mean.

The weekly assessment of the leucocyte differentiation (Figure 1E) indicated that the lymphocytes fraction in the leucocyte differentiation was significantly decreased as compared to the pre-operative values on all post-operative time points ($p \leq 0.017$). The neutrophilic granulocyte fraction was only significantly different on the second and sixth post-operative week ($p \leq 0.050$). The monocyte fraction was significantly increased in all but the second post-operative week ($p \leq 0.033$). The basophilic granulocyte fraction was significantly increased from the third post-operative week onward ($p \leq 0.038$). The eosinophilic granulocyte fraction was only significantly different at the fifth post-operative week ($p = 0.042$).

The bone morphological changes initiated by the per-operative contamination of the tibia were detectable on X-ray radiographs from the 3th post-operative week onwards (Figure 2A), when scored according to our previously described osteomyelitis scoring system (6), focussing on bone morphological changes like osteolysis, periosteal elevation and cortical thickening. The microCT data allowed *post-mortem* assessment of the bone morphological changes as a result of the established osteomyelitis, with clear evidence of osteolysis and cortical thickening (Figure 2B), confirming the X-ray data.

Figure 2 (right page): Imaging data. **A:** Sequential X-ray radiographs during follow-up. The surgical procedure can result in radiologic symptoms for osteolysis (small arrow head). Two weeks after surgery periosteal elevation can be detected (solid arrow head). After four weeks cortical thickening (double headed arrow) and osteolysis can be detected (asterisk). At six weeks the osteolysis is affecting the entire proximal part of the tibia (hash sign). Graph depicts the increase in radiological score during the developmental stage of an osteomyelitis. Radiological scores during follow-up were compared to the pre-operative radiological score, asterisk indicates $p \leq 0.05$ and error bars indicate standard error of mean. **B:** Representative *post-mortem* microCT images taken after the six weeks follow-up. The normal condition shows a clearly defined cortex without apparent signs of osteolysis, the osteomyelitis conditions shows cortical thickening, loss of cortex integrity and signs of moderate to severe osteolysis. The graph depicts the distribution of the radiological score in the experimental group. **C:** Reconstructed ^{18}F-FDG microPET data shows in increased tracer uptake in the operated area during the experimental follow-up (arrow). Graph depicts the quantification of the tracer uptake. Comparisons were made between the left and right (osteomyelitis) leg and between the uptake levels before and after surgery of the operated right leg. Tracer uptake in the affected right tibiae was significantly higher on all post-operative time points compared to the uptake in the contralateral leg. Furthermore, the tracer uptake of the affected right tibiae was significantly higher at all post-operative time points compared to the uptake before surgery. Asterisk indicates $p \leq 0.05$ and error bars indicate standard error of mean.

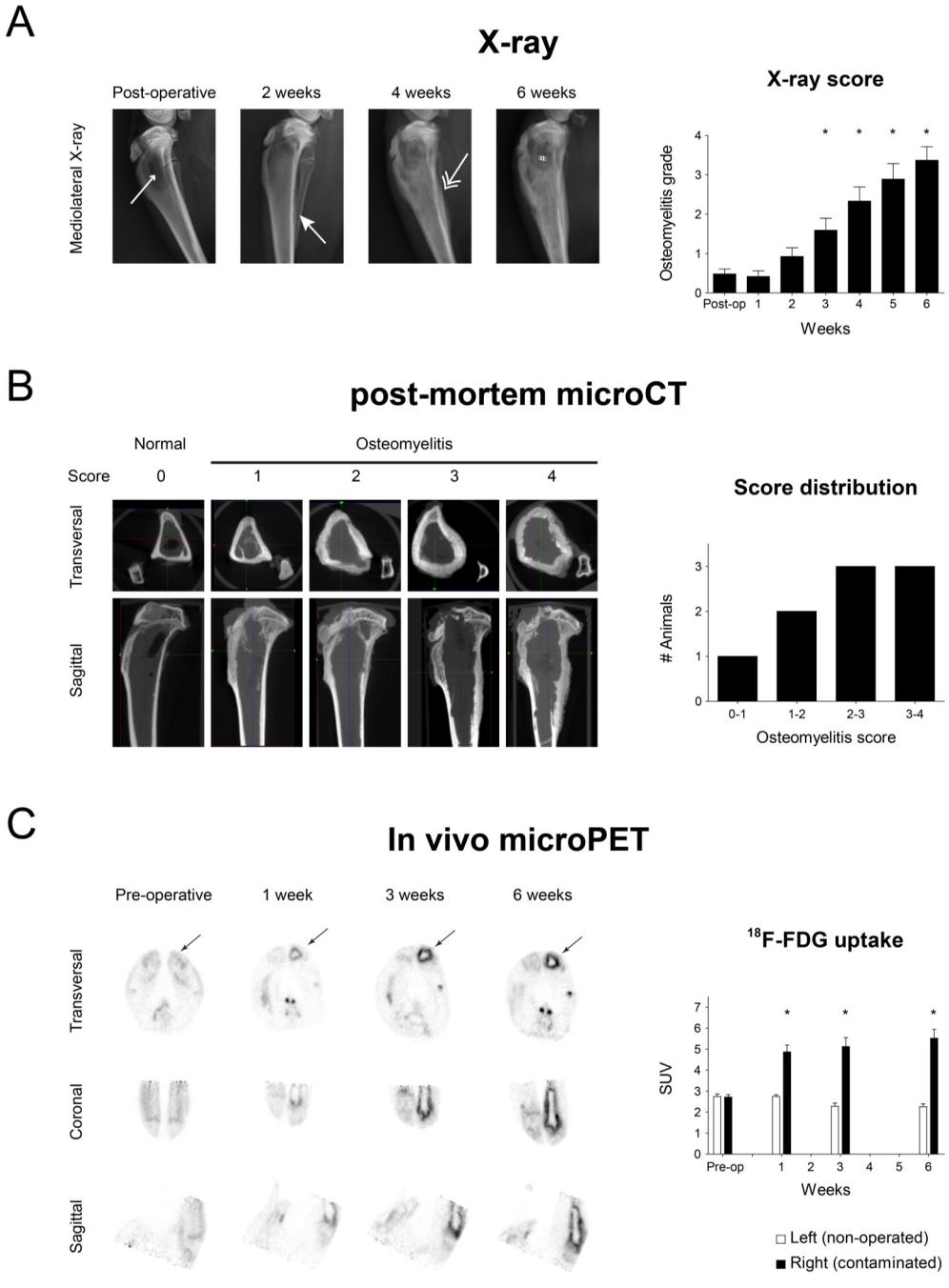
A
X-ray
Post-operative
2 weeks
4 weeks
6 weeks
Mediolateral X-ray
X-ray score
Osteomyelitis grade
Post-op
Weeks
B
post-mortem microCT
Normal
Osteomyelitis
Score
0
1
2
3
4
Transversal
Sagittal
Score distribution
Animals
0-1
1-2
2-3
3-4
Osteomyelitis score
C
In vivo microPET
Pre-operative
1 week
3 weeks
6 weeks
Transversal
Coronal
Sagittal
18F-FDG uptake
SUV
Pre-op
Weeks
Left (non-operated)
Right (contaminated)

Quantification of the microPET tracer uptake indicated that there was no statistical difference in tracer uptake in the proximal part of the tibia between the experimental pre-operative group and the historic control group (7) (left leg, p=0.371; right leg p=0.112).

There was no statistical difference in tracer uptake between the left and right leg of the combined pre-operative control group (including the historic control group) (p=0.753).

The ^{18}F-FDG uptake in the operated right leg was significantly increased at all post-operative time points compared to the uptake in the right tibia of the combined pre-operative control group (Figure 2C, pre-operative black bar compared to post-operative black bars; p≤0.001).

All post-operative time points showed an increased ^{18}F-FDG uptake, indicated by the standardized uptake value (SUV) in the operated and contaminated right leg when compared to the uncontaminated left leg (Figure 2C, white bars compared to black bars; p≤0.012).

Indicative for an active osteomyelitis, bacterial cultures of swabs taken from the knee joint cavities tested positive for *S. aureus* in 4 out of 9 cases, while bone tissue homogenate cultures tested positive for *S. aureus* in all cases (Figure 3A).

Histological staining of PMMA sections of the tibiae indicated the presence of Gram-positive cocci in the intramedullary cavity of the contaminated tibiae only (Figure 3B). Masson Goldner staining indicated a clearly defined well-structured cortex, without signs of periosteal elevation or cortical thickening in uncontaminated left tibiae, while the contaminated right tibiae showed cortical thickening and loss of cortical integrity, indicating osteomyelitis (Figure 3C).

The state of bone remodelling was assessed by calcium binding fluorophores. In normal aseptic bone remodelling closely matched fluorescent signals (calcium deposition) are to be expected whereas diseased bone remodelling would show as calcium deposition in an in outward direction in clearly defined layers (green; 2 weeks post-operative, red; 4 weeks post-operative and blue; the day before sacrifice). This allowed a clear discrimination between the normal left (unoperated and uncontaminated) and the right (operated and infected) tibia of all animals.

Figure 3 (right page): Bacterial culture and histology **A:** *Post-mortem* bacterial culture of the excised part of the tibial tuberosity of the osteomyelitic tibia, indicating bacterial presence in all tibiae. **B:** Histological confirmation of bacterial presence, by Gram stain, in the contaminated right leg only. **C:** Bone morphological changes between left and right tibia. Tibial tuberosity is missing in the section of the right leg since this was used for bacterial culture. Fluorescence microscopy (insert) indicated normal bone remodelling in the left tibia, while it indicates cortex remodelling during the experimental follow-up in the right tibia (green at two weeks, red at four weeks and blue at six weeks after surgery).

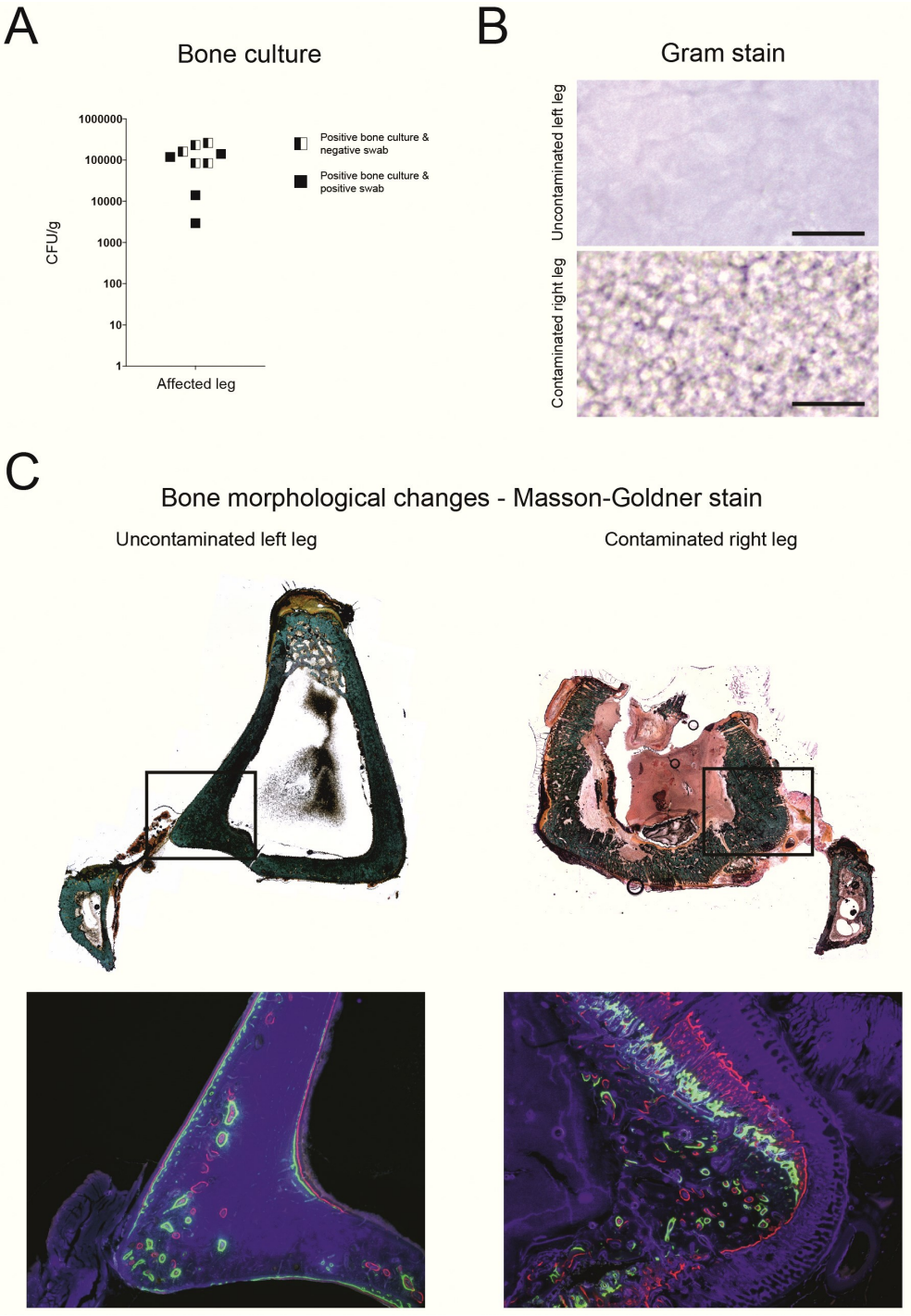
A
Bone culture
1000000
100000
10000
1000
100
10
1
CFU/g
Affected leg
Positive bone culture & negative swab
Positive bone culture & positive swab
B
Gram stain
Uncontaminated left leg
Contaminated right leg
C
Bone morphological changes - Masson-Goldner stain
Uncontaminated left leg
Contaminated right leg

The calcium binding fluorophores indicated undisputable signs of periosteal elevation and cortical thickening, in the infected tibiae (Figure 3C), these hallmarks for infection are confirmed by our previously published studies concerning orthopaedic implant infections.

4. Discussion

Osteomyelitis remains to be a major complication after an orthopaedic intervention or after bone trauma (9, 10). The herein described study was conducted to provide insight in osteomyelitic development including the accompanying bone remodelling and the use of novel diagnostic approaches in the absence of an orthopaedic implant and a sclerosing agent to support infection development. Combined the results of this study with our previously published studies on orthopaedic implant infection (6) and the use of ^{18}F-FDG to detect implant infection by PET-imaging (7), we can provide an improved perspective on how the used infection parameters differ from each other in case of (non-)implant related orthopaedic infections.

Animal models for experimental (implant-related) osteomyelitis, like ours, are being used to evaluate the application resorbable biomaterials and antimicrobial coatings and their antimicrobial properties (11-14). For this reason no sclerosing agent like sodium morrhuate was used, since it poses a threat to resorbable biomaterials, due to the denaturing capacity of sodium morrhuate (15 -18). Furthermore sodium morrhuate creates an abnormal bone anatomy by destructing the local vascularisation (5, 19).

Common haematological parameters like ESR, CRP and leucocyte differentiation are potent parameters for infection detection. However, there are some practical difficulties, the ESR is difficult to determine due to the used capillary detection system in our experimental setup, resulting in large deviations at the moment of readout. This issue makes this method of determination less accurate. The determination of the CRP concentration on the other hand is performed by ELISA, which is a very sensitive method, resulting in a more accurate readout. However both ESR and CRP show the same trend, which is increased levels in the first weeks after surgery, after which the levels slowly decrease.

The leucocyte differentiation however shows a specific increase or decrease of a specific fraction of the leucocyte pool. E.g. acute infection is generally related to a decrease in the lymphocyte fraction and a related increase in favour of the neutrophil and monocyte fraction. When we combine these haematological findings with the fact that the infection remains active, even when

the ESR and CRP are decreasing and the shift in leucocyte differentiation remains, this would suggest that the infection is stabilizing. This finding was confirmed by our previously performed study on orthopaedic implant infections.

X-ray radiographs allow detection of bone infection due to morphological changes like infection-initiated mineralisation and osteolysis. Radiography is often used on single time points. The use of multiple imaging moments during follow-up allows monitoring of the bone morphological changes in the affected region. By detecting periosteal elevation, focal loss of cortex integrity and osteolysis, an osteomyelitic lesion can be detected in time during radiological follow-up and thus allows monitoring of infection progression. Whereas the presence of an implant may disturb radiologic detection of infection hallmarks due to implant related scatter of the X-rays, nonetheless the influence (on radiologic imaging) of the implant will remain equal during follow-up which will not hamper the sequential evaluation of bone mineralisation and morphology over time.

^{18}F-FDG has been described as a clinical PET tracer for metabolic active processes (e.g. tumour growth, brain activity) (20, 21). Together with previously published data of others, our data indicates the diagnostic potential of ^{18}F-FDG as a microPET tracer for the detection of osteomyelitis in relation to other relevant infection parameters, especially since ^{18}F-FDG microPET indicates abnormal metabolically active areas in the body (2, 7, 22). Furthermore our data indicates that ^{18}F-FDG microPET allows differentiation between contaminated and uncontaminated bony tissue within one week after surgery. Due to the ability of ^{18}F-FDG microPET to distinguish between infected and uninfected tissue this could be a powerful tool to assess novel infection interventions (coatings, antibiotic treatments). However previously published studies have shown that the presence of an implant or an osteotomy/fracture can hamper early detection by PET due to implant-related scatter of the excited photons on the metallic implant surface or by tracer uptake due to a local sterile inflammation (fracture) (7, 22). This indicates that the use of ^{18}F-FDG is a very sensitive method to detect increased metabolic activity in the bony tissue, however the specificity is not only dedicated towards infection, but also towards sterile inflammation due to tissue damage (by a surgical intervention or fracture) (7, 22).

Bacterial culture is considered the golden standard for the detection of active bone infections (23-25). The additional histological analysis for bacterial presence, by Gram-staining, of the PMMA sections of the tibiae indicates the presence of bacteria in the affected tissue. While standard histological staining's indicate the bone morphological changes initiated by the bacterial infection.

The use of calcium binding fluorophores has been used in the past to follow bone remodelling and the mineralisation of teeth (26-30). In contrast to these previous studies our data shows that these calcium binding fluorophores can also be of considerable value to monitor and quantify osteomyelitis related bone remodelling, specifically the mineralisation of the periosteal elevation (6). Furthermore when these data are combined with the haematological data, it shows that the infection-mediated bone mineralisation remains progressing even after the ESR and CRP levels are decreasing, strengthening the indication for an acute stabilizing (potentially chronic) infection. Furthermore when combined with our previously published data (6, 7), these data indicate that these changes in bone remodelling are infection dependent and not associated with the presence nor absence of an implant.

Our collected data provides novel insight in osteomyelitis development and suggestions of parameter usage in both pre-clinical and clinical perspective. In the pre-clinical setting the body weight and temperature provide general information about the condition of the animal and should be regarded as such. The use of weekly assessment of the CRP levels and leucocyte differentiation, in combination with weekly X-ray radiographs, histology and bacterial culture is recommended. Although the use of ^{18}F-FDG microPET, *post-mortem* microCT and the use of calcium binding fluorophores, provide optional information on the infection and its related bone mineralisation, they are not absolutely necessary to determine if an antimicrobial coating or biomaterial is effective to prevent an osteomyelitis, X-ray radiographs, histology, bacterial culture and haematological analysis provide sufficient information. However, when interested in prophylactic approaches, the determination of delayed onset of the actual infection, or infection mediated bone remodelling and osteolysis, ^{18}F-FDG microPET, *post-mortem* microCT and the use of calcium binding fluorophores provide more in depth information about timing, metabolic activity and bone mineralisation.

When translated to the clinical situation however, the situation is different, CRP and leucocyte differentiation will still be useful and so will X-ray radiographs, but calcium binding fluorophores are not an option. Based on our data, ^{18}F-FDG PET (combined with CT/MRI in one clinical system) could considerably contribute to the early detection of an orthopaedic infection allowing early infection intervention and treatment in the clinical situation.

5. Conclusion

Our study describes the detection of different bone infection parameters and their correlations in an experimental osteomyelitis animal model (independent of the presence of an implant) and provides information on which parameters would be the most optimal infection parameters to be of use in the pre-clinical and potentially the clinical setting. Furthermore our study showed that ^{18}F -FDG PET is a potent diagnostic tool for the early detection of orthopaedic infections, which can be of great value when applied in the clinical situation.

Acknowledgements

This research forms part of the Project P4.01 NANTICO of the research program of the BioMedical Materials institute, co-funded by the Dutch Ministry of Economic Affairs.
Furthermore, the authors would like to thank the employees of the animal facility of the Maastricht University Medical Centre for their assistance during this study. We would also like to thank I. Pooters, M. Visser and C. Urbach from the Nuclear Medicine department of the Maastricht University Medical Centre for their support during this study. And we would like to thank S. Bout and P. Dijkstra for their overall support during this study.

References

1. Demirev A, Weijers R, Geurts J, Mottaghy F, Walenkamp G, Brans B. Comparison of (18 f)fdg pet/ct and mri in the diagnosis of active osteomyelitis. Skeletal Radiology. 2014 May;43(5):665-72.
2. Lankinen P, Lehtimaki K, Hakanen AJ, Roivainen A, Aro HT. A comparative 18f-fdg pet/ct imaging of experimental staphylococcus aureus osteomyelitis and staphylococcus epidermidis foreign-body-associated infection in the rabbit tibia. EJNMMI Res. 2012 Jul 23;2(1):41.
3. Makinen TJ, Lankinen P, Poyhonen T, Jalava J, Aro HT, Roivainen A. Comparison of 18f-fdg and 68ga pet imaging in the assessment of experimental osteomyelitis due to staphylococcus aureus. European Journal of Nuclear Medicine and Molecular Imaging. 2005 Nov;32(11):1259-68.
4. Norden CW. Experimental osteomyelitis. I. A description of the model. Journal of Infectious Diseases. 1970 Nov;122(5):410-8.
5. Andriole VT, Nagel DA, Southwick WO. A paradigm for human chronic osteomyelitis. Journal of Bone and Joint Surgery (American Volume). 1973 Oct;55(7):1511-5.
6. Odekerken JC, Arts JJ, Surtel DA, Walenkamp GH, Welting TJ. A rabbit osteomyelitis model for the longitudinal assessment of early post-operative implant infections. Journal of Orthopaedic Surgery and Research. 2013;8(1):38.
7. Odekerken JC, Brans BT, Welting TJ, Walenkamp GH. 18f-fdg micropet imaging differentiates between septic and aseptic wound healing after orthopedic implant placement a longitudinal study of an implant osteomyelitis in the rabbit tibia. Acta Orthopaedica. 2014;85(3):9.
8. Winkler NT. Alara concept--now a requirement. Radiologic Technology. 1980 Jan-Feb;51(4):525.
9. Acklin YP, Widmer AF, Renner RM, Frei R, Gross T. Unexpectedly increased rate of surgical site infections following implant surgery for hip fractures: Problem solution with the bundle approach. Injury. 2011 Feb;42(2):209-16.
10. Montanaro L, Speziale P, Campoccia D, Ravaioli S, Cangini I, Pietrocola G, Giannini S, Arciola CR. Scenery of staphylococcus implant infections in orthopedics. Future Microbiology. 2011 Nov;6 (11):1329-49.
11. Alt V, Lips KS, Henkenbehrens C, Muhrer D, Oliveira Cavalcanti MC, Sommer U, Thormann U, Szalay G, Heiss C, Pavlidis T, Domann E, Schnettler R. A new animal model for implant-related infected non-unions after intramedullary fixation of the tibia in rats with fluorescent in situ hybridisation of bacteria in bone infection. Bone. 2011 May 1;48(5):1146-53.
12. Kalicke T, Schierholz J, Schlegel U, Frangen TM, Koller M, Printzen G, Seybold D, Klockner S, Muhr G, Arens S. Effect on infection resistance of a local antiseptic and antibiotic coating on osteosynthesis implants: An in vitro and in vivo study. Journal of Orthopaedic Research. 2006 Aug;24(8):1622-40.
13. Moojen DJ, Vogely HC, Fleer A, Nikkels PG, Higham PA, Verbout AJ, Castelein RM, Dhert WJ. Prophylaxis of infection and effects on osseointegration using a tobramycin-periapatite coating on titanium implants--an experimental study in the rabbit. Journal of Orthopaedic Research. 2009 Jun;27 (6):710-6.
14. Nijhof MW, Stallmann HP, Vogely HC, Fleer A, Schouls LM, Dhert WJ, Verbout AJ. Prevention of infection with tobramycin-containing bone cement or systemic cefazolin in an animal model. Journal of Biomedical Materials Research. 2000 Dec 15;52(4):709-15.
15. Rogers L. A note on sodium morrhuate in tuberculosis. British Medical Journal. 1919 Feb 8;1(3032):147 -8.
16. Tunick IS, Nach R. Sodium morrhuate as a sclerosing agent in the treatment of varicose veins. Annals of Surgery. 1932 May;95(5):734-7.
17. Schaumburger J, Trum S, Anders S, Beckmann J, Winkler S, Springorum HR, Grifka J, Lechler P. Chemical synovectomy with sodium morrhuate in the treatment of symptomatic recurrent knee joint effusion. Rheumatology International. 2012 Oct;32(10):3113-7.
18. Stroncek DF, Hutton SW, Silvis SE, Vercellotti GM, Jacob HS, Hammerschmidt DE. Sodium morrhuate stimulates granulocytes and damages erythrocytes and endothelial cells: Probable mechanism of an adverse reaction during sclerotherapy. Journal of Laboratory and Clinical Medicine. 1985 Nov;106 (5):498-504.
19. Cremieux AC, Carbon C. Experimental models of bone and prosthetic joint infections. Clinical Infectious Diseases. 1997 Dec;25(6):1295-302.

20. Toyama H, Ichise M, Liow JS, Modell KJ, Vines DC, Esaki T, Cook M, Seidel J, Sokoloff L, Green MV, Innis RB. Absolute quantification of regional cerebral glucose utilisation in mice by 18f-fdg small animal pet scanning and 2-14c-dg autoradiography. Journal of Nuclear Medicine. 2004 Aug;45(8):1398-405.
21. Toyama H, Ichise M, Liow JS, Vines DC, Seneca NM, Modell KJ, Seidel J, Green MV, Innis RB. Evaluation of anesthesia effects on (18f)fdg uptake in mouse brain and heart using small animal pet. Nuclear Medicine and Biology. 2004 Feb;31(2):251-6.
22. Jones-Jackson L, Walker R, Purnell G, McLaren SG, Skinner RA, Thomas JR, Suva LJ, Anaissie E, Miceli M, Nelson CL, Ferris EJ, Smeltzer MS. Early detection of bone infection and differentiation from post-surgical inflammation using 2-deoxy-2-(18f)-fluoro-d-glucose positron emission tomography (fdg-pet) in an animal model. Journal of Orthopaedic Research. 2005 Nov;23(6):1484-9.
23. Trampuz A, Zimmerli W. Antimicrobial agents in orthopaedic surgery: Prophylaxis and treatment. Drugs. 2006;66(8):1089-105.
24. Woods GL, Walker DH. Detection of infection or infectious agents by use of cytologic and histologic stains. Clinical Microbiology Reviews. 1996 Jul;9(3):382-404.
25. Waldvogel FA, Medoff G, Swartz MN. Osteomyelitis: A review of clinical features, therapeutic considerations and unusual aspects. New England Journal of Medicine. 1970 Jan 22;282(4):198-206.
26. Pautke C, Tischer T, Vogt S, Haczek C, Deppe H, Neff A, Horch HH, Schieker M, Kolk A. New advances in fluorochrome sequential labelling of teeth using seven different fluorochromes and spectral image analysis. Journal of Anatomy. 2007 Jan;210(1):117-21.
27. Pautke C, Vogt S, Tischer T, Wexel G, Deppe H, Milz S, Schieker M, Kolk A. Polychrome labeling of bone with seven different fluorochromes: Enhancing fluorochrome discrimination by spectral image analysis. Bone. 2005 Oct;37(4):441-5.
28. van Gaalen SM, Kruyt MC, Geuze RE, de Bruijn JD, Alblas J, Dhert WJ. Use of fluorochrome labels in in vivo bone tissue engineering research. Tissue engineering Part B, Reviews. 2010 Apr;16(2):209-17.
29. Rittmann WW, Perren SM. Corticale knochenheilung nach osteosynthese und infektion. Biomechanik und biologie: Springer-Verlag, Berlin; 1974.
30. Feith R. Side-effects of acrylic cement implanted into bone. Thesis. 1975.

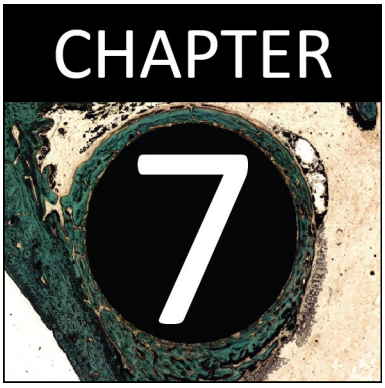

A novel polymer-based osteoconductive drug-eluting coating for orthopaedic implants

J.C.E. Odekerken

A.J. Dirks

J.A. Loontjens

B.T. Brans

L .N.D. Rijk

J.J.C. Arts

T.J.M. Welting

G.H.I.M. Walenkamp

Patent filed, 2014. Manuscript to be submitted

Abstract

Introduction: Orthopaedic implant infection is a severe complication with a high impact on the patient's life and the health care system. In prophylaxis as well as in treatment the use of systemically applied antibiotics is often supported or replaced by locally delivering antibiotic carriers as antibiotic loaded bone cement, eventually in the form of PMMA spacers or beads. However when no antibiotic loaded bone cement is used, as in uncemented joint prostheses or osteosynthesis, there is a need for a biocompatible coating that can act as a carrier of an antibacterial compound to prevent infection of the implant or to facilitate one stage revisions of implant infections.

Methods: We therefore explored the properties of a polymer coating which allows easy application on a titanium implant surface, release of the antiseptic chlorhexidine, and actively facilitates bone apposition.
Coated titanium implants were evaluated *in vitro* on the release and the effectiveness of chlorhexidine and *in vivo* on the infection prevention as well as the osteoconductive capacity of the implant surface.

Results: *In vitro* evaluation of the coating proved antiseptic activity of the released chlorhexidine against *S. aureus* growth, but *in vivo* evaluation indicated that the released dose of chlorhexidine resulted only in a delayed onset of the implant infection. In addition *in vivo* evaluation indicated that the polymer coating allowed more bone apposition on the coated surface as compared to uncoated titanium, even when the coating was loaded with chlorhexidine.

Conclusions: We here present the development and evaluation of a novel osteoconductive polymer coating concept that allows the incorporation of an antibacterial component, like chlorhexidine, which remains active after the initial release *in vitro* and *in vivo*.

Keywords: Infection, animal model, antimicrobial coating, osteoconduction, bone apposition, molecular imaging.

1. Introduction

Orthopaedic infection is a serious healthcare-associated infection with a high burden for the patient and is associated with a prolonged hospital stay, multiple reconstructive surgical procedures and expensive invasive antibiotic treatment resulting in high costs for the healthcare system (1-3).

Increasing numbers of joint prostheses are implanted every year, due to improved surgical techniques and enhanced uncemented prosthesis designs. In combination with a general prolonged life expectancy and even with an unchanged relative low incidence of implant infections, the prevalence of prostheses infections will increase due to the increased number of implants being placed (4-6). Consequently, prophylaxis of these infections becomes increasingly important. Furthermore all methods to improve the treatment of established infections are of great value.

In prophylaxis as well as in treatment, antibiotics are systemically and locally applied (delivered by a carrier like PMMA beads or bone cement in case of cemented prostheses). In joint prostheses placement, prophylaxis of postoperative infection is performed with antibiotic admixture in the PMMA bone cement (7-10). The same efficacy of the antibiotic elution is shown in the revision of infected prostheses, since the results achieved with antibiotic loaded bone cement are superior to bone cement without antibiotics in one stage as well as in two stage procedures (7, 8). However an increasing number of uncemented (often hydroxyapatite coated) prostheses are being implanted, lacking this protection by locally delivered antibiotics. This is even more troublesome in the revision procedure of infected uncemented prostheses, especially since more and more uncemented prosthesis are used for re-implantation.

PMMA bone cement admixed with gentamicin, clindamycin, tobramycin or vancomycin is the most commonly used local prophylactic measure for cemented prosthesis. However, more and more bacterial resistance towards these antibiotics are being reported (11, 12).

Therefore antiseptic compounds might prove to be valuable for the treatment of these infections, since they are being used for decades in disinfecting lotions, soaps and adhesives with limited reports on acquired antibiotic resistance against these antiseptic chemicals (13-17). Chlorhexidine is such an antiseptic compound and is being used as an antiseptic since the 1950s, after which it has been used in various applications ranging from toothpaste to chemical vasectomy in pets (13, 15, 18, 19). Its sclerosing mode of function is based on the disruption of cellular membrane,

precipitation of cytoplasmic proteins and nucleic acids, resulting in cell death (15, 17, 20). Therefore a combination of chlorhexidine and alcohol provides an effective antimicrobial solution with limited reports on potential hypersensitivity of the patient (13, 15), while direct intravenous injection of chlorhexidine is considered toxic, potentially even lethal (21). In medical device applications chlorhexidine is a frequently explored compound due to its antiseptic capacity and its thermal and chemical stability. Therefore it has been used in dentistry in mouthwash liquids and coatings, to protect against caries-initiated tooth decay (22) or as a protective agent in orthodontic adhesives and cements (14, 23). It is also used in the clinic as a releasing component in central venous catheters (Arrowg+ard Blue & Arrowg+ard Blue PLUS, Teleflex Medical, USA) to prevent biofilm formation and bacterial infection. Still the implementation of chlorhexidine as a prophylactic to prevent or support the treatment of orthopaedic implant infections, has never been explored to our knowledge.

The optimal orthopaedic implant coating for the prevention of direct post-operative infection, should possess the following properties:

- Provide an advantage in favour of the host tissue instead of potential pathogens like bacteria in “the race for the surface” (24, 25).
- Effective in the prevention of deep infection
- Improve the results of re-implantation after infection revision for implants with various fixation technologies.
- The coating backbone must be osteoconductive, to allow the host tissue to achieve local bone remodelling before the development of a bacterial biofilm on the implant surface.
- The coating composition and procedure must allow the incorporation of antibacterial substances during the production process and allow the release of these substances when applied in patients.

We here evaluated the prophylactic and osteoconductive potential of a novel polymer coating. The developed coating is expected to promote bone apposition and allow the incorporation and release of the antiseptic chlorhexidine (CHX) to prevent infection. The coating properties were evaluated in an *in vitro* microbiological efficacy test, an *in vivo* systemic toxicity screening and in an *in vivo* infection model.

2. Materials and methods

2.1 Coating production and procedure

The base-coating formulation was prepared by a mixture of "***Compound α***", "***Compound β***" and "***Compound γ***". In case of loading with chlorhexidine the base-coating formulation was supplemented after the incubation with 15 ml ethanol containing either 0.17 mmol chlorhexidine diacetate (Sigma-Aldrich, CAS 56-95-1) for a low dose coating (3 µg/cm^2) or 1.7 mmol chlorhexidine diacetate for a high dose coating (30 µg/cm^2). If the coating contained no chlorhexidine only 15 ml ethanol was added.

The compiled coating mixtures (either with or without the supplementation of chlorhexidine diacetate) were used for the coating of grit-blasted medical grade titanium (TiAl6V4) rods (DePuy). Rods were dip coated in 2 phases (to obtain full surface coverage) at a dip speed of 2.0 mm/s (PL 3201, Specialty Coating Systems) with a sequential curing step (at temperature "***X***" for "***Y***" hours in a stove) after each coating phase. After the final curing step the rods were individually packed for sterilisation by autoclaving (20 minutes at 121 ^{o}C) or gamma sterilisation.

Due to the possible patentability of the coating for other applications, the coating composition and preparation is intentionally blinded.
Patent EP14186637: Medical Coating Composition.

2.2 *In vitro* efficacy of released chlorhexidine

To evaluate the *in vitro* antimicrobial efficacy and the effect of the sterilisation procedure (autoclaved or gamma-sterilized) on the *in vitro* antimicrobial efficacy of the coating, two identically manufactured coating groups (except for the final sterilisation step) were tested. Each group contained a coated subgroup without chlorhexidine and 2 subgroups with a chlorhexidine containing coating (low dose; 3 µg/cm^2 and a high dose; 30 µg/cm^2). Coated titanium rods were incubated for 48h at 37^{o}C in 2 ml sterile phosphate-buffered saline (PBS, pH 7.4) to assess the antimicrobial properties of the eluted chlorhexidine.

After 48 hours 100 µl of the eluate was used in a bacterial growth inhibition test, in which 1.7x10^5 CFU *Staphylococcus aureus* ATCC 49230 (a clinical isolate from a patient with chronic

osteomyelitis), in tryptic soy broth (Bacto, Beckton Dickinson, France), was subjected to the eluate in comparison to a dose response curve of standard concentrations of chlorhexidine ranging from a final concentration of 0 to 100 ug/ml chlorhexidine, which served as a reference (fig 1, column 1-3). After 24h of incubation at 37°C, the bacterial growth was assessed by bacterial culture on tellurite glycine agar plates (Difco, Becton Dickinson, France).

2.3 *In vivo* experiments: animal choice, welfare and ethics

The toxicity of the coating was evaluated in 15 Specified Pathogen Free (SPF) female New Zealand White (NZW) rabbits (Charles River, France). For the evaluation of the *in vivo* coating efficacy 33 SPF female NZW rabbits (Charles River, France) were used in combination with an historic uncontaminated control group of 11 SPF female NZW rabbits (26, 27). All animals were within a weight range of 3.5 - 4 kg. After arrival the animals were allowed to acclimatize in group housing for 2 weeks before surgery was performed.
In each experiment the population was randomly divided in surgical groups containing 5-8 animals. Each animal received a 20 mm long, 4 mm wide (un)coated grit-blasted titanium rod ($TiAl_6V_4$) (DePuy, USA) in the proximal tibia.

In the coating toxicity study, 15 animals were randomly assigned to 3 separate groups of 5 rabbits, an unloaded coating group (coating without chlorhexidine), a low dose coating group (3 µg/cm^2 chlorhexidine) and a high dose coating group (30 µg/cm^2 chlorhexidine). Each study group consisted of 5 animals.

In the coating efficacy study, 33 animals were randomly assigned to 3 separate groups, 1 uncontaminated implant control group coated with the high dose chlorhexidine coating and 2 contaminated implant groups with either an uncoated or coated (30 µg/cm^2 chlorhexidine) titanium implant. The historic uncontaminated uncoated implant group served as a treatment control group (26, 27). So each group consisted out of 11 animals with a total of 44 animals, of which 11 originated from a previously performed study and functioned as an historic control group. Surgical groups were maintained during the entire follow-up period.
Animal housing, feeding, pain treatment, humane endpoints and sacrifice were performed according to our previously described studies (26, 27).

This study was approved by the Maastricht University Animal Ethics Committee (DEC-UM, Protocol 2010-089, Maastricht, the Netherlands).

2.4 Animal surgery and follow-up

The anaesthesia and surgical procedure was performed according our previously described studies (26, 27). A titanium rod was introduced through a cylindrical cavity in the tibia plateau in the proximal left tibia using a comparable operative technic as in intramedullary nailing of fractures in human patients.

In case of the coating efficacy experiments the animals received a per-operative contamination with 100 µl saline containing $1.8x10^6$ CFU/ml *S. aureus* ATCC 49230. The inoculum was freshly prepared before surgery of each animal. *S. aureus* was cultured in tryptic soy broth (Bacto, Beckton Dickinson, France). Inocula were prepared by inoculation of an inoculation loop of fresh overnight culture in 20 ml tryptic soy broth. After 3 to 4 hours the OD600 of the bacterial culture was determined, the bacteria were harvested at an OD600 of 0.5 by centrifugation (5 minutes, 1800xg). The pellet was resuspended and diluted with sterile saline to a concentration of $1.8x10^6$ CFU/ml, based on OD600 (Amersham Biosciences, GE Healthcare, USA) measurements. The bacterial count of every inoculum was verified by quantitative culture on tellurite glycine agar, before and after surgery to confirm inoculum size.

Animals were clinically monitored during a 6 weeks follow-up, observing the use of the hind legs, aspect of the wound and general signs of infection. Body weight and temperature were measured pre-operative at the day of surgery and every week thereafter until the end of the experiment. Blood was collected by venipuncture before surgery and every week thereafter until the end of the experiment to check for changes in leucocyte differentiation (Euregio Laboratory, the Netherlands), C-reactive protein levels (Rabbit CRP ELISA, E-15CRP, Immunology Consulants Laboratory, USA) and changes in erythrocyte sedimentation rate (Kabe Labortechnik, Germany).

2.5 Imaging

Bone morphological changes were assessed by antero-posterior and lateral X-ray radiographs, acquired at 85 kV and 20 mAs (Polymobil, Siemens, Germany). Post-mortem microCT data was acquired with a field of view of 10 cm in diameter, a source-to-axis distance of 30 cm and a source-

to-detector distance of 62 cm, at 80 kVp, with an isotropic spacing of 102 µm and 2.14 mm Al added filtration (X-rad 225, Precision X-ray, USA). Increased metabolic turnover of glucose was assessed by ^{18}F-FDG microPET, after reconstruction by an attenuation-weighed 2-dimensional ordered-subsets expectation maximisation (OSEM2D) protocol with an isotropic voxel size of 0.87 mm (Focus 120 MicroPET, Siemens, Germany). All these imaging procedures were performed according to our previously described studies (26, 27).

2.6 Bacteriology

After sacrifice the tibiae were dissected aseptically. Swaps were taken from the knee joint cavity and tibial plateau. To assess soft tissue infection, swaps were evaluated for the presence of *S. aureus* on tellurite glycine agar plates. *S. aureus* growth was identified by the presence of black colonies, due to the coagulase positive character of the species. Other contaminating, coagulase negative, bacterial species would appear as white colonies. The *tuberositas tibiae* were excised from the tibia with a surgical drill (SM 12, Nouvag, Switzerland) and homogenized in 10 ml sterile saline (Ultra-Turrax T25, Ika, Germany) at 6000 rpm. The homogenates were cultured on tellurite glycine agar plates. After 24 hours, culture dishes were quantified for the specific bacterial growth. Cultures were deemed inconclusive in case of specific bacterial growth on only one of two agar plates, or less than 5 colonies present on the agar plates).

2.7 Histology

During the experimental follow-up of 6 weeks, 3 different calcium binding fluorophores were administered at intermitted time points allowing monitoring of bone apposition and mineralisation over time. At week 2 of the experimental follow-up, 25 mg/kg Calcein Green (Fluka, Sigma Aldrich, Germany) was injected, 30 mg/kg Xylenol Orange (Fluka, Sigma Aldrich, Germany) was injected at week 4 and 25 mg/kg Calcein Blue (Fluka, Sigma Aldrich, Germany) was injected on day 41 (the day before sacrifice).

After sacrifice and sampling for bone culture, tibiae were fixated in 4% formaldehyde/PBS for 4 weeks, after which the tibiae were dehydrated by increasing ethanol concentrations, followed by embedding in polymethyl methacrylate (PMMA) (Technovit 9100, Hereaus-Kulzer, Germany). After polymerisation sections were stained according to Masson-Goldner (Carl Roth, Germany) and

Gram (without a safranin counterstain). After staining, cover slides were glued on the section surface with UV-polymerizing glue (Permacol, the Netherlands) and subsequently 50 µm sections were obtained using a saw microtome (SP 1600, Leica, Germany). Sections were analysed and digitized by light microscopy (Axioscope A1, Axiovision LE release 4.8.2, Carl Zeiss, Germany). The localisation of calcium binding fluorophores in the bony tissue was visualized by fluorescence microscopy (Leica DMRB, Leica IM50 version 1.2 release 19, Leica, Germany) on unstained PMMA sections. Acquired images were merged using Photoshop CS3 (Adobe Systems, USA) to generate overview images. Histological sections were analysed blinded by 3 independent observers for multiple signs of osteomyelitis and scored accordingly.

2.8 Statistical analysis

SPSS 22 (IBM, USA) was used for the statistical analyses. Data were checked for normality with the Shapiro-Wilk test. Differences between groups were determined by a Mann-Whitney U test for non-parametric significance. Differences within groups were determined by a Wilcoxon's signed ranks test for related samples. The significance level was determined at $p<0.05$. Graphical representation of the data was performed in GraphPad Prism 5 (GraphPad, USA).

3. Results

3.1 *In vitro* efficacy of the released chlorhexidine from the coating

The coating composition was prepared and applied to the titanium rods, followed by sterilisation by either autoclaving or gamma irradiation. To evaluate the effect of the sterilisation procedure on the *in vitro* antimicrobial efficacy of the coating, two identically manufactured coating groups (except for the final sterilisation step) were evaluated. Each group contained a coated subgroup without chlorhexidine and 2 subgroups with a chlorhexidine containing coating (low dose; 3 µg/ cm^2 and a high dose; 30 µg/cm^2). After elution for 48 hours in PBS, the eluate was evaluated on bacterial growth inhibition in triplicate.

Eluates from the unloaded coating did not result in inhibition of bacterial growth in both the gamma-sterilized and autoclaved samples (Figure 1, C4-12; F4-12). Eluates of the low dose chlorhexidine loaded samples failed to inhibit bacterial growth in 1 out of 3 samples when

sterilized by gamma-irradiation (Figure 1, D4-12). Eluates from the autoclaved low dose loaded samples however, did show successful inhibition of bacterial growth in all samples (Figure 1, G4-12). The eluates from all samples with the high dose chlorhexidine loaded coating, autoclaved as well as gamma-sterilized, were effective in inhibiting bacterial growth (Figure 1, E4-12 and H4-12). These data indicate that the loaded chlorhexidine retained its antimicrobial properties after being released from the coating. Based on these dosis experiments we concluded that the autoclaved coating containing 30 μg/cm^2 chlorhexidine was the preferable coating for further *in vivo* evaluation of infection prevention.

Figure 1 (right page): *In vitro* evaluation of the unloaded and loaded coating on the bactericidal efficacy of the released chlorhexidine, indicated by bacterial growth inhibition. Each well contained 1.7 x 10^5 CFU *S. aureus*, which was exposed to a release sample to determine the bactericidal properties of the released chlorhexidine in the specific sample (triplicates). Column 1-3 served as chlorhexidine reference samples for the evaluated eluates. A4-6 represents a positive control culture to check for bacterial growth. A7-9 serve as positive control cultures for the absence of antibacterial properties of the elution buffer. A10-12 serve as negative control cultures due to the absence of bacteria.

The titanium without coating did not have bactericidal properties indicated by the bacterial growth (B4-12). Also the coated implants without chlorhexidine did not show bacterial growth inhibition, independent from their sterilisation procedure (C4-12 and F4-12). The 3 μg/cm^2 chlorhexidine containing γ-sterilized coating indicated bactericidal properties in 2 out of 3 samples (D4-12), while its autoclaved coating version did show bactericidal properties in all samples (G4-12). The 30 μg/cm^2 chlorhexidine containing coating was able to prevent bacterial growth in all samples, independent from their sterilisation procedure (E4-12 and H4-12). These data indicate that the 30 μg/cm^2 chlorhexidine containing coating is the preferable coating for further *in vivo* evaluation of infection prevention.

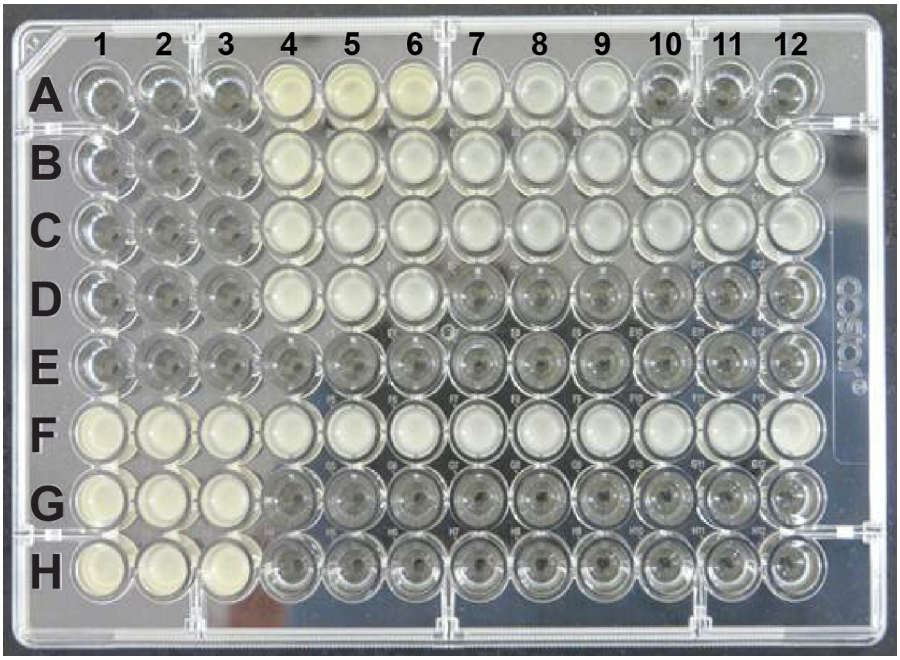

	1-3	**4-6**	**7-9**	**10-12**
A	Bacterial dose response curve **100 µg/ml CHX**	Positive control culture ***S. aureus***	Positive control culture **Elution buffer**	Negative control culture **No bacteria**
B	Bacterial dose response curve **50 µg/ml CHX**	Sterile titanium **no coating** (sample 1)	Sterile titanium **no coating** (sample 2)	Sterile titanium **no coating** (sample 3)
C	Bacterial dose response curve **25 µg/ml CHX**	*γ-sterilized* Coating **without** CHX (sample 1)	*γ-sterilized* Coating **without** CHX (sample 2)	*γ-sterilized* Coating **without** CHX (sample 3)
D	Bacterial dose response curve **12.5 µg/ml CHX**	*γ-sterilized* Coating **3 µg/cm^2** CHX (sample 1)	*γ-sterilized* Coating **3 µg/cm^2** CHX (sample 2)	*γ-sterilized* Coating **3 µg/cm^2** CHX (sample 3)
E	Bacterial dose response curve **5 µg/ml CHX**	*γ-sterilized* Coating **30 µg/cm^2** CHX (sample 1)	*γ-sterilized* Coating **30 µg/cm^2** CHX (sample 2)	*γ-sterilized* Coating **30 µg/cm^2** CHX (sample 3)
F	Bacterial dose response curve **2.5 µg/ml CHX**	*Autoclaved* Coating **without** CHX (sample 1)	*Autoclaved* Coating **without** CHX (sample 2)	*Autoclaved* Coating **without** CHX (sample 3)
G	Bacterial dose response curve **1.25 µg/ml CHX**	*Autoclaved* Coating **3 µg/cm^2** CHX (sample 1)	*Autoclaved* Coating **3 µg/cm^2** CHX (sample 2)	*Autoclaved* Coating **3 µg/cm^2** CHX (sample 3)
H	Bacterial dose response curve **0 µg/ml CHX**	*Autoclaved* Coating **30 µg/cm^2** CHX (sample 1)	*Autoclaved* Coating **30 µg/cm^2** CHX (sample 2)	*Autoclaved* Coating **30 µg/cm^2** CHX (sample 3)

3.2 *In vivo* evaluation of systemic toxicity and bone apposition

Three groups of 5 rabbits each received an intramedullary titanium implant coated with the autoclaved coating and either unloaded, loaded with a low dose (3 µg/cm^2) or loaded with a high dose (30 µg/cm^2) chlorhexidine. One animal of the unloaded coating group was lost during the initial surgery. Liver and kidney function of all animals were assessed weekly and compared to their corresponding pre-operative values. Serum creatinine levels (Figure 2A) fluctuated within normal ranges during follow-up (28, 29). Serum albumin levels (Figure 2B) increased slightly in all experimental animals, but remained within the normal range (28, 29). Aspartate transaminase (Figure 2 C), alanine transaminase (Figure 2D) and glutamate dehydrogenase levels (Figure 2E) showed elevated levels at the sixth post-operative week. These elevated values were specifically related to two sick animals, one animal of the unloaded coating group and one animal of the low dose chlorhexidine coating (diagnosed with hepatic lipidosis). Two veterinarians determined that the hepatic lipidosis in these two animals was not caused by the implanted material but more likely due to environmental stress. Furthermore the aspartate transaminase (Figure 2 C), alanine transaminase (Figure 2D) and glutamate dehydrogenase levels (Figure 2E) levels in the high dose chlorhexidine coating remained within the normal range (28, 29). Alkaline phosphatase levels (Figure 2F) remained within the normal ranges in all animals (28, 29).

After euthanization of the animals the tibiae containing the implants were excised and fixed in buffered formaldehyde and subsequently embedded in polymethyl methacrylate for histological sectioning. A historic control group of implanted uncoated titanium implants in 11 rabbit tibiae served as a bone apposition reference (implant material, surgical procedure and follow-up time points were identical to the coated groups). The average circumferential bone coverage in the control group was 71.5% within 6 weeks (Figure 3A, (26)). The unloaded coating clearly showed increased bone apposition on the implant surface with an almost complete circumferential coverage in all cases of 98.8% (Figure 3B). Fluorescence microscopy of the calcium binding fluorophores indicates that the majority of bone apposition took place within the first 4 weeks after implantation (Figure 3B). The high dose chlorhexidine coating resulted in a less pronounced increased circumferential coverage of 81.3% on average (Figure 3C). Also in this experimental group the majority of bone apposition took place within the first 4 weeks after implantation (Figure 3C). Based on these data we continued with the evaluation on the in vivo antimicrobial efficacy of the high dose chlorhexidine coating.

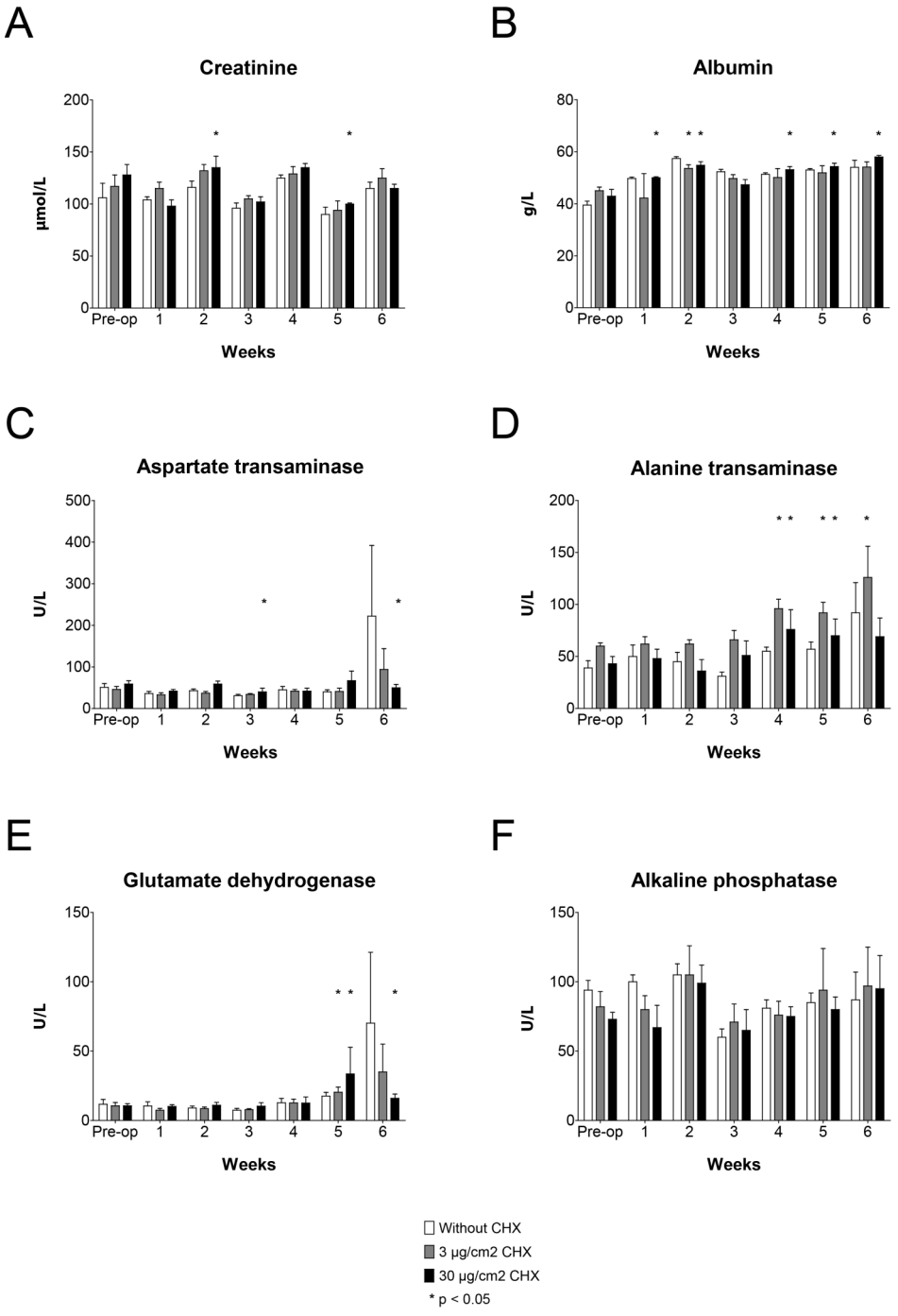

Figure 2: *In vivo* determination of kidney (A) and liver (B-F) toxicity in rabbit serum. Asterisk indicates $p < 0.05$.

A

Titanium - no coating

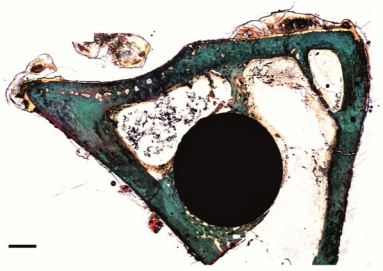

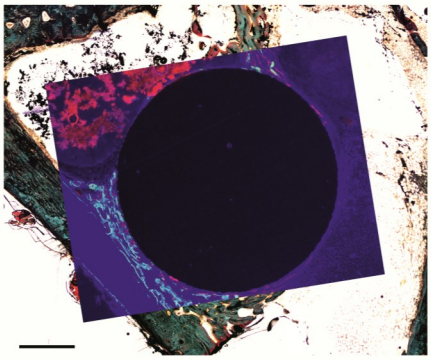

Bone apposition on surface: **71.5%**

B

Coating without CHX

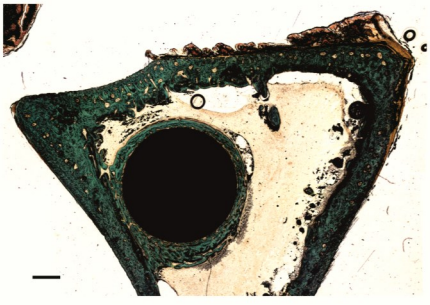

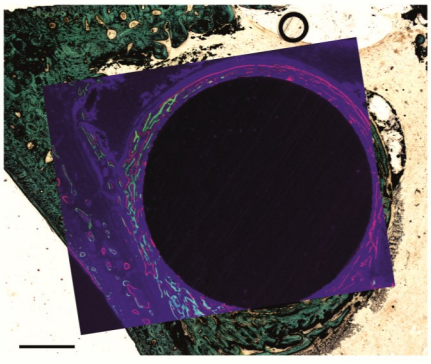

Bone apposition on surface: **98.8%**

C

Coating with 30 µg/cm^2 CHX

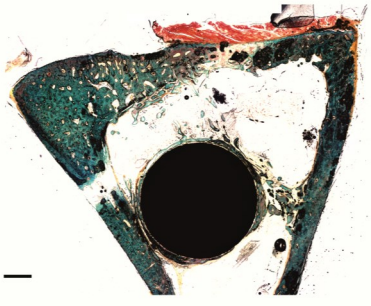

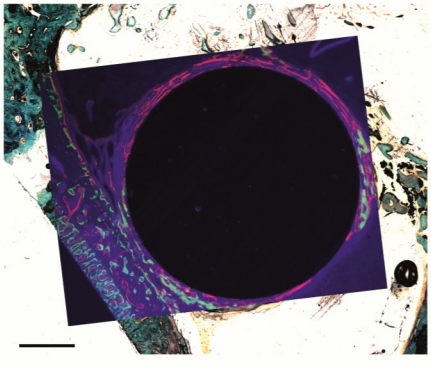

Bone apposition on surface: **81.3%**

Figure 3 (left page): Histomorphological analysis of the bone apposition on the implant surface. **A:** Bone apposition on blank titanium implants without coating (historic control group (26)). **B:** Bone apposition on the titanium implants with the unloaded coating. **C:** Bone apposition on the titanium implants with the high dose chlorhexidine coating after the release of chlorhexidine from the coating surface. Size bars indicate 1 mm; inserts in lower images originate from fluorescent microscopic analysis of sequential histological sections.

3.3 *In vivo* evaluation of the infection prophylactic capacity of the high dose chlorhexidine coating

To evaluate whether only the high dose chlorhexidine coating was able to function as an implant infection prophylactic, the coating was assessed in a rabbit tibial nail infection model (26, 27). Uncoated titanium nails served as control implants in both the presence and absence of a perioperative bacterial contamination.

In the historic control group (uncontaminated uncoated titanium implant) 2 out of 11 animals did not recover from the initial surgery (26). Three rabbits from the contaminated uncoated titanium implant group were sacrificed due to humane endpoint complications (severe soft tissue infection, 8 out of 11 rabbits remaining). In the uncontaminated chlorhexidine implant group, 2 out of 11 rabbits did not recover from the initial surgery (9 rabbits remaining). Four rabbits from the contaminated chlorhexidine coated implant group were sacrificed due to humane endpoint complications (severe soft tissue infection, 7 out of 11 rabbits remaining). In total 33 rabbits completed the experimental follow-up.

Our previous study (26) has shown that weight change, the lymphocyte fraction of the leucocyte differentiation and the CRP levels are robust indicators for the development of an implant infection in this specific animal model. In the results of this study the weight change indicated that the contaminated implant groups did not reach their pre-operative weight, while the uncontaminated implant groups did regain their pre-operative weight (Figure 4A). The lymphocyte fraction remained stable during follow-up in the uncontaminated implant groups while it decreased in the contaminated implant groups, indicating an implant infection (Figure 4B). Also CRP measurements indicated elevated concentrations in the contaminated implant groups while CRP remained low within the uncontaminated implant groups (Figure 4C). Taken together the clinical and haematological parameters indicated the development of an implant infection in both contaminated implant groups, suggesting that the released chlorhexidine was not sufficient to fully prevent the development of a deep implant infection and that it therefore does not function as a prophylactic coating at the current released concentration.

^{18}F-FDG microPET scans were acquired during the experimental follow-up to diagnose and quantify the implant infection at the early post-operative phase (27). MicroPET data quantification indicated that there was no statistical difference in tracer uptake between the saline control groups at the corresponding time points (Figure 5A). The uptake in the contaminated blank titanium group was significantly higher compared to the uptake in uncontaminated blank titanium group at the 6th post-operative week (Figure 5A). The uptake in the contaminated CHX coated implant group was significantly higher compared to the uptake in the uncontaminated CHX coated implant group at the 3th and 6th post-operative week (Figure 5A). No significant difference in tracer uptake was found between both contaminated implant groups on all post-operative time points (Figure 5A). However a trend was observed suggesting a lower tracer uptake, at the first post-operative week, in the contaminated CHX coated implant group when compared to the contaminated uncoated implant group. The increased tracer uptake in both contaminated implant groups was compared to their respective control groups, indicating an increased metabolic turnover of glucose in the area surrounding the contaminated implants, indicative for the presence of an implant infection at the end of the experimental follow-up in both contaminated implant groups.

The presence of an infection was further confirmed by microCT imaging (and scoring according our previously described radiological scoring system (26), also see page 229), indicating normal bone morphology in the uncontaminated implant groups, while in both contaminated implant groups clear radiological changes indicative for an implant-related osteomyelitis were observed (cortical thickening, osteolysis, loss of normal bone morphology and minimal bone apposition on the implant surface) (Figure 5B). There was no statistical difference in radiological osteomyelitis score between both uncontaminated implant groups and between both contaminated implant groups, while the osteomyelitis score was significantly higher in the contaminated implant groups when compared to the osteomyelitis score of the saline control groups (Figure 5B).

In vivo bone remodelling after implantation and bone apposition on the implant surface was evaluated by the use of calcium binding fluorophores. Histological sections of both saline control groups show the presence of clearly defined cortical bone and bone apposition on the implant surface (Figure 6). The histological sections of the contaminated implant groups showed the absence of bone apposition on the implant surface and disturbed cortical bone with indications of osteolysis (loss of the Calcein Green signal) and osteomyelitis progression (disorderly outward stacking of the Calcein Green, Xylenol Orange and Calcein Blue signal) (Figure 6). There was no

statistical difference in the histological osteomyelitis score (according our earlier described histological scoring system (26), also see page 230) between both uncontaminated implant groups and between both contaminated implant groups. However the histological osteomyelitis score was significantly higher in the contaminated implant groups compared to the saline control groups (Figure 6). All combined these data indicate that the prophylactic capacity of the chlorhexidine loaded coating is not sufficient to prevent an implant related osteomyelitis in this animal model.

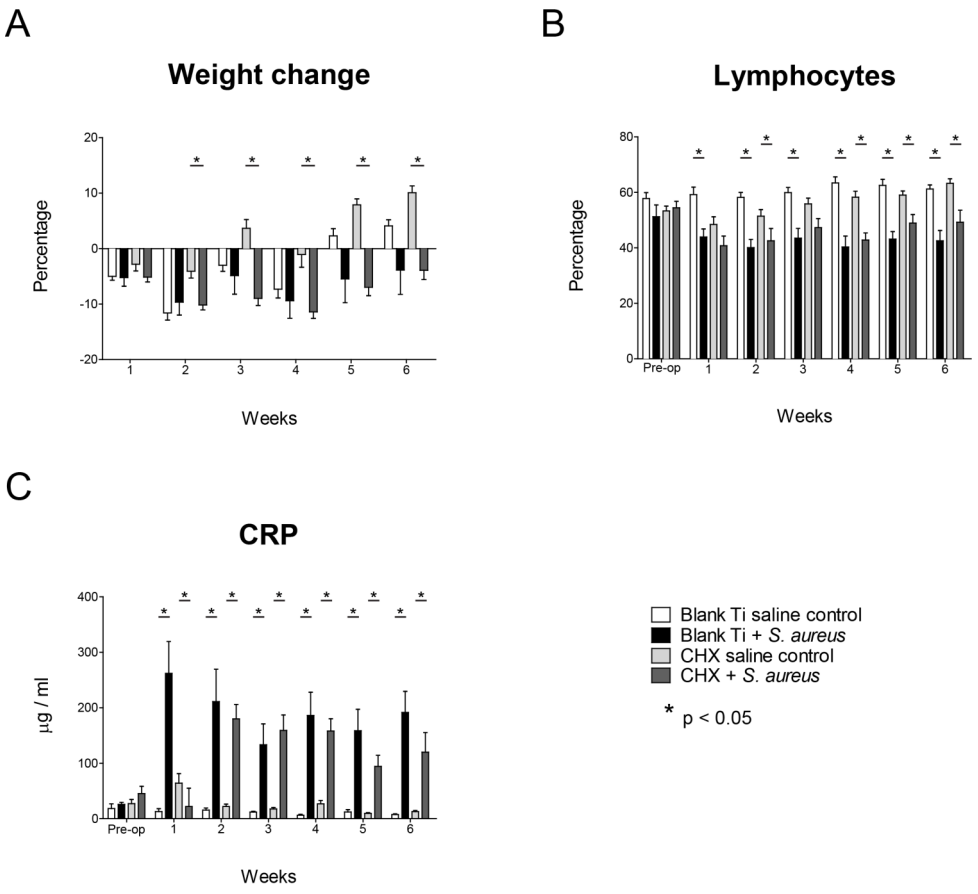

Figure 4: *In vivo* evaluation of the bactericidal efficacy of the CHX containing coating, based on clinical and haematological analysis. **A:** Weight change **B:** Leucocyte differentiation **C:** CRP levels. Asterisk indicates $p < 0.05$.

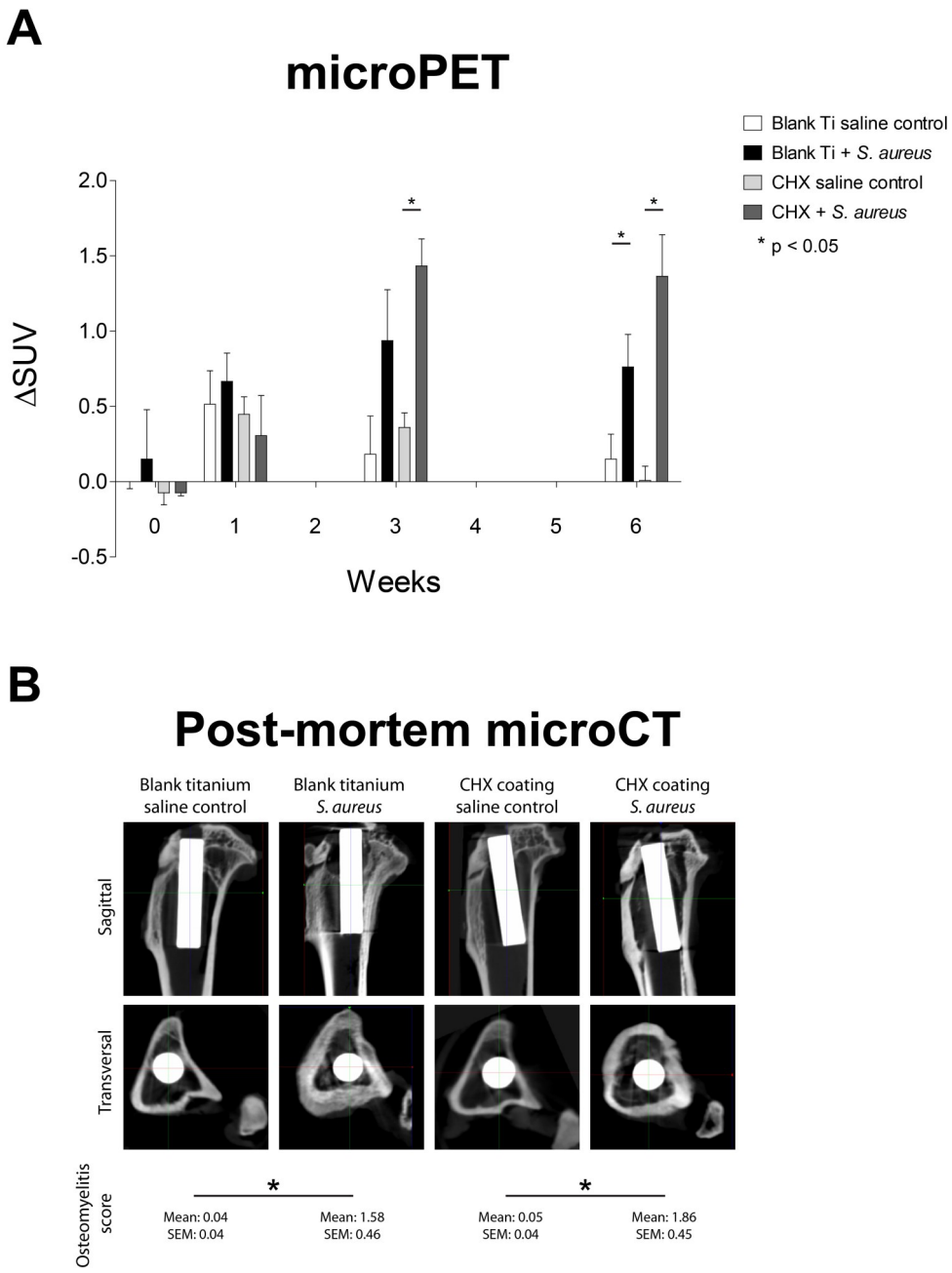

Figure 5: *In vivo* evaluation of the bactericidal efficacy of the high dose CHX containing coating based on *in vivo* and *ex vivo* imaging. **A:** Quantification of the *in vivo* ^{18}F-FDG microPET data **B:** Quantification of *ex vivo* microCT imaging. Asterisk indicates $p < 0.05$.

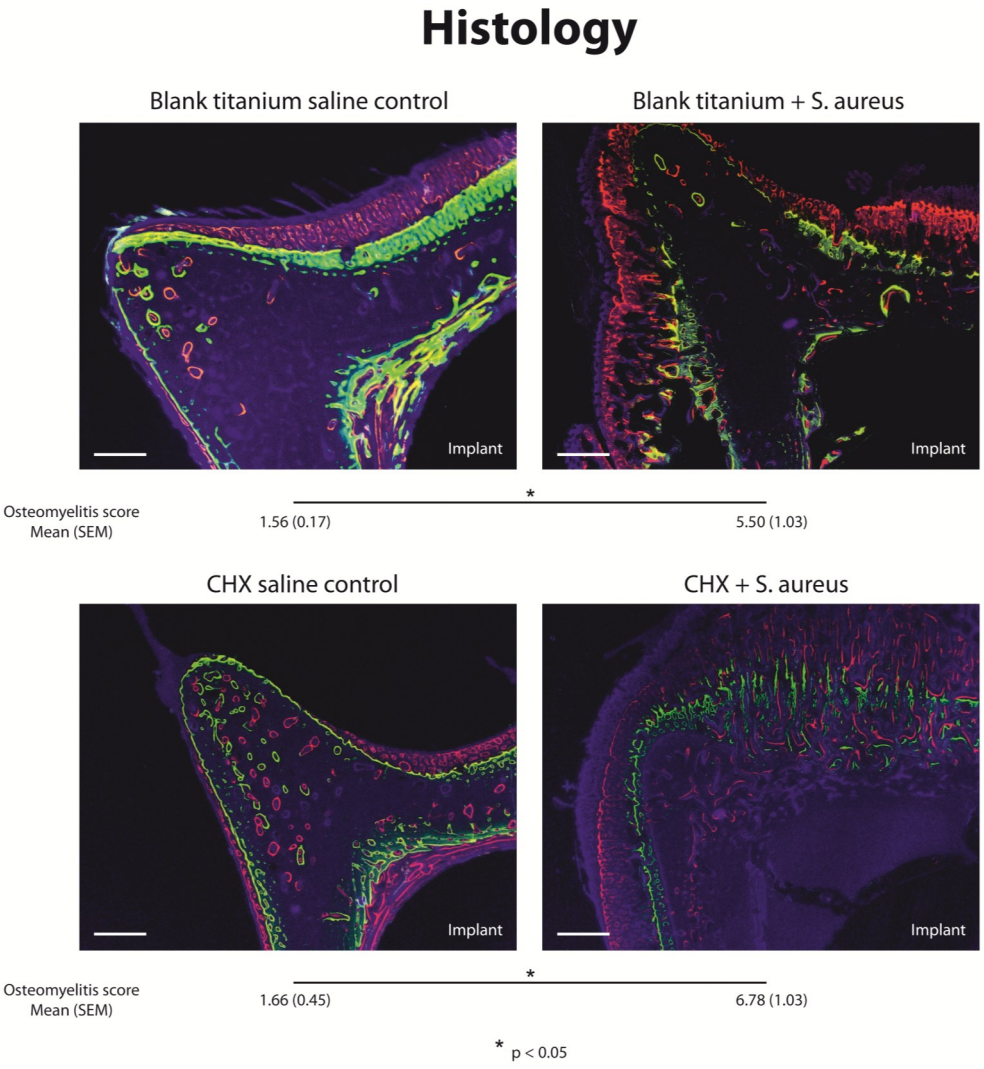

Figure 6: Calcium binding fluorophores indicate the bone apposition on specific time points during the experimental follow-up. Green stands for 2 weeks after surgery, red stands for 4 weeks and blue stands for the bone apposition at the end of the experimental follow-up (6 weeks). The control groups show clearly defined and structured bone mineralisation, while the S. aureus groups show unstructured expansion in bone apposition away from the implant as a result of an implant infection. White bars indicate 500 µm, asterisk indicates $p < 0.05$.

4. Discussion

The herein described study was performed to evaluate the prophylactic and osteoconductive properties of a novel polymer coating. Our results indicate that the polymer coating is suitable as an osteoconductive surface. The loading of the base-coating with chlorhexidine however was not sufficient as a prophylaxis for implant infection.

4.1 Coating composition

Currently used clinical osteoconductive coatings are sintered on the metallic implant surface. However, sintering makes incorporation of antibiotics in these coatings almost impossible. This means that a novel coating approach is preferable; we therefore combined techniques from different fields like industrial coatings and decontaminating chemicals like chlorhexidine.
Due to the composition of the coating it can be expected that chlorhexidine does not interact with the base-coating components so that it functions as a carrier-coating which serves as a vessel for local drug delivery (in our case chlorhexidine, but might be substituted by gentamicin or other antibacterial compounds). And because of the coating thickness it is very likely that the chlorhexidine release from the coating happens in a burst-like fashion, limiting the effective time span of the coating, making it suitable for infection prophylaxis.

4.2 Coating evaluation

Our novel polymer coating concept was evaluated in 3 separate study parts, an *in vitro* antimicrobial efficacy study, an *in vivo* toxicity and bone-apposition study and an *in vivo* antimicrobial efficacy study.
The *in vitro* evaluation on antimicrobial efficacy indicated that the released chlorhexidine remained to be active as an antimicrobial compound when being incorporated in the coating on the titanium implant surface and after the subsequent release *in vitro*. The difference in *in vitro* efficacy depending on the use of autoclaving or gamma-irradiation might be a result of cross-linking within the polymer composition due to the exposure to gamma-radiation. This might have resulted in structural and chemical changes in the coating and thus in a change of antimicrobial properties.

Many studies only proved a successful *in vitro* efficacy of an antibiotic containing coating concept, often they do not report on the *in vivo* evaluation of these coatings (30-32), while *in vivo* coating efficacy and thus evaluation is crucial if not essential. In our *in vivo* study, the *in vivo* bone apposition, as indicated by the *in vivo* bone remodelling surrounding the titanium implant after 6 weeks of implantation in a sterile environment in a rabbit, was enhanced by the base coating itself (without CHX). The coating loaded with CHX also showed an increased bone apposition, compared with an uncoated titanium implant despite the local release of chlorhexidine. Furthermore, the *in vivo* test for toxicity indicated that there was no risk for systemic toxicity caused by the coating components. The 2 events of animal illness were probably related to stress and not to the loaded chlorhexidine (1 unloaded coating and 1 low dose coated implant).

In vivo evaluations of osteoconductive and drug-eluting coatings have been performed in literature in several comparable models, often, but not solely, in a rabbit. In many of these models the coated or drug eluting biomaterials are implanted in the bacterial contaminated proximal tibia or distal femur (33-39). In these studies the antimicrobial compound released from the carrier is very effective in prevention and treatment of the orthopaedic infection (33-42). This indicates that it is feasible, in the model we used, to prevent infection onset by providing a potent antimicrobial compound to serve as an infection prophylactic. The evaluation on the *in vivo* efficacy of the released chlorhexidine indicated that the *in vivo* release was not sufficient to serve as a prophylactic to prevent the implant infection onset. This might be related to the sclerosing effect prescribed to chlorhexidine, as it might cause comparable tissue damage as sodium morrhuate. As such it would destroy local vasculature and negatively influence the local immune response, which results in an advantage for the bacterial contaminant to cause a local infection, while it should have been bactericidal in the first place. This effect possibly explains the discrepancy between the *in vitro* and *in vivo* antimicrobial efficacy of the CHX loaded coating

However the finding that our proposed base-coating allowed incorporation of an antiseptic compound and was able to release this compound, indicated that this base-coating composition was able to serve as a bone conductive antibacterial carrier for future implant coatings. Furthermore the base coating should technically allow incorporation of other antimicrobial substances like gentamicin or vancomycin.

Future studies should include further research to elucidate the possible applications of this coating composition for the use on medical devices, like metallic or plastic orthopaedic implants. This may for instance result in plastic implants which do not require a metallic carrier to achieve bone

apposition, or in plastic osteoconductive loadbearing prostheses (intervertebral body cages). Also the efficacy of other antibiotic or antiseptic substances to be released from this coating should be explored.

5. Conclusion

To our knowledge this is the first α-β-γ-based polymer coating which facilitates bone formation *in vivo*, making it a promising concept for medical applications.
Furthermore, combining the results of our *in vitro* as well as *in vivo* study indicated that *in vivo* efficacy is the most import study phase in coating evaluation since this phase actually assures coating function and efficacy in a living subject.

Concluding remark
There is a patent application pending on the herein described coating, its composition, its applications and its functionality. Therefore this entire chapter has been modified to avoid jeopardizing the patentability of future applications and modifications of the herein described coating. Patent EP14186637: Medical Coating Composition.

Acknowledgements

This research forms part of the Project P4.01 NANTICO of the research program of the BioMedical Materials institute, co-funded by the Dutch Ministry of Economic Affairs.
Furthermore, the authors would like to thank the employees of the animal facility of the Maastricht University Medical Centre for their assistance during this study. We would also like to thank I. Pooters, M. Visser and C. Urbach from the Nuclear Medicine department of the Maastricht University Medical Centre for their support during this study. And we would like to thank S. Bout and P. Dijkstra for their overall support during this study.

References

1. Surveillance of healthcare-associated infections in europe. http://www.ecdc.europa.eu/en/publications/Publications/120215_SUR_HAI_2007.pdf (Accessed October 2014): European Centre of Disease prevention and Control; 2007.
2. Surveillance report: Annual epidemiological report, reporting on 2009 surveillance data and 2010 epidemic intelligence data. http://ecdc.europa.eu/en/publications/publications/0910_sur_annual_epidemiological_report_on_communicable_diseases_in_europe.pdf (Accessed October 2014): European Centre for Disease prevention and Control; 2011.
3. Healthcare-associated infections - fact sheet. http://www.who.int/gpsc/country_work/gpsc_ccisc_fact_sheet_en.pdf (Accessed October 2014): World Health organisation; 2012.
4. Acklin YP, Widmer AF, Renner RM, Frei R, Gross T. Unexpectedly increased rate of surgical site infections following implant surgery for hip fractures: Problem solution with the bundle approach. Injury. 2011 Feb;42(2):209-16.
5. Dale H, Hallan G, Espehaug B, Havelin LI, Engesaeter LB. Increasing risk of revision due to deep infection after hip arthroplasty. Acta Orthopaedica. 2009 Dec;80(6):639-45.
6. Kurtz SM, Lau E, Ong KL, Carreon L, Watson H, Albert T, Glassman S. Infection risk for primary and revision instrumented lumbar spine fusion in the medicare population. Journal of Neurosurgery: Spine. 2012 Oct;17(4):342-7.
7. Garvin KL, Evans BG, Salvati EA, Brause BD. Palacos gentamicin for the treatment of deep periprosthetic hip infections. Clinical Orthopaedics and Related Research. 1994 Jan(298):97-105.
8. Langlais F. Can we improve the results of revision arthroplasty for infected total hip replacement? Journal of Bone and Joint Surgery (British Volume). 2003 Jul;85(5):637-40.
9. Parvizi J, Saleh KJ, Ragland PS, Pour AE, Mont MA. Efficacy of antibiotic-impregnated cement in total hip replacement. Acta Orthopaedica. 2008 Jun;79(3):335-41.
10. Buchholz HW, Engelbrecht H. [depot effects of various antibiotics mixed with palacos resins]. Chirurg. 1970 Nov;41(11):511-5.
11. Limbago BM, Kallen AJ, Zhu W, Eggers P, McDougal LK, Albrecht VS. Report of the 13th vancomycin-resistant staphylococcus aureus isolate from the united states. Journal of Clinical Microbiology. 2014 Mar;52(3):998-1002.
12. Tang HJ, Chen CC, Cheng KC, Wu KY, Lin YC, Zhang CC, Weng TC, Yu WL, Chiu YH, Toh HS, Chiang SR, Su BA, Ko WC, Chuang YC. In vitro efficacies and resistance profiles of rifampicin-based combination regimens for biofilm-embedded methicillin-resistant staphylococcus aureus. Antimicrobial Agents and Chemotherapy. 2013 Nov;57(11):5717-20.
13. Block SS. Disinfection, sterilisation, and preservation. 4th ed. Philadelphia: Lea & Febiger; 1991. xvi, 1162 p. p.
14. Lim BS, Cheng Y, Lee SP, Ahn SJ. Chlorhexidine release from orthodontic adhesives after topical chlorhexidine treatment. European Journal of Oral Sciences. 2013 Jun;121(3 Pt 1):211-7.
15. Lim KS, Kam PC. Chlorhexidine--pharmacology and clinical applications. Anaesthesia and Intensive Care. 2008 Jul;36(4):502-12.
16. Cookson BD, Bolton MC, Platt JH. Chlorhexidine resistance in methicillin-resistant staphylococcus aureus or just an elevated mic? An in vitro and in vivo assessment. Antimicrobial Agents and Chemotherapy. 1991 Oct;35(10):1997-2002.
17. Russell AD. Chlorhexidine: Antibacterial action and bacterial resistance. Infection. 1986 Sep-Oct;14 (5):212-5.
18. Barnett BD. Chemical vasectomy of domestic dogs in the galapagos islands. Theriogenology. 1985 Mar;23(3):499-509.
19. Pineda MH, Dooley MP. Surgical and chemical vasectomy in the cat. American Journal of Veterinary Research. 1984 Feb;45(2):291-300.
20. Pineda MH, Hepler DI. Chemical vasectomy in dogs. Long-term study. Theriogenology. 1981 Jul;16(1):1 -11.

21. Ishigami S, Hase S, Nakashima H, Yamada H, Dohgomori H, Natsugoe S, Aikou T. Intravenous chlorhexidine gluconate causing acute respiratory distress syndrome. Journal of Toxicology: Clinical Toxicology. 2001;39(1):77-80.
22. Symington JM, Perry R, Kumar A, Schiff R. Efficacy of a 10% chlorhexidine coating to prevent caries in at-risk community-dwelling adults. Acta Odontologica Scandinavica. 2014 Jan 27.
23. Hiraishi N, Yiu CK, King NM, Tay FR. Chlorhexidine release and antibacterial properties of chlorhexidine -incorporated polymethyl methacrylate-based resin cement. J Biomed Mater Res B Appl Biomater. 2010 Jul;94(1):134-40.
24. Arciola CR, Campoccia D, Speziale P, Montanaro L, Costerton JW. Biofilm formation in staphylococcus implant infections. A review of molecular mechanisms and implications for biofilm-resistant materials. Biomaterials. 2012 Sep;33(26):5967-82.
25. Gristina AG. Biomaterial-centered infection: Microbial adhesion versus tissue integration. Science. 1987 Sep 25;237(4822):1588-95.
26. Odekerken JC, Arts JJ, Surtel DA, Walenkamp GH, Welting TJ. A rabbit osteomyelitis model for the longitudinal assessment of early post-operative implant infections. Journal of Orthopaedic Surgery and Research. 2013;8(1):38.
27. Odekerken JC, Brans BT, Welting TJ, Walenkamp GH. 18f-fdg micropet imaging differentiates between septic and aseptic wound healing after orthopedic implant placement a longitudinal study of an implant osteomyelitis in the rabbit tibia. Acta Orthopaedica. 2014;85(3):9.
28. Hein J, Hartmann K. Labordiagnostische referenzbereiche bei kaninchen. Tierarztliche Praxis. 2003;31 (K):8.
29. Hewitt CD, Innes DJ, Savory J, Wills MR. Normal biochemical and hematological values in new zealand white rabbits. Clinical Chemistry. 1989 Aug;35(8):1777-9.
30. Rauschmann MA, Wichelhaus TA, Stirnal V, Dingeldein E, Zichner L, Schnettler R, Alt V. Nanocrystalline hydroxyapatite and calcium sulphate as biodegradable composite carrier material for local delivery of antibiotics in bone infections. Biomaterials. 2005 May;26(15):2677-84.
31. Neut D, Kluin OS, Crielaard BJ, van der Mei HC, Busscher HJ, Grijpma DW. A biodegradable antibiotic delivery system based on poly-(trimethylene carbonate) for the treatment of osteomyelitis. Acta Orthopaedica. 2009 Oct;80(5):514-9.
32. Castelli C, Marone P, Monzillo V, Segú K. Antistaphylococcal activity of antibiotic impregnated bone cement. The Knee. 1995;2(2):219-22.
33. Koort JK, Makinen TJ, Suokas E, Veiranto M, Jalava J, Knuuti J, Tormala P, Aro HT. Efficacy of ciprofloxacin-releasing bioabsorbable osteoconductive bone defect filler for treatment of experimental osteomyelitis due to staphylococcus aureus. Antimicrobial Agents and Chemotherapy. 2005 Apr;49 (4):1502-8.
34. Moojen DJ, Vogely HC, Fleer A, Nikkels PG, Higham PA, Verbout AJ, Castelein RM, Dhert WJ. Prophylaxis of infection and effects on osseointegration using a tobramycin-periapatite coating on titanium implants--an experimental study in the rabbit. Journal of Orthopaedic Research. 2009 Jun;27 (6):710-6.
35. Nijhof MW, Stallmann HP, Vogely HC, Fleer A, Schouls LM, Dhert WJ, Verbout AJ. Prevention of infection with tobramycin-containing bone cement or systemic cefazolin in an animal model. Journal of Biomedical Materials Research. 2000 Dec 15;52(4):709-15.
36. Alt V, Bitschnau A, Bohner F, Heerich KE, Magesin E, Sewing A, Pavlidis T, Szalay G, Heiss C, Thormann U, Hartmann S, Pabst W, Wenisch S, Schnettler R. Effects of gentamicin and gentamicin-rgd coatings on bone ingrowth and biocompatibility of cementless joint prostheses: An experimental study in rabbits. Acta Biomater. 2011 Mar;7(3):1274-80.
37. Darouiche RO, Mansouri MD, Zakarevicz D, Alsharif A, Landon GC. In vivo efficacy of antimicrobial-coated devices. Journal of Bone and Joint Surgery (American Volume). 2007 Apr;89(4):792-7.
38. Moskowitz JS, Blaisse MR, Samuel RE, Hsu HP, Harris MB, Martin SD, Lee JC, Spector M, Hammond PT. The effectiveness of the controlled release of gentamicin from polyelectrolyte multilayers in the treatment of staphylococcus aureus infection in a rabbit bone model. Biomaterials. 2010 Aug;31 (23):6019-30.
39. Alt V, Bitschnau A, Osterling J, Sewing A, Meyer C, Kraus R, Meissner SA, Wenisch S, Domann E, Schnettler R. The effects of combined gentamicin-hydroxyapatite coating for cementless joint

prostheses on the reduction of infection rates in a rabbit infection prophylaxis model. Biomaterials. 2006 Sep;27(26):4627-34.

40. Walenkamp GH. Gentamicin pmma beads and other local antibiotic carriers in two-stage revision of total knee infection: A review. Journal of Chemotherapy. 2001 Nov;13 Spec No 1(1):66-72.
41. Walenkamp GH, Kleijn LL, de Leeuw M. Osteomyelitis treated with gentamicin-pmma beads: 100 patients followed for 1-12 years. Acta Orthopaedica Scandinavica. 1998 Oct;69(5):518-22.
42. Walenkamp GH, van Rens TJ. [chains of gentamicin-pmma beads: A new method for the local treatment of osteomyelitis]. Nederlands Tijdschrift voor Geneeskunde. 1982 Nov 20;126(47):2136-42.

General discussion and conclusion

Nosocomial infections, also called hospital acquired infections (HAI) are a major healthcare issue with an estimated incidence of hundreds of millions of patients per year worldwide of which approximately 4.1 million patients per year in Europe (1, 2). The surveillance of HAI is often subdivided in more specific surveillances like, infections in intensive care units (e.g. infections related to pulmonary ventilators) or surgical site infections (SSI) (e.g. infections related to abdominal and orthopaedic surgery). Orthopaedic infections are often a subject in SSI surveillance programs since they are one of the most severe complications in orthopaedic and trauma surgery.
Besides the considerable financial impact on the healthcare system, an orthopaedic infection has a tremendous impact on the patient. These infections often require multiple major revision surgeries in combination with aggressive and long-term antibiotic treatment regimens. If an antibiotic treatment is not successful (due to the severity of the infection or the presence antibiotic-resistant bacteria), such infections can lead to severe disabilities, loss of limb, bacterial sepsis and in some cases even death. Further advances in surgical procedure, antimicrobial prophylaxis and treatment are necessary to reduce the infection incidence and to improve the outcome of infection treatment.

In this thesis experimental models and diagnostic tools are described to evaluate (novel) antimicrobial approaches:

- An ELISA-based assay to determine gentamicin and vancomycin concentrations in protein-rich samples, to allow prospective longitudinal evaluation of novel antibiotic release systems *in vitro* and *in vivo* (Chapter 3).
- An acute implant infection model in NZW rabbits, for the evaluation of prophylactic coatings for orthopaedic implant infections (Chapter 4).
- The use of ^{18}F-FDG PET as a specific imaging tool for the detection of orthopaedic infections and to follow the infection progression or treatment outcome (Chapter 5).
- An acute osteomyelitis model in NZW rabbits, for e.g. the evaluation of osteomyelitis development in the absence of an orthopaedic implant or for the assessment of antimicrobial bone substitute materials (Chapter 6).
- The evaluation of a novel polymer-based osteoconductive drug-releasing coating for application on metallic implants (Chapter 7).

1. Experimental orthopaedic infection models

Whereas osteomyelitis itself is probably as old as the existence of vertebrates (since it was determined in dinosaurs (e.g. *Mosasaurus hoffmanni*, Collection Maastricht Natural History Museum) and Neanderthals (3-5)), the first dedicated experimental models to evaluate osteomyelitis development was described by Becker in 1883 and by Rodet in 1884 (6-8).

Although the first models described the development of osteomyelitis by contamination with *Staphylococcus aureus*, many different bacterial species can cause an orthopaedic (implant) infection or osteomyelitis (e.g. coagulase-negative *Staphylococci*, *Streptococci*, *Enterococci* and gram-negative bacilli) (9, 10). Still 50 - 60% of the current orthopaedic infections are initiated by *Staphylococci*, either being coagulase-positive (often found in early post-operative infections) or being coagulase-negative (often found in late or low-grade infections) and sensitive or resistant to specific antibiotics (9-11). Of the available *Staphylococci* strains, methicillin sensitive *S. aureus* is the most commonly found bacterial strain in orthopaedic infections (9-11). Based on the clinical relevance and its frequent use in experimental models, a methicillin sensitive strain of *S. aureus* was chosen for the herein described experimental models.

Since many inflammatory reactions mimic infection, the current golden standard for infection determination in experimental studies is bacterial culture of the infected tissue (Chapter 1, Table 3). Still bacterial culture at the end of a study only indicates the presence or absence of living bacteria at that specific endpoint; but this does not necessarily mean that there has not been an infectious event during the study when a culture turns out to be negative at the end of the study. To achieve a positive culture at the end of a study, the inoculation dose should be high enough to establish an osteomyelitis, but low enough to not result in the loss of experimental animals. In general the bacterial load required to establish an (implant-related) osteomyelitis in an experimental model has been described to be between 10^3 – 10^9 colony forming units (CFU), depending of the virulence of the bacteria (12-18). Still the clinical relevance of these numbers is not likely to be realistic, since it is not to be expected that such large amounts of CFU will inoculate the surgical site during implantation, while this might be the case in trauma surgery. Byrne *et al.*, Davis *et al.* and Jonsson *et al.* focussed on the per-operative wound contamination by analysing the bacterial presence in the wound by taking swabs (19-22). These studies indicated that per-operative contamination is nearly inevitable due to the surgical procedure and that this contamination may cause implant infection, unfortunately no quantitative culture was performed

to determine the amount of CFU present in the wound (19-21). It can be expected that the higher inoculation dose in the experimental models results in an earlier onset of osteomyelitis, while low dose inoculations may result in natural clearance by the host immune system (12, 23-25). This was confirmed by a dose-finding study in rabbits in which the low dose bacterial contamination of the surgical bed lead to bacterial clearance within a period of 6 weeks after surgery, while a high dose bacterial contamination did not result in bacterial clearance but in osteomyelitis development (Chapter 4). In turn this might explain the rationale behind the use of a sclerosing agent (like sodium morrhuate) in experimental studies to support the development of an orthopaedic infection at lower bacterial dosages (14, 26-31). A sclerosing agent disrupts local vascularisation and the local immune response providing an advantage for a possible contaminant to overcome the host immune system and cause an infection (14, 26-29). The additional use of a sclerosing agent is a non-natural situation and may therefore be not preferable in certain experimental approaches. When translated to the clinical situation the establishment of an orthopaedic infection is depending on multiple factors like patient health status and patient history on infections, where relatively low bacterial contaminations can result in severe infections (32, 33). Another aspect is the time needed to develop an infection and the infection incidence. Both aspects can be positively influenced (decrease in time and increase in incidence) in pre-clinical experiments by the use of a sclerosing agent (30, 31).

Review of the literature (Chapter 1, Table 3) showed that most experimental studies on orthopaedic infections focussed only on mere endpoint measurements (where multiple experimental groups were sacrificed on different time points). However, an experimental group should ideally be followed at sequential time points during follow-up. With such a sequential follow-up of an experimental group one does not only measure experimental outcome but also disease development and progression. Besides, a sequential follow-up in every animal improves the statistical power of a study and it reduces the overall required number of animals (34). For the experimental studies described in this thesis (Chapter 4, 5, 6 and 7) such a sequential experimental follow-up was chosen to monitor disease progression and to assess disease-related changes in clinical and haematological parameters combined with bone morphological changes. The herein described experimental setup describes an (implant-related) osteomyelitis in a tibial intramedullary contamination model in NZW rabbits.

There is a general lack of a sequential follow-up in combination with the assessments of single parameters in the studies on orthopaedic infection development in previously described

experimental studies (Chapter 1, Table 3). To the author's opinion a thorough evaluation on biological infection related processes and antibiotic treatment efficacy could only be determined by a multi-parameter sequential follow-up. Only an extensive combination of the procedures mentioned below can provide a detailed overview on infection development or on antimicrobial coating efficacy.

For the assessment of experimental orthopaedic infection, infection prophylaxis and treatment, we preferred a combination of several assessments:

- Weekly measurement of standard clinical parameters (body temperature and body weight).
- Weekly determination of haematological parameters (erythrocyte sedimentation rate (ESR), leukocyte differentiation and C-reactive protein levels (CRP)).
- Weekly assessment of bone morphological changes by X-ray radiographs.
- Bi-weekly injection of calcium binding fluorophores (to assess *in vivo* bone apposition and bone remodelling during follow-up).
- ^{18}F-FDG microPET at 1, 3 and 6 weeks after contamination (^{18}F-FDG is a proposed infection tracer, where increased local tracer uptake indicates the presence of infection).
- *Post-mortem* microCT (high-resolution assessment of the infected bone morphology (density and micro-architecture).
- *Post-mortem* bacterial culture (to determine the infectious state of the animals).
- *Post-mortem* histological analysis (to evaluate bone morphology, bone remodelling and bacterial presence).

Such an experimental approach allows evaluation of the progression of an orthopaedic infection in every animal on all of the above-mentioned parameters. In Chapter 7 the above mentioned infection parameters were used in our implant infection model to evaluate the potential of a novel proposed osteoconductive and prophylactic implant coating with the ability to release an antimicrobial compound.

2. Diagnostics and material testing

2.1 Orthopaedic infection and imaging

Techniques like standard radiographs (X-rays), CT, MRI and several types of bone scintigraphy (^{67}Ga-citrate, ^{99m}Tc or ^{111}In-labelled leukocytes or leukocyte antibodies) have been applied to specifically assess the infection of the skeletal tissue (35, 36). Positron emission tomography (PET) is an emerging imaging modality in clinical diagnostics, especially its use within orthopaedic infections. PET scanning (available since the 1970's, (37, 38)) has proven to be a successful imaging modality to assess brain activity (39-42), the cardiovascular system (42, 43) or tumour tissue (42, 44, 45), with indications for successful application within orthopaedics (36, 42, 46-53). The last 15 years, studies have focussed on the potential of PET scanning for the assessment of bone remodelling (^{18}F-NaF) and orthopaedic infections (^{18}F-FDG) (36, 42, 46-53).

The labelling of a glucose derivative (deoxyglucose) with a radionuclide originating from Fluor (^{18}F) allowed the production of a PET tracer (^{18}F-FDG) mimicking metabolic active glucose (42, 46, 54). A locally increased metabolic turnover of glucose, as present in infections, results in a locally increased tracer uptake, with a locally increased positron emission by the tracer eventually detected by a PET scanner. From these data the standardized uptake value (55) was calculated. In case of an orthopaedic implant infection a local increased metabolic turnover is expected (and thus an increase in SUV) due to the presence of bacteria and leukocytes in the tissue surrounding the implant (46, 50).

Clinical and experimental studies currently prefer ^{18}F-FDG due to its universal character (30, 35, 36, 51, 56-58). Several experimental studies indicate the potential of ^{18}F-FDG as a tracer for diagnosing orthopaedic infections (30, 51, 56-60). The tracer uptake can be quantified by the calculation of the standardized uptake value (SUV), which represents the relation between the total amount of injected tracer, the local tracer uptake and the weight of the subject. This allows a qualitative and quantitative comparison of the tracer uptake between experimental groups and between specific time points. The in this thesis described studies indicate the potential of ^{18}F-FDG not only as a reliable diagnostic tool for early diagnosis of implant infection, but also to monitor infection progression or healing over time. Chapter 5 describes the potential of ^{18}F-FDG as an infection tracer in an orthopaedic implant infection context with a sequential follow-up of 6 weeks. This study showed that the infection onset takes up to three weeks after the initial surgery before

^{18}F-FDG allows differentiation from an uninfected implant. This is mainly caused by the sterile post-surgical inflammation, which also results in a slightly elevated PET-tracer uptake, hampering the early detection of infection. This effect is also seen with radionuclide labelled leukocytes, due to the high uptake caused by sterile inflammation and the surgical procedure itself (35). Chapter 6 indicated that the sensitivity of ^{18}F-FDG PET is even higher in the absence of the orthopaedic implant. This allows detection of an early post-operative infection/osteomyelitic lesion within 1 week after the initial surgery, when compared to sterile inflammation and wound healing, confirming the findings of Jones-Jackson *et al.* (56). These findings also suggest that the presence of an orthopaedic implant negatively influences early orthopaedic infection diagnosis, possibly as a result of implant-induced scatter of photons during detection. This effect should be considered when ^{18}F-FDG is applied in combination with metallic implants in a (pre-) clinical study context.

However ^{18}F-FDG is considered by some authors to be not specific enough for an infection-specific tracer. Instead, the use of radionuclide labelled leukocytes (or anti-leukocyte antibodies) was proposed to be a more suitable way to detect implant infection, since this approach directly detects the locally present leukocytes in infected tissue (35, 61-63), however this method has some important disadvantages. Because of its patient's specificity it requires the isolation and labelling of the patient's leukocytes before the initial scanning, besides, the patient is also exposed to a higher level of radiation (35, 64). Also the use of ^{67}Ga-citrate exposed the patient to a high level of radiation and is not specific enough for infection (35). All these methods are currently still in use within the clinic, but because of the universal character of ^{18}F-FDG and the disadvantages of the patient-specific leukocyte scan, leukocyte scintigraphy, bone scintigraphy and ^{67}Ga-citrate, the use of the latter methods decreases for the detection of orthopaedic infections (35, 61, 62, 64).

The findings described in this thesis indicate that the sensitivity of ^{18}F-FDG depends on the local metabolic turnover (and not as much the presence of leucocytes, as in leukocyte scintigraphy) and the presence of a metallic implant due to the resulting scattering (an effect also evident in other nuclear imaging modalities) (35). The sequential follow-up of multiple time point data supported the single time point data of independent research groups indicating the potential of ^{18}F-FDG as an orthopaedic infection PET tracer (30, 56). The major difference is that the in this thesis described studies define a timeframe in which a differentiation between infection and aseptic wound healing can be made, while previously described studies only describe the infection status at a specific time point in follow-up. Furthermore the herein described studies, for the first time, allow assessment of orthopaedic (implant) infection development during a sequential follow-up in each

animal over time, where previously published studies only describe single time points in single animals.

Although each nuclear imaging modality (e.g. ^{18}F-FDG, leucocyte scintigraphy, bone scintigraphy, ^{67}Ga-citrate) roughly provides comparable information, often combined with an additional assessment by X-ray/CT, MRI or haematological screening to allow a clinician to come to the initial diagnosis of an orthopaedic infection, each clinician (or hospital) has its own diagnostic preferences for orthopaedic infection diagnosis (35, 36). All together ^{18}F-FDG has been shown to be a suitable infection tracer with a high sensitivity and specificity in our experimental model. The herein presented results indicate that ^{18}F-FDG microPET can be an effective tool to assess antibiotic loaded carriers for therapeutic and prophylactic purposes in our experimental model. Still our findings should be confirmed in a comparable experimental setup with different bacterial strains to assess the full diagnostic potential of ^{18}F-FDG microPET. Furthermore our herein described studies (supported by pre-clinical and clinical findings in literature) suggest that ^{18}F-FDG PET might be a useful tool to assess orthopaedic infections in the clinic, this however should be evaluated in first, pre-clinical studies (osteomyelitis caused by other bacterial contaminants than *S. aureus*) then followed by future patient series.

2.2 Quantification of released antibiotics

In the development and evaluation of antimicrobial release systems the determination of the release by a coating or biomaterial is important but may be very difficult. Antibiotics being released by coatings or biomaterials have been determined in the past by the semi-quantitative evaluation of bacterial growth inhibition zones on agar plates in correspondence with known stock solutions (65, 66). The use of fluorescence or spectrophotometric based detection methods resulted in improved detection limits, which were further improved by the introduction of high performance liquid chromatography (HPLC)-based protocols (67-71). However both methods are negatively influenced by samples with high protein content. Enzyme linked immunosorbent assay (ELISA)-based methods have been established to detect antibiotics like gentamicin or vancomycin in dairy products like milk (72) and in serum or plasma (73-76). However these methods were not applied to the human situation nor for the assessment of releasing biomaterials or coatings, neither did they allow direct modification to facilitate the detection of other antibiotics. It is remarkable that

ELISA-based detection of antibiotics has never been implemented in the field of orthopaedic research to validate currently clinically used antibiotic release systems (personal communications).
The ELISA procedure is depending on the availability of a microtiter plate with the respective antibiotic coated to the microtiter plate wells. Unfortunately, antibiotic molecules cannot be coated to a microtiter plate directly because of their small size; it therefore requires the antibiotic to be cross-linked with a larger protein-like structure. The group of Fujiwara described cross-linking with N-(γ-maleimidobutyryloxy)succinimide (GMBS) which functions as a connecting short spacer-arm between protein and antibiotic (76). The group of Chianelli described the use of synthetic molecularly imprinted polymer nanoparticles (nanoMIPS) to function as a protein-antibiotic hapten substitute (75). While the group of Haasnoot described a more preferable method by cross-linking BSA and the antibiotic of choice with N-(3-Dimethylaminopropyl)-N'-ethylcarbodiimide hydrochloride (EDC). This method is depending on the presence of carboxyl groups or amine groups in the molecular structure of the antibiotic to allow cross-linking with a protein and thus formation of a coatable hapten (72). EDC does not introduce a spacer-arm between protein and antibiotic and therefore excludes the risk of an antibody response towards such spacer-arm structures. Furthermore the availability of a specific antibody directed against the respective antibiotic is essential, if not it can be developed in-house by immunisation (with e.g. a KLH-antibiotic conjugate) of a small animal (mouse or rabbit). Both described ELISA's (Chapter 3) are specific for the antibiotic of choice with limited to no interference due to other compounds in serum, plasma or wound exudate, like proteins. Furthermore the protocol described in chapter 3 of this thesis can be modified (with relatively minor effort) to establish ELISA's to detect other antibiotic compounds such as tobramycin and kanamycin in a comparable experimental setting, depending on the availability of a specific antibody directed against the corresponding antibiotic compound.
These ELISA-based antibiotic detection assays can be used to *in vitro* and *in vivo* validate novel antibiotic release systems and compare them with the currently clinically applied antibiotic release modalities like antibiotic loaded bone cement, acrylic or synthetic beads and PMMA spacers.

3. Implant coatings

3.1 Coatings and bone

Frequently used terms for orthopaedic coating properties are osteocompatibility, osteoconduction and osteoinduction. In general osteocompatibility describes the tolerance of osteogenic cells and skeletal tissue towards the proposed osteocompatible material and that the material allows direct bone bonding to its surface without the formation of soft tissue at the implant interface. Osteoconduction and osteoinduction are material properties that describe the interaction of the proposed material surface or coating with the osteogenic cells and tissue. Osteoconduction is when a surface modification not actively initiates bone apposition on the surface, but does allow cell attachment, proliferation and bone matrix deposition on its surface (77-79). Osteoinduction is when a surface modification actively initiates bone formation around or on the implant surface without the presence of osteogenic factors (77-79).

Osteoconductive surface modifications have been developed since the late 1980's, of which the application of hydroxyapatite on an implant surface, by Geesink and colleagues, is the most well-known (80-85). The thermal application of calcium phosphates to metallic implants creates a stable rough calcium phosphate layer on the implant surface. The composition of this bone-like layer allows the adherence of osteoblasts which eventually results in bone matrix formation and mineralisation, leading to implant fixation, providing an advantage of the host's osteogenic cells in "the race for the surface" (82, 83, 86). The clinical follow-up of these implant coatings is currently over 15 years with minimal loss of follow-up due to aseptic loosening or osteolysis, indicating an excellent long time survival (85). Still there have been reports that the rough surface forms a risk for biofilm formation and subsequent implant infection (18, 87). Loading of hydroxyapatite-based coatings with antibiotics is proposed as a possible solution to this increased infection risk (16). Also porous titanium implants coated with hydroxyapatite have been shown to promote osteoconductivity and bone tissue ingrowth, furthermore the porous structure of the titanium also allows the loading of antibiotics, like gentamicin and tobramycin, to serve as an effective prophylaxis for implant infection (16, 88, 89). Unfortunately these products are currently not yet on the market, because according to the Food and Drug Administration (FDA) regulations these implants are no longer a medical device, but due to their antibiotic releasing character they are considered as a drug. Because of this the antibiotic releasing device has to be subjected to a

separate set of clinical trials to validate its safety and efficacy, before further commercialisation (90).

Osteoinductive surface modifications are currently only available in experimental stages; this mainly concerns coating procedures that locally release growth factors. One of the most widely used growth factors in such applications is bone morphogenetic protein 2 (BMP-2), which initiates *in vitro* mesenchymal stem cell differentiation towards bone matrix-producing osteoblasts (91-94). However clinical application of BMP-2 might contribute to the development of cancerous tissue in the application zone since BMP-2 is also associated with cancer cell proliferation, differentiation and apoptosis (95). Another approach to promote bone tissue development is the use of RGD-based coatings (RGD is a tripeptide composed of arginine, glycine and aspartate), which has been shown to generate significantly increased bone-formation when compared to uncoated surfaces. Furthermore these coatings are proposed to further enhance bone formation on the coated surface when combined with hydroxyapatite (88, 89, 96). Currently RGD coatings are only explored in *in vitro* and pre-clinical studies.

Chapter 7 describes the evaluation of a novel coating concept that can serve as a drug delivery system. It was shown that the base coating provides an osteoconductive surface *in vivo.* This conclusion is based on the large amount of bone apposition on the coated implant surface within 4 weeks after implantation in a rabbit tibia. The described coating seems to be the first non-degradable polymer-based drug carrier coating to show *in vivo* osteoconductive properties even after the release of the sclerosing antiseptic chlorhexidine (patent EP14186637, Medical Coating Composition). This indicates the high potential of this coating based on its osteconductive properties and the optional possibility of the coating to serve as a drug carrier, to contribute to infection prophylaxis when implanting uncemented prostheses. Furthermore due to the application procedure of the coating, it may also be applied to polymer substrates, providing an osteoconductive surface on polymer-based implants (e.g. vertebral body spacers, prosthesis parts). This would generate a new range of prostheses and prosthesis parts because with such a coating e.g. plastic prosthesis parts do not require a metallic hydroxyapatite coated carrier anymore to achieve fixation by bone apposition.

3.2 Antimicrobial efficacy

The local use of antibiotic carriers in orthopaedic surgery to treat and prevent orthopaedic infections is currently considered common practice, originating from the initial ideas of Buchholz (loading of bone cement with antibiotics, for implant fixation) and Klemm (the use of gentamicin loaded PMMA-beads to treat infections locally) in the 1970's (97-101). Antibiotic loaded bone cement is used as a prophylactic measure for (re-)infection of a cemented orthopaedic implant. Unfortunately this prophylactic measure is currently not available for uncemented implants. Considering this niche, an antimicrobial compound releasing coating could serve as a prophylactic measure on uncemented prosthesis. Such an antimicrobial coating is required to support bone apposition on the coating surface in combination with the release of an antimicrobial substance like an antibiotic or antiseptic. Up till now a few experimental studies have been published, reporting on the effective *in vitro* (65, 67, 68) and *in vivo* (16, 88, 89, 102, 103) efficacy of antibiotic (gentamicin, vancomycin, tobramycin and rifampicin) releasing coatings.

Chapter 7 describes the evaluation of a chlorhexidine (CHX) eluting and osteoconductive coating concept. The *in vitro* data showed that the released CHX caused effective bacterial growth inhibition, however *in vivo* evaluation of this drug eluting coating concept may indicate that the current dose of CHX being released from the coating may not be sufficient to serve as an effective prophylactic tool for implant infection in an animal implant infection model. This illustrates very well that *in vitro* evaluation is not sufficient enough to describe the actual potential of an antimicrobial coating and that *in vivo* evaluation is crucial to evaluate the true antimicrobial efficacy.

Possibly other antiseptics might be more effective when applied in a coating, depending on their mode of operation. The supposed efficacy of CHX as an antiseptic is based on its sclerosing effect on cells (104, 105). CHX might therefore even contribute to the establishment of an implant infection in our animal model due to its function as a sclerosing agent, by the local disruption of vascularisation and immune system, an effect also seen with the use of sodium morrhuate (frequently used in experimental models as a sclerosing agent (14, 26-31)). The use of other antibacterial substances for the release from our herein described coating should therefore be explored *in vitro* as well as *in vivo*.

When we established our herein described animal model we performed a bacterial dose finding study to check which bacterial dose is required for an intramedullary contamination to develop an

osteomyelitis in the tibia of a rabbit (Chapter 4). Such a dose finding study is also required for the assessment of antibiotic coatings, by evaluating the antimicrobial efficacy of coatings with several dosages, releasing different amounts of antibiotics/antiseptics. This approach would result in a thorough *in vivo* screening of the coating efficacy over a wide antibiotic/antiseptic concentration range and when a potentially effective dose is found, this dose should be evaluated in a large scale study to validate the antimicrobial coating efficacy. Based on previous reports and our own findings presented in this thesis, the most important follow-up parameters that should be assessed weekly are: body weight, CRP-levels, leucocyte differentiation and X-ray radiographs, supplemented with bi-weekly injections with calcium binding fluorophores and assessment with ^{18}F-FDG microPET at 1, 3 and 6 weeks after surgery. *Post-mortem* assessment should include quantitative bacterial culture and histological evaluation of the per-implant tissue. Combined these parameters will allow thorough evaluation of *in vivo* coating efficacy on both bone apposition and prophylactic capacity.

4. Conclusion

During the last 30 years significant improvements have been made in the field of orthopaedic infection treatment (antibiotic loaded bone cement, beads spacers and bone substitutes) and prevention (improved operating theatres, surgical gowns and experimental antibiotic-releasing (polymer) coatings) (16, 19-21, 88, 89, 97-99, 101, 106, 107). However the prevalence of infected implants is increasing since an increasing number of implants/prostheses are being placed (108-110). Although animal models are available to evaluate novel treatments and implants, an antimicrobial coating to successfully treat and prevent orthopaedic (implant) infections still remains to be found. The solution for orthopaedic infection prevention and treatment will be a multifactorial approach, with the focus on:

- Prevention of per-operative contamination (e.g. specified operating theatre, specific surgical gowns and hospital code of conduct).
- The use of systemic antibiotics before surgery (oral or i.v.), with a possible risk of the induction of antibiotic resistant bacterial strains.
- The use of a local prophylactic for the first days after surgery (by implant coating or cement).
- Prevention of post-operative bacteraemia.

- In case of infection treatment, remove the implant and the surrounding diseased bone and soft tissue by rigorous debridement and irrigation of the wound.
- In case of uncemented prostheses, osteoconductive (potentially antibiotic releasing) surface treatments on implants (hydroxyapatite or polymer-based coatings).
- Systemic antibiotic therapy after debridement and revision surgery.
- Follow-up (annually with X-ray and/or ^{18}F-FDG PET/CT).

Overall the above suggestions are already known and probably the most positive effect will be dependent on novel implant surface treatments (osteoconductive/osteoinductive coatings able to function as a drug-carrier) and not so much on surgical procedure or the used implant materials itself since these have already been optimised during the last 30 years.

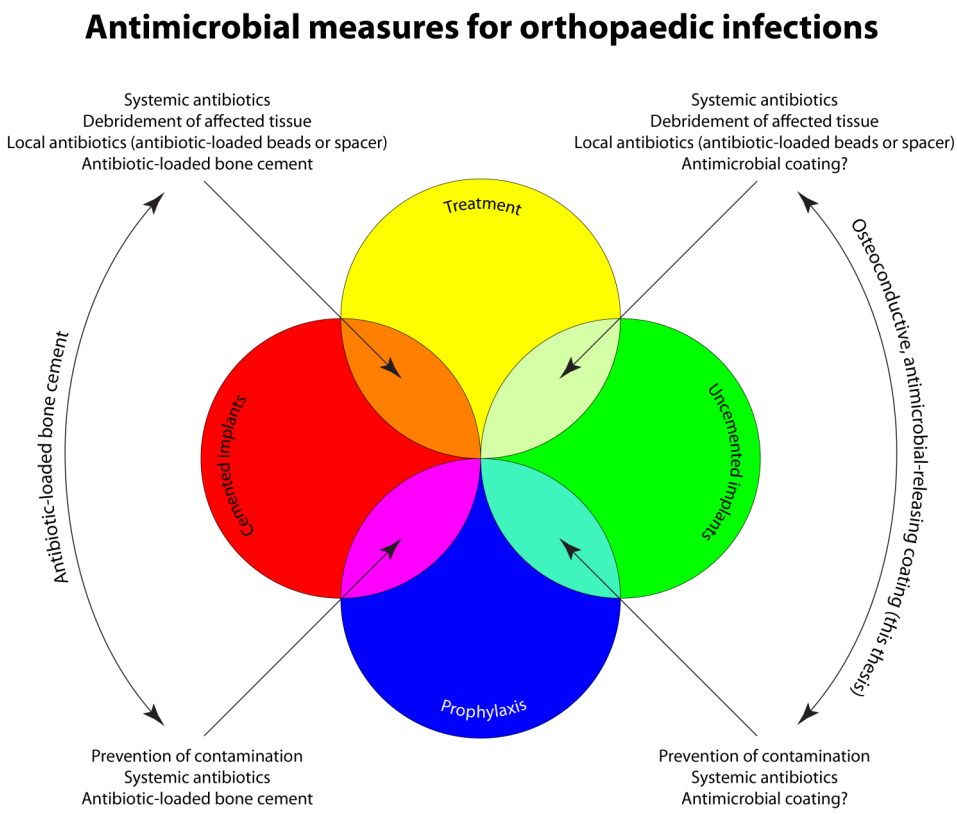

Figure 1: Graphical overview of the relation between treatment and prophylaxis of orthopaedic infections with respect to (un)cemented implants.

Besides the establishment of novel clinical diagnostic modalities, including molecular laboratory tests to evaluate drug release from coatings or biomaterials, novel implant coating concepts have been developed which allow drug release from the coating surface. An osteoconductive coating was developed which has the potential to elute antimicrobial compounds, however further research remains to be conducted to elucidate the remaining issues concerning the appropriate concentration of the antimicrobial for the release from the coating. This coating could potentially provide a solution to the current lack of an infection prophylaxis for uncemented implants (Figure 1).

Suggestions for future research are:

- Evaluate the potential of ^{18}F-FDG PET for the diagnosis of orthopaedic infection in combination with other bacterial contaminants, especially in low grade infections.
- Expand the range of antibiotics to be detected by the herein described ELISA protocol.
- Incorporate an antibiotic (e.g. gentamicin or vancomycin) in the herein described novel drug-releasing coating and evaluate the in vitro release profile in comparison to current delivery systems e.g. antibiotic loaded acrylic beads or bone cement. This would allow comparison of the prophylactic capacity of an implant coating in contrast to e.g. bone cement.
- Evaluate the in vivo prophylactic efficacy of the above-mentioned antibiotic loaded coating in comparison to current prophylactic release systems e.g. antibiotic loaded bone cement, to address the current lack of an infection prophylactic in uncemented prosthesis.
- Evaluate the clinical diagnostic value of ^{18}F-FDG PET in patients under suspicion of orthopaedic infection in addition to the current standard diagnostic protocol to evaluate the potential added value of ^{18}F-FDG PET in clinical diagnostics for orthopaedic infections.
- Initiate a pilot study in large animals and possibly patients to evaluate the osteoconductive properties of the herein described novel osteoconductive polymer-based coating.

References

1. Surveillance of healthcare-associated infections in europe. http://www.ecdc.europa.eu/en/publications/Publications/120215_SUR_HAI_2007.pdf (Accessed October 2014): European Centre of Disease prevention and Control; 2007.
2. Surveillance report: Annual epidemiological report, reporting on 2009 surveillance data and 2010 epidemic intelligence data. http://ecdc.europa.eu/en/publications/publications/0910_sur_annual_epidemiological_report_on_communicable_diseases_in_europe.pdf (Accessed October 2014): European Centre for Disease prevention and Control; 2011.
3. Rega E, Holmes RB, Tirabaso A. Habitual locomotor behaviour inferred from manual pathology in two late cretaceous chasmosaurine ceratopsid dinosaurs, chamsosaurus irvinensis (cmn41357) and chasmosaurus belli (rom 843). In: Ryan MJ, editor. New perspectives on horned dinosaurs: The royal tyrrell museum ceratopsian symposium. Life of the past: Indiana University Press; 2010.
4. Burri C. Posttraumatische osteitis. Bern: Hans Huber; 1979.
5. Schulp AS, Walenkamp GHIM, Hofman PAM, Stuip Y, Rothschild BM. Chronic bone infection in the jaw of mosasaurus hoffmanni (squamata). Oryctos. 2006;6:41-52.
6. Becker. Deutsche Medizinische Wochenschrift. 1883;9(46).
7. Vanarsdale WW. Ii. On the present state of knowledge in bacterial science in its surgical relations (continued): Osteomyelitis. Annals of Surgery. 1886 Mar;3(3):221-6.
8. Rodet A. Etude expérimentale sur l'osteomyelite infectieuse. Comptes rendus hebdomadaires des Séances de l'Académie des Sciences. 1884;99:569-71.
9. Trampuz A, Zimmerli W. Antimicrobial agents in orthopaedic surgery: Prophylaxis and treatment. Drugs. 2006;66(8):1089-105.
10. Montanaro L, Speziale P, Campoccia D, Ravaioli S, Cangini I, Pietrocola G, Giannini S, Arciola CR. Scenery of staphylococcus implant infections in orthopedics. Future Microbiology. 2011 Nov;6(11):1329-49.
11. Singh JA, Sperling JW, Schleck C, Harmsen WS, Cofield RH. Periprosthetic infections after total shoulder arthroplasty: A 33-year perspective. Journal of Shoulder and Elbow Surgery. 2012 Nov;21(11):1534-41.
12. Andriole VT, Nagel DA, Southwick WO. Chronic staphylococcal osteomyelitis: An experimental model. Yale Journal of Biology and Medicine. 1974 Mar;47(1):33-9.
13. Bowers WH, Wilson FC, Greene WB. Antibiotic prophylaxis in experimental bone infections. Journal of Bone and Joint Surgery (American Volume). 1973 Jun;55(4):795-807.
14. Norden CW. Experimental osteomyelitis. I. A description of the model. Journal of Infectious Diseases. 1970 Nov;122(5):410-8.
15. Reizner W, Hunter JG, O'Malley NT, Southgate RD, Schwarz EM, Kates SL. A systematic review of animal models for staphylococcus aureus osteomyelitis. Eur Cell Mater. 2014;27:196-212.
16. Moojen DJ, Vogely HC, Fleer A, Nikkels PG, Higham PA, Verbout AJ, Castelein RM, Dhert WJ. Prophylaxis of infection and effects on osseointegration using a tobramycin-periapatite coating on titanium implants--an experimental study in the rabbit. Journal of Orthopaedic Research. 2009 Jun;27(6):710-6.
17. Poultsides LA, Papatheodorou LK, Karachalios TS, Khaldi L, Maniatis A, Petinaki E, Malizos KN. Novel model for studying hematogenous infection in an experimental setting of implant-related infection by a community-acquired methicillin-resistant s. Aureus strain. Journal of Orthopaedic Research. 2008 Oct;26(10):1355-62.
18. Vogely HC, Oosterbos CJ, Puts EW, Nijhof MW, Nikkels PG, Fleer A, Tonino AJ, Dhert WJ, Verbout AJ. Effects of hydrosyapatite coating on ti-6a1-4v implant-site infection in a rabbit tibial model. Journal of Orthopaedic Research. 2000 May;18(3):485-93.
19. Byrne AM, Morris S, McCarthy T, Quinlan W, O'Byrne J M. Outcome following deep wound contamination in cemented arthroplasty. International Orthopaedics. 2007 Feb;31(1):27-31.
20. Davis N, Curry A, Gambhir AK, Panigrahi H, Walker CR, Wilkins EG, Worsley MA, Kay PR. Intraoperative bacterial contamination in operations for joint replacement. Journal of Bone and Joint Surgery (British Volume). 1999 Sep;81(5):886-9.

21. Jonsson EO, Johannesdottir H, Robertsson O, Mogensen B. Bacterial contamination of the wound during primary total hip and knee replacement. Median 13 years of follow-up of 90 replacements. Acta Orthopaedica. 2014 Apr;85(2):159-64.
22. Whyte W, Hodgson R, Tinkler J. The importance of airborne bacterial contamination of wounds. Journal of Hospital Infection. 1982 Jun;3(2):123-35.
23. Petty W, Spanier S, Shuster JJ, Silverthorne C. The influence of skeletal implants on incidence of infection. Experiments in a canine model. Journal of Bone and Joint Surgery (American Volume). 1985 Oct;67(8):1236-44.
24. Southwood RT, Rice JL, McDonald PJ, Hakendorf PH, Rozenbilds MA. Infection in experimental hip arthroplasties. Journal of Bone and Joint Surgery (British Volume). 1985 Mar;67(2):229-31.
25. Odekerken JC, Arts JJ, Surtel DA, Walenkamp GH, Welting TJ. A rabbit osteomyelitis model for the longitudinal assessment of early post-operative implant infections. Journal of Orthopaedic Surgery and Research. 2013;8(1):38.
26. Andriole VT, Nagel DA, Southwick WO. A paradigm for human chronic osteomyelitis. Journal of Bone and Joint Surgery (American Volume). 1973 Oct;55(7):1511-5.
27. Kaarsemaker S, Walenkamp GH, vd Bogaard AE. New model for chronic osteomyelitis with staphylococcus aureus in sheep. Clinical Orthopaedics and Related Research. 1997 Jun(339):246-52.
28. Norden CW, Keleti E. Experimental osteomyelitis caused by pseudomonas aeruginosa. Journal of Infectious Diseases. 1980 Jan;141(1):71-5.
29. Power ME, Olson ME, Domingue PA, Costerton JW. A rat model of staphylococcus aureus chronic osteomyelitis that provides a suitable system for studying the human infection. Journal of Medical Microbiology. 1990 Nov;33(3):189-98.
30. Lankinen P, Lehtimaki K, Hakanen AJ, Roivainen A, Aro HT. A comparative 18f-fdg pet/ct imaging of experimental staphylococcus aureus osteomyelitis and staphylococcus epidermidis foreign-body-associated infection in the rabbit tibia. EJNMMI Res. 2012 Jul 23;2(1):41.
31. Makinen TJ, Veiranto M, Knuuti J, Jalava J, Tormala P, Aro HT. Efficacy of bioabsorbable antibiotic containing bone screw in the prevention of biomaterial-related infection due to staphylococcus aureus. Bone. 2005 Feb;36(2):292-9.
32. Cierny G, 3rd, Mader JT, Penninck JJ. A clinical staging system for adult osteomyelitis. Clinical Orthopaedics and Related Research. 2003 Sep(414):7-24.
33. Zimmerli W. Infection and musculoskeletal conditions: Prosthetic-joint-associated infections. Best Practice & Research: Clinical Rheumatology. 2006 Dec;20(6):1045-63.
34. Russell W, Burch R. The principles of humane experimental technique. United States of America: Johns Hopkins University; 1959.
35. Glaudemans AW, Galli F, Pacilio M, Signore A. Leukocyte and bacteria imaging in prosthetic joint infection. Eur Cell Mater. 2013;25:61-77.
36. Demirev A, Weijers R, Geurts J, Mottaghy F, Walenkamp G, Brans B. Comparison of [18 f]fdg pet/ct and mri in the diagnosis of active osteomyelitis. Skeletal Radiology. 2014 May;43(5):665-72.
37. Hoffmann EJ, Phelps ME, Mullani NA, Higgins CS, Ter-Pogossian MM. Design and performance characteristics of a whole-body positron transaxial tomograph. Journal of Nuclear Medicine. 1976 Jun;17(6):493-502.
38. Phelps ME, Hoffman EJ, Mullani NA, Ter-Pogossian MM. Application of annihilation coincidence detection to transaxial reconstruction tomography. Journal of Nuclear Medicine. 1975 Mar;16(3):210-24.
39. Toyama H, Ichise M, Liow JS, Modell KJ, Vines DC, Esaki T, Cook M, Seidel J, Sokoloff L, Green MV, Innis RB. Absolute quantification of regional cerebral glucose utilisation in mice by 18f-fdg small animal pet scanning and 2-14c-dg autoradiography. Journal of Nuclear Medicine. 2004 Aug;45(8):1398-405.
40. Toyama H, Ichise M, Liow JS, Vines DC, Seneca NM, Modell KJ, Seidel J, Green MV, Innis RB. Evaluation of anesthesia effects on [18f]fdg uptake in mouse brain and heart using small animal pet. Nuclear Medicine and Biology. 2004 Feb;31(2):251-6.
41. Huang SC, Phelps ME, Hoffman EJ, Sideris K, Selin CJ, Kuhl DE. Noninvasive determination of local cerebral metabolic rate of glucose in man. American Journal of Physiology. 1980 Jan;238(1):E69-82.
42. Kim EE. Clinical pet : Principles and applications. New York: Springer; 2004. xviii, 394 p. p.

43. Marsboom G, Wietholt C, Haney CR, Toth PT, Ryan JJ, Morrow E, Thenappan T, Bache-Wiig P, Piao L, Paul J, Chen CT, Archer SL. Lung (1)(8)f-fluorodeoxyglucose positron emission tomography for diagnosis and monitoring of pulmonary arterial hypertension. American Journal of Respiratory and Critical Care Medicine. 2012 Mar 15;185(6):670-9.
44. Tang G, Wang M, Tang X, Luo L, Gan M. Synthesis and evaluation of o-(3-[18f]fluoropropyl)-l-tyrosine as an oncologic pet tracer. Nuclear Medicine and Biology. 2003 Oct;30(7):733-9.
45. Huang T, Civelek AC, Li J, Jiang H, Ng CK, Postel GC, Shen B, Li XF. Tumor microenvironment-dependent 18f-fdg, 18f-fluorothymidine, and 18f-misonidazole uptake: A pilot study in mouse models of human non-small cell lung cancer. Journal of Nuclear Medicine. 2012 Aug;53(8):1262-8.
46. Bleeker-Rovers CP, Vos FJ, Corstens FH, Oyen WJ. Imaging of infectious diseases using [18f] fluorodeoxyglucose pet. Quarterly Journal of Nuclear Medicine and Molecular Imaging. 2008 Mar;52 (1):17-29.
47. Crymes WB, Jr., Demos H, Gordon L. Detection of musculoskeletal infection with 18f-fdg pet: Review of the current literature. Journal of Nuclear Medicine Technology. 2004 Mar;32(1):12-5.
48. Guhlmann A, Brecht-Krauss D, Suger G, Glatting G, Kotzerke J, Kinzl L, Reske SN. Fluorine-18-fdg pet and technetium-99m antigranulocyte antibody scintigraphy in chronic osteomyelitis. Journal of Nuclear Medicine. 1998 Dec;39(12):2145-52.
49. Nawaz A, Torigian DA, Siegelman ES, Basu S, Chryssikos T, Alavi A. Diagnostic performance of fdg-pet, mri, and plain film radiography (pfr) for the diagnosis of osteomyelitis in the diabetic foot. Molecular Imaging and Biology. 2010 Jun;12(3):335-42.
50. Schmitz A, Risse HJ, Kalicke T, Grunwald F, Schmitt O. [fdg-pet for diagnosis and follow-up of inflammatory processes: Initial results from the orthopedic viewpoint]. Zeitschrift für Orthopädie und Ihre Grenzgebiete. 2000 Sep-Oct;138(5):407-12.
51. Stumpe KD, Dazzi H, Schaffner A, von Schulthess GK. Infection imaging using whole-body fdg-pet. European Journal of Nuclear Medicine. 2000 Jul;27(7):822-32.
52. van der Bruggen W, Bleeker-Rovers CP, Boerman OC, Gotthardt M, Oyen WJ. Pet and spect in osteomyelitis and prosthetic bone and joint infections: A systematic review. Seminars in Nuclear Medicine. 2010 Jan;40(1):3-15.
53. Czernin J, Satyamurthy N, Schiepers C. Molecular mechanisms of bone 18f-naf deposition. Journal of Nuclear Medicine. 2010 Dec;51(12):1826-9.
54. Schlyer DJ. Pet tracers and radiochemistry. Annals of the Academy of Medicine, Singapore. 2004 Mar;33(2):146-54.
55. Jones-Jackson L, Walker R, Purnell G, McLaren SG, Skinner RA, Thomas JR, Suva LJ, Anaissie E, Miceli M, Nelson CL, Ferris EJ, Smeltzer MS. Early detection of bone infection and differentiation from post-surgical inflammation using 2-deoxy-2-[18f]-fluoro-d-glucose positron emission tomography (fdg-pet) in an animal model. Journal of Orthopaedic Research. 2005 Nov;23(6):1484-9.
56. Jones-Jackson L, Walker R, Purnell G, McLaren SG, Skinner RA, Thomas JR, Suva LJ, Anaissie E, Miceli M, Nelson CL, Ferris EJ, Smeltzer MS. Early detection of bone infection and differentiation from post-surgical inflammation using 2-deoxy-2-[18f]-fluoro-d-glucose positron emission tomography (fdg-pet) in an animal model. Journal of Orthopaedic Research. 2005 Nov;23(6):1484-9.
57. Koort JK, Makinen TJ, Knuuti J, Jalava J, Aro HT. Comparative 18f-fdg pet of experimental staphylococcus aureus osteomyelitis and normal bone healing. Journal of Nuclear Medicine. 2004 Aug;45(8):1406-11.
58. Stumpe KD, Strobel K. 18f fdg-pet imaging in musculoskeletal infection. Quarterly Journal of Nuclear Medicine and Molecular Imaging. 2006 Jun;50(2):131-42.
59. Odekerken JC, Brans BT, Welting TJ, Walenkamp GH. 18f-fdg micropet imaging differentiates between septic and aseptic wound healing after orthopedic implant placement a longitudinal study of an implant osteomyelitis in the rabbit tibia. Acta Orthopaedica. 2014;85(3):9.
60. Odekerken JCE, Walenkamp GHIM, Brans BT, Welting TJM, Arts JJC. The longitudinal assessment of osteomyelitis development by molecular imaging in a rabbit model. Biomed Research International. 2014;424652.
61. Palestro CJ, Love C, Miller TT. Infection and musculoskeletal conditions: Imaging of musculoskeletal infections. Best Practice & Research: Clinical Rheumatology. 2006 Dec;20(6):1197-218.

62. Al-Zahrani A, El-Saban K, Al-Sakhri H. Diagnosis of bone infection by complementary role of technetium -99m mdp and technetium-99m hexamethylpropylene-amineoxime-leukocytes. Indian Journal of Nuclear Medicine. 2012 Jul;27(3):164-71.
63. Palestro CJ, Love C, Bhargava KK. Labelled leukocyte imaging: Current status and future directions. Quarterly Journal of Nuclear Medicine and Molecular Imaging. 2009 Feb;53(1):105-23.
64. El-Maghraby TA, Moustafa HM, Pauwels EK. Nuclear medicine methods for evaluation of skeletal infection among other diagnostic modalities. Quarterly Journal of Nuclear Medicine and Molecular Imaging. 2006 Sep;50(3):167-92.
65. Castelli C, Marone P, Monzillo V, Segú K. Antistaphylococcal activity of antibiotic impregnated bone cement. The Knee. 1995;2(2):219-22.
66. Rauschmann MA, Wichelhaus TA, Stirnal V, Dingeldein E, Zichner L, Schnettler R, Alt V. Nanocrystalline hydroxyapatite and calcium sulphate as biodegradable composite carrier material for local delivery of antibiotics in bone infections. Biomaterials. 2005 May;26(15):2677-84.
67. Lewis G, Janna S. The in vitro elution of gentamicin sulfate from a commercially available gentamicin-loaded acrylic bone cement, versabond ab. J Biomed Mater Res B Appl Biomater. 2004 Oct 15;71(1):77-83.
68. Neut D, Kluin OS, Crielaard BJ, van der Mei HC, Busscher HJ, Grijpma DW. A biodegradable antibiotic delivery system based on poly-(trimethylene carbonate) for the treatment of osteomyelitis. Acta Orthopaedica. 2009 Oct;80(5):514-9.
69. Manyanga V, Kreft K, Divjak B, Hoogmartens J, Adams E. Improved liquid chromatographic method with pulsed electrochemical detection for the analysis of gentamicin. Journal of Chromatography A. 2008 May 2;1189(1-2):347-54.
70. Stypulkowska K, Blazewicz A, Fijalek Z, Sarna K. Determination of gentamicin sulphate composition and related substances in pharmaceutical preparations by lc with charged aerosol detection. Chromatographia. 2010 Dec;72(11-12):1225-9.
71. Stallmann HP, Faber C, Bronckers AL, Nieuw Amerongen AV, Wuisman PI. In vitro gentamicin release from commercially available calcium-phosphate bone substitutes influence of carrier type on duration of the release profile. BMC Musculoskeletal Disorders. 2006;7:18.
72. Haasnoot W, Stouten P, Cazemier G, Lommen A, Nouws JF, Keukens HJ. Immunochemical detection of aminoglycosides in milk and kidney. Analyst. 1999 Mar;124(3):301-5.
73. Jin Y, Jang JW, Han CH, Lee MH. Development of elisa and immunochromatographic assay for the detection of gentamicin. Journal of Agricultural and Food Chemistry. 2005 Oct 5;53(20):7639-43.
74. Jin Y, Jang JW, Lee MH, Han CH. Development of competitive direct enzyme-linked immunosorbent assay for the detection of gentamicin residues in the plasma of live animals. Asian-Australasian Journal of Animal Sciences. 2005 Oct;18(10):1498-504.
75. Chianella I, Guerreiro A, Moczko E, Caygill JS, Piletska EV, De Vargas Sansalvador IM, Whitcombe MJ, Piletsky SA. Direct replacement of antibodies with molecularly imprinted polymer nanoparticles in elisa--development of a novel assay for vancomycin. Analytical Chemistry. 2013 Sep 3;85(17):8462-8.
76. Fujiwara K, Yoshizaki Y, Shin M, Miyazaki T, Saita T, Nagata S. Immunocytochemistry for vancomycin using a monoclonal antibody that reveals accumulation of the drug in rat kidney and liver. Antimicrobial Agents and Chemotherapy. 2012 Nov;56(11):5883-91.
77. Albrektsson T, Johansson C. Osteoinduction, osteoconduction and osseointegration. European Spine Journal. 2001 Oct;10 Suppl 2:S96-101.
78. Blokhuis TJ, Arts JJ. Bioactive and osteoinductive bone graft substitutes: Definitions, facts and myths. Injury. 2011 Sep;42 Suppl 2:S26-9.
79. Hannink G, Arts JJ. Bioresorbability, porosity and mechanical strength of bone substitutes: What is optimal for bone regeneration? Injury. 2011 Sep;42 Suppl 2:S22-5.
80. Geesink RG. Hydroxyapatite-coated total hip prostheses. Two-year clinical and roentgenographic results of 100 cases. Clinical Orthopaedics and Related Research. 1990 Dec(261):39-58.
81. Geesink RG. Osteoconductive coatings for total joint arthroplasty. Clinical Orthopaedics and Related Research. 2002 Feb(395):53-65.
82. Geesink RG, de Groot K, Klein CP. Chemical implant fixation using hydroxyl-apatite coatings. The development of a human total hip prosthesis for chemical fixation to bone using hydroxyl-apatite coatings on titanium substrates. Clinical Orthopaedics and Related Research. 1987 Dec(225):147-70.

83. Geesink RG, de Groot K, Klein CP. Bonding of bone to apatite-coated implants. Journal of Bone and Joint Surgery (British Volume). 1988 Jan;70(1):17-22.
84. ten Broeke RH, Alves A, Baumann A, Arts JJ, Geesink RG. Bone reaction to a biomimetic third-generation hydroxyapatite coating and new surface treatment for the symax hip stem. Journal of Bone and Joint Surgery (British Volume). 2011 Jun;93(6):760-8.
85. Capello WN, D'Antonio JA, Jaffe WL, Geesink RG, Manley MT, Feinberg JR. Hydroxyapatite-coated femoral components: 15-year minimum followup. Clinical Orthopaedics and Related Research. 2006 Dec;453:75-80.
86. Gristina AG. Biomaterial-centered infection: Microbial adhesion versus tissue integration. Science. 1987 Sep 25;237(4822):1588-95.
87. Laure B, Besnier JM, Bergemer-Fouquet AM, Marquet-Van Der Mee N, Damie F, Quentin R, Favard L, Rosset P. Effect of hydroxyapatite coating and polymethylmethacrylate on stainless steel implant-site infection with staphylococcus epidermidis in a sheep model. J Biomed Mater Res A. 2008 Jan;84(1):92-8.
88. Alt V, Bitschnau A, Bohner F, Heerich KE, Magesin E, Sewing A, Pavlidis T, Szalay G, Heiss C, Thormann U, Hartmann S, Pabst W, Wenisch S, Schnettler R. Effects of gentamicin and gentamicin-rgd coatings on bone ingrowth and biocompatibility of cementless joint prostheses: An experimental study in rabbits. Acta Biomater. 2011 Mar;7(3):1274-80.
89. Alt V, Bitschnau A, Osterling J, Sewing A, Meyer C, Kraus R, Meissner SA, Wenisch S, Domann E, Schnettler R. The effects of combined gentamicin-hydroxyapatite coating for cementless joint prostheses on the reduction of infection rates in a rabbit infection prophylaxis model. Biomaterials. 2006 Sep;27(26):4627-34.
90. Moriarty TF, Grainger DW, Richards RG. Challenges in linking preclinical anti-microbial research strategies with clinical outcomes for device-associated infections. Eur Cell Mater. 2014;28:112-28; discussion 28.
91. Kim HJ, Kim SH. Tanshinone iia enhances bmp-2-stimulated commitment of c2c12 cells into osteoblasts via p38 activation. Amino Acids. 2010 Nov;39(5):1217-26.
92. Kim IS, Song YM, Cho TH, Kim JY, Weber FE, Hwang SJ. Synergistic action of static stretching and bmp-2 stimulation in the osteoblast differentiation of c2c12 myoblasts. Journal of Biomechanics. 2009 Dec 11;42(16):2721-7.
93. Liu R, Ginn SL, Lek M, North KN, Alexander IE, Little DG, Schindeler A. Myoblast sensitivity and fibroblast insensitivity to osteogenic conversion by bmp-2 correlates with the expression of bmpr-1a. BMC Musculoskeletal Disorders. 2009;10:51.
94. Handschel J, Berr K, Depprich RA, Kubler NR, Naujoks C, Wiesmann HP, Ommerborn MA, Meyer U. Induction of osteogenic markers in differentially treated cultures of embryonic stem cells. Head & Face Medicine. 2008;4:10.
95. Cooper GS, Kou TD. Risk of cancer after lumbar fusion surgery with recombinant human bone morphogenic protein-2 (rh-bmp-2). Spine (Phila Pa 1976). 2013 Oct 1;38(21):1862-8.
96. Kantlehner M, Schaffner P, Finsinger D, Meyer J, Jonczyk A, Diefenbach B, Nies B, Holzemann G, Goodman SL, Kessler H. Surface coating with cyclic rgd peptides stimulates osteoblast adhesion and proliferation as well as bone formation. Chembiochem: A European Journal of Chemical Biology. 2000 Aug 18;1(2):107-14.
97. Buchholz HW, Engelbrecht H. [depot effects of various antibiotics mixed with palacos resins]. Chirurg. 1970 Nov;41(11):511-5.
98. Klemm K. [gentamicin-pmma-beads in treating bone and soft tissue infections (author's transl)]. Zentralblatt für Chirurgie. 1979;104(14):934-42.
99. Walenkamp GH, van Rens TJ. [chains of gentamicin-pmma beads: A new method for the local treatment of osteomyelitis]. Nederlands Tijdschrift voor Geneeskunde. 1982 Nov 20;126(47):2136-42.
100. Walenkamp GH, Vree TB, van Rens TJ. Gentamicin-pmma beads. Pharmacokinetic and nephrotoxicological study. Clinical Orthopaedics and Related Research. 1986 Apr(205):171-83.
101. Walenkamp GH, Kleijn LL, de Leeuw M. Osteomyelitis treated with gentamicin-pmma beads: 100 patients followed for 1-12 years. Acta Orthopaedica Scandinavica. 1998 Oct;69(5):518-22.
102. Moskowitz JS, Blaisse MR, Samuel RE, Hsu HP, Harris MB, Martin SD, Lee JC, Spector M, Hammond PT. The effectiveness of the controlled release of gentamicin from polyelectrolyte multilayers in the

treatment of staphylococcus aureus infection in a rabbit bone model. Biomaterials. 2010 Aug;31 (23):6019-30.

103. Kalicke T, Schierholz J, Schlegel U, Frangen TM, Koller M, Printzen G, Seybold D, Klockner S, Muhr G, Arens S. Effect on infection resistance of a local antiseptic and antibiotic coating on osteosynthesis implants: An in vitro and in vivo study. Journal of Orthopaedic Research. 2006 Aug;24(8):1622-40.
104. Lim KS, Kam PC. Chlorhexidine--pharmacology and clinical applications. Anaesthesia and Intensive Care. 2008 Jul;36(4):502-12.
105. Pineda MH, Hepler DI. Chemical vasectomy in dogs. Long-term study. Theriogenology. 1981 Jul;16(1):1 -11.
106. Walenkamp GH. Gentamicin pmma beads and other local antibiotic carriers in two-stage revision of total knee infection: A review. Journal of Chemotherapy. 2001 Nov;13 Spec No 1(1):66-72.
107. Hooper GJ, Rothwell AG, Frampton C, Wyatt MC. Does the use of laminar flow and space suits reduce early deep infection after total hip and knee replacement?: The ten-year results of the new zealand joint registry. Journal of Bone and Joint Surgery (British Volume). 2011 Jan;93(1):85-90.
108. Dale H, Hallan G, Espehaug B, Havelin LI, Engesaeter LB. Increasing risk of revision due to deep infection after hip arthroplasty. Acta Orthopaedica. 2009 Dec;80(6):639-45.
109. Acklin YP, Widmer AF, Renner RM, Frei R, Gross T. Unexpectedly increased rate of surgical site infections following implant surgery for hip fractures: Problem solution with the bundle approach. Injury. 2011 Feb;42(2):209-16.
110. Kurtz SM, Lau E, Ong KL, Carreon L, Watson H, Albert T, Glassman S. Infection risk for primary and revision instrumented lumbar spine fusion in the medicare population. Journal of Neurosurgery: Spine. 2012 Oct;17(4):342-7.

Summary

Chapter 1

An infection has always been one of the most problematic orthopaedic complications. The disease itself has been determined in fossilized specimens of dinosaurs and Neanderthals and has been described in ancient Egyptian and Roman manuscripts. To date the treatment of orthopaedic infections still is a challenging task for the clinician with a high impact on the patient's daily life. Treatment often consists out of high-dosed antibiotics and surgical debridement of the affected tissue. In general the treatment regimen is time consuming and results in a long recovery period for the patient. Orthopaedic infections are difficult to cure and often become a chronic condition.

Although the necessary precautions in the use of antibiotics, the incidence of bacterial strains resistant to specific antibiotic treatment is increasing, also those responsible for orthopaedic infections (in most cases *Staphylococci*, like MRSA and MRSE). Orthopaedic infections caused by such antibiotic resistant bacteria are more difficult to treat, therefore antibiotic therapy should be applied with caution due to the limited collection of effective antibiotics. This indicates that improvement of the current treatment regimen is an option that has to be considered.

Infection prevention is an important measure to reduce the incidence of post-operative orthopaedic infections. The per-operative use of systemic antibiotics is a known effective measure, so is the use of bone cement admixed with antibiotics for the fixation of cemented prostheses. Currently such a prophylactic measure is not available for uncemented prostheses; a coating capable of releasing an antiseptic compound is expected to function as such a prophylactic measure. Currently such coatings are not yet suitable for clinical application and require further research into its (pre-)clinical efficacy.

Pre-clinical evaluation of such coatings and implants require a validated and reproducible pre-clinical implant infection model which allows thorough assessment of infection specific parameters. An overview of the available clinical diagnostics and experimental models was made to assess possible improvement options. Infection specific imaging was one of the diagnostic modalities which have shown to generate inconclusive results in the past. The diagnostic potential of scintigraphy has shown its limitations especially in the early phase of infection and in low-grade infections. PET scanning is expected to provide in a more discriminative diagnostic power in those cases. Furthermore a review on the available pre-clinical models indicated that there is room for improvement, since there are only a few animal models which use a multitude of infection specific parameters to assess infection development.

This indicates that considerable improvements can be made when focussing on the currently used diagnostic tools and the experimental setup of the animal infection models. An infection model, in which a multitude of infection specific parameters is being determined, combined with the use of multiple diagnostic imaging tools, could result in a more complete experimental model.

Chapter 2

Metallic implants are being used in the field of orthopaedic and trauma surgery for the stabilisation of fractures and osteotomies and for joint prosthesis. For the fixation of uncemented prostheses it is essential that the implant surface allows bone apposition, this can be enhanced with a coating like the well-known hydroxyapatite coating. However there is currently no coating available in the clinic which allows bone apposition on the implant surface and the ability to release an antimicrobial substance to function as a prophylactic measure for implant infection. A review of the current literature indicated that every coating has its advantages and disadvantages in fabrication and application and that there is a multitude of evaluation methods to assess the functionality of such novel coatings *in vitro*, *in vivo* and *ex vivo*.

Chapter 3

Current methods for the local delivery of antibiotics in patients (e.g. antibiotic-loaded bone cement or bone substitutes) result in diffusion of the antibiotic compound in the haematoma and the surrounding tissues. To determine the efficacy of the release of the antibiotic from the material, it is essential to determine the antibiotic load in patient material, like wound exudate and serum. The available methods to detect and measure the released amount of antibiotics are not optimal since they are hampered by the presence of proteins in patient material, which negatively influences the detection of the antibiotics present in the samples. An ELISA was established to determine the concentration of gentamicin and vancomycin in buffer, wound exudate and serum. In contrast to HPLC and fluorescence based methods, an ELISA based approach is more sensitive and less prone to interference caused by proteins. The established ELISA allows to specifically determine gentamicin concentrations within a range of 2 – 500 ng/ml, while the vancomycin ELISA can specifically determine concentrations within a range of 20 – 5000 ng/ml in protein containing samples.

Chapter 4

Pre-clinical evaluation of coatings and implants require a validated and reproducible pre-clinical model. After careful consideration of the available pre-clinical models (**Chapter 1**) and evaluation methods (**Chapter 2**), an experimental model in rabbits was chosen. In this model, rabbits received a titanium nail in the proximal tibia. In 50% of the rabbits the intramedullary cavity was contaminated per-operatively with $3.8x10^5$ CFU *S. aureus* prior to the implantation of a titanium nail, while the remainder of the rabbits received an intramedullary injection with sterile saline before implantation. After surgery the rabbits were followed for a period of 6 weeks to assess the development of an orthopaedic implant infection. During this 6 week follow-up period the rabbits were evaluated weekly on changes in weight, temperature and haematological values in combination with X-ray radiographs of the affected leg. Every 2 weeks the rabbits also received an injection with calcium binding fluorophores to register bone remodelling at that specific time point in follow-up. After 6 weeks the rabbits were sacrificed to evaluate the affected tibiae for infection by microCT, bacterial culture and histology. In total this approach resulted in a wide collection of infection specific parameters determined at multiple time points in a dedicated population, this resulted in a reproducible model for orthopaedic implant infections.

Data analysis indicated that an elevated erythrocyte sedimentation rate was indicative for infection presence early in follow-up. The changes in body weight were only indicative for the presence of an infection later on in follow-up. Leucocyte differentiation, C-reactive protein levels and X-ray radiographs allowed differentiation between uninfected and infected implants within the first 2 weeks of the experimental follow-up, these data were supported by the microCT, bacterial culture and histological data.

Chapter 5

In the described rabbit implant infection model we also investigated the use of ^{18}F-FDG as a PET-tracer for infection specific imaging. The systemic use of a radionuclide labelled glucose molecule (^{18}F-FDG) results in an accumulation in metabolically active regions, like active infections. The ^{18}F-FDG microPET scan was able to visualize and quantitatively determine infection presence at 3 weeks after surgery (possibly even after 2 weeks). Furthermore, the histological data confirmed that the PET-tracer uptake in the infected tissue corresponded with the infection mediated bone

morphological changes of the affected tissue. Therefore, ^{18}F-FDG can be used as an infection specific diagnostic imaging tool for the detection of early post-operative orthopaedic implant infections in this animal model.

Chapter 6

The presence of an implant is not a necessity for an orthopaedic infection. Also this situation requires an experimental model, not just to assess infection development but also for the evaluation of future bone replacement materials. An equal approach as described in **Chapter 4** was used for the infection model, only with the absence of an intramedullary nail, merely an empty defect in the proximal tibia. Also in this model the extensive experimental follow-up resulted in evident clinical, radiological and histological data on infection development and progression. The absence of a metallic implant was an advantage in the evaluation of the X-ray radiographs, microCT and microPET imaging data, due to the lack of implant mediated scattering induced by the necessary ionising radiation. As a result the X-ray radiographs, microCT and ^{18}F-FDG microPET data were able to differentiate between septic and aseptic wound healing at earlier time points. As such, ^{18}F-FDG allowed the detection of an orthopaedic infection within the first weeks after surgery. Also in this study the use of calcium binding fluorophores provided detailed information about the infection mediated structural changes of the tibial cortex and the presence or absence of osteolysis. Combined this allowed determination of infection mediated bone morphological changes from the 2nd post-operative week onward.

Chapter 7

The established rabbit implant infection model described in **Chapter 4** and **5** was ultimately used for the evaluation of a novel implant coating, with a proposed prophylactic function. The coating consisted out of a polymer admixed with the antiseptic chlorhexidine, resulting in a gradual release of chlorhexidine in the surrounding tissue. *In vitro* evaluation indicated that the coating was able to release a sufficient amount of chlorhexidine to reach bacteriostatic levels. The chlorhexidine containing polymer coating was subsequently evaluated on *in vivo* systemic toxicity. In 3 groups of 5 animals each, polymer coated titanium nails were implanted: a coating without chlorhexidine, a low dose and a high dose chlorhexidine containing coating. This part of the study indicated that

there was no systemic toxicity. The histological data of the legs with a titanium nail coated with the polymer coating without chlorhexidine indicated that, the surface of this "base-coating" was covered with bone within 4 weeks after implantation and is therefore able to serve as an excellent osteoconductive surface.

The *in vivo* antimicrobial efficacy study indicated that the high dose chlorhexidine coating was not able to prevent the onset of an implant infection in our animal model. However the ^{18}F-FDG microPET data did show a lower uptake at the first post-operative week in the rabbits with the chlorhexidine coated nail, when compared to the uptake in rabbits with an uncoated titanium nail. This suggests that the released chlorhexidine was not sufficient for a complete bacterial kill-off and as such resulted in a decreased virulence of the bacteria present in the contaminated tibial intramedullary cavity. Furthermore, the potential sclerosing effect of chlorhexidine might have resulted in a temporarily constrained local immune response.

As a result this study evaluated 2 separate coatings. First, a novel polymer based coating without further additions, which is able to function as an osteoconductive surface. And a second coating, a chlorhexidine loaded coating, which is able to release the antiseptic chlorhexidine. Unfortunately the released dose was not sufficient to reach *in vivo* bacteriostatic levels and was therefore not able to prevent an orthopaedic implant infection in our experimental model.

Conclusion

The main findings described in this thesis are:

- ELISA is a suitable method for the detection of gentamicin and vancomycin in patient material.
- A rabbit infection model is a suitable model for the evaluation of novel implant coatings and biomaterials.
- ^{18}F-FDG PET can be considered as a valid diagnostic imaging tool for the early detection of orthopaedic infections, with and without the presence of an implant.
- The current chlorhexidine containing polymer coating is inadequate as a prophylactic measure against orthopaedic implant infections.
- The studied polymer coating can serve as an osteoconductive surface for orthopaedic implants.
- This thesis also contains detailed descriptions of pre-clinical orthopaedic infection models, for the evaluation of orthopaedic infections, novel coatings and biomaterials. It also provides in histological and radiological scoring systems for the quantitative assessment of orthopaedic infections in these models.

Samenvatting

Hoofdstuk 1

Infecties zijn altijd al een van de meest problematische orthopaedische aandoeningen geweest. Botinfecties werden reeds vastgesteld bij dinosauriërs en Neanderthalers en werden tevens omschreven in oude Egyptische en Romeinse geschriften. Nog steeds is het behandelen van bot- en gewrichtsinfecties een uitdaging voor zowel de behandelend specialist als voor de patient. De behandeling vereist doorgaans een hoog gedoseerde antibioticumkuur en het operatief debrideren van het geïnfecteerde weefsel. De behandelingen en herstelperioden duren doorgaans lang. Botinfecties zijn moeilijk te genezen en resulteren dan ook vaak in een chronische aandoening.

Ondanks de nodige beperkingen in het antibioticumgebruik is er een toename van antibioticaresistentie bij een groot aantal bacteriestammen, onder andere die, die verantwoordelijk zijn voor orthopaedische infecties (in de meeste gevallen *S. aureus* en *S. epidermidis* (MRSA en MRSE)). Orthopaedische infecties veroorzaakt door resistente bacteriën zijn beduidend lastiger te behandelen. Er dient voorzichtig omgegaan te worden met de huidige beschikbare effectieve antibiotica en zo is het verbeteren van huidige behandelmethoden een mogelijke oplossing.

Om de incidentie van orthopaedische postoperatieve infecties terug te dringen, zijn diverse preventieve maatregelen van belang. Naast het gebruik van systemische antibiotica perioperatief, is in gecementeerde prothesen de bijmenging van antibiotica in het botcement effectief. In ongecementeerde prothesen bestaat die mogelijkheid niet en zou een coating op een orthopaedisch implantaat, welke een antiseptische stof vrijgeeft, eenzelfde bescherming kunnen bieden. Echter een dergelijke coating is op dit moment klinisch niet beschikbaar en dient nog ontwikkeld te worden alvorens deze geschikt is.

Het pre-klinisch testen van zulke coatings vereist een representatief en reproduceerbaar pre-klinisch implantaat infectie diermodel dat mogelijkheden biedt om alle aspecten van de infectie nauwkeurig te volgen. Daarom wordt er een overzicht gegeven van de beschikbare klinische diagnostica en experimentele modellen. Met name de infectie specifieke imaging is in het verleden teleurstellend gebleken, omdat in vooral de vroege fase van infecties en in low-grade infecties de scintigrafieën te weinig specifiek waren. PET scanning zou dat mogelijk beter inzichtelijk kunnen maken. Uit een literatuur overzicht van osteomyelitis diermodellen blijkt dat er maar weinig

diermodellen zijn die een compleet arsenaal aan infectie parameters gebruiken om de infectie te volgen.
De conclusie is dat door zowel wat betreft diagnostische middelen als wat betreft de diermodellen verbeteringen mogelijk zijn, en een combinatie van een verbeterd diermodel met meerdere infectieparameters en diagnostica zou kunnen resulteren in een optimaal experimenteel diermodel.

Hoofdstuk 2

Metalen implantaten worden al jaren gebruikt in het orthopaedisch en traumatologisch werkveld, voor de stabilisatie van fracturen en osteotomieën, maar ook voor gewrichtsprotheses. In geval van een ongecementeerde prothese is het voor de fixatie ervan nodig dat de prothese goed hecht of vastgroeit aan het bot, zoals bijvoorbeeld het geval is met een hydroxyapatiet coating. Het is gunstig als er adequate bot appositie plaatsvindt aan het oppervlak van het metalen implantaat. Er bestaat echter nog geen klinisch toepasbare coating die zowel botaangroei mogelijk maakt maar ook tegenlijk een antibacteriële stof afstaat die preventief werkzaam is tegen een infectie van de prothese. Het literatuuroverzicht laat niet alleen duidelijk zien dat iedere coating specifieke voor- en nadelen heeft bij zowel fabricage als ook bij klinische toepassing, maar ook dat er meerdere methoden zijn om de toepasbaarheid van deze coatings te evalueren, zowel *in vitro*, *in vivo* en *ex vivo*.

Hoofdstuk 3

De huidige methoden voor de lokale afgifte van antibiotica in de patiënt (zoals antibiotica houdende botcementen of botsubstituten) zorgen voor een diffusie van het antibioticum in het wondhematoom en de omliggende weefsels. Om de effectiviteit van zo'n lokale afgifte te kunnen bepalen is het nodig antibioticum concentraties te meten in onder andere wondvocht en serum. De reeds beschikbare meetmethoden om deze antibiotica afgifte te meten zijn niet optimaal met name vanwege de aanwezigheid van eiwitten in het patientmateriaal wat een negatieve invloed heeft op de concentratiebepaling van de antibiotica. Daarom is er een ELISA opgezet om de concentratie van gentamicine en vancomycine te bepalen in buffer, wondvocht en serum. Deze nieuwe methode is gevoeliger dan de reeds beschikbare methoden (zoals HPLC en methoden

gebaseerd op fluorescente detectie van antibiotica) en is minder gevoelig voor interferentie door eiwitrijke oplossingen. De ontwikkelde ELISA staat specifiek toe om gentamicine concentraties te bepalen binnen een bereik van 2 – 500 ng/ml, waar de vancomycin ELISA specifiek in staat is om concentraties te bepalen binnen een bereik van 20 – 5000 ng/ml in eiwitrijke oplossingen.

Hoofdstuk 4

Het pre-klinisch testen van coatings vereist een representatief en reproduceerbaar diermodel. Op grond van de bestudering van de bestaande experimentele modellen (**Hoofdstuk 1**) en evaluatie methoden (**Hoofdstuk 2**), werd gekozen voor een diermodel in konijnen. In dit model werd bij konijnen, in de proximale mergholte van de tibia, een titanium staafje geplaatst. Bij de helft van de de geopereerde konijnen werd het de mergholte vlak voor het implanteren gecontamineerd met met $3{,}8x10^5$ CFU *S. aureus*, de andere helft van de konijnen ontving een equivalent volume aan steriele buffer in de mergholte. Postoperatief werden de konijnen 6 weken gevolgd om zo de ontwikkeling van een implantaat infectie te bestuderen. Gedurende deze 6 weken werden de konijnen naast de dagelijkse algemene controle, iedere week onderzocht op afwijkende waarden in lichaamstemperatuur, gewicht en bloedwaarden. In diezelfde periode werden er ook Röntgen opnames gemaakt van de aangedane poot en werden er om de 2 weken fluorescente calcium markers toegediend ter registratie van bot remodellering op het tijdstip van injectie. Na 6 weken werden de konijnen geëuthanaseerd, waarna van de aangedane poot een microCT werd gemaakt, weefselkweken werden afgenomen en histologisch onderzoek werd verricht. Alle onderzoeken samen leverden een grote hoeveelheid aan infectie specifieke parameters op meerdere meetmomenten op, wat resulteerde in een informatief en reproduceerbaar diermodel voor implantaat infecties.

Analyse van deze infectie parameters liet zien dat in dit diermodel de bezinking al vroeg uitsluitsel kon geven of er een infectie bestond. Het lichaamsgewicht kon alleen op latere tijdspunten betrouwbaar dienen als een indicator voor de infectie. De leucocyten differentiatie en de C-reactief proteine concentratie stonden evenals de Röntgen opnames toe om al van de eerste à tweede postoperatieve week een onderscheid te kunnen maken tussen ongeïnfecteerde en geïnfecteerde implantaten, wat ondersteund werd door de microCT, de bacteriekweken en de histologische secties.

Hoofdstuk 5

In het konijnen infectiemodel werd gebruik gemaakt van microPET scanning ter evaluatie van de tracer ^{18}F-FDG voor infectie specifieke beeldvorming. Het gebruik van een radioactief gelabeld glucose molecuul (^{18}F-FDG) zorgt hierbij voor een lokale verhoogde glucose opname in het weefsel rondom de infectiehaard. De ^{18}F-FDG microPET scan stond toe het geïnfecteerde weefsel in beeld te brengen en te kwantificeren vanaf een postoperatieve periode van 3 weken, mogelijk al na 2 weken. Vergelijking met de histologisch onderzoeks gegevens toonde aan dat de opname van de PET tracer correspondeerde met het door de infectie aangedane weefsel. Kortom, ^{18}F-FDG microPET is in dit diermodel een betrouwbaar en specifiek diagnostisch hulpmiddel voor het detecteren van orthopaedische implantaat infecties, ook in een vroeg postoperatief stadium.

Hoofdstuk 6

Er zijn ook situaties waarbij er botinfecties optreden in de afwezigheid van een implantaat. Ook deze situatie behoeft een pre-klinisch model, niet alleen om de ontwikkeling van zulke infecties in kaart te brengen maar ook ter evaluatie van toekomstige botvervangende materialen. Zo werd er gebruik gemaakt van de gelijke opzet als beschreven in **Hoofdstuk 4** maar dan in de afwezigheid van een implantaat, dus enkel een leeg botdefect in de mergholte van de proximale tibia. De experimentele opzet zorgde ook hier voor een duidelijk klinisch, radiologisch en histologisch beeld van de ontwikkeling van een infectie. Door de afwezigheid van een implantaat was er minder storing van de Röntgen, microCT en ^{18}F-FDG microPET opnamen: er is minder storing van het signaal doordat er geen weerkaatsing meer is van de ioniserende straling aan het implantaat oppervlak. Deze verlaagde achtergrond zorgde voor een betere beoordeling van de verkregen gegevens van de Röntgen-opnamen, microCT en ^{18}F-FDG microPET, waardoor er op eerdere tijdstippen kon worden vastgesteld of er een infectie aanwezig was dan wanneer er wel een implantaat aanwezig was. Zodoende kon met behulp van ^{18}F-FDG PET al vanaf één week na de operatie het onderscheid gemaakt worden tussen geïnfecteerd en gezond weefsel. Ook in deze studie leverde het gebruik van fluorescente markers gedetailleerde informatie op omtrent de structuur van de tibiale cortex en de aan- of afwezigheid van osteolyse. Gecombineerd zorgde dit, in het geval van een infectie, voor een detecteerbaar verlies van bot en vervorming van de tibiale cortex vanaf de 2^{e} week na de operatie.

Hoofdstuk 7

Het in **Hoofdstuk 4** en **5** beschreven infectie model in het konijn werd ingezet voor de evaluatie van een nieuwe coating, met een beoogde profylactische werking. De coating bestaat uit een polymeer waarin het antisepticum chloorhexidine is vermengd, waarbij chloorhexidine geleidelijk wordt afgegeven aan de omgeving. *In vitro* evaluatie liet zien dat deze coating in staat was om genoeg chloorhexidine af te staan om bactericide concentraties te bereiken. In het konijnen model is deze chloorhexidine bevattende polymeer coating vervolgens getest op systemische toxiciteit. In drie groepen, van 5 konijnen ieder, werden met polymeer gecoate titanium staafjes in gebracht: zonder chloorhexidine, met een lage concentratie en met een hoge concentratie chloorhexidine. Geconcludeerd kon worden dat er in geen van de groepen systemische toxiciteit optrad. Opvallend was dat de histologie, van tibiae waarin de polymeer coating zonder chloorhexidine was gebruikt, aantoonde dat het oppervlak van deze "basis" coating binnen 4 weken na implantatie grotendeels bedekt was met bot, en dus in staat is om te dienen als uitstekend osteoconductief oppervlak.

Uit een vervolgstudie bleek echter dat de coating met chloorhexidine niet in staat was om het ontstaan van een infectie van een gecoat titanium implantaat in een gecontamineerde konijnen tibia te voorkomen. Desalniettemin registreerde de ^{18}F-FDG PET scan wel een verminderde tracer opname bij de gecoate implantaat groep in de eerste postoperatieve week ten opzichte van de groep konijnen met een gecontamineerd titanium implantaat zonder coating. Dit zou kunnen betekenen dat er een onvolledige eliminatie van de ingebrachte bacteriën bestond en dat de antiseptische werking van chloorhexidine zorgde voor slechts een vermindering van de virulentie van de bacteriepopulatie, die enkel van korte duur was. Daarnaast is het mogelijk dat chloorhexidine door zijn cel beschadigende werking de lokale cellulaire afweer tijdelijk heeft geremd.

Zodoende resulteerde dit gedeelte van de studie feitelijk in een tweetal mogelijke coatings. Allereerst een polymere coating zonder verdere toevoegingen, welke dienst kan doen als een osteoconductief oppervlak. En in een coating voorzien van chloorhexidine welke instaat is om die chloorhexidine vrij te geven, maar waarvan de vrijgekomen dosis niet afdoende was om een orthopaedisch infectie te voorkomen in ons experimentele diermodel.

Conclusie

De belangrijkste bevindingen beschreven in dit proefschrift zijn:

- ELISA is een geschikte methode voor de detectie van gentamicine en vancomycine in patientmateriaal.
- Een infectiemodel in konijnen is een geschikt model voor de evaluatie van antimicrobiële coatings van biomaterialen.
- Beeldvorming met behulp van ^{18}F-FDG PET is een geschikt diagnostisch hulpmiddel voor de zeer vroege detectie van orthopaedisch infecties met en zonder implantaat.
- De huidige chloorhexidine bevattende polymeer coating is niet geschikt als een profylaxe voor orthopaedische implantaat infecties.
- De bestudeerde polymeer coating is in staat te dienen als een osteoconductief oppervlak.
- Daarnaast voorziet deze thesis in gedetailleerde omschrijvingen van pre-klinische orthopaedische infectie modellen voor het bestuderen van orthopaedische infecties, antimicrobiële implantaat coatings en biomaterialen. Daarnaast voorziet deze thesis in de bij deze modellen behorende scoringssystemen voor het beoordelen van pre-klinische orthopaedische infecties.

Osteomyelitis scoring system

Radiology: X-ray

(During follow-up, without implant)

Lateral

Grade 0
Normal

Grade 1
Mild periosteal reaction

Grade 2
Periosteal reaction
Mild metaphyseal osteolysis

Grade 3
Periosteal reaction with
subperiostal calcification
Mild cortical thickening
More extensive
metaphyseal osteolysis

Grade 4
Cortical thickening
Osteolysis extending into
diaphysis

Radiology: X-ray

(During follow-up, with implant)

Lateral

Grade 0
Normal

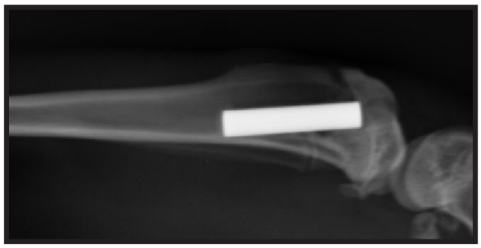

Grade 1
Mild periosteal reaction
Mild osteolysis immediate
around implant

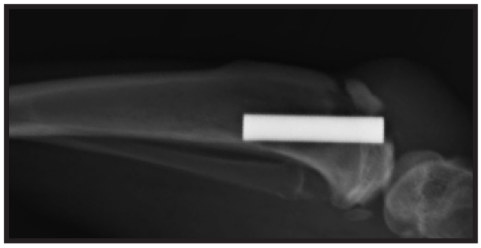

Grade 2
Periosteal reaction
Evident osteolysis
around implant

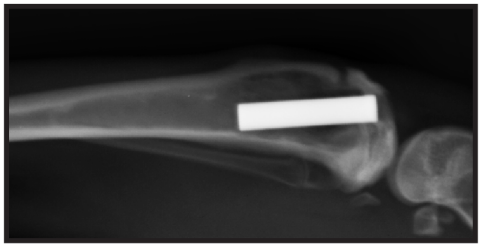

Grade 3
Periosteal reaction with
subperiostal calcification
Mild cortical thickening
More extensive
metaphyseal osteolysis

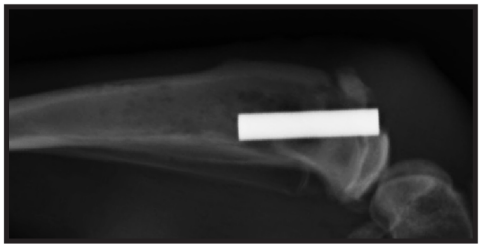

Grade 4
Cortical thickening
Osteolysis extending into
diaphysis

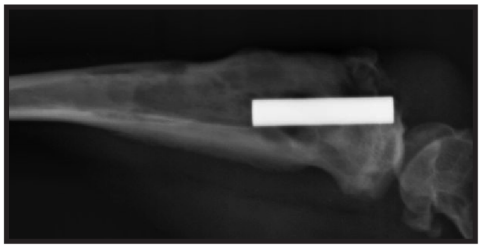

Radiology: *post-mortem* microCT

(Without implant)

	Sagittal	Lateral
Grade 0 Normal	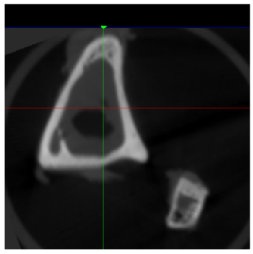	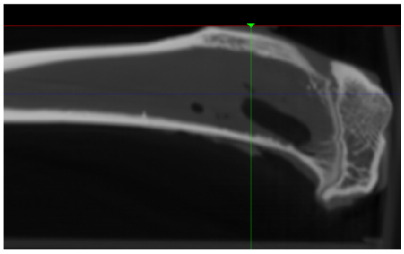
Grade 1 Mild periosteal reaction Mild cortical thickening	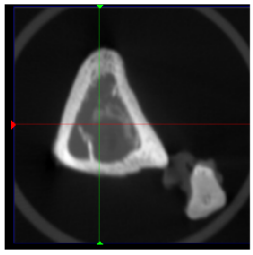	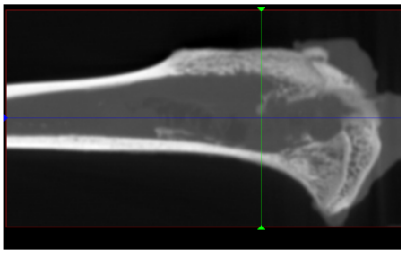
Grade 2 Evident periosteal reaction Evident cortical thickening Mild Osteolysis	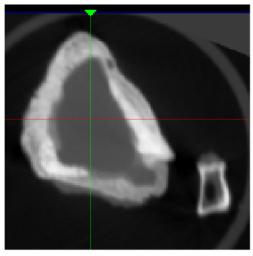	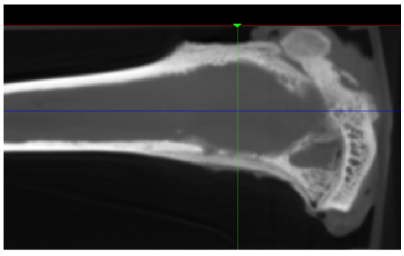
Grade 3 Extensive cortical thickening Focal loss of cortical wall Evident osteolysis	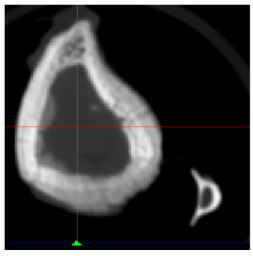	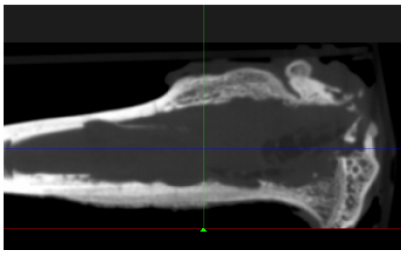
Grade 4 Extensive cortical thickening Loss of cortical morphology Loss of spongeous morphology Extensive osteolysis	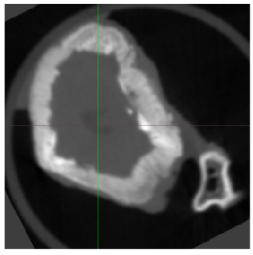	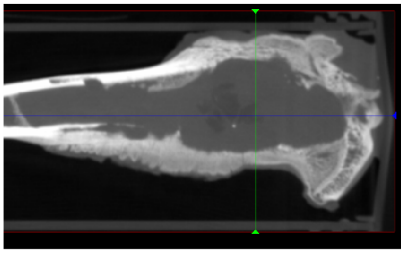

Radiology: *post-mortem* microCT

(With implant)

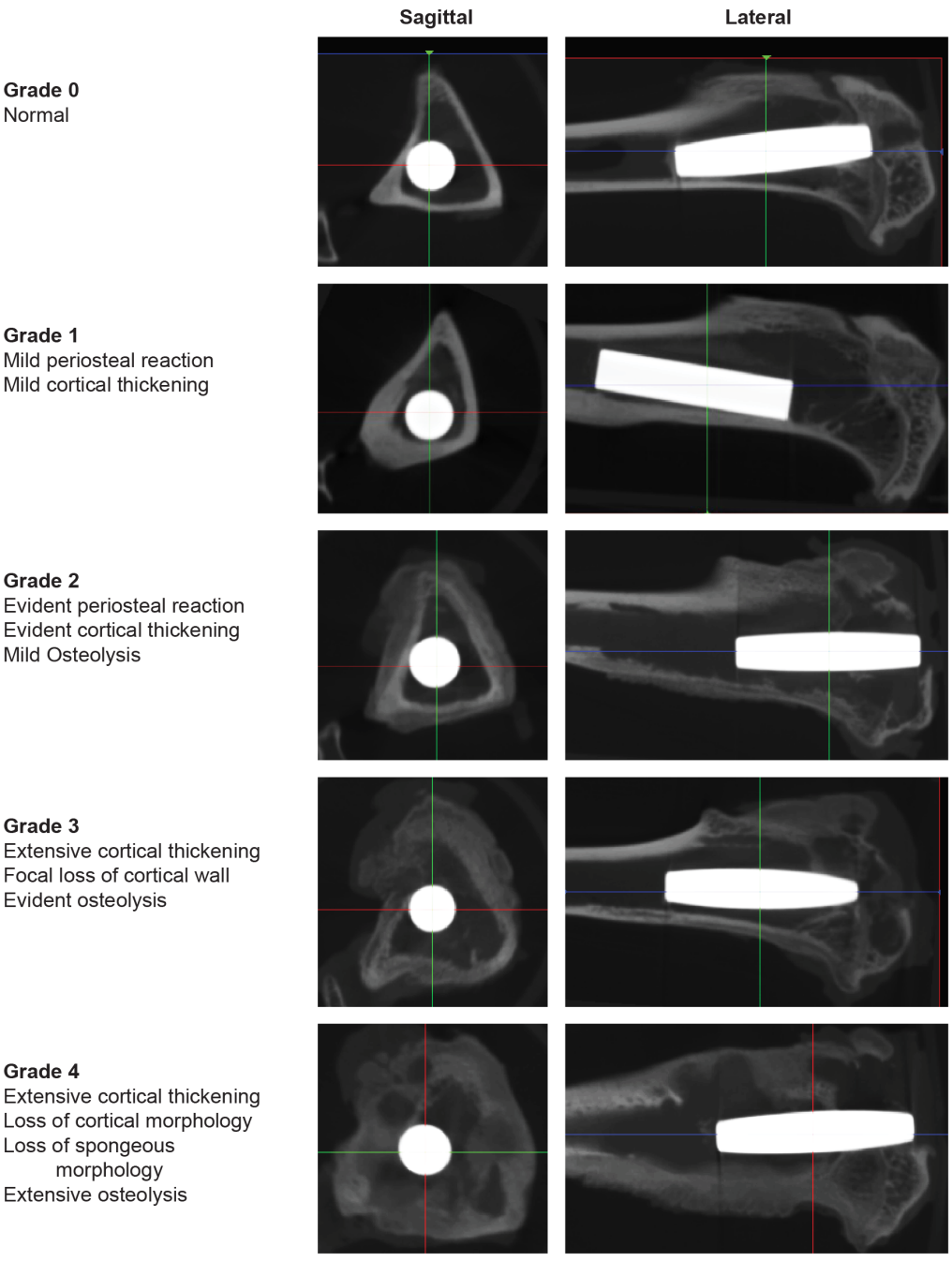

Histology

(Parameters independent from implant presence/absence)

	Score = 0	Score = 1	Score = 2
Cortical thickening (Masson Goldner) (Distal sections, 25 - 100x)	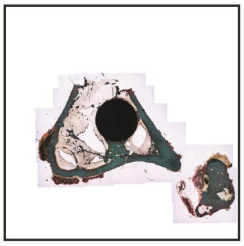	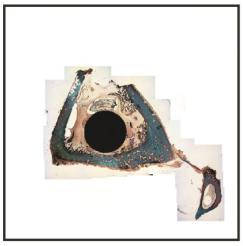	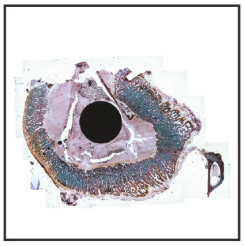
Presence of microabcesses (Masson Goldner) (Proximal and distal sections, 25x)	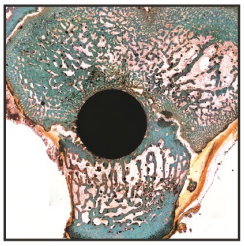	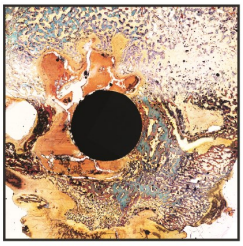	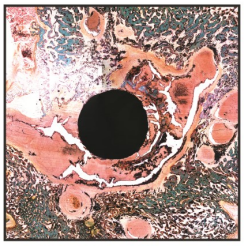
Enlarged Haversian canals (Masson Goldner) (Distal sections, 100 -200x)	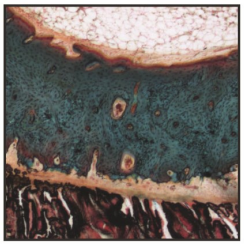	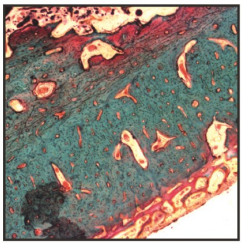	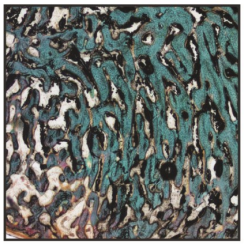
Periosteal elevation (Unstained section) (Calcium binding fluorophores) (Distal sections, 16x)	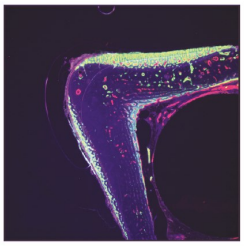	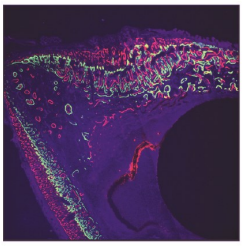	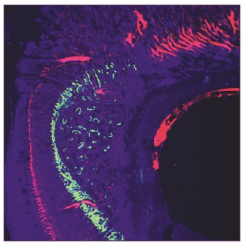
Gram stain (Modified Gram stain) (Distal sections, 400x, only with cam, modif. exposure and diaphragm)	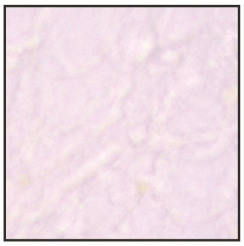		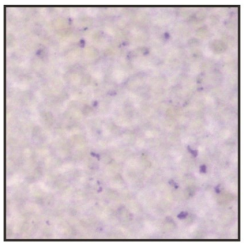

Morphological	**Histological staining**	**Score (per abnormality)**
Cortical thickening	Masson-Goldner	0: Absent 1: Mild to moderate 2: Moderate to severe
Presence of Enlarged Haversian		
Periosteal elevation	Calcium binding	
Gram stain	Modified Gram stain	0: Negative 2: Positive

Total histological score	**Osteomyelitis grade**
0 – 3	Not infected
>3 – 5	Mild
>5 – 7	Moderate
>7 – 10	Severe

Valorisation

Socioeconomic impact

Healthcare-associated infections, also called nosocomial infections, are considered to be the biggest healthcare related complication worldwide. HAI annually affects hundreds of millions of patients worldwide with approximately 4.1 million patients in Europe and about 1.7 million patients in the United States The costs related to these infections are considerable and are mainly a result of prolonged hospital stay and costs related to the treatment of the patient (US: $ 10 billion/year). One of the most common nosocomial infections are surgical site infections (e.g. orthopaedic implants) with an incidence of up to 15%, mainly depending on the surgical treatment and general health of the patient. (data World Health Organisation).

In general an orthopaedic infection has a tremendous impact on the patient's daily life. These infections require multiple major revision surgeries in combination with aggressive antibiotic treatment regimens. If an antibiotic treatment is not successful (due to the severity of the infection or the presence antibiotic resistant bacteria), such infections can lead to severe disabilities, loss of limb, bacterial sepsis and in some cases even death. In most cases orthopaedic infections are the result of the use of foreign material within the patient's body.

Treatment of these infections with antimicrobial substances is a challenging task, mainly due to the high incidence of resistant bacterial strains. Together with the potential risk of systemic toxicity of some broad-spectrum antibiotics, local antibiotic delivery and thus local treatment is the key to success. Currently, infection treatment consists of retraction of the implant and systemic antibiotics in combination with local delivery of antibiotics by antibiotic release from acrylic beads or spacers.

Prevention of orthopaedic infections is achieved by the incorporation of antibiotics in the bone cement used for the fixation of cemented prosthesis. However, there is no local prophylactic measure in case of an uncemented prosthesis, an osteoconductive antimicrobial coating is the proposed solution to this problem.

This thesis describes both experimental models and diagnostic tools for the evaluation of novel biomaterials and orthopaedic implant coatings and also brings these evaluation methods to practise by the assessment of a novel osteoconductive antimicrobial coating.

Collaborations

The majority of the work described within this thesis was funded by the BioMedical Materials program (BMM) which in turn was co-funded by the Dutch Ministry of Economic Affairs. BMM is a Dutch initiative initiated in 2007 to establish a nationwide consortium to promote collaboration in scientific research between academic and industry partners. In general this consortium comprises 18 research projects with a total budget of € 90+ million and holds research positions for over 400 researchers divided over 50 public or private partners.

Close collaboration with other Dutch research consortia like TiPharma (60 projects, 72 partners, € 260 million), CTMM (22 projects, 119 partners, € 300 million) and TeRM (6 projects, 13 partners, € 25 million) enables open communication and discussion resulting in innovation in medical science all originating from Dutch soil.

BMM comprises multiple projects and the herein described research was part of the BMM NANTICO project (Nonadhesive ANTImicrobial COatings for biomedical implants). This project was a collaboration between 4 academic partners (University Medical Centre Groningen, Amsterdam Medical Centre, Utrecht University and Maastricht University Medical Centre) and 2 industrial partners (DSM and Dolphys Medical), with the general focus on antimicrobial coating development and coating evaluation for biomedical implants (e.g. urinary catheters, vascular catheters and metal prosthesis).

This thesis mainly focusses on the implementation and evaluation of antimicrobial coatings for orthopaedic implants, which was mainly a joined effort of DSM Biomedical (coating development and the application to titanium implants) and the department of Orthopaedic Surgery of the Maastricht University Medical Centre (experimental model development and coating evaluation).

Innovation, product development and contribution to the field

The studies described in this thesis is of interest to multiple target groups within the field of biomedical and biomaterial research.

Physicians & patients:

The herein described animal studies and experimental approaches provide in tools to develop and evaluate novel products to eventually enhance patient health and mobility. With the main focus on the development and evaluation of novel implant coatings, biomaterials, antibiotics and diagnostic imaging modalities.

Also the herein described use of ^{18}F-FDG PET as a diagnostic tool allows the early diagnosis of orthopaedic infections. This method has been used in the clinical with positive results in specific cases, still it has not been accepted as a diagnostic standard for orthopaedic infections.

Researchers:

This thesis describes an experimental approach to evaluate novel biomaterials and implant coatings on osteocompatibility and antimicrobial efficacy.

This thesis also provides in a protocol to detect and quantify the presence of antibiotic compounds in liquid media (including patient material). Our method allows the evaluation of antibiotic release systems in a laboratory environment. This method could also contribute to the optimisation of the current antibiotic treatment regimen to minimize the initiation of antibiotic resistant bacterial strains during patient infection treatment.

Industry:

As in research, the described biomaterial and coating evaluation models and protocols can contribute to the development of more effective products, to assist in patient care and treatment.

Furthermore the findings concerning our novel osteoconductive coating are of high potential value (patent pending) to the medical device industry.

The herein described coating allows incorporation and release of an antimicrobial compound while remaining its osteoconductive surface properties.

Furthermore the use of this coating is not necessarily limited to metallic implants; the application of this coating to non-metallic substrates could initiate a complete new line of medical plastics

with an osteoconductive surface. Together with the upcoming plastic 3D-printing techniques the medical applications for plastics can become practically limitless (at least in combination with bone).

Product certified for clinical use?

This thesis describes the evaluation of a novel osteoconductive coating which allows the release of an antimicrobial compound. Before bringing this product to the market several aspects need to be arranged.

- The coating should be patented (currently in progress) before continuing further (pre-) clinical steps.
- After the patent has been filed, initiate the procedure to get the coating and application CE-certified and further investigate the incorporation of antibiotic substances into the coating to serve as a local prophylactic for implant infection.
- The clinical efficacy of the osteoconductive coating should be investigated, preferably supported by a research grant (e.g. STW Valorisation grant). A research group should initiate this grant to establish the means for a small pilot study followed by a randomised controlled trial to evaluate the clinical efficacy of the herein described coating.
- When the coating is fit for clinical application, a marketing strategy should be established to achieve visibility in the field.
  This can be achieved by informing:
  - Insurance companies
  - Clinicians
  - Patients
  - Contribute to scientific conferences

Overall this will be a process which will take several more years to finalize.

Current publicity

The in this thesis described studies have been presented at relevant scientific conferences by oral presentations (Orthopaedic Research Society, San Francisco, USA, 2012; European Bone and Joint Infection Society, Montreux, Switzerland, 2012; Dutch society for Biomaterials and Tissue Engineering, Lunteren the Netherlands, 2012; Dutch Orthopaedic Association (NOV), Amsterdam, the Netherlands, 2013; the European Bone and Joint Infection Society, Utrecht, the Netherlands, 2014 and at the Dutch Orthopaedic Association (NOV), Maastricht, the Netherlands, 2015) and poster presentations (Dutch society for Biomaterials and Tissue Engineering, Lunteren the Netherlands, 2010, 2011; European Cells and Materials XII conference, Davos, Switzerland, 2011 and at the Orthopaedic Research Society, Los Angeles, USA, 2011). Furthermore, our findings have been published in scientific journals relevant to the field (Journal of Orthopaedic Surgery and Research, Acta Orthopaedica and BioMed Research International).

Furthermore the evaluated coating and its composition have been filed as a patent, EP14186637: Medical Coating Composition, 2014.

Acknowledgements

Zo, hier ligt ie dan... Mijn boekje... Eindelijk...

Dit boekje was er nooit gekomen zonder de hulp van veel mensen (en konijnen), toch wil ik graag een aantal mensen in het bijzonder bedanken.

Allereerst mijn promotieteam, Prof. Dr. G.H.I.M. Walenkamp, Dr. T.J.M. Welting en Dr. J.J.C. Arts.

Beste Geert, wat begon met “Beste Professor Walenkamp” in de mailcorrespondentie en een geruststellend koud biertje op de markt in Groningen (m’n eerste NANTICO meeting), kunnen we na 5 jaar afsluiten met “Beste Geert” in de mailcorrespondentie en gezellig een biertje drinken op het feest. Hartelijk dank voor het geduld, de uitleg (zowel de klinische, wetenschappelijke maar zeker ook de “politieke” uitleg) en sturing die ik de afgelopen jaren heb mogen ontvangen, ik heb hier heel veel van geleerd en ook al vaak kunnen toepassen.

Beste Tim, hoewel je hart ligt bij kraakbeen en RNase MRP, ben ik je dankbaar voor de mogelijkheden en het vertrouwen dat je me gegeven hebt als promovendus op een “bot/infectie” gerelateerd onderwerp. Ookal was dat soms lastig te combineren met al het kraakbeen-werk dat op de agenda stond. Daarnaast heb ik graag meegewerkt aan het uitbreiden van de labfaciliteiten (het regelen van de aanschaf van nieuwe apparatuur... en dat zijn er nogal wat geweest...) en de reparaties van apparatuur nadat deze eigenlijk afgeschreven, maar toch onmisbaar was (glutaaraldehyde en plastic ventilatortjes gaan immers niet samen...).

Beste Chris, de communicatie onderling was wellicht niet altijd optimaal, maar toch hebben we een hele raffel aan projecten opgezet, aangepakt en succesvol afgerond. Ik heb veel van je geleerd, van communicatie naar bedrijven toe tot het leggen van contacten op congressen, waarvoor hartelijk dank.

Prof. Dr. L.W. van Rhijn, beste Lodewijk, hoewel we elkaar niet heel vaak gesproken hebben wil ik je toch graag bedanken voor je eerlijkheid en de interesse in mijn onderzoek en de daarbij behorende resultaten.

Dr. P.J. Emans, beste Pieter bedankt voor de mogelijkheden die je me gegeven hebt, eenerzijds met Fusebone en anderzijds met het Intech boekhoofdstuk. Dit waren de net wat andere onderzoeken die er voor zorgden dat ik een breed blikveld ben blijven houden.

Dr. B.T. Brans, beste Boudewijn, het was altijd even zoeken naar een gaatje in de agenda om even te overleggen of bij te praten over de status van de experimenten en het verwerken van de data. Ik heb het een geweldige kans en uitdaging gevonden om samen met de afdeling nucleaire geneeskunde te mogen samenwerken. Ik heb hier heel veel

van geleerd en veel nieuwe ideeën opgedaan. Ik denk dan ook dat er een paar hele mooie publicaties uit voort zijn gekomen en ik hoop dat er in de toekomst nog meer van zulke samenwerkingsverbanden met de afdeling mogen volgen.

Zo ook mijn collega (bijna) "lotgenoten" Marjolein, Ilona, Laura, Shennah, Mandy, Eva, Marloes, Guus, Alex, Toon, Maarten, Ufuk, Tessy, Michiel en Pieter. Allemaal hebben we hetzelfde doel voor ogen, goed en gedegen onderzoek afleveren om zo uiteindelijk te mogen promoveren (sommigen hebben dit inmiddels al gedaan, Top!!!). Het was erg fijn om met jullie alle ervaringen te mogen delen (al dan niet onder het genot van een biertje met nootjes en chips). Zo waren de avondjes bij Thembi altijd een succes en was er bij "Het bier van de maand" altijd een vaste groep aanwezig. Ook de avondjes tijdens de congres bezoeken waren altijd erg gezellig.

Don en Andy, tijdens mijn experimenten hebben jullie de nodige schoenzolen versleten tijdens het uitlezen van de röntgenplaten bij radiologie om ze vervolgens weer te retourneren naar het CPV waar de foto's gemaakt werden. Jullie maakten het (eigenlijk belachelijk) drukke protocol een stukje draaglijker. Thanks guys.

Zo passeerden ook de nodige studenten de labvloer... Loubna, Robin en Dorien. Ik hoop dat ik jullie iets heb kunnen leren, ik heb in ieder geval veel van jullie geleerd. Veel succes met jullie carrière (heb ik alle vertrouwen in) en bedankt voor jullie inzet.

Liesbeth en Margareth, waar kon ik anders terecht als ik mijn hart even moest luchten. Jullie zijn een geweldig team dat naar mijn mening vaak meer waardering verdiend dan dat het krijgt. Heel erg bedankt voor de verhelderende gesprekken en het luisterend oor.

Paul en Jan, bedankt voor de prettige samenwerking gedurende alle "nevenprojecten" om het maar even zo te noemen. Ookal lag er niet altijd de focus en vereiste het enig geduld van jullie zijde, toch heb ik altijd graag deelgenomen aan jullie studies.

Ralph en Kim, bedankt voor de prettige communicatie en het verzorgen (en soms zoeken) van de röntgenfoto's. Zonder jullie waren de studies een stuk lastiger te interpreteren geweest.

Marielle, Christian en Ivo bedankt voor het verzorgen van de ^{18}F-FDG spuitjes en de prettige samenwerking.

Marjanne, Sandra, Martine en Pascal, altijd waren jullie geinteresseerd in de experimentele opzet die ik weer eens bedacht had. Bedankt voor het gepuzzel met de goedkeuringen en de gesprekken over vanalles en nog wat.

Zo ook Joyce, Petra, Sanne, Frans, Femke, Richard, Peter, Nadine, Angeli en Barry zonder jullie was het werk op het CPV een stuk lastiger geweest.

Maar werken op het CPV kan niet zonder dat een onderzoeker een “geweten” heeft welke een oogje in het zeil houdt... Sanne oa. jij vervulde deze taak met verve, bedankt daarvoor. Zo ook Saskia, ik realiseer me ter degen dat ik niet altijd even gemakkelijk ben geweest, maar ik ben je wel enorm dankbaar dat je me met m’n neus op de feiten drukte (ookal was ik daar op dat moment niet altijd even gelukkig mee). Ik ben je daarom ook erg dankbaar dat we altijd een open discussie hebben kunnen voeren om zo het beste uit de experimenten te halen zonder dat dit resulteerde in onnodig ongerief of verlies van dieren. Dit heeft namelijk geresulteerd in een aantal mooie publicaties en zo ook in dit boekje.

De dames van het secretariaat Orthopaedie, bedankt voor de prettige communicatie als ik weer eens inzage moest hebben in de agenda van een van de specialisten. En de talloze gesprekken over koetjes en kalfjes (en konijntjes).

De Orthopaedische staf en assistenten wil ik ook graag bedanken voor hun interesse en voor hun kritische blik op het onderzoek tijdens de pizzameetings en daarbuiten.

De leden van het NANTICO-consortium wil ik ook graag bedanken voor hun feedback en open discussies omtrent de gehele studie. In het bijzonder Ton, Ton, Heidrun en Llewellyn over de discussies omtrent de uiteindelijke coating en Bas en Martijn voor hun input omtrent de microbiologische aanpak.

Marieke & Benjamin (en Dastan), Carla & Ronald, Dionne & Guy (en Sophie), Felix & Anke en Anouk, we kennen elkaar nu ruim 12 jaar, veel dingen zijn er gebeurd, maar altijd zijn we een hechte groep gebleven. Uit de grond van mijn hart, ik heb van mensen buiten mijn familie nog nooit zo veel steun mogen ontvangen als van jullie. Jullie zijn geweldige vrienden... Ik hoop dan ook dat er nog veel gezellige avondjes, uitstapjes, feestjes, BBQ’s en motor-ritjes mogen volgen.

Mijn familie wil ik ook graag bedanken voor hun interesse gedurende de afgelopen jaren. Ik hoop dat mijn inzet en uitleg in combinatie met dit boekje jullie een duidelijker beeld heeft kunnen geven over de noodzaak van dit soort onderzoeken, en de resultaten die men ermee kan bereiken.

Dan mijn paranimfen...

Felix wij kennen elkaar al sinds het HLO en daar zaten we al direct op een lijn (niet zeuren, maar doen...) en dat is altijd zo gebleven. Ik heb je mening altijd bijzonder gewaardeerd ookal was die soms ongelooflijk direct. Ik vind het dan ook geweldig dat je paranimf wilde zijn bij mijn promotie.

Roy, breurke, ondanks dat we zo veel verschillen, zijn we toch uit het zelfde hout gesneden. We hebben samen het nodige meegemaakt, zowel op het voetbalveld als bij

het vellen van een denneboom. Ik kon me dan ook niemand anders wensen die ik aan mijn zijde wilde hebben staan bij mijn promotie, je bedacht je dan ook geen moment toen ik je vroeg als paranimf, waarna de vraag volgde “wat houdt dat eigenlijk in?”.

Pap en Mam, bedankt voor alle kansen die jullie Roy en mij hebben gegeven, ik denk dat wij twee deze ook zo goed als volledig benut hebben. Bedankt voor alle vertrouwen, steun en bemoedigende woorden (zeker de afgelopen jaren), dat heeft mij altijd op de been gehouden (zonder het avondeten dat altijd klaar stond na de lange dagen tijdens mijn experimenten was dit overigens sowieso niet gelukt). Zonder jullie input stond ik nu niet hier en was er ook geen boekje...

Lieve Daisy, bedankt voor je geduld en steun gedurende de afrondende fase van mijn promotie. Het boekje is nu klaar, nu is er weer meer tijd om samen dingen te ondernemen en ik hoop dat nog heel lang met je te mogen doen. Ik hou van je...

Illustration by E. Noyons, reprint with permission from Dr. R. Feith

Curriculum Vitae

Jim Odekerken was born on January 31st 1985 in Houthem - St. Gerlach, the Netherlands. In 2002 he graduated at the Higher General Secondary Education (HAVO) of the Stella Maris College in Meerssen. In September 2002 he started the study of Biomedical Laboratory Research at the Zuyd University of Applied Sciences (Hogeschool Zuyd) in Heerlen, where he received his "Bachelor of Applied Science" degree in 2006.

After receiving his Bachelor's degree he started the study of Clinical Molecular Sciences at the Maastricht University, where he received his "Master in Science" degree in 2008.

In 2009 he started working as "Research Technician Genotyping" at the Department of Clinical Genomics of the Maastricht University. Later on that year he started his PhD-trajectory at the Department of Orthopaedic Surgery of the Maastricht University Medical Centre under supervision of Professor Dr. G.H.I.M. Walenkamp, Dr. T.J.M. Welting and Dr. J.J.C. Arts. He presented his work on several national and international conferences, of which several have been described in this thesis.

In October 2014 he continued his career as a researcher and lecturer at the Zuyd University of Applied Sciences where he joined fellow scientists and lecturers to train the next generation of technicians.

Scientific contributions

Peer-reviewed publications

J.C.E. Odekerken, A.J. Dirks, J.A. Loontjens, B.T. Brans, L.N.D. Rijk, J.J.C. Arts, T.J.M. Welting, G.H.I.M. Walenkamp. A novel polymer-based osteoconductive drug-eluting coating for orthopaedic implants. 2014, Patent filed (EP14186637), manuscript to be submitted.

J.C.E. Odekerken, D.M.W. Logister, L. Assabre, J.J.C. Arts, G.H.I.M. Walenkamp, T.J.M. Welting. ELISA-based detection of gentamicin and vancomycin in protein-containing samples. 2015, Submitted.

J. Song, **J.C.E. Odekerken**, D.W.P.M. Löwik, P.M. López-Pérez, T.J.M. Welting, F. Yang, J.A. Jansen, S.C.G. Leeuwenburgh. Release Kinetics of Antibiotics from Gelatin Micro- and Nanospheres Depend on Physicochemical Properties of Antibiotics. 2015, Submitted.

J.C.E. Odekerken, G.H.I.M. Walenkamp, B.T. Brans, J.J.C. Arts, T.J.M. Welting. The longitudinal assessment of osteomyelitis development by molecular imaging in a rabbit model. BioMed Research International. 2014, Article ID 424652.

J.C.E. Odekerken, B.T. Brans, T.J.M. Welting, G.H.I.M. Walenkamp. ^{18}F-FDG microPET imaging differntiates between septic and aseptic wound healing after orthopedic implant placement: A longitudinal study of an implant osteomyelitis in the rabbit tibia. Acta Orthopaedica. 2014 Jun;85 (3):305-13.

J.L. Lansdowne, D. Devine, U. Eberli, P.J. Emans, T.J.M. Welting, **J.C.E. Odekerken**, D. Schiuma, M. Thalhauser, L. Bouré, S. Zeiter. Characterisation of an ovine bilateral critical sized bone defect iliac wing model to examine treatment modalities based on bone tissue engineering. BioMed Research International. 2014, Article ID 250958.

C.J.D. Bergmann, **J.C.E. Odekerken**, T.J.M. Welting, F. Jungwirth, L.W. van Rhijn, R. Telle, H. Fischer, P.J. Emans. Calcium phosphate based three-dimensional cold plotted bone scaffolds for critical size bone defects. BioMed Research International. 2014, Article ID 852610.

J.C.E. Odekerken, J.J.C. Arts, D.A.M. Surtel, G.H.I.M. Walenkamp, T.J.M. Welting. A rabbit osteomyelitis model for the longitudinal assessment of early post-operative implant infections. Journal of Orthopaedic Surgery and Research. 2013;8:38.

P.H.J. van Bilsen, L. Jaspers, M.S. Lombardi, **J.C.E. Odekerken**, E.N. Burright, and W.F. Kaemmerer. Identification and allele-specific silencing of the mutant Huntington allele in Huntington's disease patient-derived fibroblasts. Human Gene Therapy. 2008 Jul;19(7):710-9.

Book chapters

J.C.E. Odekerken, T.J.M. Welting, J.J.C. Arts, G.H.I.M. Walenkamp and P.J. Emans. Modern orthopaedic implant coatings – Their pro's, con's and evaluation methods. Modern Surface Engineering Treatments (Intech), 2013, ISBN 980-953-307-959-7.

Patents

EP14186637: Medical Coating Composition, DSM/MUMC.

Oral presentations

J.C.E. Odekerken, D.M.W. Logister, L. Assabre, J.J.C. Arts, G.H.I.M. Walenkamp, T.J.M. Welting. ELISA-based detection of gentamicin and vancomycin. Annual meeting of the Dutch Orthopaedic Association (NOV), Maastricht, the Netherlands, February 2015
* Nominated for the Rik Huiskes Award

J.C.E. Odekerken, D.M.W. Logister, L. Assabre, J.J.C. Arts, G.H.I.M. Walenkamp, T.J.M. Welting. ELISA-based detection of gentamicin and vancomycin. Annual meeting of the European Bone and Joint Infection Society (EBJIS), Utrecht, the Netherlands, September 2014.
* Nominated for the Best Paper Award

J.C.E. Odekerken, J.J.C. Arts, G.H.I.M. Walenkamp, T.J.M. Welting. The evaluation of a novel antimicrobial coating: the use of chlorhexidine to prevent orthopaedic implant infection. Annual meeting of the BioMedical Materials program, Ermelo, the Netherlands, June 2013.

J.C.E. Odekerken, B.T. Brans, J.J.C. Arts, T.J.M. Welting, G.H.I.M. Walenkamp. In vivo imaging of osteomyelitis with ^{18}F-FDG microPET. Annual meeting of the Dutch Orthopaedic Association (NOV), Amsterdam, the Netherlands, February 2013.
* Nominated for the Rik Huiskes Award

J.C.E. Odekerken, J.J.C. Arts, D.A.M. Surtel, T.J.M. Welting, G.H.I.M. Walenkamp. A reproducible implant infection model in rabbits. Annual meeting of the Netherlands society for Biomaterials and Tissue Engineering (NBTE), Lunteren, the Netherlands, December 2012.
* Nominated for the Best Presentation Award

J.C.E. Odekerken, B.T. Brans, T.J.M. Welting, G.H.I.M. Walenkamp. In vivo imaging of osteomyelitis with ^{18}F-FDG microPET. Annual meeting of the European Bone and Joint Infection Society (EBJIS), Montreux, Switzerland, September 2012.
* Nominated for the Best Paper Award

J.C.E. Odekerken, J.J.C. Arts, D.A.M. Surtel, T.J.M. Welting, G.H.I.M. Walenkamp. A reproducible implant infection model in rabbits. Annual meeting of the European Bone and Joint Infection Society (EBJIS), Montreux, Switzerland, September 2012.

J.C.E. Odekerken, T.J.M. Welting, B.T. Brans, J.J.C. Arts, G.H.I.M. Walenkamp. A reproducible implant infection model in rabbits, for evaluating antibacterial coatings on orthopaedic implants. Annual meeting of the Orthopaedic Research Society (ORS), San Francisco, USA, February 2012.

Poster presentations

J.C.E. Odekerken, D.M.W. Logister, L. Assabre, J.J.C. Arts, G.H.I.M. Walenkamp, T.J.M. Welting. ELISA-based detection of Gentamicin and Vancomycin. Annual meeting of the Orthopaedic Research Society (ORS), New Orleans, USA, March 2014.

J.C.E. Odekerken, J.J.C. Arts, G.H.I.M. Walenkamp, T.J.M. Welting. A reproducible osteomyelitis model in rabbits. Annual meeting of the BioMedical Materials program, Ermelo, the Netherlands, September 2012.

J.C.E. Odekerken, T.J.M. Welting, B.T. Brans, J.J.C. Arts, G.H.I.M. Walenkamp. A reproducible osteomyelitis model in rabbits. Annual meeting of the Care and Public Health Research Institute (CAPHRI), Maastricht, the Netherlands, April 2012.

J.C.E. Odekerken, T.J.M. Welting, B.T. Brans, J.J.C. Arts, G.H.I.M. Walenkamp. A reproducible osteomyelitis model in rabbits. eCM XII: Implant Infection conference, Davos, Switzerland, June 2011.

J.C.E. Odekerken, T.J.M. Welting, J.J.C. Arts, G.H.I.M. Walenkamp. A preface to a reproducible osteomyelitis model in rabbits Annual meeting of the BioMedical Materials program, Ermelo, the Netherlands, May 2011.

T.J.M. Welting, P.J. Emans, **J.C.E. Odekerken**, C.J.D. Bergmann, J.J.C. Arts, L. Bouré, D. Devine, R. Telle, H. Fischer, L.W. van Rhijn. Low Temperature 3D printing of β-TCP-based scaffolds. Annual meeting of the Orthopaedic Research Society (ORS), Los Angeles, USA, January 2011.

J.C.E. Odekerken, T.J.M. Welting, J.J.C. Arts, G.H.I.M. Walenkamp. Antibacterial coatings for titanium substrates. Annual meeting of the Netherlands society for Biomaterials and Tissue Engineering (NBTE), Lunteren, the Netherlands, December 2010.

J.C.E. Odekerken, T.J.M. Welting, J.J.C. Arts, G.H.I.M. Walenkamp. Antibacterial coatings for titanium substrates. Annual meeting of the BioMedical Materials program, Ermelo, the Netherlands, April 2010.

J.C.E. Odekerken, T.J.M. Welting, J.J.C. Arts, G.H.I.M. Walenkamp. Antibacterial coatings for titanium substrates. Annual meeting of the Care and Public Health Research Institute (CAPHRI), Maastricht, the Netherlands, March 2010.
* Winner CAPHRI Poster Award

List of Abbreviations

A

Ab	Antibiotic
ALP	Alkaline phosphatase assay
ASTM	American Society for Testing and Materials
ATCC	American Type Culture Collection

B

BMM	BioMedical Materials institute
BMP (-2, -4, -7)	Bone morphogenetic protein (-2, -4, -7)
BSA	Bovine serum albumin

C

CDC	Centers of Disease Control and Prevention
CFU	Colony forming unit
CHX	Chlorhexidine
CLHAS	Cross-linked high amylose starch,
CRP	C-reactive protein
CT	Computed tomography

D

DAPI	4',6-diamidino-2-phenylindole
DEC	Animal Ethics Committee
Det.	Detector
DEXA	Dual energy X-ray absorptiometry
DNA	Deoxyribonucleic acid

E

E. coli	*Escherichia coli,*
ECL	Enhanced chemiluminescence
EDC	N-(3-Dimethylaminopropyl)-N'-ethylcarbodiimide hydrochloride
ELISA	Enzyme-linked immunosorbent assay
ESR	Erythrocyte sedimentation rate

F

FCS	Foetal calf serum
FDA	Fluorescein diacetate
FDA	Food and Drug Administration

G

GFP	Green fluorescent protein
GMBS	N-(γ-Maleimidobutyryloxy)succinimide
Gmd-1C11	Anti-glucosamidase monoclonal antibody

H

HA	Hydroxyapatite
HAI	Healthcare-associated infections
HD-PE	High density polyethylene
HPLC	High performance liquid chromatography
HRP	Horseradish peroxidase

I

I.v.	Intravenous
ISO	International Organisation for Standardisation

J

JIS	Japanese Industrial Standard

K

kDa	Kilodalton
keV	Kiloelectron volt
KLH	Keyhole limpet haemocyanin
kV	Kilovolt
kVp	Kilovolt peak

L

Leucoc.	Leucocyte count/differentiation
L-PRP	Leucocyte- and platelet-rich plasma

M

mAs	Milliampere second
MBC	Minimal bactericidal concentration
MBq	Megabecquerel
MEC	Medical Ethics Committee
MIC	Minimal inhibitory concentration
MRI	Magnetic resonance imaging
MRSA	Methicillin-resistant *Staphylococcus aureus*
MRSE	Methicillin-resistant *Staphylococcus epidermidis*
MTS	3-(4,5-dimethylthiazol-2-yl)-5-(3-carboxymethoxyphenyl)-2-(4-sulfophenyl)-2H-tetrazolium
MTT	3-(4,5-Dimethylthiazol-2-yl)-2,5-Diphenyltetrazolium Bromide

N

nanoMIPS	Molecular imprinted polymer nanoparticles
NANTICO	Non-adhesive antimicrobial coatings for biomedical implants
NZW	New Zealand White

O

OD	Optical density
OSEM-2D	2-dimensional ordered-subsets expectation maximisation

P

P. acnes	*Propionibacterium acnes*
P. aeruginosa	*Pseudomonas aeriginosa*
P. mirabilis	*Proteus mirabilis*
P3HB	Poly-3-hydroxybutyrate
P3HB/HA	Poly-3-hydroxybutyrate/hydroxyapatite

PA	Peri-apatite
PBS	Phosphate-buffered saline
PCL	Polycarprolactone
PCR	polymerase chain reaction
PE	Polyethylene
PET	Positron emission tomography
pHA	Partial hip arthroplasty
PHA	Polyhydroxyalkanoate
PL:PG	Polylactide/polyglycolide
PLA	Polylactic acid
PLA-PL:CG	Polylactic acid-polylactide/polyglycolide
PLGA	Polylactic-co-glycolic acid
PLGA-PEG	Polylactic-co-glycolic acid – polyethylene glycol
PLLA	Poly-L-lactide,
PMMA	Polymethyl methacrylate
PMTC	Poly(trimethylene carbonate)
PolyA	Polyanhydride
PPF	Polypropylene fumarate
PTFE	Polytetrafluoroethylene
PVC	Polyvinyl chloride
PVDF	Polyvinylidene fluoride

R

RAMPO	Rabbit anti-mouse peroxidase
RGD	Arginine-glycine-asparagine
RNA	Ribonucleic acid
ROI	Region of interest
rpm	Rotations per minute

S

S. aureus	*Staphylococcus aureus*
S. canis	*Streptococcus canis*
S. epidermidis	*Staphylococcus epidermidis*
Scint.	Scintigraphy
SDS-PAGE	Sodium dodecyl sulphate polyacrylamide gel electrophoresis
SEM	Scanning electron microscopy
SPECT	Single photon emission computed tomography
SPF	Specified pathogen free
SUV	Standardized uptake value
SWARPO	Swine anti-rabbit peroxidase

T

TCP	Tricalcium phosphate
TEM	Transmission electron microscopy
Temp.	Temperature
TGF-β	Transforming growth factor beta
TKA	Total knee arthroplasty
TMB	3,3',5,5'-Tetramethylbenzidine

U

UHMWPE	Ultra-high molecular weight polyethylene
UV	Ultraviolet

V

VBA	Visual Basic for Applications
VOI	Volume of interest
VRSA	Vancomycin-resistant *Staphylococcus aureus*

W

WHO	World Health Organisation

X

XTT	2,3-bis-(2-methoxy-4-nitro-5-sulfophenyl)-2H-tetrazolium-5-carboxanilide

Isotopes and tracers

^{18}F-FDG	(^{18}Fluor) fluorodeoxyglucose
^{18}F-NaF	(^{18}Fluor) sodium fluoride
^{57}Co	^{57}Cobalt
^{67}Ga-citrate	^{67}Gallium citrate
^{99m}Tc-MDP	^{99m}Technetium-methyl diphosphonate
^{111}In	^{111}Indium

Sponsors

cambioceramics

Anna Fonds

Nederlands
Orthopedisch
Research en
Educatie
Fonds

NBTE

Nederlandse vereniging voor
Biomaterialen en Tissue Engineering
Netherlands society for Biomaterials
and Tissue Engineering

caphri

BUITEN STATE
WWW.BUITENSTATE.NL

aelmans
www.aelmans.com

Marcel van de Laar
Korinthe 10 Klimmen
T 045 574 0878
I www.vdlaaradvies.nl

vdLAAR
Financiële DienstVerlening

Financieringen
Hypotheken
Verzekeren
Sparen

Ger Horsmans
Timmer-montagebedrijf

Ger Horsmans
Hogeweg 75
6367 BC Voerendaal
Tel: 045-5750298
Mobiel: 06-20465160
Fax: 045-8501619
ghorsmans@hotmail.com

frissen
GROEN TECHNIEK
Valkenburg a/d Geul • www.frissen.nl

BMM